UNIVERSIDAD COMPLUTENSE DE MADRID
FACULTAD DE CIENCIAS QUÍMICAS

TESIS DOCTORAL

Posttranslational modifications of endosomal GTPases.
Implications in intracellular localization and traffic

Modificaciones postraduccionales de GTPasas endosomales
implicaciones en localización y tráfico intracelular

MEMORIA PARA OPTAR AL GRADO DE DOCTORA
PRESENTADA POR

Clara Lillian Oeste Villavieja

Directora

María Dolores Pérez-Sala Gozalo

Madrid, 2015

UNIVERSIDAD COMPLUTENSE
DE MADRID

CENTRO DE INVESTIGACIONES
BIOLÓGICAS (CSIC)

Posttranslational modifications of endosomal GTPases. Implications in intracellular localization and traffic

Modificaciones postraduccionales de GTPasas endosomales. Implicaciones en localización y tráfico intracelular

By

Clara Lillian Oeste Villavieja

A thesis
in Biochemistry and Molecular Biology

Submitted to
Universidad Complutense de Madrid
in fulfillment of the requirements for the degree of

Doctor in Philosophy

Tutor
Mª Dolores Pérez-Sala Gozalo
Centro de Investigaciones Biológicas, CSIC

Madrid, 2015

"Satisfaction of one's curiosity is one of the greatest sources of happiness in life."

Linus Pauling

ACKNOWLEDGEMENTS

This work was supported by the "Formación de Personal Investigador" doctoral fellowship program (BES-2010-033718), including the "Estancias Breves" program (EEBB-I-12-04482), from MINECO within the framework of grants SAF2009-11642 and SAF2012-36519, and by RETIC RIRAAF from ISCIII (RD07/0064/0007 and RD12/0013/0008). Funding from the CSIC JAE-Intro program as well as the FEBS Summer Fellowship program is also acknowledged.

This work wouldn't have been possible without Dr. Pérez-Sala's kind and ceaseless support. Thank you for sharing your never-ending keenness for science, and for catalyzing my transition from theoretical science to hands-on research with such patience and enthusiasm, as well as a scientific thoroughness that I hope never to stray from.

I would also like to thank the constant help of Mª Jesús Carrasco. Muchas gracias por los buenos ratos y ánimos en todos estos años. I would especially like to thank all my colleagues at the lab for their help and warmth, particularly Irene, Ruth, Bea and Marta, and more recently Fran, whose unrelenting eagerness to help has filtered into this thesis unawares.

The help of many people at the Centro de Investigaciones Biológicas (CIB) has been crucial for this work, specifically that of Maite Seisdedos at the confocal imaging unit, and Dr. Blanca Pérez Maceda and Carmen Doñoro at the cell culture facility. Furthermore, I would like to thank collaborators here at the CIB, particularly Dr. Miguel A. Peñalva for the opportunity of exploring the stunning *Aspergillus nidulans* cell trafficking model, and Mario and Elena for their help in setting it up. Thanks to Dr. Patricia Boya for autophagy studies and Esther for experimental input.

It is essential to show my gratitude towards all who helped me during stays abroad, for both their mentoring and kind welcome. Thanks to Prof. Harald Stenmark and all the members of the lab at the Radium Hospital in Oslo, including Andreas, Viola, and especially Kay for help with super-resolution imaging. I would also like to thank Prof. Marja Jäättelä as well as Dr. Nikolaj H. T. Pedersen and all other colleagues at the Kræftens Bekæmpelse in Copenhagen.

The scientific curiosity that lead me on the path to research was initially awakened by Dr. Diana Wrigley de Basanta, whom I would like to thank for so brilliantly introducing the concept of cell biology in her classes in 9th grade. I am deeply indebted to many other teachers that have awakened my awareness on many subjects.

Muchísimas gracias a mi maravillosa familia (a mis tíos Antonio, Esther, Manuel, Mary Tere, etc. y todos mis primos) por su apoyo y alegría. Es una suerte teneros cerca porque vuestra compañía me llena de felicidad. Gracias especialmente a mi prima y mejor amiga Mayte por sus arengas y por las risas. También agradecer su apoyo a mis amigos, que siempre siguen ahí a pesar de mis negligencias o de la distancia.

Querría ante todo dar las gracias a mis padres. Gracias Ma por tu amor y dulzura incondicionales, y por transmitirme tu fortaleza mental para aprender a relativizar: es la lección más importante que he aprendido en la vida. Esta tesis es por y para ti. Thanks Dad, for your love and for keeping up your delightful and charming character, just like grandma Florence, regardless of your troubles. Gracias Sister, por ser mi role model desde pequeñas con tu inteligencia y esfuerzo, además de por tu cariño y apoyo, tan presentes aun en la distancia. Gracias también por tu empeño en compartir con nosotros la alegría de esa maravilla que es Sofía.

Finalmente, quería dar las gracias a la persona que más afectada se ha visto por el desarrollo de este trabajo, sin cuyo amor y comprensión hubiese sido casi irrealizable. Adrián, mi persona favorita, me haces más feliz cada día desde hace ya tantos años que el único agradecimiento posible es esforzarme en poder hacer lo mismo por ti siempre. *The light of my life and the beat of my heart.*

ABBREVIATIONS

15d-PGJ_2	15-deoxy-$\Delta^{12,14}$-Prostaglandin J_2
2-BP	2-bromopalmitate
AP	Heterotetrameric adaptor protein complexes
BAEC	Bovine aortic endothelial cell(s)
BLOC	Biogenesis of lysosome-related organelles complex
C-terminal	Carboxy-terminal
CD	Clusters of differentiation
CHS	Chediak-Higashi Syndrome
COX	Cyclooxygenase
cyPG	Cyclopentenone prostaglandin(s)
DBB	Dibromobimane
EGFR	Epidermal growth factor receptor
ER	Endoplasmic reticulum
ESCRT	Endosomal sorting complex required for transport
FT	Farnesyl transferase(s)
GAP	GTPase-activating protein(s)
GDI	GDP dissociation inhibitor(s)
GDP	Guanosine diphosphate
GEF	Guanine nucleotide exchange factor(s)
GGT	Geranylgeranyl transferase(s)
GPCR	G-protein coupled receptor(s)
GTP	Guanosine triphosphate
HPS	Hermansky-Pudlak Syndrome
Hrs	Hepatocyte growth factor-regulated tyrosine kinase substrate
ILV	Intraluminal vesicle(s)
KD	Knock-down
Lamp1	Lysosome-associated membrane protein 1
LBPA	Lysobisphosphatidic acid (a.k.a. BMP)
LRO	Lysosome-related organelle(s)

LTR	Lysotracker® Red
Lyst	Lysosomal trafficking regulator
M6P	Mannose 6-phosphate
MHC	Major histocompatibility complex
MVB	Multivesicular body/bodies
NF-κB	Nuclear factor kappa-light-chain-enhancer of activated B cells
NPC	Niemann-Pick type C disease
PAGE	Polyacrylamide gel electrophoresis
PAO	Phenylarsine oxide
PAT	Palmitoyl transferase(s)
PE	Phosphatidylethanolamine
PI(3)P	Phosphatidylinositol 3-phosphate
PS	Phosphatidylserine
Rab	Ras-related in brain
Ras	Rat sarcoma
Rep	Rab escort protein
Rho	Ras homolog
SDS	Sodium dodecyl sulfate
SIM	Structured illumination microscopy
TEM	Tetraspanin-enriched microdomain(s)
Tsg101	Tumor susceptibility gene 101
WB	Western blot(s)
ZGA	Zaragozic acid

Other abbreviations not shown here follow IUPAC nomenclature.

TABLE OF CONTENTS

LIST OF FIGURES

LIST OF TABLES

INTRODUCTION

1. Small GTPase proteins

The Rat sarcoma (Ras) superfamily of small GTPases is made up of a plethora of 20 to 40 kDa proteins that share the ability to bind to a GTP nucleotide and hydrolyze it to GDP, which determines their activation state. The Ras, Rho, Rab, Arf and Ran protein families represent the majority of proteins in this family (Figure 1), which share some similar domains but also contain specific structural determinants that endow each protein with unique conformational and signaling characteristics, as reviewed in (Takai et al., 2001). This superfamily is named after the first small GTPases that were studied: the Ras proteins (Barbacid, 1987). Some of the first oncogenes identified are part of this family and play crucial roles in cell survival, proliferation and signaling, as reviewed in (Ridley, 2001; Schmitz et al., 2000).

The Rho protein family was identified as containing sequences homologous to Ras (**R**as **ho**molog) and includes three Rho isoforms (RhoA, B and C), three Rac isoforms (Rac1, 2 and 3) as well as Cdc42, among others (Bustelo et al., 2007; Madaule and Axel, 1985). Rho proteins regulate cytoskeletal functions such as actin stress fiber induction (RhoA) or lamellipodia and filopodia formation (Rac and Cdc42, respectively), as reviewed in (Hall, 2005; Matozaki et al., 2000). Another member, RhoB, is known to induce stress fibers but also plays a role in vesicular transport (Aspenström et al., 2004; Gampel et al., 1999), as will be discussed below in detail. The Rab GTPases (**Ra**s-related in **b**rain) comprise the largest of the Ras families, with more than 60 isoforms identified in humans (Touchot et al., 1987). They are responsible for membrane trafficking processes including endocytosis, exocytosis, transcytosis, and general vesicle maturation, as reviewed in (Stenmark, 2009).

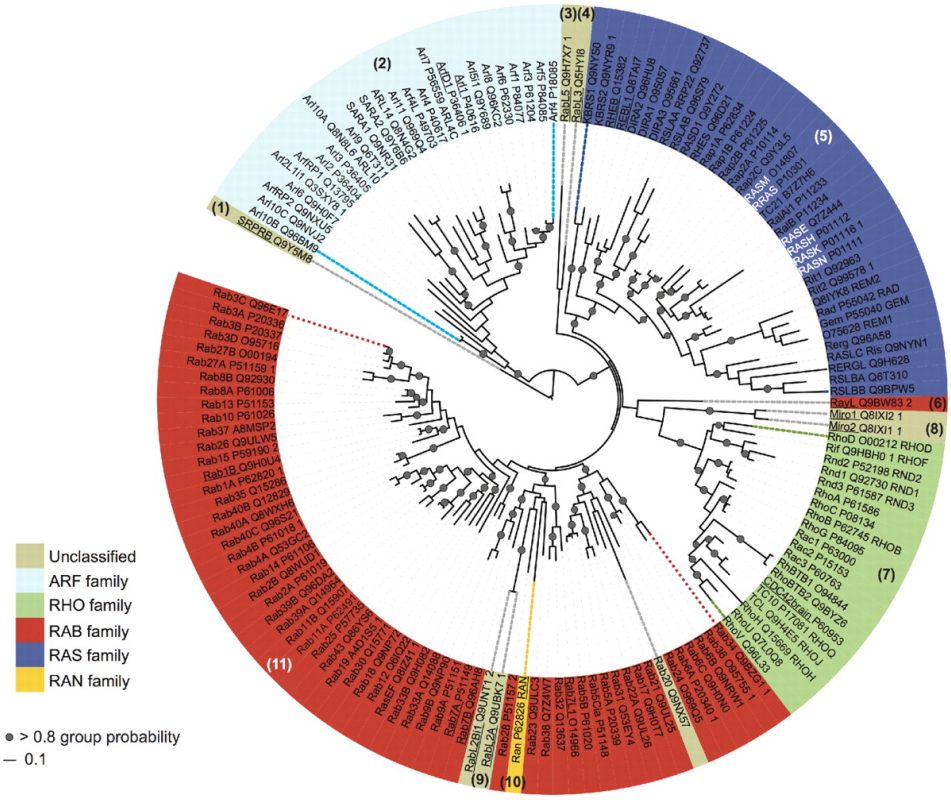

Figure 1. Human Ras superfamily phylogenetic tree.

Representation of the different Ras families from a phylogenetic standpoint, as represented by the tree inside the circle. The major Ras groups are shown in different colors, i.e. blue for the Ras family, green for Rho, red for Rab, cyan for Arf, and yellow for Ran. ©Rojas et al., 2012. Originally published in The Journal of Cell Biology. doi: 10.1083/jcb.201103008. (Rojas et al., 2012)

Small GTPases act as molecular switches, transitioning between a GDP-bound, inactive state and a GTP-bound, active state, as depicted in Figure 2. Their activation is mediated by varied stimuli, which can initiate signaling cascades affecting guanine nucleotide exchange factors (GEF), which favor GTP incorporation, as reviewed in (Geyer and Wittinghofer, 1997). Active states of small GTPases arise from conformational changes that allow these proteins to bind to effectors and hence propagate signals intracellularly. Considering that the intrinsic GTPase activity of these proteins is rather low, they require GTPase activating proteins (GAP) to effectively hydrolyze GTP to GDP, returning to their inactive state. A further level of regulation involves specific GDP dissociation inhibitors (GDI), which bind to inactive Ras superfamily proteins to detach them from membranes, thus retaining them in the cytosol (Figure 2).

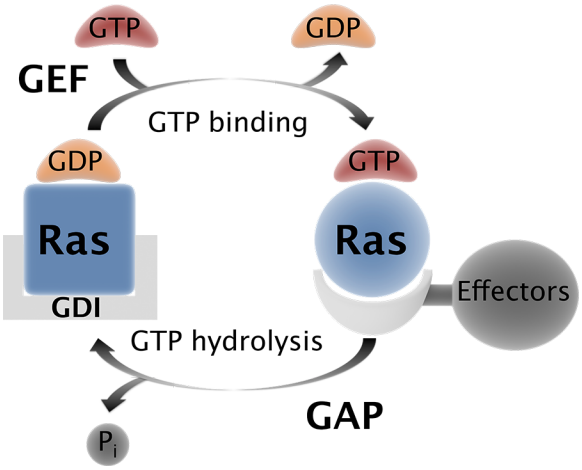

Figure 2. Small GTPase GDP/GTP cycle.

The inactive form of the Ras superfamily protein (square Ras) is bound to GDP. For some GTPases, binding to RhoGDI stabilizes this inactive form. Small GTPase binding to GTP is facilitated by GEF and allows interaction with effectors to induce signal transduction (circular Ras). Enzymatic hydrolysis of GTP for GDP is stimulated by GAP and leads to GTPase inactivation, terminating its effector binding and activation.

GEF, GAP and GDI proteins are inherent to the process of Ras protein regulation, so that each subfamily is modulated by a specific subset of activators, inhibitors or overall modulators, each with their feedback or feed-forward regulation. Thus, this complex network of Ras protein-related effectors generates fine-tuned signaling cascades within the cell, as reviewed extensively in (Cherfils and Zeghouf, 2013). It is therefore evident that small GTPases entail tight regulatory mechanisms to correctly carry out their intracellular functions (Matozaki et al., 2000).

1.1 Endolysosomal GTPases

Numerous members of the Ras superfamily appear at endolysosomal compartments, particularly Rab proteins, as well as the Ras proteins Rap2A, Rap2B, and H-Ras, or the Rho proteins TC10 and RhoB (Valero et al., 2010), as will be described throughout this work. Specific members of the Rab protein family associate at defined vesicles along the endocytic pathway and assist in the maturation of these membrane compartments by mediating vesicle budding, fusion, motility, coating and uncoating, which endows endomembranes with an extremely dynamic quality (Stenmark, 2009). The core endosomal Rabs may be laterally segregated into specific domains of the same

vesicles, which allows for a flexible flow of compartments within the cell. Except in the case of Ran proteins, which contain a nuclear import signal, lipids modify proteins belonging to the Ras superfamily posttranslationally in order to associate with membranes. The combination of these lipid anchors and other structural determinants gives rise to subcellular localizations at specific membrane compartments, as discussed below for RhoB in greater detail.

1.2 RhoB

RhoB is located on the cytoplasmic side of the plasma membrane and late endosomes, from which it plays important roles in trafficking of signaling molecules (Gampel et al., 1999). It is a short-lived protein with a half-life of approximately 2-3 hours, which differs from the relative stability of other Rho proteins (24-hour half-lives) (Engel et al., 1998; Stamatakis et al., 2002). RhoB is an immediate early response gene that is rapidly induced by DNA damage or growth factors (Fritz and Kaina, 1997; Malcolm et al., 2003). Therefore, maintaining a high RhoB turnover ensures the rapid response of RhoB levels to various stimuli. Though *in vitro* studies have shown similar effectors for RhoA and RhoB, cellular approaches have shown that each has its own set of interactors to carry out specific functions. As summarized in Figure 3, RhoB presents unique functions that set it apart from other Rho proteins by controlling endocytic traffic and affecting the sorting of growth factor receptors or signaling kinases (Fernández-Borja et al., 2005; Huang et al., 2007b; Mellor et al., 1998; Sandilands et al., 2004; Wherlock et al., 2004). Hence, there are associated consequences for growth factor signaling, cell survival, proliferation, and apoptosis, which contribute to the proposed dual role of RhoB as both a tumor suppressor and an angiogenesis inducer (Gerald et al., 2013; Huang et al., 2006; Liu et al., 2001). RhoB is involved in modulating cell death through genotoxic stress (Fritz and Kaina, 2000; Liu et al., 2001) and controlling c-myc stability (Huang et al., 2006), as well as signaling and trafficking of Akt kinase (Adini et al., 2003). Furthermore, RhoB could play a role in apoptosis following Ras inhibition (Kamasani et al., 2004; Liu et al., 2001). RhoB has also been shown to mediate actin dynamics upstream of Dia1 (Diaphanous-related formin 1), which is necessary for actin coat formation around endosomes (Fernández-Borja et al., 2005). Additionally, reduced

cell spreading and adhesion to different substrates was noted in several RhoB-depleted cell types, which could be due to the concomitant reduction of surface β1 integrin levels in these cells and accountable for decreased focal adhesions, resulting in increased migration rates (Vega et al., 2012).

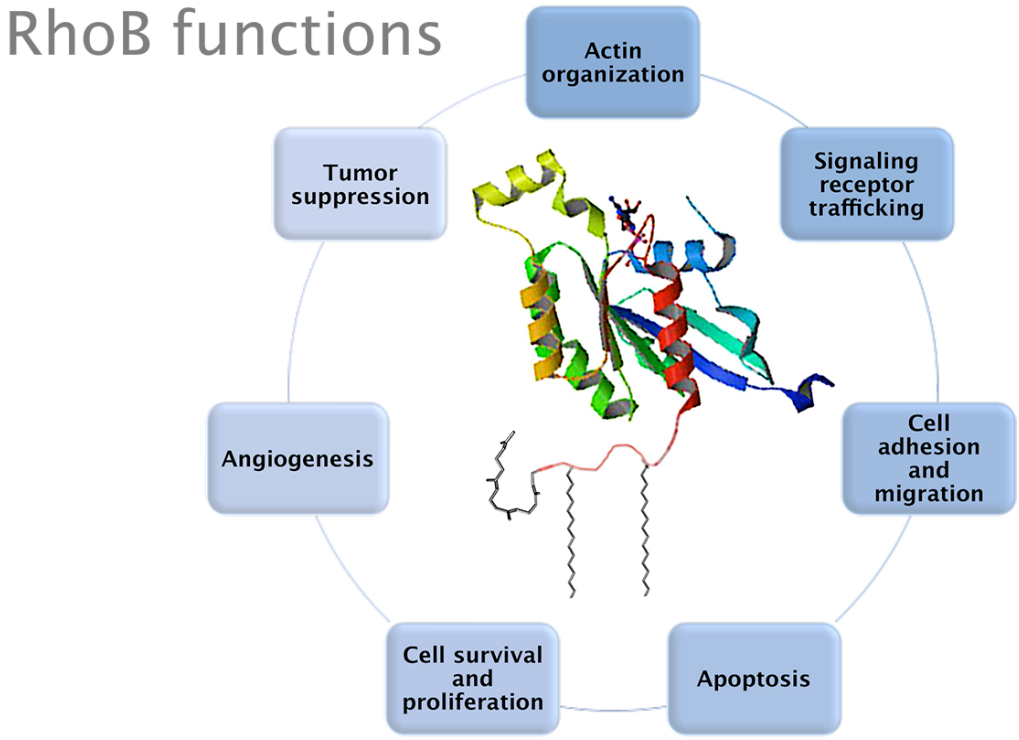

Figure 3. Schematic of RhoB functions.

A ribbon diagram of the RhoB structure attached to an isoprenoid moiety (curved, gray chain) and two palmitates (straight chains) is shown in the center. The small GTP-binding protein RhoB performs specific tasks within the cell that set it apart from other proteins of the Ras superfamily, including roles in cancer progression related to angiogenesis or apoptosis, regulating receptor trafficking or actin polymerization at endosomes, and cell migration. See text for details.

RhoB is highly homologous to RhoA in structural terms, though under resting conditions, RhoGDI retains RhoA in the cytosol (Dransart et al., 2005) whereas RhoB is bound to the plasma membrane or endolysosomal membranes (Oeste et al., 2014; Pérez-Sala et al., 2009; Stamatakis et al., 2002). These differences in localization are related to the distinct residues present at the carboxy-terminal (C-terminal) hypervariable region (Chiu et al., 2002; Gorfe et al., 2007), which contains the –CAAX box and could bear phosphorylation sites as well as sites for additional lipidation (Hancock et al., 1989; Wennerberg and Der, 2004), as will be described in detail below.

In the case of RhoB, upon isoprenylation of its –CAAX box cysteine (C193), two nearby cysteines (C189 and C192) are further modified by palmitate moieties (Wang and Sebti, 2005), whereas RhoA fosters a polybasic sequence.

RhoB therefore presents several distinguishing features that endow it with unique cellular behavior. The specific lipidation sequence at its C-terminus acts as a plasma membrane and endolysosomal anchor. Furthermore, these lipid modifications determine RhoB degradation through a lysosomal pathway distinct from the proteasomal degradation typical of other GTPases of its family (Pérez-Sala et al., 2009; Stamatakis et al., 2002).

2. Posttranslational modifications of GTPases

Posttranslational modifications constitute an essential regulatory mechanism for protein function, activation, localization and half-life. Most of these changes result in conformational shifts that alter activation states, allow modified proteins to interact with effectors or expose otherwise hidden motifs within their sequence. Common posttranslational modifications include processes such as phosphorylation, hydroxylation and nitrosylation (inorganic residue addition), ubiquitination and glutathionylation (peptide addition), or isoprenylation, myristoylation and palmitoylation (lipid addition), among many others, as reviewed in (Walsh et al., 2005). The resulting functional outcomes range from marking proteins to be degraded, as in ubiquitination, to direct activation for effector interaction, i.e. phosphorylation.

Ras superfamily proteins undergo several posttranslational modifications, including irreversible alteration of their carboxy-terminal sequence by isoprenylation and proteolysis, as well as methylation and further lipidation by palmitate moieties in some instances. Other residues within these proteins can undergo other modifications such as peptidyl-prolyl isomerization, phosphorylation, ubiquitination, glycosylation,

nitrosylation, and ADP ribosylation, as reviewed in (Ahearn et al., 2012). As will be discussed below, some of these modifications alter Ras protein localization, in turn determining the effectors with which they can interact and ultimately their activation patterns.

2.1 Lipidation at C-terminal ends

Lipidation involves covalent attachment of lipids to protein residues and can take place spontaneously or through enzymatic mechanisms. Isoprenylation and myristoylation are irreversible enzymatic modifications that significantly increase protein hydrophobicity, thus elevating the probability of their interaction with membranes. Whereas myristoylation takes place at a glycine residue located in the first position of the protein sequence (after methionine removal), isoprenylation occurs at cysteines in the C-terminal segment. Palmitoylation usually takes place at cysteines that are in the vicinity of isoprenylated or myristoylated residues and confers a more flexible, reversible mode of regulation of protein localization, as reviewed in (Aicart-Ramos et al., 2011). Several Ras proteins become palmitoylated following isoprenylation to better anchor them to membranes, as will be discussed below in further detail. Protein modification by lipids is therefore a crucial tool to modulate subcellular localization and hence site-specific activation and recruitment of proteins, affecting a myriad of signaling platforms.

2.1.1 Isoprenylation

Isoprenylation is an enzymatic process affecting more than 300 proteins in humans by which isoprenoid lipids bind to cysteines through a thio-ether bond, as reviewed in (McTaggart, 2006). Specific prenyl transferases recognize particular sequences to catalyze farnesylation, in the case of farnesyl transferase (FT) or geranylgeranylation, in the case of geranylgeranyl transferases (GGT) I and II. Many Ras proteins contain a "-CAAX box" at their C-terminus, where "C" is the cysteine amenable to isoprenylation, "A" stands for aliphatic residues and "X" can be any amino

acid (Hancock et al., 1989). As depicted in Figure 4, -CAAX boxes undergo modifications including isoprenylation, proteolysis and methylation.

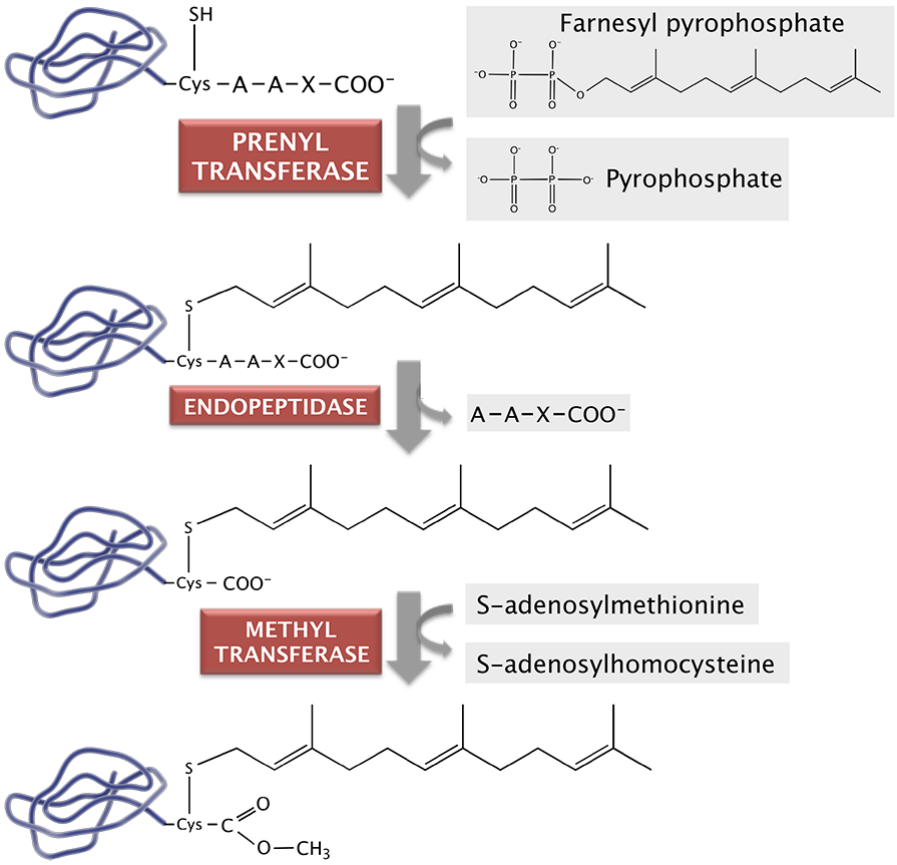

Figure 4. Protein isoprenylation and CAAX box processing.

Proteins containing a CAAX box undergo posttranslational processing, beginning with isoprenylation by prenyl transferases. An endopeptidase cleaves the last three amino acids (-AAX), and methylation of the C-terminal end is brought about by a methyl transferase. Shown here is farnesyl pyrophosphate (C15), though some proteins become geranylgeranylated by GGT using a geranylgeranyl pyrophosphate moiety (C20) as a substrate. See text for details.

In the case of FT- and GGT I-mediated isoprenylation, the X residue in –CAAX boxes of target proteins determines whether the cysteine will be modified by a farnesyl or geranylgeranyl isoprenoid. FT modifies proteins in which the X residue is methionine, serine, alanine or glutamine, whereas GGT I acts on proteins bearing a leucine residue. However, certain proteins can be modified by either FT or GGT I depending on other biochemical features of the –CAAX box surroundings (Hartman et al., 2005) or on isoprenoid availability (Whyte et al., 1997). FT and GGT-I share an α subunit and possess specific β subunits that recognize CAAX motifs and transfer either

farnesyl pyrophosphate or geranylgeranyl pyrophosphate, respectively. In contrast, GGT II requires an accessory protein, Rab escort protein (Rep) that recognizes whole Rab proteins and presents them to the catalytic subunit (Nguyen et al., 2010). GGT II is responsible for single or double geranylgeranylation of Rab proteins at their C-terminal –CAC, -CC, -CCX, -CCXX, -CCXXX or –CXXX motif cysteines (Desnoyers et al., 1996; Leung et al., 2006; Maurer-Stroh et al., 2003). Once isoprenylation has taken place, the amino acids that remain at the carboxy end of the isoprenylated cysteine are cleaved by a specific endoprotease and the carboxyl group of the cysteine is methylated by a specific methyltransferase for isoprenylated proteins (Pérez-Sala et al., 1991; Sinensky, 2000; Tan et al., 1991).

2.1.2 Palmitoylation

Palmitoylation is the addition of a palmitate moiety (C16:0) to a cysteine residue through a thioester bond, as reviewed in (Dietrich and Ungermann, 2004). As shown in Figure 5, the cysteine sulfhydryl group needs to be in its thiolate form, i.e. unprotonated, in order to carry out a nucleophilic attack on the α carbon of palmitoyl-CoA. This reaction can occur spontaneously depending on the cysteine pK_a, which is determined by the intra- and intermolecular surroundings, but is greatly enhanced when catalyzed by palmitoyl transferases (PAT), a.k.a. protein acyl transferases, which contain a conserved aspartate-histidine-histidine-cysteine (DHHC) active site rich in cysteine residues, as reviewed in (Aicart-Ramos et al., 2011). These enzymes and the substrate palmitoyl-CoA are present on membranes, so that proteins that are to be palmitoylated need to come in close contact with PAT-containing membranes (Dunphy et al., 1996). Isoprenylation increases the probability of a protein to bind to membranes, and palmitoylation presents a further structural determinant that stabilizes membrane association, as reviewed in (Smotrys and Linder, 2004; Smotrys et al., 2005). Depalmitoylation is mediated by palmitoyl-protein thioesterases (Verkruyse and Hofmann, 1996), allowing proteins to undergo repeated cycles of palmitoylation/depalmitoylation (Aicart-Ramos et al., 2011).

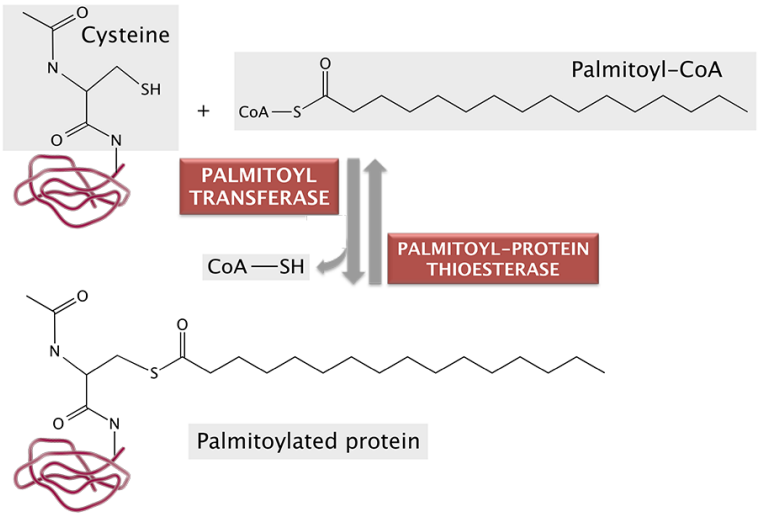

Figure 5. Protein palmitoylation.

In red, a random protein structure with its palmitoylation cysteine depicted chemically. The cysteine thiolate group produces a nucleophilic attack on the electrophilic carbon on the palmitoyl-CoA chain to yield a palmitoylated protein and free CoA. This reaction can take place spontaneously or be catalyzed by palmitoyl transferases. Depalmitoylation is catalyzed by palmitoyl-protein thioesterases. Adapted from (www.lipidlibrary.aocs.org).

Many protein families provide examples of palmitoylation-mediated membrane association. Such is the case of a multitude of integral membrane proteins such as heterotrimeric G-proteins, tetraspanins, the mannose 6-phosphate (M6P) receptor, or synaptotagmins, all involved in general endocytic trafficking processes (Schweizer et al., 1996; Stipp et al., 2003; Veit et al., 1996). These proteins, though already spanning the membrane, are able to associate at specific microdomains such as lipid rafts and hence form signaling platforms, as is the case for transmembrane adaptor proteins, e.g. LAT (Linker of Activation for T cells) (Stepanek et al., 2014). Furthermore, membrane anchors of peripheral membrane proteins often consist in palmitoylation either close to myristoylated residues, as for Src tyrosine kinases, or in the vicinity of previously isoprenylated cysteines, as is the case for the Ras protein superfamily (Aicart-Ramos et al., 2011), and is described as follows.

Within the Ras family of proteins, H-Ras is palmitoylated at two cysteine residues present in the hypervariable domain (C181 and C184), N-Ras contains a single palmitoylation site (C181) and K-Ras4B possesses no cysteine residues but its interaction with cellular membranes is favored by the presence of a polybasic domain that is attracted to negatively charged polar head groups of membrane phospholipids, much like RhoA. In the case of H-Ras, localization is mainly at the plasma membrane

and various intracellular structures, including the endoplasmic reticulum (ER), the Golgi complex, recycling endosomes (Gómez and Daniotti, 2005; Hancock and Parton, 2005) and to randomly moving nanoparticles known as rasosomes (Rotblat et al., 2006). These differences are critical to determine the specific trafficking and site of action of the different Ras proteins, as reviewed in (Omerovic et al., 2007; Pérez-Sala, 2007). Other proteins that also contain additional cysteines close to the isoprenylation site that are amenable to palmitoylation include TC10, Rap2, or RhoB (Aicart-Ramos et al., 2011; Michaelson et al., 2001; Uechi et al., 2009). TC10 has been detected at the plasma and perinuclear membranes, identified as components of secretory or endosomal compartments (Michaelson et al., 2001; Watson et al., 2003), whereas Rap2 has been detected in secretory granules (Mollinedo et al., 1993) and recycling endosomes (Uechi et al., 2009). Fully lipidated RhoB is both isoprenylated and bipalmitoylated (Wang and Sebti, 2005), which is required for its association with endolysosomes (Pérez-Sala et al., 2009).

2.2 Cyclopentenone prostaglandins

In addition to lipidation by isoprenoid or palmitate moieties, proteins may suffer modification by reactive lipid species of varied structure. Cell metabolism under both basal and pathological conditions gives rise to products derived from lipid peroxidation that can form stable adducts with particular protein residues (Bogatcheva et al., 2005). Oxidative and nitrosative stress produce many of these products, which play a role in numerous pathologies such as neurodegenerative diseases (Dianzani, 2003), vascular alterations (Lee and Park, 2013), and cancer (Garzón et al., 2011). Amongst the many electrophilic lipids that are produced in cells, cyclopentenone prostaglandins (cyPG) are a family of reactive lipid species with anti-inflammatory, anti-viral and anti-tumoral effects, which makes them a forthcoming option as exogenous therapeutic compounds (Sánchez-Gómez et al., 2004; Straus and Glass, 2001). cyPG generation is increased in cells undergoing oxidative stress, whereas cyPG production in homeostatic cells is low (Ceaser et al., 2004; Koenitzer and Freeman, 2010). The electrophilic nature of cyPG allows them to react with nucleophilic residues including cysteines, in turn eliciting

structural changes within the whole protein that provide new reactivity and electrophilicity. cyPG of different structural characteristics present specificity towards particular cysteine residues, so that different cyPG enter distinctive intramolecular binding pockets even within the same protein. Moreover, cyPG bind to proteins involved in a multitude of different cellular tasks (Garzón et al., 2011; Renedo et al., 2007). These features account for dual actions: cyPG modification of proteins involved in redox regulation can modulate oxidative stress pathways, whereas binding and subsequent inhibition of NF-κB (nuclear factor kappa-light-chain-enhancer of activated B cells) pathway proteins contributes to cyPG anti-inflammatory effects (Díez-Dacal and Pérez-Sala, 2010; Kim and Surh, 2006). The pleiotropic behavior of these electrophilic lipids is therefore a reflection of the variety of intracellular targets, many of which have been discovered in the past decade through proteomic studies, as reviewed in (Garzón et al., 2011; Oeste and Pérez-Sala, 2014). Interestingly, Ras proteins are included in this expanding list of cyPG targets (Oeste et al., 2011; Stamatakis and Pérez-Sala, 2006), as discussed below in further detail.

As shown in Figure 6, cyPG are derived from peroxidation of membrane fatty acids, in particular arachidonic acid, through the action of cyclooxygenases (COX) or non-enzymatically through the isoprostane pathway (Funk, 2001; Gao et al., 2003). In the case of the COX pathway, prostaglandin synthases act on the precursor PGH_2 to give rise to PGD_2 and PGE_2 (Funk, 2001). The latter two PG can also be formed by non-enzymatic epimerization of isoprostanes through the isoprostane pathway (Gao et al., 2003), which gives rise to *trans* isomers of PG, i.e. isoprostanes such as iso-PGJ_2 and iso-PGA_2. J series cyPG arise from dehydration of PGD_2 to PGJ_2, which can be further dehydrated to form 15d-PGJ_2 (15-deoxy-$\Delta^{12,14}$-Prostaglandin J_2) or give rise to Δ^{12}-PGJ_2 through an albumin-dependent mechanism (Narumiya and Fukushima, 1985; Shibata et al., 2002). cyPG of the A series are produced upon dehydration of PGE_1 or PGE_2 (Ohno et al., 1986).

cyPG synthesized in this manner contain an α, β-unsaturated carbonyl group within their cyclopentane ring, which renders highly electrophilic -β carbons. Therefore, they are amenable to forming Michael adducts through nucleophilic attack by thiol moieties from cysteines, as seen at the bottom of Figure 6. The cysteine residues to which cyPG bind present structural characteristics allowing for the entry and

positioning of specific cyPG to form the stable, covalent Michael adducts with consequences on biological functions.

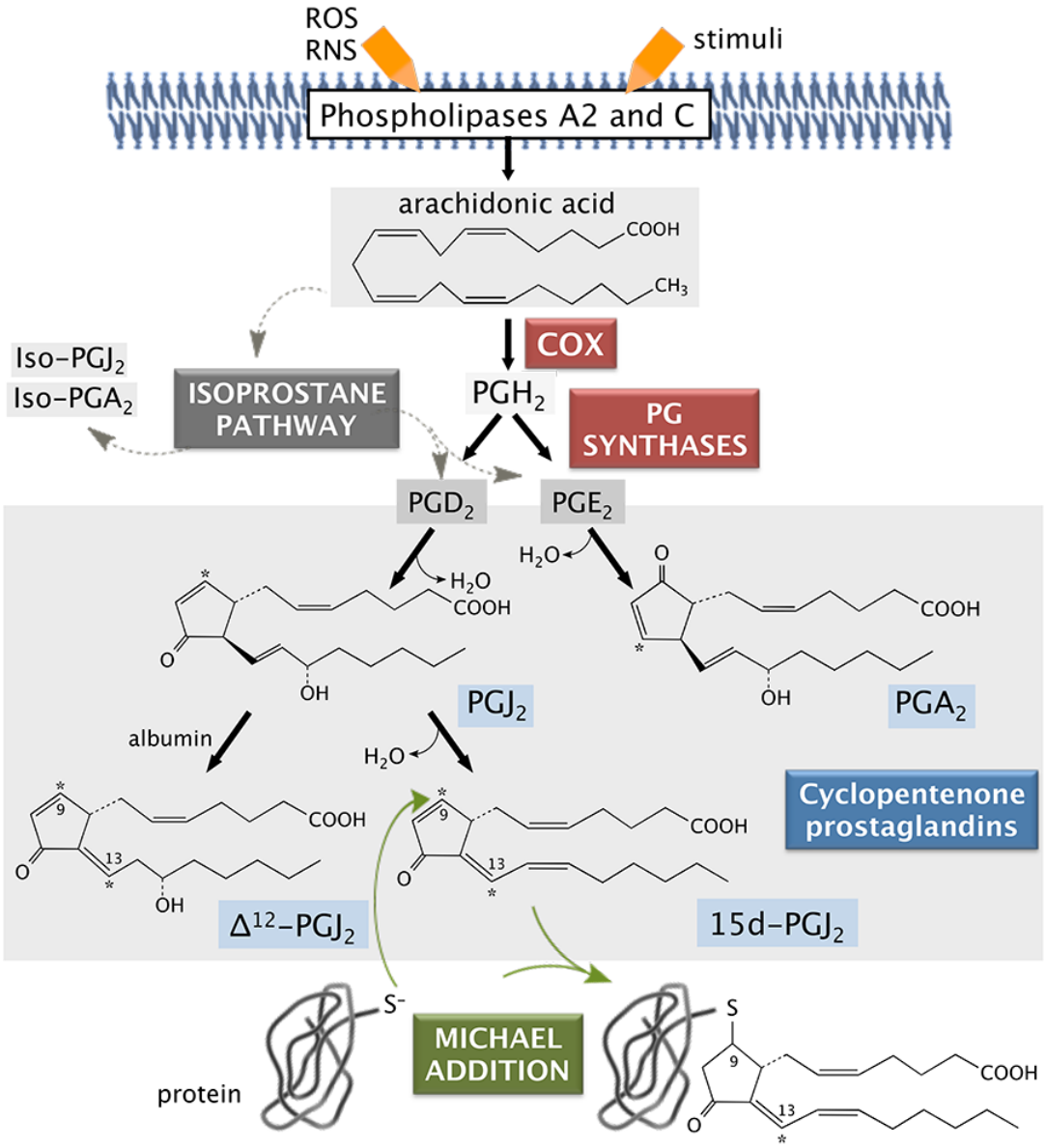

Figure 6. Cyclopentenone prostaglandin formation and covalent binding to proteins through Michael addition.

cyPG (blue shaded boxes) are formed by spontaneous dehydration of their PG precursors (gray shaded boxes). These precursors are generated in turn from unsaturated fatty acids such as arachidonic acid by the action of cyclooxygenases (COX) or through non-enzymatic processes, i.e. the isoprostane pathway (dashed arrows). Arachidonic acid is formed as a product of phospholipase A2 or C cleavage of membrane-bound phospholipids. cyPG contain electrophilic carbons (asterisks) that can undergo attack by nucleophilic groups such as cysteine thiolates and form Michael adducts (green arrows), as shown at the bottom for 15d-PGJ_2. See text for details.

2.2.1 Cyclopentenone prostaglandin modification of Ras proteins

cyPG containing either one or two electrophilic carbons, i.e. single enones or dienones, can bind to different subsets of proteins depending on the steric attributes of the cysteines in the protein to be modified. Several studies have shown that the dienone cyPG 15d-PGJ_2 can establish Michael adducts with cysteine residues of proteins as structurally and functionally different as actin, vimentin (Stamatakis et al., 2006), NF-κB, PPARγ (Peroxisome proliferator-activated receptor gamma) (Cernuda-Morollón et al., 2001; Shiraki et al., 2005), Keap1 or GSTP1-1 (Glutathione S-transferase P) (Levonen et al., 2004; Sánchez-Gómez et al., 2007). The fact that electrophilic carbon count is particularly important for selectivity is reflected by cyPG binding to Ras proteins. Various cyPG have been found to modify and activate Ras proteins in an isoform- and site-selective manner (Oliva et al., 2003). Specifically, single enone cyPG, e.g. PGA_1 or PGJ_2 bind preferentially to C118, which is present in the GTP binding site in all three Ras proteins, namely H-Ras, K-Ras and N-Ras. However, the dienone 15d-PGJ_2 can bind two cysteine residues simultaneously (C181 and C184), located at the H-Ras C-terminus (Renedo et al., 2007). Since other Ras proteins such as N- or K-Ras do not contain this sequence, they are not preferential targets for dienone cyPG binding. Interestingly, modification of the H-Ras C-terminal sequence by cyPG or other small reactive molecules elicits changes in its membrane partitioning and distribution along the endocytic pathway (Oeste et al., 2011). It is thus apparent that cyPG selectivity can fine-tune intracellular pathways by modifying not only specific proteins, but also particular cysteine residues within the same protein, which can have consequences on its subcellular sorting and localization.

3. Endolysosomal sorting and degradation

Endocytosis is the means by which cells internalize extracellular material as well as plasma membrane proteins and lipids, among many other substances. As summarized in Figure 7, this material is engulfed by plasma membrane and pinched off to produce endocytic vesicles, which undergo multiple maturation processes on their way towards lysosomes, recycling compartments, autophagosomes, or other intracellular destinations. Trafficking of these endocytic vesicles involves signaling through membrane receptors from the outside-in and recycling these components for further receptor-effector cascades or producing metabolic building blocks, hence contributing to overall cell functions, as reviewed in (Huotari and Helenius, 2011). During their maturation process, these vesicles evolve through dynamic interaction of non-discrete compartments that are in constant flow from one to another. However, distinct proteins and lipids attach to vesicles at different points in the endocytic route, aiding in their categorization into specific types of endosomes. Interestingly, accumulating evidence points at site-selective signaling within the cell, for certain signaling molecules bind to different effectors depending on their subcellular localization (Schmidt-Glenewinkel et al., 2008), and some signaling processes require previous endocytosis of their components to regulate the specificity, duration and magnitude of the signal, as reviewed in (Sadowski et al., 2009). The components that attach to vesicles during their internalization will hence define their ultimate subcellular destination and function, such as traveling back to the plasma membrane for recycling or inclusion into multivesicular bodies (MVB) for secretion or degradation (Huotari and Helenius, 2011; Platta and Stenmark, 2011).

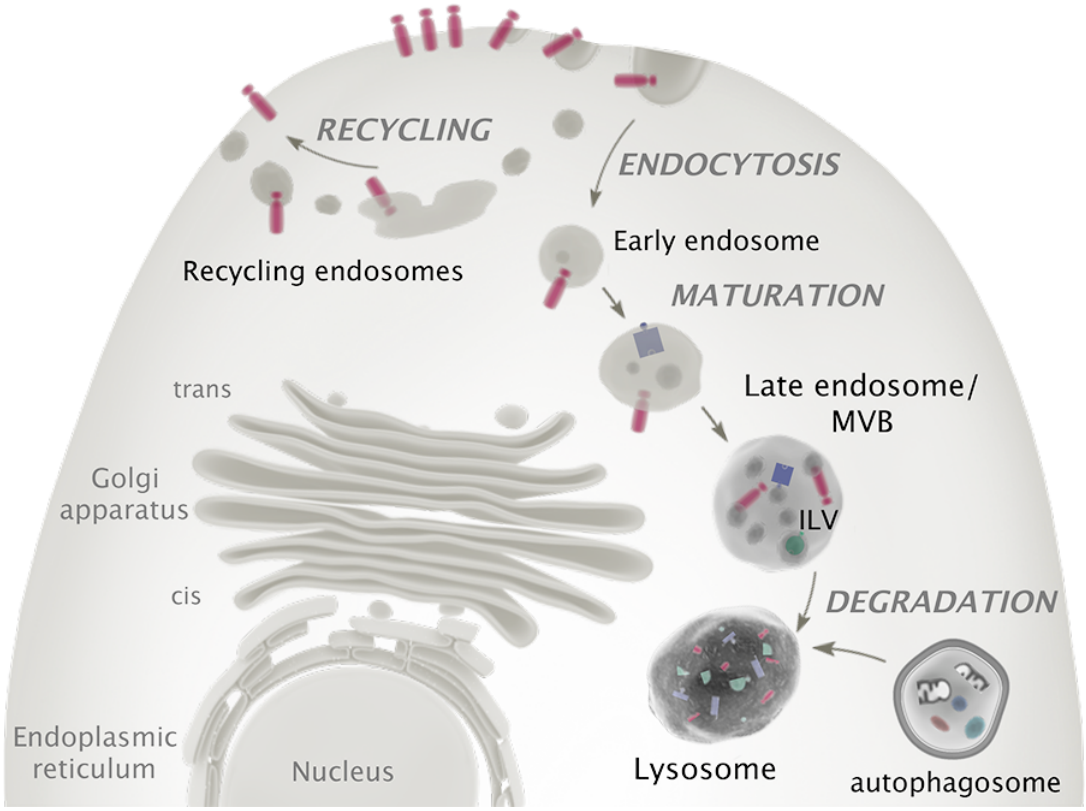

Figure 7. The endocytic pathway.

Cellular components residing at the plasma membrane such as signaling receptors (red rods) are internalized along with extracellular material during endocytosis. The vesicles that pinch off can be sent along recycling endosomes back to the plasma membrane in a process that recycles receptors for a new round of outside-in signaling at the cell surface. Alternatively, endocytic vesicles undergo a series of maturation steps from early endosomes to late endosomes/MVB, including membrane invagination to form intraluminal vesicles (ILV). Fusion with lysosomes elicits macromolecule degradation by specific enzymes working at low pH levels within these compartments, resulting in receptor down-regulation and signaling termination. Autophagosomes containing damaged organelles and cellular material for degradation also fuse to lysosomes to produce simpler components that can be reused by the cell. See text for details.

Degradation of endocytosed material implies macromolecule breakdown into its constituent parts, e.g. proteins into amino acids to use in protein synthesis. It is therefore essential for cells to be endowed with several degradation machineries. The first protein-specific degradation mechanism described within the cell was the proteasome, which is a cytosolic protease that degrades misfolded and short-lived regulatory proteins in the cytoplasm (Schwartz and Ciechanover, 2009). Proteins that are destined towards this degradation machinery are modified by several ubiquitin moieties forming a chain that is recognized by the proteasome. Ubiquitination can also mark proteins for other subcellular outcomes and is a complex, target-specific process

involving several enzymes (Sadowski et al., 2012). In the case of transmembrane proteins, a single ubiquitin molecule marks them for degradation, though this process must necessarily occur *via* vesicular transport, in particular through endosomes to the lysosome or vacuole, where degradation takes place. Lysosomes are acidic organelles containing hydrolytic enzymes and are at the crossroads of several degradation processes, for they degrade proteins with long half-lives arriving in endosomes or aid in clearing away larger elements packaged in phagosomes or autophagosomes (de Duve, 1969; Fader and Colombo, 2009; Saftig and Klumperman, 2009). It is indeed vital for cell homeostasis to tightly coordinate the complex processes encompassing vesicular biogenesis, membrane trafficking and the degradation of cellular components by means of precise macromolecular machineries.

3.1 Protein machineries involved in sorting

Intense research in the past decades on the proteins involved in endosomal sorting has uncovered a plethora of interaction networks and transport systems to shuttle cargo to and fro within the cell, as reviewed in (Bishop, 2003). Vesicle biogenesis is a topologically complicated process in which the membrane must curve forcefully and still accommodate transmembrane or peripheral membrane proteins and their effectors (McMahon and Gallop, 2005). Proteins responsible for inducing curvature, coating of developing omegas and membrane scission at the plasma membrane are key players in the initial steps of vesicle generation (Stachowiak et al., 2013). However, once endosomes are formed, their destination is tightly regulated by other sets of proteins such as Rab proteins that assemble onto the newly formed vesicles and help in their uncoating, trafficking (i.e. along microtubules), tethering, and fusion with one another (Stenmark, 2009). Furthermore, extensive maturation gives rise to vesicles that suffer internal processes of their own, such as the production of intraluminal vesicles (ILV) from the membrane of MVB mediated by the ESCRT (endosomal sorting complex required for transport) protein machinery (Raiborg and Stenmark, 2009) or acquisition of acidic pH values. The relatively recent discoveries of tethering protein complexes, namely, HOPS (homotypic fusion and vacuole protein sorting complex) (Seals et al., 2000) and CORVET (class C core vacuole/endosome tethering complex) (Peplowska et

al., 2007) unveil the role of these multi-protein machineries in homotypic fusion of endocytic compartments prior to SNARE (Soluble NSF (*N*-ethylmaleimide-sensitive factor) Attachment Protein Receptor) participation, as reviewed extensively in (Solinger and Spang, 2013). Furthermore, anterograde transport from the Golgi to late endosomes or lysosomes and vacuoles is mediated by carboxypeptidase Y and AP-3 (heterotetrameric adaptor protein complex 3) pathways, whereas retromer governs retrograde trafficking within these compartments with the help of other proteins such as sorting nexins (Cullen and Korswagen, 2012; Epp et al., 2011). However, these complexes are beyond the scope of this dissertation, in which attention will be focused on the Rab and ESCRT protein machineries involved in endolysosomal trafficking and MVB biogenesis, to contextualize the localization of the endosomal GTPases under study.

3.1.1 Rab proteins

As described above and seen in Figure 1, Rab proteins constitute the largest of the Ras subfamilies. Membrane tethering is determined by their two C-terminal geranylgeranyl moieties and the immediate upstream protein sequence (Chavrier et al., 1991), as well as binding to specific GDI or GDI recycling factors (Dirac-Svejstrup et al., 1997; Ullrich et al., 1994; Ullrich et al., 1993). The multitude of Rab proteins contained in human cells and the processes in which they are involved are reflected in Table 1.

Rab functions that are basic to cell homeostasis include trafficking between the ER, plasma membrane or endosomes and the Golgi apparatus, as well as intra-Golgi trafficking. Distinct Rab proteins also mediate early and late endosome biogenesis, maturation and fusion with lysosomes, as shown in Table 1. Endocytic recycling, exocytosis or phagosome dynamics also involve members of this protein family. Furthermore, Rab proteins also mediate other more specific, cell-type dependent transport mechanisms, such as melanosome biogenesis and transport, ciliogenesis, or tight junction assembly in epithelial cells (Stenmark, 2009). Many of these Rab proteins mediate trafficking steps, which are controlled by feedback mechanisms involving their effectors: sorting adaptors, motor adaptors for vesicle transport on actin or tubulin,

tethering factors or simply their respective GAP, GDI or GEF. These interactions are at the core of Rab protein involvement in vesicle budding, motility or fusion (Stenmark, 2009).

Rab GTPases	Function
Rab1	ER–Golgi trafficking
Rab2	Golgi–ER trafficking
Rab6, Rab33, Rab40	Intra–Golgi trafficking
Rab8	Golgi–Plasma membrane trafficking
Rab22	Golgi–early endosome transport, both directions
Rab5	Early endosome biogenesis and maturation
Rab7	Late endosome and phagosome maturation Fusion with lysosomes
Rab9	Late endosome–Golgi transport
Rab4	Fast endocytic recycling
Rab11, Rab35	Slow endocytic recycling
Rab3, Rab26, Rab27, Rab37	Regulated exocytosis
Rab33, Rab24	Autophagosome formation
Rab18	Lipid droplet formation
Rab32, Rab38	Melanosome biogenesis and transport
Rab8, Rab17, Rab23	Ciliogenesis
Rab13	Tight junction assembly

Table 1. Functions of Rab GTPases.

Rab GTPases are crucial for a wide variety of intracellular tasks, which they perform at specific subcellular localizations. Where indicated, several Rab proteins act in concert to regulate a particular trafficking or biogenesis event. See text for details.

Amongst the trafficking routes mediated by Rab proteins, the most important step in endosome biogenesis is the exchange of Rab5 for Rab7 on early endosomes maturing to late endosomes. In this process, early endosomes derived from internalization the plasma membrane are covered by Rab5, which is replaced by Rab7 following an exchange of their GEF (Poteryaev et al., 2010; Rink et al., 2005). Switching Rab5 for Rab7 implies that recycling Rabs such as Rab4 and Rab11 are lost, whereas late

endosomal Rab9 is recruited. Other concomitant endosomal maturation steps include phosphatidylinositol species turnover, acquisition of hydrolases and other proteins from the trans-Golgi network, lumen acidification by V-ATPases, and morphological or size variations (Huotari and Helenius, 2011).

Due to the importance of Rab proteins in intracellular trafficking, mutations in several of these proteins give rise to pathological scenarios including congenital disorders such as Griscelli Syndrome 2, in which Rab27a is mutated (Menasche et al., 2003; Mitra et al., 2011), or X-linked choroideremia, arising from Rep-1 mutation and subsequent deficits in Rab27a geranylgeranylation (D'Adamo et al., 1998; Seabra et al., 1993; Seabra et al., 1995). In addition, Rabs can mediate tumorigenesis (Recchi and Seabra, 2012) and are involved in infectious processes, since many pathogens hijack Rab pathways either during endocytosis while entering the cell, e.g. *Salmonella enterica* serovar Typhimurium or coxsackie virus (Coyne et al., 2007; Smith et al., 2007), or interfering with endosome maturation steps once inside the cell, e.g. *Lysteria monocytogenes* and *Helicobacter pylori* (Prada-Delgado et al., 2005; Terebiznik et al., 2006).

The concerted action of Rab proteins with other machineries adds further complexity to endosomal sorting. For example, late endosomes that have acquired Rab7 undergo internal rearrangements such as acquisition of material from the Golgi, homotypic fusion instead of fusion with early endosomes, or ILV formation giving rise to MVB (Huotari and Helenius, 2011). This latter process is catalyzed by yet another multi-protein sorting machinery, the ESCRT proteins.

3.1.2 ESCRT proteins in MVB biogenesis

There is a multitude of proteins involved in the formation of MVB that function sequentially from cargo recognition, deformation of the membrane, to internalization of cargo into ILV of MVB (Raiborg and Stenmark, 2009). The components involved in recognizing ubiquitin on cargo to be degraded were studied in yeast and termed Class E Vacuolar protein sorting (Vps) proteins (Raymond et al., 1992). It was soon determined that Vps proteins combine at MVB membranes to form the multi-subunit ESCRT machinery represented in Figure 8 to mediate ILV biogenesis.

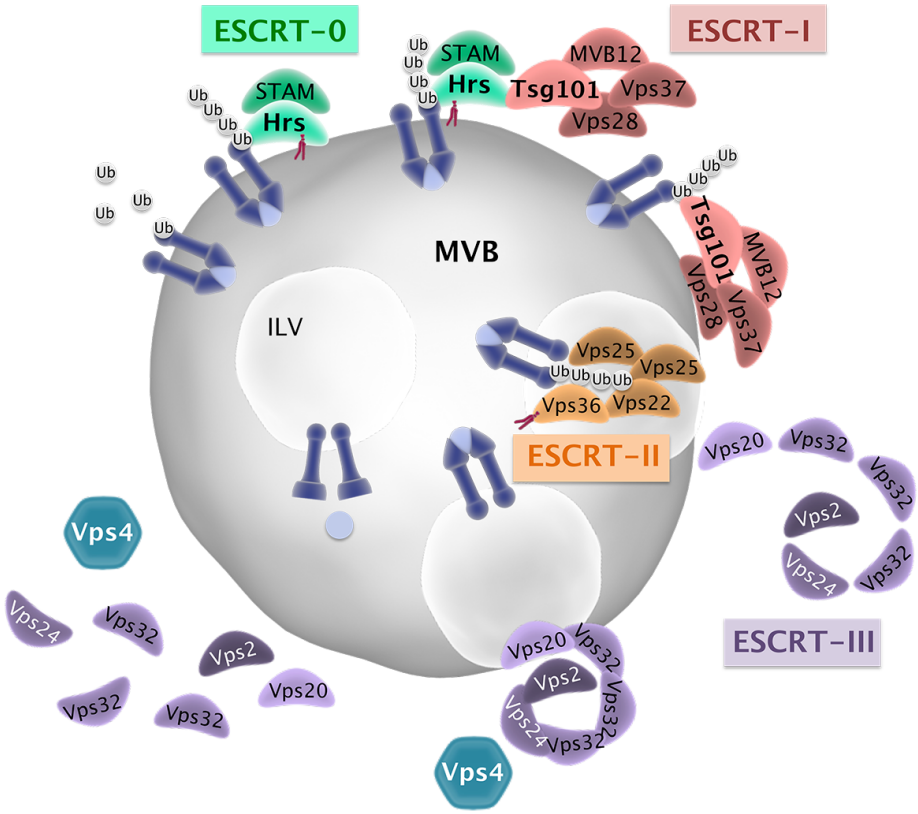

Figure 8. Schematic of the ESCRT protein machinery.

The ESCRT machinery aids in sorting endosomal cargo and MVB biogenesis through ILV production. Dark blue rods bound to light blue circles represent receptors bound to their ligand that have been internalized from the plasma membrane and arrive at the MVB limiting membrane during endocytosis. Ubiquitin binds to these receptors and is recognized by ESCRT-0 (green components) through binding of Hrs to PI(3)P (red phospholipid). ESCRT-I (red shapes) is recruited by this machinery and cargo is transferred along the pathway such that ESCRT-I together with ESCRT-II (orange shapes) gives rise to MVB membrane invagination. ESCRT-III (purple spiral) binds to ESCRT-II along with other associated proteins responsible for deubiquitinating cargo. ESCRT-III forms spiral filaments surrounding the forming vesicle neck to induce its pinching off from the limiting membrane to form an ILV. Ultimately, the ATPase Vps4 (teal hexagon) is recruited by ESCRT-III and promotes its disassembly to recycle components. The nomenclature used here refers mostly to yeast proteins, though alternative nomenclatures have developed for mammalian orthologues. Adapted from (Rusten et al., 2012).

As addressed above, protein complexes aid vesicles in diverse maturation steps along the endocytic route (see Figure 7), including membrane budding events that elicit multivesicular compartment formation. The ESCRT –I, -II and –III complexes were described as assemblies of Vps proteins, each involved in a specific step of MVB biogenesis (Babst et al., 2002a; Babst et al., 2002b; Katzmann et al., 2001). A fourth complex, ESCRT-0, was defined later on, though it is the first to act by recognizing ubiquitinated cargo such as monoubiquitinated cytosolic domains of membrane receptors and forming a protein mesh on endosomes (Raiborg et al., 2001; Raiborg and

Stenmark, 2009). The fundamental ESCRT-0 protein is Vps27p, or Hrs (Hepatocyte growth factor-regulated tyrosine kinase substrate) in humans (Figure 8, green). Hrs recognizes ubiquitinated cargo and also contains a phosphoinositol-3-phosphate (PI(3)P) binding domain termed FYVE. ESCRT-I is responsible for binding to ubiquitinated cargo and ESCRT-0 simultaneously (Katzmann et al., 2001). Vps23p or its homolog in humans, Tsg101 (Figure 8, red), is at the core of ESCRT-I, for it directly binds to cargo and Hrs. Once ESCRT-0 is recycled, ESCRT-I can interact with ESCRT-II (Figure 8, orange), which aids in early steps of membrane curvature and in assembling the next complex (Babst et al., 2002b). ESCRT-III function is one of the most important steps in MVB biogenesis, since a subset of its subunits is in charge of generating membrane curvature to accommodate ILV production, while other proteins in this complex aid in vesicle abscission (Babst et al., 2002a; Hanson et al., 2008). Currently, there is still debate as to how ESCRT-III subunits (in humans, charged multivesicular proteins, or CHMP) assemble to deform membranes, with two main hypotheses still standing, i.e. the helical and dome models, represented by purple spirals in Figure 8, as reviewed in (Henne et al., 2013). In turn, several ESCRT-associated proteins perform crucial tasks such as deubiquitinating cargo or aiding in membrane deformation (Clague and Urbe, 2006). Vps4 is an ATPase that is in charge of terminating ILV formation by providing energy for membrane scission at the vesicle neck and promoting ESCRT-III dissociation from the MVB (Shim et al., 2008). Interestingly, ESCRT machineries do not accompany cargo into ILV, but rather are all recycled for subsequent rounds of endolysosomal sorting (Babst et al., 1998; Williams and Urbe, 2007).

Though the canonical ESCRT sorting pathway begins with cargo ubiquitination, several studies have shown that this route can also be responsible for ubiquitin-independent sorting. In yeast, acid trehalase is targeted to lysosomes via MVB in an ubiquitin-independent manner (Huang et al., 2007a). In mammalian cells, several cytokine receptors and the G-protein coupled receptors (GPCR) DOR (delta opioid receptor) and PAR1 (protease-activated receptor 1) are similarly sorted into MVB through ubiquitin-independent mechanisms involving at least part of the ESCRT machinery (Amano et al., 2011; Dores et al., 2012; Hislop et al., 2004). A recent study further suggests that binding to any ESCRT protein can mediate ubiquitin-independent

sorting, such that weak affinity for ESCRT and strong membrane association will mediate internalization into MVB, whereas a strong interaction with ESCRT but weaker membrane binding will send proteins along the recycling pathway to the plasma membrane, regardless of their ubiquitination state (Mageswaran et al., 2014). Therefore, some MVB cargo contains structural determinants that allow for ESCRT-dependent sorting into ILV in the absence of ubiquitin.

The ILV inside MVB can have different fates. If retained in the endosomal route, they will be taken to the lysosome to be degraded (Futter et al., 1996). Alternatively, ILV can be liberated to the extracellular space after fusion of MVB with the plasma membrane, hence becoming exosomes, as reviewed in (Simons and Raposo, 2009). Whether degradative and exocytic ILV are contained within distinct MVB or can be found in the same MVB has been the subject of much debate. Recently, two subpopulations of ILV have been shown to coexist within the same MVB (Edgar et al., 2014), as depicted in Figure 9.

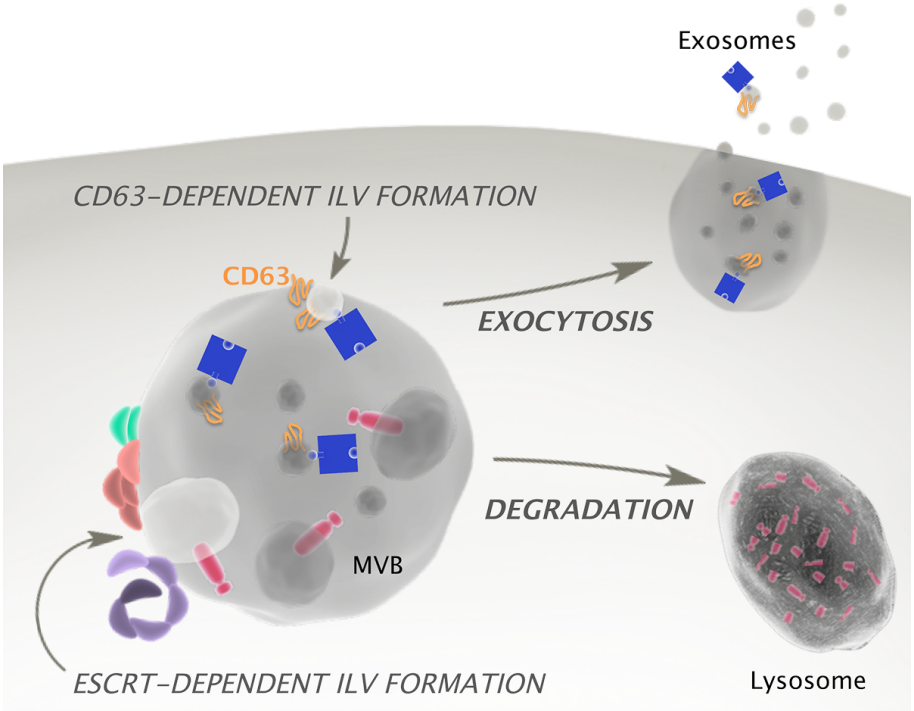

Figure 9. ILV biogenesis and destination.

The limiting membrane of MVB invaginates to form either large ILV through ESCRT-dependent mechanisms (machinery shown in green, red and purple) or to form small ILV in a process involving CD63 (shown in orange). In this model, the same MVB holds both types of ILV, as described recently (Edgar et al., 2014); however, it is not yet clear whether this is the case or if specific MVB exist for each type of ILV. Small ILV containing CD63 and material to be secreted (blue squares) are released into the extracellular milieu upon fusion of the MVB with the plasma membrane during exocytosis. On the other hand, large ILV containing cargo such as signaling receptors (red rods) fuse with lysosomes to elicit degradation of ILV content.

The two types of ILV differ in size, biogenesis and cellular fate. Large, sorting ILV are formed Hrs-dependently, whereas small, exocytic ILV appear due to sorting mediated by the tetraspanin CD63, as will be explained below. It is therefore possible that both ESCRT-dependent and -independent ILV generation occur simultaneously within the cell, giving rise to specific types of vesicles with unique destinations. This point is further substantiated by the fact that CD63-positive ILV still appear in the absence of members of all ESCRT complexes, suggesting that ESCRT-independent mechanisms of MVB biogenesis are still operative in this setting (Stuffers et al., 2009). Indeed, the major histocompatibility complex-II (MHC-II) in dendritic cells can be sorted to lysosomal ILV when ubiquitinated under resting conditions *via* an ESCRT-dependent process, whereas cell activation abolishes MHC-II ubiquitination and promotes its internalization into exosomal ILV that are liberated towards the T cells with which they interact (Buschow et al., 2009).

Though represented as distinct processes in Figure 9, crosstalk most likely exists between degradative or exocytic ILV biogenesis pathways, as reflected in a recent report presenting an RNA interference screen of 23 ESCRT proteins. Several ESCRT proteins, e.g. Hrs or Tsg101, were found necessary not only for degradative ILV formation but also for exosome biogenesis, suggesting that exosomes can be formed by the ESCRT machinery as well as by ESCRT–independent pathways (Colombo et al., 2013).

3.1.3 CD63-mediated sorting

The role of CD63 in formation of exosomal ILV highlights the fact that this tetraspanin is inextricably involved in late endosomal trafficking, as reviewed in (Pols and Klumperman, 2009). Tetraspanins are a family of proteins containing four transmembrane domains, glycosylated residues and most contain cysteines amenable to palmitoylation, as is the case for CD63, as reviewed in (Hemler, 2005). These posttranslational modifications aid in homo- and heteroligomerization to produce tetraspanin-enriched microdomains (TEM) in which tetraspanins of several types along with receptors, integrins, metalloproteinases and cholesterol occupy a tightly packed area of membrane, particularly on the plasma membrane (Yang et al., 2002). In fact, as

shown in Figure 10, a cholesterol-palmitoyl interaction is also established by the palmitates bound to tetraspanins, further stabilizing these TEM (Charrin et al., 2003).

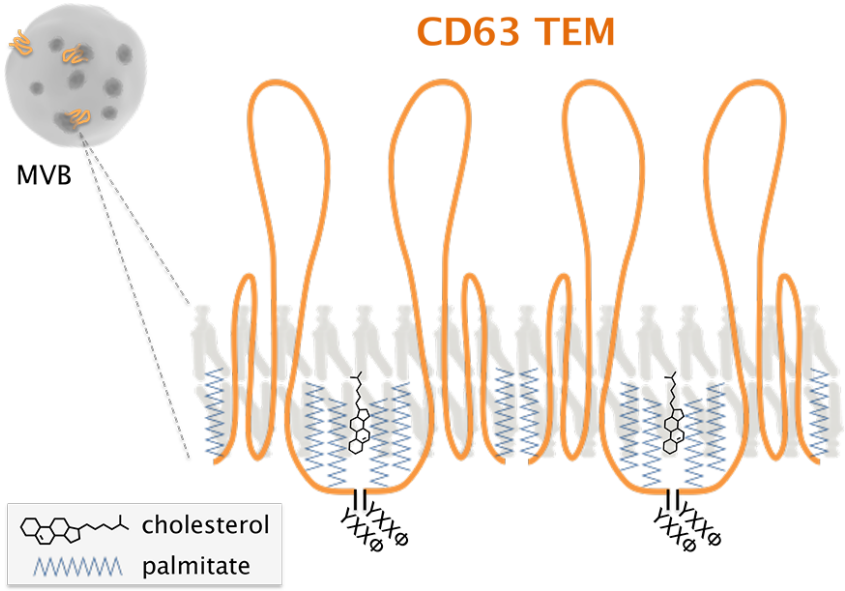

Figure 10. CD63 tetraspanin-enriched microdomains.

Zoom-in of a membrane from an ILV destined for exosomal release. CD63 molecules are shown in orange, containing four transmembrane domains and two loop domains. Cysteine residues at their N- and C-termini become palmitoylated (blue zigzags), which allows for interaction with membrane-embedded cholesterol (black structures). The C-terminal YXXΦ motifs that interact with AP complexes for intracellular shuttling are also depicted. Tetraspanins associate with each other to form oligomers, as shown here for four CD63 molecules, to form tetraspanin-enriched microdomains (TEM).

In the case of CD63, its association with late endosomes and ILV usually predominates over plasma membrane localization. Specifically, ILV destined for exosome formation are enriched in several tetraspanins including CD63 (Escola et al., 1998). This tetraspanin contains the lysosomal targeting sequence "YEVM", which follows a "YXXΦ" pattern recognized by adaptor protein complexes, in which a crucial tyrosine residue is followed by any two amino acids (X) and an aliphatic, bulky residue (Φ), as reviewed in (Bonifacino and Traub, 2003). Therefore, CD63 contains several structural determinants that direct it to the late endocytic pathway.

A newly synthesized CD63 polypeptide chain undergoes glycosylation and palmitoylation at the Golgi prior to export to the plasma membrane, cycling back inward when its sorting signal is recognized by AP-2 and traveling further from recycling endosomes to late endosomes/MVB and lysosomes via AP-3 binding, as reviewed in (Pols and Klumperman, 2009). Following these pathways, it has been

reported that CD63 could be involved in trafficking of MHC-II in dendritic cells (Vogt et al., 2002) or recycling of the H^+/K^+ ATPase pump in gastric parietal cells (Duffield et al., 2003). Additionally, a truncated form of CD63 was shown to down-regulate chemokine receptor CXCR4 plasma membrane levels due to receptor internalization in T lymphocytes (Yoshida et al., 2008). Once localized at late endosomes/MVB, CD63 can mediate ESCRT-independent sorting of certain proteins, as is the case for specific domains of the melanosomal protein Pmel17 (Theos et al., 2006; van Niel et al., 2011). Furthermore, CD63 plays a central role in ESCRT-independent exosome biogenesis, as described above, which is also reflected by its use as an exosomal marker, as reviewed in (Andreu and Yáñez-Mo, 2014). Recently, the direct role of TEM in exosome formation has been set forth by a comprehensive high-throughput proteomic analysis that highlights their importance in selecting receptors and signaling proteins for exosomal packaging (Pérez-Hernández et al., 2013). It is interesting to note that though CD63 is involved in sorting proteins of various origins, its knock-out (KO) mouse model is viable and displays normal lysosomal function, though these mice suffer kidney pathologies. However, considering the amount of tetraspanins expressed in cells, there could be redundancies such that other members of this protein family could compensate for CD63 loss (Schröder et al., 2009).

Though MVB biogenesis and cargo sorting require proteins such as CD63 or ESCRT components, it also depends on the lipid composition in which membrane proteins are embedded. It has been proposed that specific membrane domains and the lipids contained therein can play a part in the invagination of the MVB limiting membrane to form ILV (Matsuo et al., 2004). Moreover, it has been described that certain lipid compositions favor the formation of MVB in the absence of protein components, both in liposome models and in cells (Matsuo et al., 2004; Trajkovic et al., 2008), as will be described in the following section.

3.2 Lipid involvement in endosomal sorting

Lipids are distributed unevenly among cellular membranes and hence play a significant role in the distribution of membrane proteins in different organelles. As schematized in Figure 11, intracellular membranes have been proposed to be divided

into two distinct environments according to lipid properties: the biosynthetic, pre-Golgi system that includes the ER, and the secretory-endocytic, post-Golgi system that includes the plasma membrane and endocytic vesicles (Lippincott-Schwartz and Phair, 2010). Following this model, ER/cis-Golgi membranes contain monounsaturated lipids usually with neutral head groups that favor interactions with cytosolic proteins preferring lipid-packing defects. On the other hand, the trans-Golgi, plasma membrane and endocytic compartments include more negatively charged lipids packed tightly (i.e. phospholipids with more saturated acyl chains) to favor electrostatic interactions (Figure 11). Other specialized lipids appear at specific subcellular locations. For instance, cholesterol and glycosphingolipids reside on both leaflets of the plasma membrane, while phosphatidylethanolamine (PE) and phosphatidylserine (PS) remain at its inner leaflet, as reviewed in (Bigay and Antonny, 2012). Furthermore, scarce but highly specialized phosphoinositides appear at different membrane sites throughout the cell. The plasma membrane contains PI(4,5)P_2 and PI(3,4,5)P_3 whereas PI(3)P appears at early endosomes and controls many endocytic processes through proteins with PI(3)P binding domains (Gillooly et al., 2000; Schink et al., 2013). The specialized phospholipid, 2,2'-dioleoyl lysobisphosphatidic acid (LBPA, a.k.a. BMP) (Kolter and Sandhoff, 2005) is exclusively localized to late endosomes, particularly ILV of MVB (Kobayashi et al., 1999), and has the ability to deform membranes *in vitro*, thus possibly playing a role in MVB invagination, as discussed below (Matsuo et al., 2004). Therefore, the dynamic nature of membrane trafficking depends not only on protein-based sorting complexes, but also on organelle identity conferred to specific endomembranes by lipids of varied acyl composition, head group charge and overall physicochemical structure.

Lipid gradients exist along the biosynthetic pathway, so that there is more cholesterol density and sphingolipids from the ER towards the PM (Maxfield and van Meer, 2010), as depicted in Figure 11. Cholesterol and sphingolipids are responsible for thickening the membrane bilayer, which is reflected by the transmembrane span of proteins (Sharpe et al., 2010). In particular, cholesterol is enriched in recycling endosomes, as well as in ILV of MVB (Möbius et al., 2003). Cholesterol has been found to appear at particularly high curvature regions (Wang et al., 2007), which could explain its concentration in ILV. This sterol also stabilizes fluid phosphoinositide domains, which could be involved in forming signaling platforms that require concentrating these

scarce phospholipids into an area that accommodates interactions between signaling proteins (Jiang et al., 2014). Furthermore, in the context of signaling receptors, several GPCR have been shown to directly interact with cholesterol through their palmitoyl moieties (Cherezov et al., 2007; Zheng et al., 2012), similarly to tetraspanins (Charrin et al., 2003).

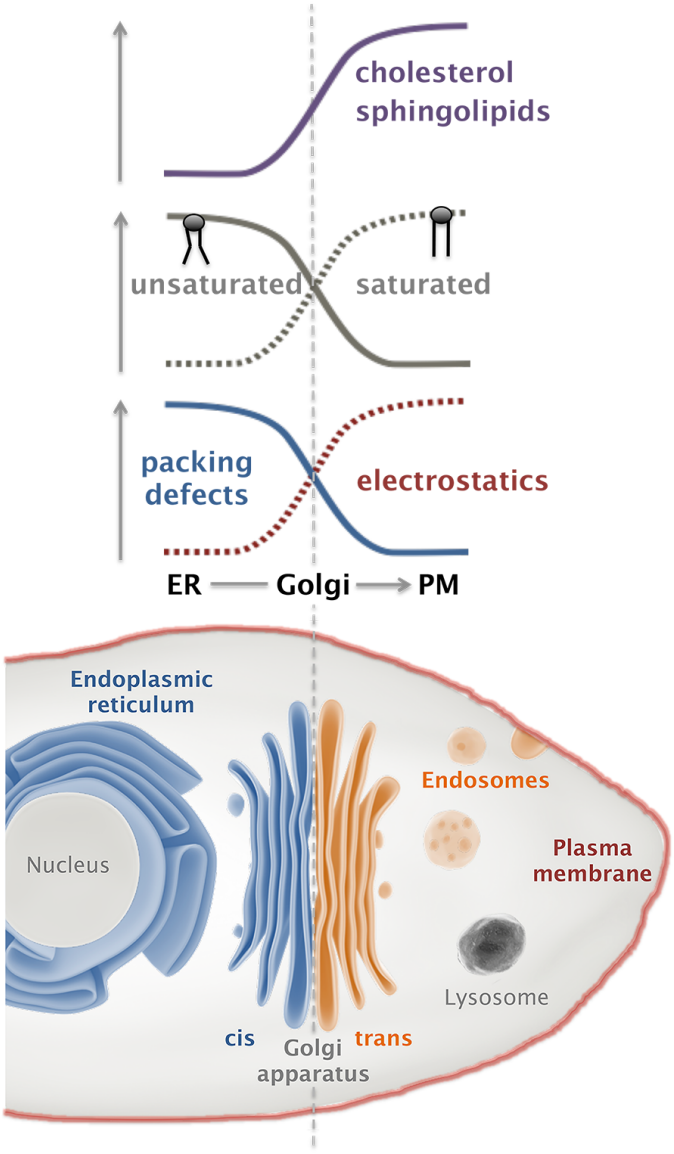

Figure 11. Lipid properties defining membrane environments within the cell.

Studies based on lipidomics and probe detection point to two distinct membrane environments within the cell. As shown to the left of the dashed line (blue structures), the ER and cis-Golgi membranes are characterized by lipid-packing defects due to the unsaturated chains that their phospholipids contain, whose head groups are weakly charged. Furthermore, they present low levels of cholesterol and sphingolipids, producing thin membranes. In contrast, trans-Golgi, endosomal and plasma membranes (orange and red components to the right of the dashed line) are characterized by inner leaflet phospholipids with negatively charged polar groups (high electrostatics) and saturated chains, as well as elevated cholesterol and sphingolipid levels, rendering them thicker and more tightly packed. Adapted from (Bigay and Antonny, 2012).

Regarding the formation of ILV of MVB, several *in vitro* studies have shown that lipids alone can mediate membrane invagination on liposomes with particular compositions (Matsuo et al., 2004; Trajkovic et al., 2008). The specialized lipid LBPA could be involved in the ESCRT-dependent formation of degradative ILV (Matsuo et al., 2004), whereas the sphingolipid ceramide induces the formation of ILV destined to become exosomes (Trajkovic et al., 2008) (see Figure 9). These findings are in line with studies describing high levels of LBPA in ILV of MVB within the cell, whereas exosomes are not enriched in this lipid (Laulagnier et al., 2004; Wubbolts et al., 2003). Another report suggests that cholesterol-rich MVB are destined for exosome formation and cholesterol-poor vesicle populations are sent to the lysosome to be degraded (Möbius et al., 2003). Furthermore, ILV have been shown to undergo back-fusion and blend back into the MVB limiting membrane via an LBPA-mediated process employed by certain pathogens to escape their degradation, as reviewed in (Falguières et al., 2009). However, there is still debate regarding whether exosome biogenesis is dependent on ESCRT and its associated proteins, e.g. Hrs, Alix (Baietti et al., 2012; Colombo et al., 2013; Gibbings et al., 2009) or mostly lipid-based and perhaps involving CD63 (Trajkovic et al., 2008). It is therefore probable that ILV themselves or even specific microdomains of the MVB limiting membrane, though thoroughly dependent on their lipid composition, are regulated by tight interplay with complex protein machineries owing to their highly dynamic nature (Bissig and Gruenberg, 2013).

Lipid composition also has its effects on peripheral membrane proteins such as Ras and Rho proteins, since their trafficking depends on lipid modifications, as described above. In the case of proteins that are both isoprenylated and palmitoylated, isoprenylation could be responsible for a weak interaction with the membrane, whereas single or double palmitoylation would aid in its binding to membranes with a particular composition (Rocks et al., 2005). These palmitate moieties are saturated chains that occupy a small space and can therefore force their way into tightly packed membranes containing saturated phospholipids, such as the plasma membrane and late endocytic vesicles. An elegant *in silico* model suggests that H-Ras forms clusters at the interface of lipid domains with its palmitate chains preferentially oriented towards liquid ordered domains (L_o, cholesterol-rich, with saturated phospholipids), whereas its polyunsaturated farnesyl moiety is directed towards the liquid disordered membrane

domain (L_d), hence increasing membrane curvature (Janosi et al., 2012). H-Ras was indeed found to cycle between L_d and L_o domains in its GTP- or GDP-bound form, respectively, underscoring the importance of lateral segregation of peripheral proteins on their function (Prior et al., 2001). Lipid packing, electrostatics or curvature could play a further role in membrane selectivity, as is the case for members of the Rho family (Rac1 and Rac2) or the Ras protein, K-Ras4B, which contain basic residues at their C-terminus that allow electrostatic interactions with PS on membranes (Ahearn et al., 2012; Bigay and Antonny, 2012). It is therefore apparent that lipid composition is crucial for peripheral membrane proteins to accomplish their biological roles at distinct subcellular locations.

3.3 Other sorting and degradation pathways

Early stages of protein sorting within the cell involve bulk flow of many proteins towards the *cis* Golgi upon translation at the ER. However, post-Golgi trafficking events become increasingly specialized for the proteins to be sorted, so that more cargo-specific sorting machineries appear further along the endocytic route towards lysosomes, secretion or recycling. Along with the pivotal Rab and ESCRT protein sorting machineries described above, other mechanisms act in parallel to coordinate the busy flow of material in later stages of protein shuttling within the cell. Many proteins contain sequences that are recognized by sorting entities (Bonifacino and Traub, 2003), as exemplified by soluble acid hydrolases, which are modified by M6P and recognized by M6P receptors in the Golgi apparatus that will accompany them to the lysosome, as reviewed in (Ghosh et al., 2003). However, other M6P-independent mechanisms involving the sorting proteins sortilin or lysosomal integral membrane protein 2 (LIMP-2) also work in the cell to transfer soluble proteins into lysosomes (Coutinho et al., 2012; Ghosh et al., 2003). As for lysosomal transmembrane proteins, their targeting sequences contain tyrosines (such as the "YXXΦ" motif in CD63 mentioned above) or dileucine motifs that are recognized by specific AP complexes, as extensively reviewed in (Bonifacino and Traub, 2003). Distinct AP complexes are present on membranes such as the plasma membrane, Golgi, endosomes and others, from which they recognize motifs in cargo proteins and mediate their transport (Bonifacino and Traub, 2003).

Additionally to protein-specific sorting, cell type-dependent processes are responsible for the formation and transport of certain specialized vesicles, such as lysosome-related organelles (LRO), e.g. melanosomes for pigmentation; basophil, azurophil and lytic granules or MHC class II compartments for immune responses; and platelet-dense granules for coagulation, as reviewed in (Dell'Angelica et al., 2000). Their biogenesis is mediated by yet another protein machinery termed BLOC 1-3 (biogenesis of lysosome-related organelles complex), containing proteins that are mutated in the lysosomal disorder Hermansky-Pudlak syndrome (HPS), which will be considered below, as reviewed in (Dell'Angelica, 2004).

3.3.1 Autophagy

The term “autophagy”, literally “self-eating”, originally was designated for a process in which proteins and even organelles are surrounded by double membranes of varied origin called phagophores, which mature to autophagosomes and fuse with lysosomes to degrade these large amounts of cellular material (Mizushima et al., 2008). The explosion of research in this field has led to the discovery of numerous autophagic pathways, so that the original term is now referred to as macroautophagy, to differentiate it from the other two main forms of autophagy, i.e. microautophagy, implying direct lysosomal internalization, and chaperone-mediated autophagy, in which the chaperone Hsc70 unfolds proteins prior to their internalization into the lysosome to be degraded (Cuervo and Dice, 1996; Lee et al., 2012). Cells undergo these degradation processes to redeliver the necessary biosynthetic building blocks to the cytosol when they detect a nutrient or energetic shortage, or under stress conditions including pathogen invasion and excessive protein aggregation, as reviewed in (Yang and Klionsky, 2010). The autophagy-related proteins (Atg) are the core molecular machinery of canonical autophagy and work together in sequential complexes during phagophore maturation towards autophagosomes, as reviewed in (Mizushima et al., 2011). Though autophagy was first regarded as a degradation and cell death mechanism, numerous reports now corroborate its role in survival, bioenergetics, cell differentiation, immunity, and tumor suppression, as reviewed in (Boya et al., 2013).

Interaction between autophagy and endolysosomal sorting is obvious at the point of autophagosome-lysosome fusion, but some instances of autophagosome fusion to early and late endosomes have been documented (Berg et al., 1998; Dunn, 1994; Liou et al., 1997). In fact, the fusion of endocytic vesicles such as MVB and autophagosomes gives rise to structures called amphisomes, which further fuse to lysosomes for degradation (Eskelinen, 2005). Moreover, some studies suggest that Rab11 could play a role in MVB-autophagosome fusion to form amphisomes, whereas Rab7 would mediate the next step of fusing to lysosomes, as reviewed in (Fader and Colombo, 2009). Other members of the Rab family also appear at the crossroads of endolysosomal and phagocytic pathways, such as Rab1 at the initial formation of the phagophore and Rab9 during non-canonical Atg5/Atg7-independent autophagy, among others, as reviewed in (Chua et al., 2011). Studies both in mammalian cells and *Drosophila* lacking certain ESCRT proteins showed impaired autophagy and accumulation of ubiquitin-positive aggregates, again revealing that correct MVB function is necessary for autophagy progression (Rusten and Simonsen, 2008). It has also recently come to light that it is common for autophagic cargo to become ubiquitinated and sorted by autophagy receptors containing ubiquitin-binding domains (Boya et al., 2013). Furthermore, connections between autophagy and exosomal MVB have been established, since autophagy induction by several methods inhibits exosome release and points to a selective MVB fate depending on cellular energy needs (Baixauli et al., 2014). Once again, the boundaries between distinct organelles are often blurred during crosstalk between intracellular trafficking pathways.

4. Lysosomal storage diseases

Lysosomal storage diseases are quite a numerous group of rare inherited metabolic disorders resulting from mutations in specific lysosome-related genes (Ballabio and Gieselmann, 2009; Fuller et al., 2006). Though initially attributed to acid hydrolases of the lysosomal lumen, it has become evident that both lysosomal integral membrane and luminal proteins, among others, are involved in certain lysosomal storage disorders (Saftig and Klumperman, 2009). There are as many as 60 lysosomal protein deficiencies that give rise to accumulation of material from incomplete degradation or trafficking in degradative compartments (Sagne and Gasnier, 2008). Some of these disorders arise from problems in LRO biogenesis, mediated by transporters and tethering or sorting factors (Huizing et al., 2008). In most cases, manifestations appear during childhood and often include varying degrees of neurodegeneration and immune deficiencies that can cause death at a relatively early age unless palliated by bone marrow transplantation or recently developed treatments such as enzyme replacement therapy, as reviewed in (Platt et al., 2012). Table 2 summarizes several lysosomal storage diseases and the proteins altered by mutations in their respective genes.

There are many pathological scenarios involving malfunction of lipid transport routes, but here the focus will be on alterations of late endosome lipids. In Niemann-Pick type C (NPC) disease, a set of lysosomal integral membrane proteins that act as cholesterol transporters at late endosomes (NPC1/NPC2) are deficient (Table 2). Late endosomes and lysosomes in NPC patients accumulate massive amounts of cholesterol and glycosphingolipids due to abnormal low-density lipoprotein processing within the endocytic pathway (Mukherjee and Maxfield, 2004). Furthermore, this cholesterol buildup induces Rab9 sequestration, possibly in its inactive form, which disrupts M6P

receptor trafficking (Ganley and Pfeffer, 2006). It has been described that NPC1 cells could be inducing the release of exosomes loaded with cholesterol, perhaps as a means of circumventing the cytotoxic effects of generalized cholesterol buildup within the cell (Strauss et al., 2010). Alterations of lipid homeostasis are quite severe due to cholesterol and LBPA accumulation in late endosomes and subsequent endolysosomal dilation in several cell types (Carstea et al., 1997; Kobayashi et al., 1999). In fact, this phenotype can be mimicked by treatment with the hydrophobic amine U18666A that has therefore been used to generate NPC-like cells (Mukherjee and Maxfield, 2004; Sobo et al., 2007).

Lysosomal storage disease	Mutated proteins
Niemann–Pick Type C (NPC)	NPC1 or NPC2
Hermansky–Pudlak Syndrome (HPS)	
• HPS–1, HPS–4	BLOC–3
• HPS–2	AP–3
• HPS–3, HPS–5, HPS–6	BLOC–2
• HPS–7, HPS–8	BLOC–1
Chediak–Higashi Syndrome (CHS)	LYST

Table 2. Lysosomal storage diseases and mutated proteins.

Lysosomal storage diseases are caused by point mutations in genes that code for proteins involved in late endocytic trafficking. NPC proteins are involved in cholesterol transport, whereas proteins responsible for the various forms of HPS mediate vesicular transport of lysosome-related organelles (BLOC) or general late endosomal trafficking (AP-3). Many point mutations have been described for the Lyst gene, all of which give rise to CHS of varying degrees of severity.

Mutations in several LRO biogenesis-related proteins give rise to recognizable hypopigmentation disorders due to malfunction of melanosome biogenesis or trafficking, as reviewed in (Dessinioti et al., 2009). Such is the case for Hermansky-Pudlak syndrome (HPS), in which mutation of several specific proteins can elicit similar phenotypes, and Chediak-Higashi syndrome (CHS), resulting from mutations in the Lysosomal trafficking regulator (Lyst) protein, as will be discussed in detail below. There are eight human HPS subtypes (Table 2), which arise from mutations in key LRO trafficking and maturation machinery proteins, i.e. BLOC-3 mutations in HPS-1 and HPS-4, AP-3 in HPS-2, BLOC-2 in HPS-3, HPS-5 and HPS-6, and BLOC-1 in HPS-7 and HPS-8, as reviewed in (Wei, 2006). Apart from LRO machineries, certain Rab

family proteins have been shown to play a role in HPS mouse models and perhaps in human pathology, for BLOC-3 acts as a Rab-GEF for Rab38 and Rab32 to recruit these proteins to premelanosomal membranes. Furthermore, Rab38 co-localizes with BLOC-2 and AP-3 at endosomal membranes, suggesting a role for this Rab in cargo trafficking during LRO biogenesis, as reviewed in (Krzewski and Cullinane, 2013).

4.1 Chediak-Higashi Syndrome

CHS is a rare autosomal recessive lysosomal storage disorder characterized by enlarged granules in many cell types, including melanocytes, neutrophils, leukocytes and neurons, among others. The large, dense granules are either lysosomes or LRO destined for secretion and involved in diverse cellular functions such as immune responses, pigmentation or coagulation. These functions are compromised in CHS patients, as reflected by their clinical manifestations which include partial oculocutaneous albinism, bleeding disorders, neutropenia, recurrent infection and neurological dysfunction, that can lead to death associated to a severe phase due to uncontrolled proliferation of cytotoxic T lymphocytes (Ward et al., 2000).

The genetic defects that underlie CHS consist of mutations in the CHS1/LYST gene, homologous to the *beige* gene in mice. This gene codifies a cytosolic protein of 3801 amino acids (approximately 429 kDa) with still unclear functions (Huizing et al., 2001). The LYST protein is a member of the BEACH (BEige And Chediak–Higashi) protein family and mutations that are phenotypically similar to CHS have been found in numerous mammalian species (Ward et al., 2000). Enlarged lysosomes and LRO are found mainly at the perinuclear region of CHS cells, pointing to a disruption in vesicle trafficking (Burkhardt et al., 1993).

There are several functional studies on CHS cells or murine *beige* models that describe alterations in late vesicular traffic and their cellular impact. Similarly to HPS, deficiency in CHS melanosome secretion underlies oculocutaneous albinism in these patients (Stinchcombe et al., 2004). Under physiological conditions, it has been established that cells are able to use their lysosomes as Ca^{2+}-regulated secretory compartments to "parch" the plasma membrane after wounding, making them crucial in membrane resealing (Reddy et al., 2001). In CHS and *beige* cells, lysosomal exocytosis

and consequent plasma membrane repair are defective (Huynh et al., 2004). Also in line with these findings, other exocytic organelles seem to be responsible for CHS immune deficiencies. CHS patients suffer from a loss of secretion at the immunological synapse, where CTL normally discharge proteins such as perforin *via* secretory lysosomes (Stinchcombe et al., 2000). Furthermore, CHS B lymphocytes present deficient peptide loading onto MHC class II as well as delayed antigen presentation as a result of defects in MHC-II transport from the TGN into MVB (Faigle et al., 1998). It has been proposed that LYST could act as a scaffold for complexes involved in LRO biogenesis that are defective in HPS pathogenesis as well, such as AP-3 or BLOC-1 (Callahan et al., 2009). Yeast two-hybrid screens using truncated forms of LYST revealed direct interaction with several proteins involved in late endosomal dynamics such as Hrs and several SNARE proteins (Tchernev et al., 2002). Rab14 interaction with a LYST homolog (LsvB) has been observed in the amoeba *Dictyostelium discoideum,* proposing that LsvB regulates lysosomal size and maturation through Rab14, though these studies are yet to be replicated in human cells (Kypri et al., 2013). Recent findings using small interfering RNA-depletion of LYST in cancer cells also point to a role for this protein in lysosome size and quantity, which could be regulated by fission or fusion events, instead of being directly responsible for LRO biogenesis or general degradation pathways (Holland et al., 2014). Indeed, in *Dictyostelium*, LsvB has been found to have an inhibitory role in vacuole fusion (Falkenstein and De Lozanne, 2014), whereas previous studies in *beige* mouse cells suggested that LYST promotes lysosomal fission (Durchfort et al., 2012). Clearly, the exact function of this remarkably large protein in endolysosomal biogenesis or sorting still warrants further studies.

AIMS AND OBJECTIVES

Small GTPases control crucial cellular functions from specific membrane localizations. Among the factors involved in their regulation, modifications at C-terminal sequences play key roles, though the involvement of lipidation and its interplay with other structural determinants in subcellular targeting of GTPases has not been fully elucidated. Therefore, the work presented in this dissertation is focused on analyzing the role of lipid modifications of RhoB cysteine residues on its intracellular sorting and determining whether its lipidation motif *per se* is able to reproduce the behavior of the full-length protein. Furthermore, the possibility that lipidation sequences could be targeted by other structurally diverse modifications, including reactive species arising in pathological scenarios, has not been explored. Therefore, the following objectives were projected:

- To study endosomal GTPase C-terminal sorting signals involved in subcellular localization.
- To evaluate the importance of C-terminal isoprenylation and palmitoylation in attachment to intracellular vesicles.
- To determine the subcellular localization of chimeras bearing the RhoB C-terminal lipidation motif.
- To assess whether the latent sorting mechanisms for the RhoB C-terminus are conserved in cells from different species.
- To explore the potential role of key molecular machineries, i.e. ESCRT complexes, CD63 or lipid dynamics, in sorting of RhoB and related chimeras.
- To set the basis for studying the potential alteration of endosomal GTPase localization and modification in experimental models of disease.

MATERIALS AND METHODS

1. Materials

1.1 General reagents

1.1.1 Cell culture reagents

Cell culture medium including DMEM, RPMI 1640, and TC100 as well as Newborn calf serum, penicillin/streptomycin, glutamine and trypsin-EDTA were from Gibco Life Technologies. NCTC 109 medium was from Sigma. Fetal bovine serum (FBS) was from Lonza Inc. Sterile plastic material for cell culture was obtained from Falcon (Beckton Dickinson). For cell imaging of live cells, 35-mm glass bottom dishes (p35) from MatTek Corp. were used.

1.1.2 Electrophoresis and Western Blotting reagents

For protein separation through polyacrylamide gel electrophoresis (PAGE), electrophoresis purity acrylamide, N,N'-methylenebisacrylamide, ammonium persulfate, N,N,N',N'-tetramethylethylenediamine (TEMED), sodium dodecyl sulfate (SDS), glycine and Tris were acquired from Bio-Rad. For DNA separation, molecular biology grade agarose from Pronadisa was used for gels. Polyvinylidene fluoride (PVDF) Immobilon-P membranes were from Millipore, the bicinchoninic acid (BCA) Protein Assay Kit for measuring protein concentration in cell lysates was from Pierce and the enhanced chemiluminescence (ECL) detection system was from Amersham Biosciences.

1.1.3 Other reagents

High purity salts, buffers and other reagents used for preparing solutions were mainly from Sigma and Merck. Milli-Q distilled water was from Millipore. Lipofectamine 2000, Lipofectamine RNAiMax, Lysotracker Red (LTR), 7-amino-4-chloromethylcoumarin (CMAC, a.k.a. CellTracker Blue), scrambled siRNA and siRNA against Hrs or Tsg101 were from Life Technologies. Chloroquine, 2-bromopalmitate, phenylarsine oxide (PAO), dibromobimane (DBB), leupeptin, filipin, carbobenzoxy-L-

leucyl-L-leucyl-L-leucinal (Z-LLL, a.k.a. MG-132), C6 ceramide, dihydroceramide C6, and ethidium bromide were from Sigma. U18666A, simvastatin and zaragozic acid (ZGA) were from Merck. Cyto-ID Green Detection Reagent for autophagy monitoring and Lyso-ID Red Detection Reagent were from Enzo Life Sciences. All prostanoids were from Cayman Chemical. Human recombinant proteins were from Calbiochem-Novabiochem (H-Ras), Jena Bioscience (RhoB and K-Ras4B) or Abcam (N-terminal His-tagged Rap2B). GFP-Trap agarose beads were from ChromoTek.

1.2 Antibodies

Antibodies for immunoblotting were: Anti-RhoB (mainly sc-180 but also sc-8048), anti-RhoGDI (sc-360), anti-Rab7 (sc-10767), anti-ubiquitin (sc-8017), anti-Hsp90 (sc-7947), and anti-LAMP1 (sc-20011) from Santa Cruz Biotechnology; anti-Tsg101 from Abcam; antiserum against Hrs, as described in (Raiborg et al., 2001); anti-pan Ras (Ab-3) from Merck; anti-Rap2 form BD Biosciences; anti-GFP from Clontech or Roche; secondary anti-mouse and anti-rabbit Immunoglobulins (Ig) conjugated with horseradish peroxidase (HRP) from Dako. Streptavidin-HRP was from GE Healthcare Life Sciences. For immunofluorescence, anti-giantin from Covance and anti-rabbit 568 from Invitrogen were used.

1.3 Primers

The primers used for sequencing or to generate plasmids by mutagenesis or PCR were synthesized automatically at the Protein Chemistry Facility at CIB-CSIC in an Applied Biosystems 3400 synthesizer and purified in Sephadex G25, NAPTM columns from Amersham.

1.4 Plasmids

Small-scale plasmid DNA preparation was carried out using the High Pure Plasmid Isolation Kit from Roche whereas large-scale plasmid isolation was performed with the EndoFree Plasmid Maxi Kit from Qiagen. All restriction enzymes are from

Promega. Digestion products were separated by electrophoresis on 1% agarose gels with 5 ng/ml ethidium bromide in Tris-acetate-EDTA (TAE) buffer prior to visualization under UV light on a Gel-Doc XR Imaging System (Bio-Rad). DNA fragment purification from agarose gels was performed with the Geneclean Turbo Kit from MP Biomedicals. The LigaFast Rapid DNA Ligation System from Promega was used for plasmid ligation. In the case of point mutations, primer pairs were designed and used with the QuikChange II XL Site-Directed Mutagenesis Kit from Agilent Technologies. All plasmids were sequence verified at the DNA Sequencing Service, Secugen S.A. at CIB-CSIC.

1.4.1 Donated and commercial plasmids

The following plasmids were kindly provided by various colleagues:

- pcDNA3-HA-RhoB (Prof. G.C. Prendergast, Lankenau Institute for Medical Research, Wynnewood, PA)
- Lamp1-GFP (Prof. J. Lippincott-Schwartz, NIH, MD)
- GFP-Rab7 (Prof. C. Bucci, University of Copenhagen, Denmark)
- GFP-Vps4 WT and E334Q (Prof. P. Woodman, University of Manchester, UK)
- GFP-Rab5 (Prof. J. Bonifacino, NIH, MD)
- GFP-2xFYVE and mCherry-2xFYVE (Prof. H. Stenmark, Radium Hospital, Oslo, Norway)
- GFP-H-Ras (Dr. J.M. Rojas, ISCIII, Majadahonda, Spain)
- RFP-LC3 (Prof. T. Yoshimori, Research Institute for Microbial Diseases, Osaka, Japan)

Other plasmids were obtained from commercial sources:

- GFP-Rab11, GFP-Rab9A, GFP-Rap2A, GFP-Rap2B, GFP-CD63 (all in a pEZ-M29 backbone for N-terminal GFP fusion) and mCherry-CD63 (pEZ-M55 backbone) were from Genecopoeia.
- pEGFP-C1, pmCherry-C1 and pDendra2-C were from Clontech.
- pTagRFP-C was from Evrogen.

The following constructs were generated by Genewiz Inc. (South Plainfield, NJ) by oligonucleotide synthesis and cloning into parent vectors:

- GFP-CINCSKVL (GFP-8-C244S, isoprenylation defective GFP-8 mutant)
- GFP-SINSCKVL (GFP-8-C240,243S, palmitoylation defective GFP-8 mutant)
- tRFP-T-CINCSKVL (tRFP-T-8-C242S)
- tRFP-T-SINSCKVL (tRFP-T-8-C238,241S)
- GFP-HA-RhoB X (expressing RhoB from *Xenopus laevis*)
- tRFP-T-HA-RhoB X
- GFP-CINCCKVL Asp (GFP-8 for *Aspergillus nidulans* transformation using p1902 as template) (Pantazopoulou and Peñalva, 2009)
- GFP-SINSCKVL Asp (GFP-8-C239,242S, palmitoylation defective GFP-8 for *A. nidulans* transformation)

1.4.2 Previously generated plasmids

Using some of the plasmids above, several constructs were previously generated and described in publications from the Pérez-Sala laboratory and colleagues:

- pEGFP-C1-HA-RhoB WT (GFP-RhoB) (Stamatakis et al., 2002)
- pcDNA3.0-GFP-CINCCKVL (GFP-8), GFP plus the last 22 amino acids of RhoB (GFP-22), and GFP-CINCCLIT (GFP-8-TC10, from the TC10 C-terminus) (Pérez-Sala et al., 2009)
- pTagRFP-RhoB (tRFP-RhoB) and pTagRFP-CINCCKVL (tRFP-8), tRFP plasmids containing a S162T mutation to improve photostability (Shaner et al., 2008): tRFP-T-RhoB and tRFP-T-8, as well as the triple mutants of GFP-HA-TC10 (K194N, K195Q, H196N; GFP-TC10-NQN) and GFP-HA-RhoB (insertion of KKH after L179, GFP-RhoB-KKH) (Valero et al., 2010)

1.4.3 Plasmids generated for this work

1.4.3.1 mCherry-8

Analogously to GFP-8, pmCherry-CINCCKVL was generated as described (Pérez-Sala 2009) using pmCherry-C1 as a template, by attaching the last eight amino acids of RhoB, a stop codon, and an EcoRI site to the C-terminus of mCherry cDNA by PCR with the following forward and reverse primers, respectively:
5'-GAGTAGAAGCTTATGGTGAGCAAGGGCGAGGAG-3'
5'-CCGAATTCTAGAGGACCTTGCAACAGTTGATACACTTGTACAGCTCGTC-CATGC-3'
PCR products were digested with HindIII and EcoRI and cloned into pcDNA3.0.

1.4.3.2 pDendra2-CINCCKVL (Dendra-8)

Analogously to mCherry-8, pDendra2-8 was generated using pDendra2-C as a template, by attaching the last eight amino acids of RhoB and an EcoRI site to the C-terminus of Dendra2 cDNA by PCR with the following forward and reverse primers, respectively:
5'-GCGCTAGCTCGAGGTACCGC-3'
5'-CCGAGCTCTAGAGGACCTTGCAACAGTTGATACACCACACCTGGCTGG-3'
PCR products were digested with HindIII and EcoRI and cloned into pDendra2-C.

1.4.3.3 mCherry-HA-RhoB

The cDNA of HA-RhoB was obtained from pEGFP-HA-RhoB by digestion with BglII and EcoRI. The fragment was purified and ligated with pmCherry-C1 previously digested with the same restriction enzymes.

1.4.3.4 Plasmids generated by site-directed mutagenesis

- *pEZ-mCh-CD63 Y235A and pEZ-GFP-CD63 Y235A:* Mutation of the YXXΦ motif tyrosine in CD63 was performed in both pEZ-mCherry-CD63 and pEZ-GFP-CD63 WT plasmids using the following oligonucleotides:
  5'-CTCGAGCTACATCACCTCGGC**GC**CACTTCTGATACTCTTC-3'
  5'-GAAGAGTATCAGAAGTG**GC**GCCGAGGTGATGTAGCTCGAG-3'

2. Methods

2.1 Cell culture

The following cell lines were used throughout this work and cultured as described:

- HeLa adenocarcinoma cells from the American Type Culture Collection (ATCC) were cultured in DMEM supplemented with 10% FBS, 100 U/ml penicillin and 100 µg/ml streptomycin at 37°C in an atmosphere with 5% CO_2.
- Bovine aortic endothelial cells (BAEC) were obtained from Lonza and cultured in RPMI1640 medium supplemented with penicillin/streptomycin and 10% calf serum at 37°C, 5% CO_2. BAEC were used between passages 5 and 12 and were grown to near confluence for experiments.
- Human primary fibroblasts from healthy subjects (AG09309 and AG10803), CHS patients (GM02075), NPC1 patients (GM03123) and HPS-2 patients (GM17890) were obtained from the NIGMS Human Genetic Cell Repository at the Coriell Institute for Medical Research, cultured in DMEM supplemented with 10% FBS and penicillin/ streptomycin at 37°C, 5% CO_2 and used up to passage 20.
- *Xenopus laevis* A6 cells were obtained from Sigma and cultured at 28°C in NCTC 109 medium supplemented with 15% distilled H_2O, 2 mM glutamine, 10% FBS and penicillin/ streptomycin.

- High Five cells, derived from ovarian cells of the cabbage looper *Trichoplusia ni*, were from Invitrogen. These cells were cultured at 28ºC in TC100 medium supplemented with 10% FBS, penicillin/ streptomycin and 10 μg/ml gentamycin.

All cell lines were passaged by trypsin-EDTA detachment, complete medium wash and centrifugation at 1000xg for 5 min, suspension in fresh medium, and plating at the desired dilution.

2.1.1 *Aspergillus nidulans* culture

Aspergillus nidulans was cultured in complete medium (MCA) or synthetic complete medium (SC) containing 1% glucose and 5 mM ammonium tartrate (i.e. 10 mM NH^{4+}) as carbon and nitrogen sources, respectively. GFP-8 and GFP-8-C239S,C242S were expressed under the control of the gpdAmini promoter, using a single-copy integration construct targeted to pyroA, as described previously (Pantazopoulou and Peñalva, 2009).

Strains used in this work:

- MAD690: yA2; argB2::[argB*-alcA^{p}::GFP]; pantoB100
- MAD4689: wA2; pyroA4::[pyroA*-gpdAmini::GFP-8]; pantoB100
- MAD4688: wA2; pyroA4::[pyroA*-gpdAmini::GFP-8-C239S,C242S]; pantoB100

2.2 Cell treatments

Treatments with the various agents described in each section were performed in the absence of serum, unless otherwise stated. As has been described for BAEC, this situation induces a near-quiescent state and does not reduce cell viability (Hernández-Perera et al. 1998). Control cells received an equivalent amount of vehicle as required.

- Inhibition of GTPase isoprenylation was elicited by treatment with 10 μM simvastatin for 24 h.

- Palmitoylation was inhibited using 2-bromopalmitate (2-BP) at 20 μM for 6 h.
- In order to disrupt the endolysosomal pathway, cells were treated with 10 μM chloroquine or U18666A for 20 h.
- For proteasome blockage, Z-LLL at 5 μM was used for 24 h.
- For cholesterol depletion, ZGA was added at 50 or 100 μM for 24 h, as indicated.
- Secretion was induced by treatment with C6 ceramide at 10 μM for 24h, using dihydroceramide C6 at the same concentration as control.
- For induction of autophagy, cells were incubated in amino acid-free medium (EBSS) for the times indicated. All further treatments and staining procedures were performed also in this medium to avoid autophagy reversion.

2.3 Transient transfections

Transient cell transfection was carried out at 80% confluence with Lipofectamine 2000 following the instructions of the manufacturer, i.e. using 1 μg of DNA and 3 μl (single transfections) or 4.5 μl (double transfections) of Lipofectamine per p35 dish. Unless otherwise indicated, after transfection, cells were allowed to recover for 24 h in complete medium before treatment with the indicated agents in the absence of serum. Imaging of live cells or biochemical analysis was performed 48 h after transfection to minimize its effects.

2.4 Cell lysis

2.4.1 Lysis of mammalian cells

In preparation for SDS-PAGE, cells were homogenized by forced passes through a 26½-gauge needle in lysis buffer containing 50 mM Tris, pH 7.5, 0.1 mM EDTA, 0.1 mM EGTA, 0.5% SDS, 0.1 mM β-mercaptoethanol, 50 mM sodium fluoride and 0.1 mM sodium orthovanadate with 2 μg/ml of the protease inhibitors leupeptin and aprotinin as well as 1.3 mM Pefabloc prior to boiling at 95°C for 5 min. Lysates for subcellular fractionation were obtained in the same buffer, without SDS. Alternatively, cells were scraped with a rubber scraper and directly lysed in Laemmli sample buffer

containing the protease and phosphatase inhibitors mentioned above by boiling at 95ºC for 5 min prior to gel loading.

For immunoprecipitation procedures, cells were lysed in radioimmunoprecipitation assay (RIPA) buffer, i.e. 10 mM Tris/Cl pH 7.5, 150 mM NaCl, 0.5 mM EDTA, 0.1% SDS, 1% NP-40, 0.5% deoxycholate plus protease and phosphatase inhibitors.

2.4.2 *Aspergillus nidulans* lysis

Total protein extracts of the *A. nidulans* strains used in this work were obtained from 200-250 mg of mycelium filtered through Miracloth (22-25 μm pore), drained, frozen in dry ice and lyophilized. The lyophilized mycelium was ruptured by a 10 second pulse in the FP120 Fast Prep Cell Disruptor (BIO101/Savant) at 4ºC using a 0.55 cm ceramic sphere. Pulverized mycelium was resuspended in alkaline lysis buffer containing 0.2 M NaOH and 0.2% β-mercaptoethanol. Proteins were precipitated by adding trichloroacetic acid to 7.5% and incubation on ice for 10 min. Samples were centrifuged at 14000 rpm for 5 min at 4 ºC and the resulting pellet was neutralized with Tris Base at 1 M. Laemmli sample buffer with protease inhibitors was added to samples, which were vortexed and boiled at 100ºC for 2 min prior to loading on 12.5% polyacrylamide gels containing 0.1% SDS.

2.5 Western blotting (WB)

Protein concentration was estimated by the BCA method. Volumes equivalent to 20 μg of protein were run on 12.5 or 15% SDS-polyacrylamide electrophoresis gels and transferred to Immobilon-P membranes using a semi-dry, Whatman filter-based method. The proteins of interest were visualized using an ECL detection system. Protein levels were estimated by image scanning of the ECL exposures and their values were corrected by the band intensities of the signal given by an antibody against a non-related protein, where indicated. Blots were quantified using ImageJ software (US National Institutes of Health, Bethesda, MD, USA).

Direct binding of DBB to recombinant proteins was assessed by visualization of the gel under UV light on a Gel-Doc XR Imaging System (Bio-Rad), as described (Sinz and Wang, 2001). Unbound DBB, which is essentially non-fluorescent, becomes fluorescent upon cysteine cross-linking (excitation maximum=385 nm, emission=477 nm).

2.6 Subcellular fractionation

For S100/P100 fractionation, total cell lysates were obtained by disrupting cells in the detergent-free buffer described above. Lysates were centrifuged at 1000xg for 5 min at 4 °C. Post-nuclear supernatants were further subjected to ultracentrifugation at 100,000xg for 1 h at 4 °C to obtain soluble and membrane cellular fractions. Supernatants (S100) were collected and pellets (P100) were resuspended in lysis buffer containing 1% NP-40 and 0.1% SDS. These fractions were loaded onto gels for WB, as described above.

2.7 Gene knock-down using siRNA

HeLa cells were depleted of ESCRT components the day after plating by transfection with 75 nM Hrs siRNA or 25 nM Tsg101 siRNA, and control cells were transfected with 50 nM scrambled (scr) siRNA using Lipofectamine RNAiMax according to the manufacturer's instructions. Cells were re-plated after 3 days, transfected with fluorescent constructs and grown for an additional 2 days before either live microscopy visualization or cell lysis and WB.

The following siRNA sequences were used:

Hrs: 5'-CGACAAGAACCCACACGUC-3'
Tsg101: 5'-CCGUUUAGAUCAAGAAGUAUU-3'

Scrambled siRNA was a double-stranded 21-mer RNA that does not correspond to any sequence encoded in the human genome.

2.8 Pull-down assays

GFP fusion proteins were immunoprecipitated using GFP-Trap agarose beads. After the described lysis, incubation with GFP-Trap took place for 1 h at 4°C. Beads were washed three times with detergent-free lysis buffer and eluted with Laemmli sample buffer for 10 min at 95°C. WB was performed on non-bound (not shown) and eluates as well as total lysates to assess protein retention.

2.9 Live cell microscopy

2.9.1 Confocal microscopy

For live visualization, cells were cultured on glass-bottom dishes, transfected with fluorescent constructs, treated with the indicated agents and visualized directly on a confocal microscope, either Leica DMRE2, Leica SP5 or Zeiss LSM 810 equipped with 405, 488, 568 and 642 nm diode lasers. Unless otherwise stated, images shown are single channels or overlays of single Z-sections for co-localization visualization. All experiments were repeated at least three times and representative results are shown. Scale bars represent 20 μm.

For live lysosome tracking, cells were stained with 25 nM LTR for 15 min at 37°C. When staining with other lysosomal or autophagosomal probes such as Lyso-ID or Cyto-ID, images were obtained shortly after staining to minimize loss of fluorescence. Care was taken to briefly observe cells under the UV lamp before imaging to minimize fading of the probes. Lyso-ID and Cyto-ID were diluted in the total volume of serum-free culture medium to be used for staining at 37 °C for 30 min to maintain endothelial cell morphology and viability during cell imaging. In experiments in which autophagy was induced by incubation of cells in EBSS, staining and washing (for autophagy reversion experiments) was also performed in this medium. In the case of Cyto-ID/LTR co-staining, LTR was added to the medium of cells that had been incubated with Cyto-ID for 15 min, left for an additional 15 min to co-stain and visualized immediately afterwards.

2.9.2 Super-resolution microscopy

In vivo super-resolution 3D structured illumination microscopy (SIM) imaging was performed on a Deltavision OMX V4 system (Applied Precision, GE Healthcare) equipped with an Olympus 60x NA 1.42 objective, cooled sCMOS cameras and 405, 488, 568 and 642 nm diode lasers. Z-stacks covering the whole cell were recorded with a Z-spacing of 125 nm. A total of 15 raw images (5 phases, 3 rotations) per plane were collected. Reconstruction and alignment of these raw images was performed using Softworx software (Applied Precision, GE Healthcare company).

2.9.3 Photoswitchable fluorescent protein tracking

Dendra-8 photoswitching and isoprenylation inhibition-and-release experiments were performed on transfected BAEC on glass-bottom dishes. The transfection medium was removed after 5 hours and replaced with serum-free medium with or without 10 μM simvastatin. Cells were observed 24 hours post-treatment on the Leica SP2 confocal microscope and photoswitching was performed by exposure to 405 nm UV light. The resulting green-to-red conversion was recorded in both channels. Simvastatin was either added or removed to the corresponding dishes in serum-free medium and photoconverted, red Dendra-8 was tracked 24 hours later by confocal microscopy.

2.9.4 *Aspergillus nidulans* microscopy

For microscopy experiments in *Aspergillus*, hyphae were cultured in Lab-Tek chambers (Thermo Fischer Scientific, 115411; 0.3 ml of medium per well) at 25–28°C in pH 6.5 'watch minimal medium' (WMM) containing 100 mM sodium acetate and 5 mM ammonium tartrate as carbon and nitrogen sources, respectively. Hyphae were visualized on an inverted fluorescence microscope (Leica DMI6000B) equipped with an EL6000 external light source with metal halide lamp epifluorescence excitation, driven by Metamorph® software (Molecular Dynamics) and coupled to a CCD camera (ORCA ER-II; Hamamatsu). Vacuoles were detected with CMAC.

2.9.5 Image analysis

Co-localization analysis was performed with LAS-AF software from Leica on single z-sections of images to obtain co-localization rates (expressed as percentages) and Pearson coefficients (coefficient r x 100). Alternatively, ImageJ (Fiji) software was used to obtain Pearson coefficients. At least 30 cells were analyzed per experimental condition. For stained cells, whole-field images were analyzed, whereas in the case of transfected cells, regions of interest (ROI) including transfected cells and excluding non-transfected cells were delimited prior to image analysis. Results are presented as mean co-localization rates or Pearson coefficients ± standard error of mean (SEM).

2.10 Immunofluorescence

For immunofluorescence with anti-giantin antibody, cells grown on glass bottom p35 were fixed in 4% paraformaldehyde for 20 min at room temperature (r.t.), washed twice in PBS and permeabilized with 0.05% saponin in PEM buffer (80 mM PIPES, 5 mM EGTA, 1 mM $MgCl_2$ pH 6.8) for 5 min. Incubation with anti-giantin at 1:500 dilution was carried out in PBS containing 0.05% saponin for 1h. After PBS washes, cells were incubated with anti-rabbit-Alexa 568 at 1:200 in 1% BSA in PBS for a further hour.

For filipin staining, fixed cells were washed 3× with PBS, incubated with 1.5 mg/mL glycine in PBS for 10 min at room temperature and subsequently with 0.05 mg/mL filipin in 10% normal goat serum in PBS for 2 h.

2.11 Mass spectrometry

Full-length H-Ras or RhoB protein or the H-Ras K170-K185 peptide were incubated at 5 μM in the presence of prostanoids, DBB or PAO at 50 μM or vehicle (DMSO) for 1 h. For some experiments, full-length protein incubation mixtures were then subjected to digestion with trypsin for 4 h at 37°C. Purification on ZipTip C18 (Millipore) was carried out prior to MALDI-TOF MS analysis on an AUTOFLEX III MALDI-TOF-TOF instrument (Bruker-Franzen Analytik) operated in the positive

mode, as reported in detail (Renedo et al., 2007). Selected peptides were further analyzed by MALDI-TOF-TOF MS-MS.

2.12 Statistical analysis

Data for WB quantification or co-localization analysis is shown as mean ± SEM of at least three independent experiments. Statistical significance was calculated by Student's *t* test for unpaired observations. A p value of less than 0.05 was considered significant and marked by asterisks, where indicated.

RESULTS

1. Structural determinants involved in RhoB endolysosomal localization

1.1 Subcellular localization of endosomal GTPases

Previous studies from the laboratory explored the subcellular localization of the small GTPase RhoB, as well as the pathways responsible for its degradation. In endothelial cells, RhoB is degraded through a lysosomal pathway, as discerned by treating cells with selective inhibitors of the major degradation pathways prior to protein analysis and microscopy studies (Pérez-Sala et al., 2009). Experiments with specific organelle markers using fluorescent RhoB fusion constructs showed RhoB association with late endosomal compartments, though their precise nature elicited further studies that are included within this section.

1.1.1 RhoB localization at endolysosomes

Several reports have shown that RhoB has a varied cell-type, activation- and lipidation-state dependent subcellular localization that comprises the plasma membrane, Golgi apparatus, early or late endosomes, MVB and lysosomes (Michaelson et al., 2001; Pérez-Sala et al., 2009; Rondanino et al., 2007; Wherlock et al., 2004). Therefore, studies were performed to define the basal subcellular localization of this GTPase under varying conditions in different cell types, as well as the structural determinants that elicit this pleiotropic distribution (Pérez-Sala et al., 2009; Valero et al., 2010). In order to do so, several fluorescent constructs of wild-type RhoB, i.e. GFP-RhoB, tRFP-T-RhoB, and mCherry-RhoB were transiently transfected into cells such as BAEC, human primary fibroblasts, HeLa cells, and others.

In BAEC, GFP-RhoB as well as a variety of specific organelle markers was employed to outline the subcellular fate of this GTPase, as shown in Figure 12. Cells were treated with the amphiphilic amino-steroid, U18666A, as a pharmacological tool to alter late endocytic lipid dynamics and induce membrane invagination into MVB, which results in enlarged endolysosomes (Marchetti et al., 2004; Sobo et al., 2007).

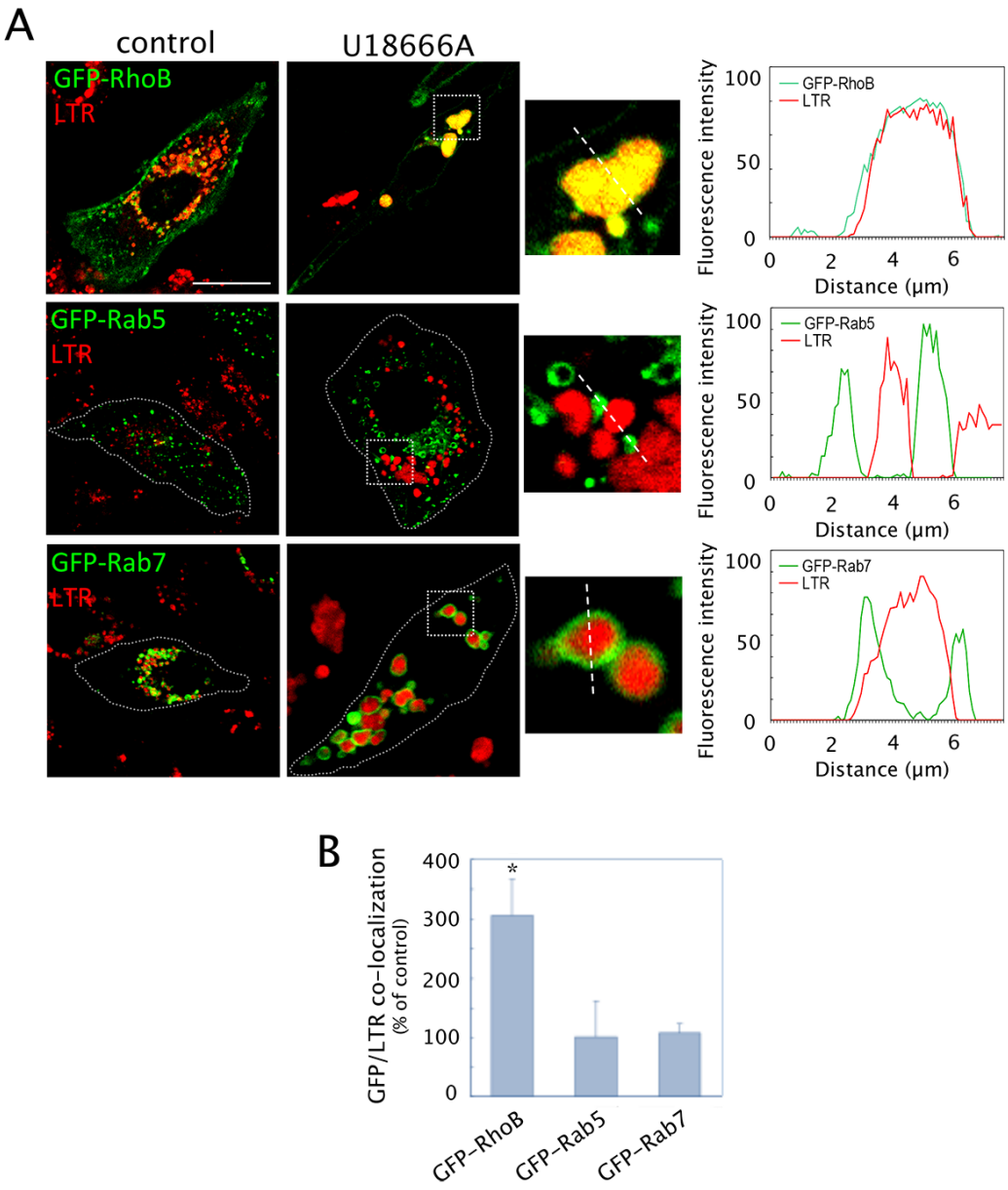

Figure 12. Subcellular distribution of GTPases following U18666A treatment.

(A) BAEC transfected with the indicated constructs were treated with U18666A as described in Methods, stained with LTR and observed live by confocal microscopy. Insets show zoom-ins of areas with dashed lines, from which profiles are derived (right panels). (B) GFP and LTR co-localization in U18666A-treated cells is used as an indicator of internalization into acidic compartments, expressed as percentage of the values compared to untreated cells. *p < 0.05 versus the same condition in the absence of U18666A.

Staining of the endolysosomal lumen is commonly performed using LysoTracker® Red (LTR), which is a widely used cationic amphiphilic drug that marks acidic compartments (Chazotte, 2011). GFP-RhoB amply co-localizes with this probe in many cell types including BAEC (Figure 12), particularly after treatment with U18666A.

In sharp contrast, a fusion protein of the early endosomal Rab5 (Bucci et al., 1992), used to mark membranes of early endosomes, does not appear at dilated endolysosomes induced by U18666A, as shown in Figure 12 by its lack of co-localization with LTR. In line with the above results, GFP-Rab5 does not co-localize with RhoB constructs (Pérez-Sala et al., 2009). However, fluorescently tagged Rab7, which has been shown to accumulate at late endocytic vesicles (Bucci et al., 2000), is present on endolysosomes, though retained at their limiting edge (Figure 12A, see profiles). As summarized from several works in Figure 13, endolysosomes containing RhoB constructs are also marked by late endocytic markers such as GFP-Rab9, Lamp1-GFP, LBPA, or cholesterol, but not considerably by the recycling endosome component, GFP-Rab11 (Patterson and Lippincott-Schwartz, 2002; Pérez-Sala et al., 2009; Ullrich et al., 1996; Valero et al., 2010).

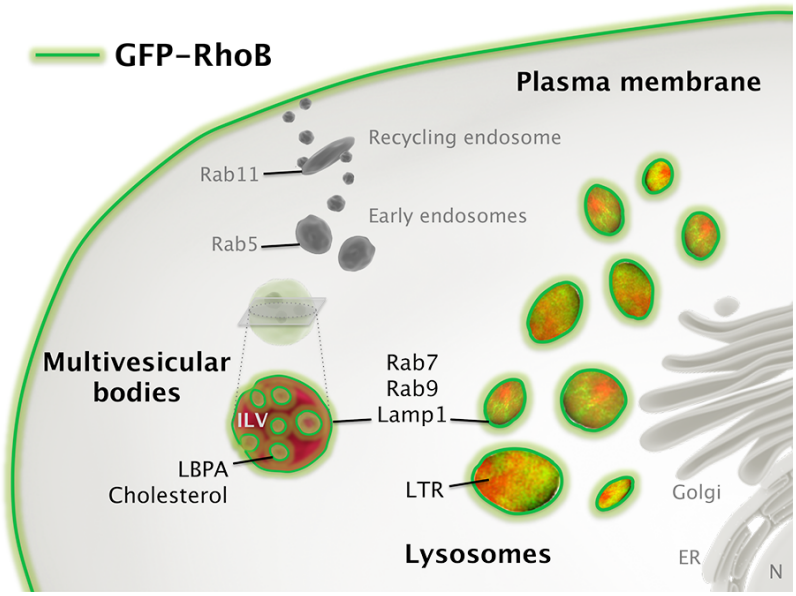

Figure 13. Schematic summary of GFP-RhoB subcellular localization.

A summary of previous work is shown here for conciseness. Full-length RhoB tagged with GFP is present at localizations depicted in green but not at those in gray. An orthogonal section of a model MVB shows its luminal content, where GFP-RhoB co-localizes with LBPA antibodies and cholesterol (stained by filipin). Likewise, the limiting membranes of both MVB and lysosomes have been found to be marked by fluorescent constructs of Rab7, Rab9 and Lamp1 that coincide with the presence of GFP-RhoB. In the lumen of MVB and lysosomes, LTR is found to co-localize with GFP-RhoB, eliciting a patchy, yellowish, red-to-green varied coloration. However, RhoB constructs tend not to overlap with the early endosomal component Rab5 or with Rab11 residing at recycling endosomes. See text for further details. ER, endoplasmic reticulum; N, nucleus.

Making use of these varied protein and lipid markers, it becomes evident that RhoB constructs appear at very specific subcellular sites, namely late endocytic vesicles such as MVB, as well as the lysosomal lumen, with varying degrees of plasma membrane localization (Figure 13).

1.1.2 Small GTPase C-terminal sequences in subcellular localization

Previous studies from our group established that RhoB degradation *via* the endolysosomal pathway is dependent on the full lipidation of its hypervariable C-terminus, i.e. isoprenylation and bipalmitoylation (Pérez-Sala et al., 2009; Stamatakis et al., 2002). However, several other small GTPases are similarly modified by these three lipids at their C-terminal sequences, as shown in Table 3, namely TC10, H-Ras, Rap2A or Rap2B.

Ras GTPase	C-terminal sequence
RhoB	-VREVF-ETATRAAL--------QKRYGSQNGCINCCKVL
TC10	-LKTVFDEAIIAILTP-KKH---TVKKRIGSRCINCCLIT
H-Ras	-VEDAFYTLV-REIRQHKLRKLNPPDESGPGCMSCKCVLS
Rap2A	-VDELFAEIV-RQMNY-------AAQPDKDDPCCSACNIQ
Rap2B	-VDELFAEIV-RQMNY-------AAQPNGDEGCCSACVIL

Table 3. C-terminal sequences of isoprenylated and bipalmitoylated GTPases.

Hypervariable regions of several small GTPases that are isoprenylated at their CAAX cysteine, shown in green, and palmitoylated at two other cysteines further upstream, shown in red. Residues removed by CAAX box proteolysis are shown in gray and basic residues are depicted in blue.

The spacing of cysteines amenable to lipidation, as well as the nature of the amino acids between them, differs among these proteins (Table 3). To explore the subcellular destination of these GTPases, fluorescent constructs were expressed in BAEC and observed by confocal microscopy. Figure 14 shows the localization of these constructs under basal conditions and upon treatment with U18666A compared to that of GFP-RhoB. An H-Ras construct shows predominant plasma membrane localization instead of accumulation at endolysosomes (Figure 14). This behavior could be due to the fact that the two amino acids between the palmitoylatable cysteines in H-Ras are

different than those of RhoB. In the case of Rap2 proteins, they become palmitoylated at contiguous cysteines, whereas RhoB contains two amino acids that separate these cysteines. As shown in Figure 14, this sequence elicits GFP-Rap2B accumulation at the limiting membrane of dilated endolysosomes, resulting in lower co-localization with LTR compared to GFP-RhoB. Therefore, though these GTPases are all isoprenylated and bipalmitoylated, differences in their lipidation sequences or other determinants could confer differential subcellular localization.

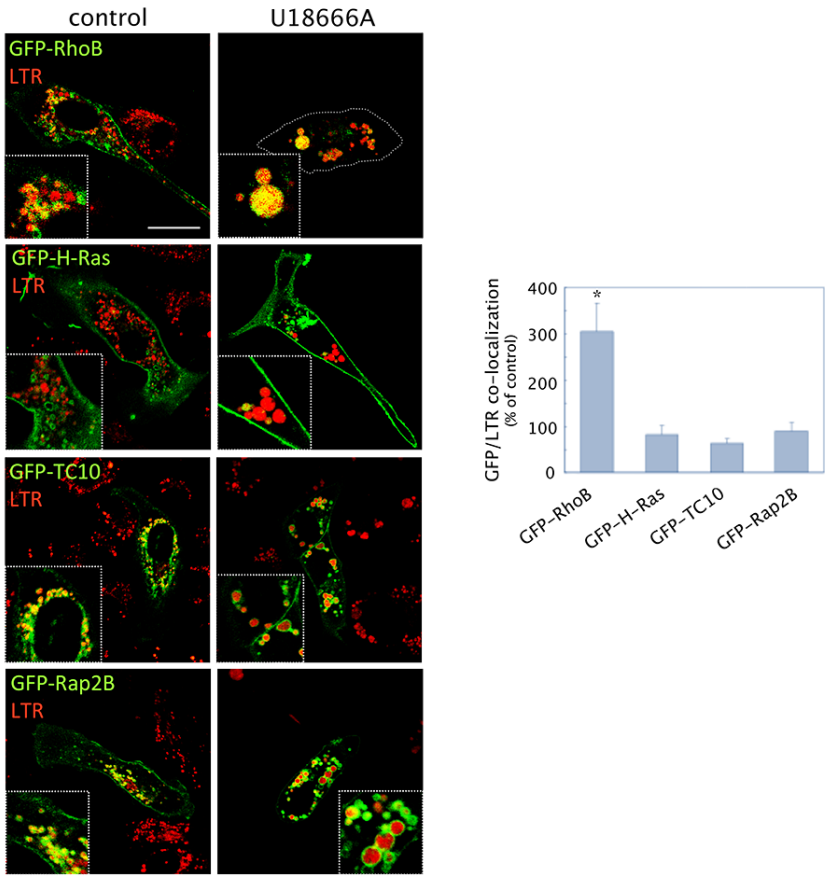

Figure 14. Localization of isoprenylated and bipalmitoylated GTPases.

BAEC transfected with the indicated constructs were treated as in Figure 12. Zoom-ins are shown in the insets. Co-localization of GFP and LTR signals was assessed as in Figure 12. *p < 0.05 versus the same condition in the absence of U18666A by Student's t-test.

RhoB and TC10 are highly homologous proteins (68% homology, 52% identity) with obvious differences in the –AAX amino acids of the CAAX box, as well as in the hypervariable region, with more basic residues present in TC10 but not RhoB. Nevertheless, their lipidation sequences are highly similar. Remarkably, when

comparing these proteins, TC10 is retained at the limiting membrane of late endocytic vesicles, instead of inside their lumen, as seen for RhoB constructs (Figure 14).

In order to study the structural determinants responsible for the differences observed between TC10 and RhoB constructs, protein chimeras of GFP fused to the last eight amino acids of these GTPases at its C-terminus were generated. Taking into account that the last three amino acids of these sequences would be cleaved after isoprenylation, the remaining sequences would be identical, as seen in Table 3. Moreover, since both CAAX boxes can undergo isoprenylation by either farnesyl or geranylgeranyl, the resulting lipidated chimeric proteins could become completely alike. Therefore, the chimeric proteins GFP-CINCCKVL (a.k.a. GFP-8, derived from RhoB, extensively described in the next section) and GFP-CINCCLIT (referred to as GFP-8-TC10) become identical once the cysteines have been lipidated. Indeed, as shown in Figure 15, the localization patterns of GFP-8 and GFP-8-TC10 are indistinguishable both in control cells and after U18666A treatment.

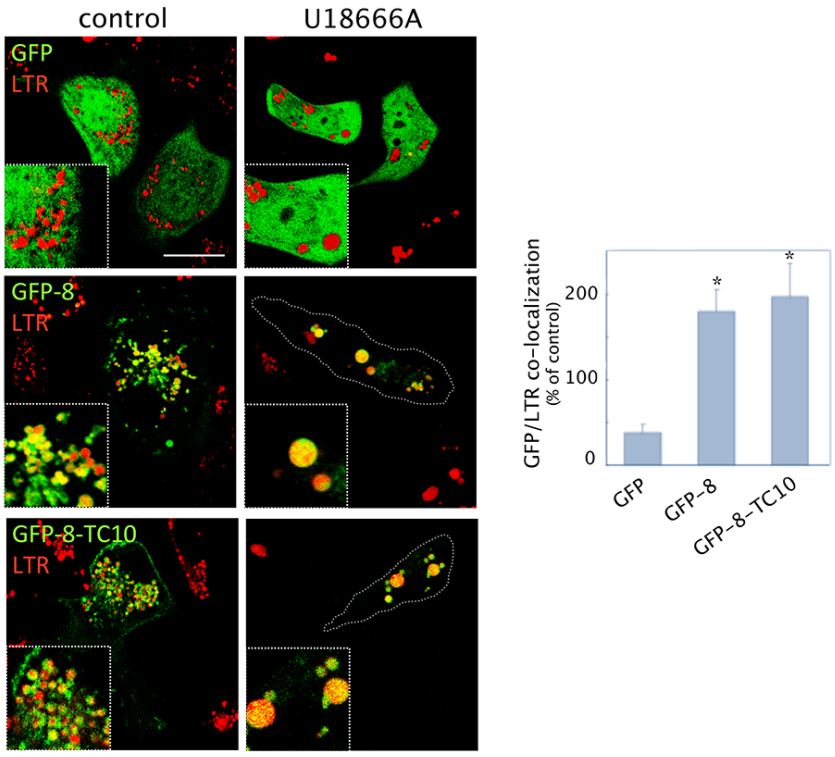

Figure 15. Localization of chimeric proteins derived from the RhoB or TC10 C-terminus.

BAEC were transfected with constructs obtained by fusing the last eight amino acids of RhoB (GFP-8) or TC10 (GFP-8-TC10) to the C-terminus of GFP, treated with U18666A, stained with LTR and visualized live by confocal microscopy. The graph shows GFP and LTR co-localization, as above. *$p < 0.05$ versus the same condition in the absence of U18666A.

In light of the results above, the TC10 sequence must contain a sorting motif upstream of these last amino acids that is responsible for full-length TC10 accumulation at the limiting membrane of MVB, as opposed to GFP-8-TC10 predominant localization inside endolysosomes. Indeed, TC10 contains a basic amino acid patch, "-KKH", that hinders its entry into the lumen of late endocytic compartments (Table 3). As seen in Figure 16, mutation of the basic amino acid patch in TC10 (TC10 NQN, Figure 16A) promotes entry into the endolysosomal lumen, as reflected by a significant increase in co-localization with LTR upon U18666A treatment (Figure 16C). Conversely, insertion of the basic amino acid patch into the RhoB sequence (RhoB KKH, Figure 16A) retains this chimera at the limiting membrane of endolysosomes (Figure 16B).

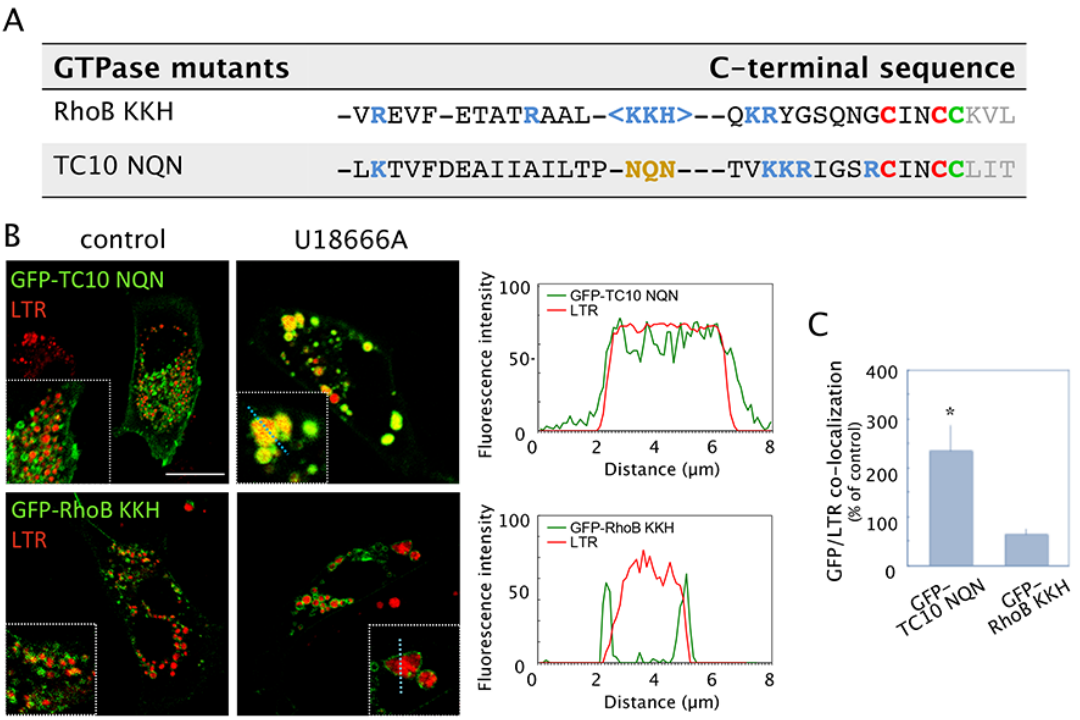

Figure 16. Role of basic residues in the hypervariable regions of TC10 and RhoB in subcellular localization.

(A) Sequences of the GTPase mutants generated by introducing either a basic residue patch (blue, in brackets) into RhoB (RhoB KKH) or a neutral amino acid patch (in yellow) into TC10 (TC10 NQN). Isoprenylation cysteines are shown in green and palmitoylation cysteines in red. (B) BAEC transfected with the indicated constructs were treated as above. Insets show zoom-ins of areas with dashed lines, from which profiles are derived (right panels). (C) GFP and LTR co-localization in U18666A-treated cells was assessed as above. *$p < 0.05$ versus the same condition in the absence of U18666A.

Therefore, fine-tuned regulation of small GTPase subcellular localization is determined by isoprenylation or palmitoylation cysteines and charged or uncharged amino acids positioned at strictly specific positions within their hypervariable C-terminal regions. The basic amino acids in TC10 "rescue" the protein from lysosomal degradation. Since this motif is not present in RhoB, it is constitutively sent towards the lysosome. However, posttranslational modifications altering the charge or the interactions of the hypervariable sequence of RhoB could hinder its entry into the degradative compartments and change its localization and/or degradation patterns.

1.2 RhoB C-terminus: CINCCKVL

1.2.1 Co-localization with endocytic markers

Studies from the laboratory using BAEC and chimeric fluorescent proteins bearing sequentially smaller parts of the RhoB sequence at their C-terminal end, from the last 22, 8 to 4 amino acids, determined that the minimum sequence eliciting endolysosomal localization and degradation corresponds to the motif that includes all three lipidated cysteines and the –CAAX box, namely –CINCCKVL (GFP-8) (Pérez-Sala et al., 2009). Since subcellular localization mechanisms are finely regulated and may be cell type-dependent, localization of GFP-8 was studied in greater detail in several additional cell types.

As shown in Figure 17, in human primary fibroblasts under resting conditions, co-transfection of tRFP-T-CINCCKVL (tRFP-T-8) with the fluorescent constructs of several endocytic components highlighted the appearance of tRFP-T-8 inside vesicles surrounded by GFP-Rab7 and Lamp1-GFP. Only marginal co-localization of tRFP-T-8 was observed with GFP-Rab11, which is used as a recycling endosome marker (Ullrich et al., 1996). Co-localization with the early endosome marker, GFP-Rab5 was negligible. Therefore, as seen for GFP-8 in BAEC, tRFP-T-8 in human fibroblasts displays a predominantly luminal endolysosomal localization, as deduced from the profiles in Figure 17.

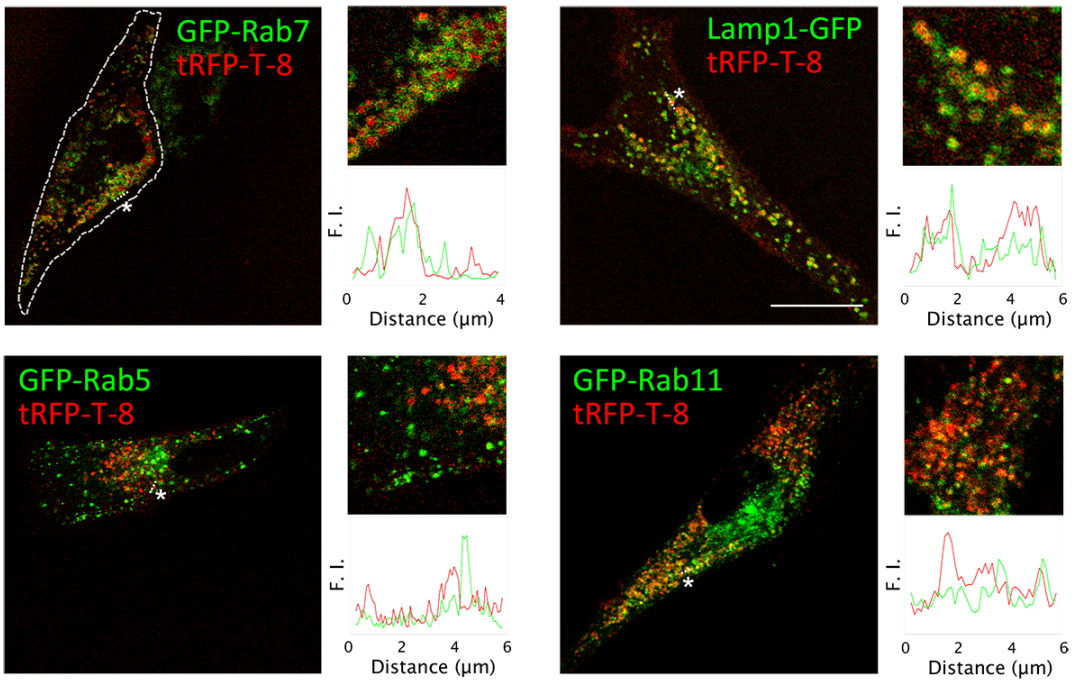

Figure 17. Localization of CINCCKVL chimeras in human primary fibroblasts

Human primary fibroblasts were co-transfected with tRFP-T-8 and the indicated endocytic membrane markers and observed live by confocal microscopy after 16 h in serum-depleted medium. Zoom-ins of original pictures and fluorescence intensity profiles along a section (marked by dotted lines and asterisks) appear to the right of every condition. F.I., fluorescence intensity.

The association of CINCCKVL chimeras with endolysosomal compartments was also confirmed in the widely used human adenocarcinoma cell line, HeLa. Similarly to the results shown in primary fibroblasts, tRFP-T-8 appeared inside Lamp1-GFP-positive vesicles in this cell line (Oeste et al., 2014). The specific localization of CINCCKVL chimeras in the context of endolysosomes was further pinpointed by co-transfecting HeLa with GFP-8 and the mCherry fluorescent construct of CD63, which is used as a marker of ILV of MVB. As described in the Introduction, different populations of ILV could exist within MVB (Edgar et al., 2014). However, the resolution provided by confocal microscopy is not able to discern discrete ILV, so that localization at these small vesicles appears as luminal fluorescence within endolysosomes. As seen in Figure 18, of all the probes and fluorescent proteins used to characterize CINCCKVL chimeras, mCherry-CD63 displayed the highest degree of co-localization (Pearson coefficient = 0.77 ± 0.015).

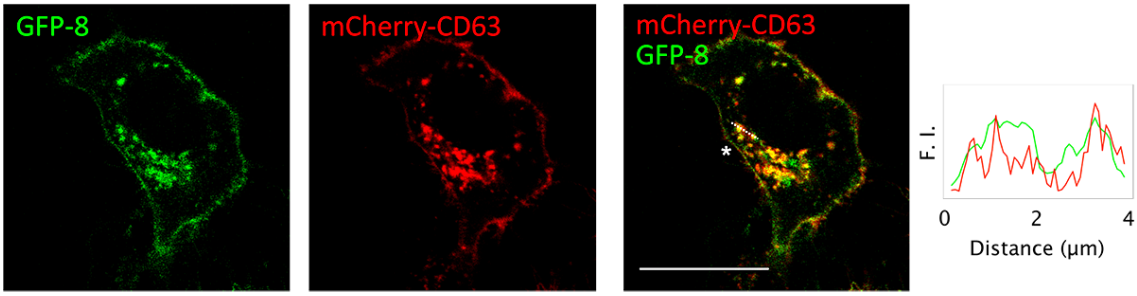

Figure 18. GFP-8 co-localization with the MVB marker, mCherry-CD63.

HeLa cells were co-transfected with GFP-8 and mCherry-CD63 and cultured in serum-depleted medium for 16 h prior to live confocal fluorescence microscopy. Fluorescence intensity profiles along a section (marked by dotted lines and asterisks) appear to the right of the overlay. F.I., fluorescence intensity.

A closer look at these specific structures was obtained using higher resolution *in vivo* three-dimension structured illumination microscopy (SIM), which provides super-resolution imaging, as seen in Figure 19.

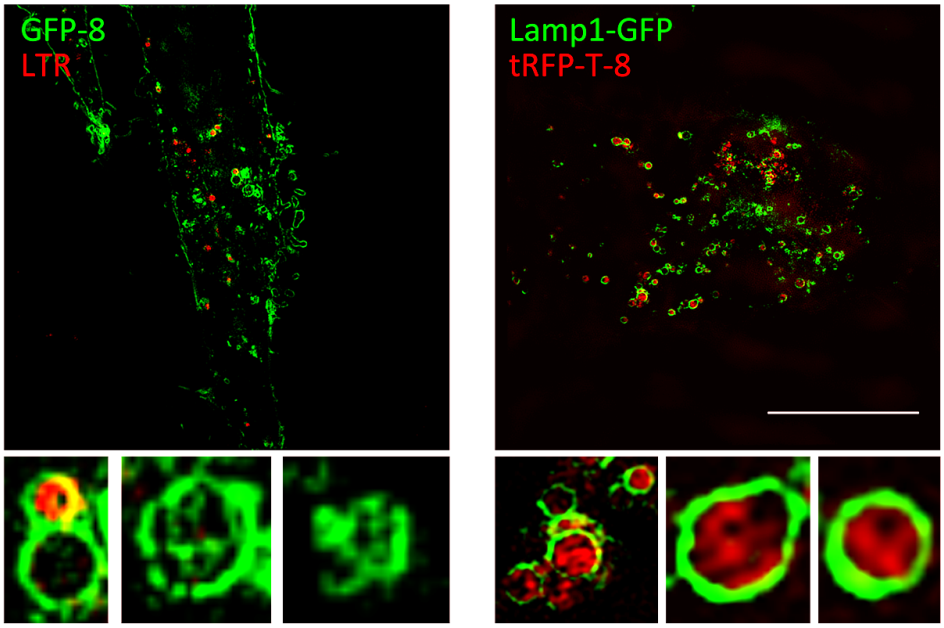

Figure 19. Super-resolution imaging of CINCCKVL chimeras.

HeLa cells were transiently transfected with the indicated constructs and stained with LTR as indicated in the Methods section, prior to live super-resolution microscopy. Lower panels show zoom-ins of compartments with internal vesicles marked by CINCCKVL constructs.

HeLa cells transfected with either GFP-8 or tRFP-T-8 revealed the unequivocal presence of these chimeras in vesicles consistent with ILV of MVB (Figure 19). Inside these compartments, whereas tRFP-T-8 showed a more diffuse pattern, GFP-8 outlined

the inner membranes, which could be due to the decrease in GFP fluorescence resulting from its quenching in acidic pH environments (Kneen et al., 1998). It is thus apparent that the –CINCCKVL sequence can target proteins to specific domains of endolysosomes, some of which are ultimately internalized to form vesicles inside MVB.

1.2.2 Lack of –CINCCKVL chimera co-localization with autophagy markers

As mentioned earlier, -CINCCKVL-mediated RhoB sorting to endolysosomes results in rapid lysosomal degradation, a behavior that also holds for other chimeras with this sequence attached to their C-terminal ends (Pérez-Sala et al., 2009). Considering the lysosomal degradation fate of RhoB and CINCCKVL chimeras as well as the high degree of intracellular crosstalk between endolysosomal and autophagic pathways, autophagy could be involved in breakdown of this GTPase and related constructs. This degradation pathway is often monitored by microscopy in live cells using constructs of the microtubule-associated protein 1 light chain 3 protein, LC3 (Bampton et al., 2005), as shown in Figure 20.

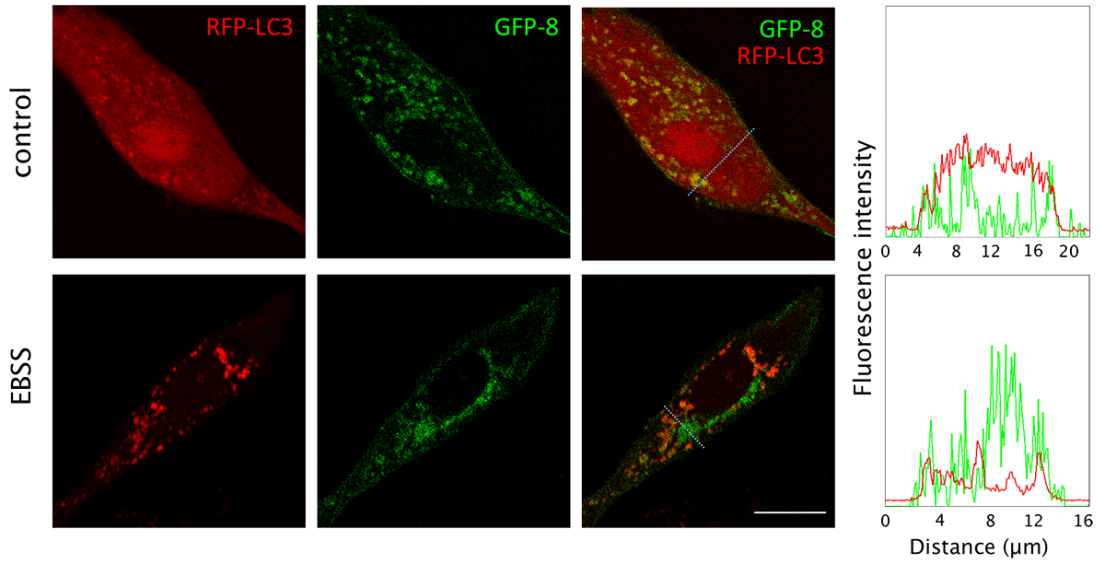

Figure 20. Lack of co-localization between GFP-8 and the autophagic probe, RFP-LC3.

BAEC were co-transfected with GFP-8 and RFP-LC3 and incubated in serum-free medium (control) or amino acid-depleted medium (EBSS) for 20 h prior to live confocal visualization. The right panels show fluorescence intensity of the single channels along the lines pictured in the images.

Upon autophagy induction by e.g. amino acid depletion, LC3 becomes lipidated by a phosphatidylethanolamine moiety, forming LC3-II (Barth et al., 2010; Kabeya et al., 2000; Mizushima and Yoshimori, 2007), which attaches to autophagosomal membranes that can be readily detected by fluorescence microscopy (Barth et al., 2010; Mizushima et al., 2010). Taking advantage of this behavior, RFP-LC3 was co-transfected with GFP-8 in BAEC (Figure 20), in which the autophagic pathway had not yet been described or characterized. We observed that, under normal cell culture conditions, RFP-LC3 showed a diffuse distribution. Following autophagy induction by incubation in the amino-acid free medium, Earle's Balanced Salt Solution (EBSS), RFP-LC3 adopted a punctate pattern characteristic of autophagosome formation. Remarkably, co-localization of GFP-8 with RFP-LC3 was negligible under both conditions, as shown in Figure 20. A similar lack of co-localization with other autophagy markers such as monodansylcadaverine or CytoID was also observed (Oeste et al., 2013). These results indicate that GFP-8 and LC3-positive vesicles are distinct entities, namely endolysosomes and autophagosomes, so that GFP-8 incorporation into the autophagic pathway is unlikely.

1.2.3 CINCCKVL chimera endolysosomal localization depends on lipid modifications

Membrane association of full-length, endogenous RhoB depends on a series of modifications at its C-terminus, including irreversible isoprenylation and reversible bipalmitoylation (Adamson et al., 1992). To confirm whether this is the case for CINCCKVL chimeras, mutants corresponding to the cysteine residues amenable to lipid modification were used in fractionation and microscopy studies. Cells transfected with GFP constructs of these mutants were subjected to whole cell lysis (Figure 21, upper panels) or subcellular fractionation (Figure 21, lower panels) into S-100 (soluble) or P-100 (membrane) fractions to assess the extent of membrane attachment. WB analysis showed that untagged GFP was fully soluble, whereas GFP-8 was detectable only in the membrane fraction. Cysteine mutants that cannot be isoprenylated (GFP-8-C244S) or palmitoylated (GFP-8-C241,243S) and therefore have restricted access to membranes appear mostly in the soluble fraction, with minimal membrane association. Of note,

lower levels of GFP-8 than of GFP or the mutated constructs were detected in whole cell lysates (Figure 21, upper panels), consistent with a rapid turnover of this endolysosome-targeted protein.

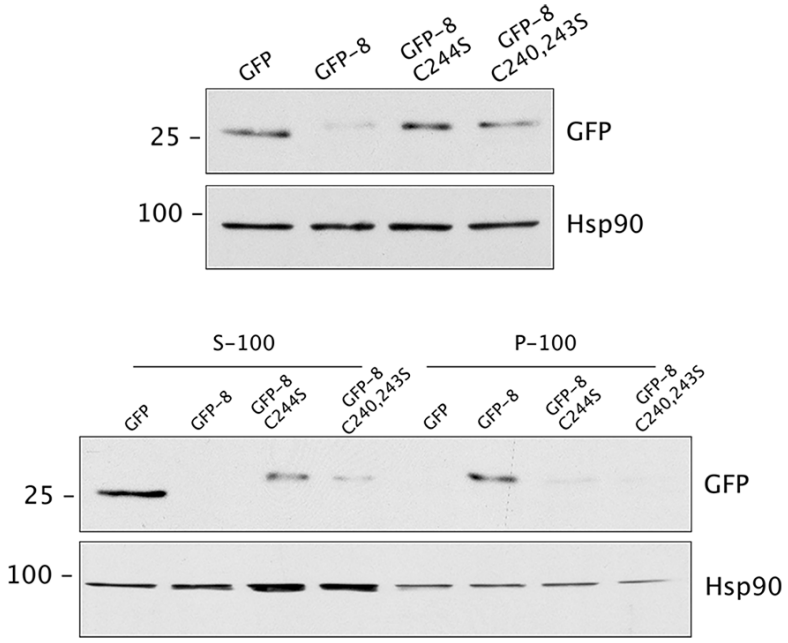

Figure 21. Subcellular fractionation of GFP-8 posttranslational modification mutants.

HeLa cells were transfected with GFP-8 or its indicated lipidation-deficient cysteine mutants. Cell lysis and fractionation were performed as described in the Methods section. Upper panels show total cell lysates whereas lower panels correspond to chimeric protein levels in the soluble (S-100) or particulate (P-100) fraction, assessed by WB with an anti-GFP antibody. Hsp90 was used as a loading control and 25 or 100 kDa markers are shown for electrophoretic mobility reference.

In order to study membrane localization of CINCCKVL cysteine mutants, confocal microscopy studies were carried out. In contrast to the high degree of localization between GFP-8 and LTR (co-localization rate: 62.6±2.5%), the palmitoylation-deficient mutant GFP-8-C241,243S presents a cytosolic distribution that excludes the nucleus (Figure 22), as expected for a mono-prenylated construct bearing only a CAAX box (Pérez-Sala et al., 2009). Furthermore, the isoprenylation mutant (GFP-8-C244S) appears as a cytosolic, non-lipidated protein that excludes some small organelles, thus following a pattern indistinguishable from that of untagged GFP (Figure 22, last two panels). This last construct does indeed contain the palmitoylation cysteines, but the fact that it does not associate with membranes indicates the dependence of palmitoylation on previous isoprenylation and CAAX processing (Wang and Sebti, 2005).

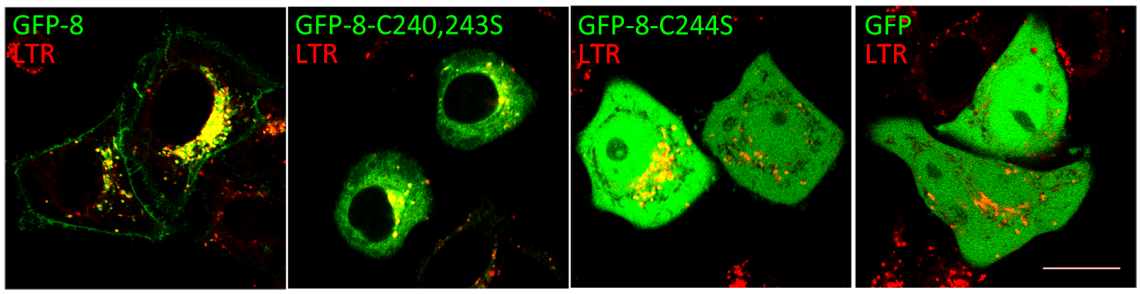

Figure 22. Endolysosomal localization of GFP-8 depends on posttranslational lipidation.

HeLa cells were transfected with GFP-8, its palmitoylation-deficient mutant (GFP-8-C240,243S), the isoprenylation-deficient mutant (GFP-8-C244S), or untagged GFP. Cells were stained with LTR prior to live confocal microscopy observation.

It has been previously described for several Ras family members that they shuttle from the plasma membrane to the Golgi in a palmitoylation-dependent manner (Rocks et al., 2005). Indeed, whereas GFP-8 did not present high co-localization with the Golgi protein giantin (Figure 23, first panel), in the case of the isoprenylated but palmitoylation-deficient mutant GFP-8-C241,243S, cells contained cytoplasmic accumulations that co-localized to a greater extent with the Golgi (Figure 23, second panel). In turn, the isoprenylation mutant as well as untagged GFP showed a similar pattern in which Golgi localization was only partial and collateral to its diffuse distribution (Figure 23, last two panels). Therefore, Golgi localization of GFP-8 probably occurs transiently when its CAAX motif has been isoprenylated and awaits further processing through bipalmitoylation.

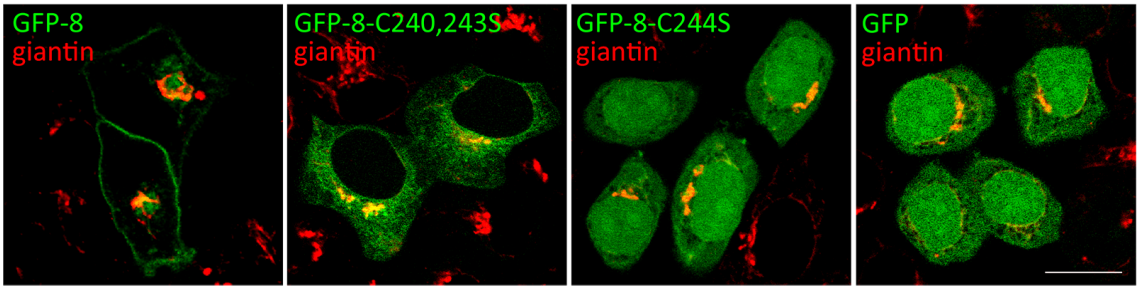

Figure 23. Golgi staining of cells transfected with GFP-8 and its lipidation mutants.

HeLa cells were transfected with the indicated constructs and fixed after 16 h in serum-depleted medium. The Golgi compartment was marked by immunofluorescence using anti-giantin antibodies, as explained in Methods.

As a proof of concept, GFP-8 isoprenylation and palmitoylation inhibition were carried out pharmacologically rather than through cysteine mutation. Treatment with

2-bromopalmitate to block palmitoylation elicited a GFP-8 subcellular localization similar to the corresponding mutant, i.e. diffuse cytosolic and excluding the nucleus (Figure 24A, left panel). Similarly, simvastatin treatment for inhibition of isoprenoid biosynthesis resulted in a totally diffuse pattern, as observed for the equivalent cysteine mutation (Figure 24A, right panel). It is hence possible to pharmacologically modulate the selective localization of CINCCKVL proteins to subcellular membranes by inhibiting lipidation of the C-terminal cysteines.

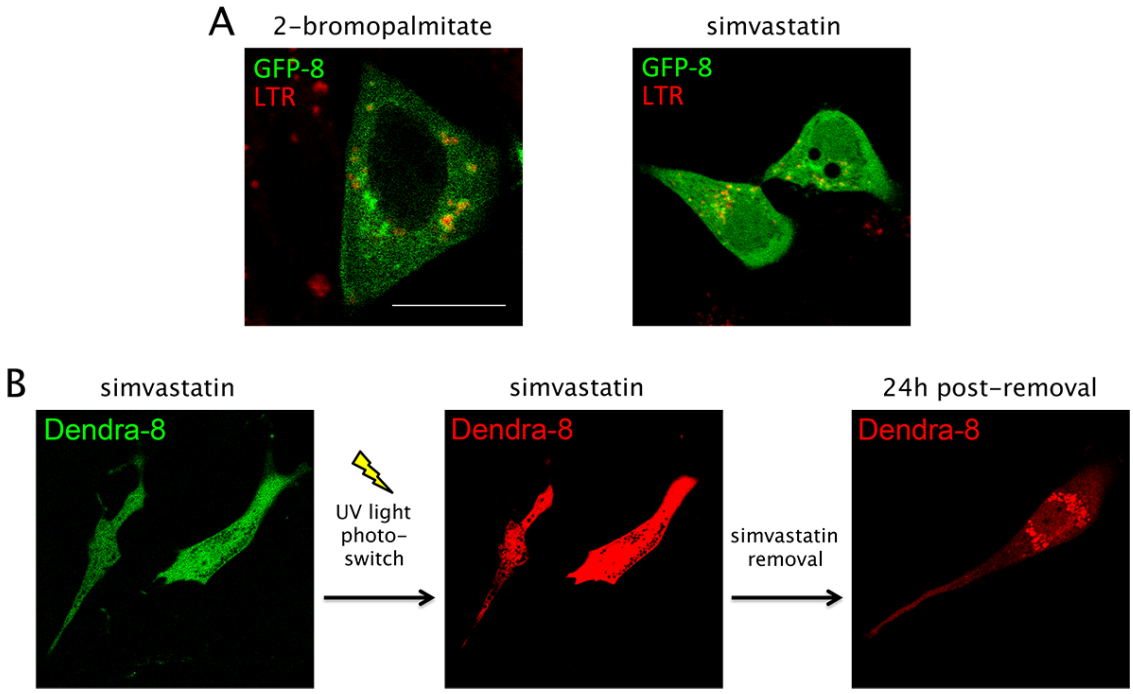

Figure 24. Lipidation inhibition by pharmacological treatment of cells expressing CINCCKVL-chimeras.

(A) HeLa cells were transfected with GFP-8 and treated with 2-bromopalmitate to inhibit palmitoylation or simvastatin to block isoprenylation, as described in Methods, prior to LTR staining and live observation under a confocal microscope. (B) BAEC were transfected with Dendra-8 and treated with simvastatin for 24 h (left panel) prior to UV light exposure to induce green-to-red photoswitching (middle panel). Simvastatin was removed directly after photoswitching and 24 h later subcellular localization of the photoconverted red protein was monitored (right panel).

A question that remains unanswered in this field is whether lipid posttranslational modifications occur only on newly synthesized proteins, or whether a previously existing pool of non-lipidated protein in the cytosol can be processed and subsequently attach to membranes. As seen above, simvastatin treatment elicits a fully cytosolic population of GFP-8 and can therefore be used to address this issue.

Furthermore, the photoswitchable fluorescent protein Dendra2 switches from green to red fluorescence emission after UV light exposure and can be used to track transfected cells before and after photoexcitation. Taking advantage of these tools, BAEC were transfected with a Dendra2-CINCCKVL fusion protein (Dendra-8) and treated with simvastatin to obtain a pool of green, fully cytosolic construct with no lipid modifications (Figure 24B, left). Specific cells were then exposed to UV light on a confocal microscope for photoswitching, providing a pool of red, unprocessed Dendra-8 to be followed (Figure 24B, middle). Simvastatin was removed immediately following green to red conversion to release isoprenylation inhibition, which, as shown in Figure 24, right, allowed endolysosomal targeting of the red protein that had previously been diffuse throughout the cytosol. Therefore, pre-existing cytosolic CINCCKVL proteins may be sorted to endolysosomal localizations upon C-terminal processing, indicating that this process does not need to occur directly on nascent proteins.

1.3 CINCCKVL sorting is conserved from fungi to human cell models

We have shown that RhoB and CINCCKVL-chimeric proteins are targeted to endolysosomal membranes in several mammalian cell types, including human primary fibroblasts, HeLa cells or BAEC. This behavior is consistent with the fact that the C-terminal sequence of RhoB is conserved in mammalian species and birds (Table 4), which must necessarily contain the cellular machinery required for RhoB sorting. However, organisms from other branches of evolution contain either a RhoB protein with a different C-terminal sequence or Ras- or Rho-related proteins with similarities to RhoB that have not been identified as *bona fide* RhoB homologs (Table 4). These proteins contain CAAX boxes and nearby cysteines that could become palmitoylated, but the different spacing between these residues along with other structural determinants could elicit unique subcellular localization patterns, as seen in Section 1.1 for other GTPases. It was therefore uncertain whether non-mammalian organisms that do not present the CINCCKVL sequence in any of their proteins could sort these chimeras to their specific endolysosomal/MVB destinations.

Species	Protein	Accession no.	C-terminal sequence
(synthetic construct)	**GFP-8**	N/A	TAAGITLGMDELYKCINCCKVL
(synthetic construct)	**tRFP-T-8**	N/A	RYCDLPSKLGHKLNCINCCKVL
Homo sapiens	RhoB	NM_004040	TRAALQKRYGSQNGCINCCKVL
Bos taurus	RhoB	NM_001077922	TRAALQKRYGSQNGCINCCKVL
Mus musculus	RhoB	AF481943	TRAALQKRYGSQNGCINCCKVL
Gallus gallus	RhoB	NM_204909.1	TRAALQKRYGTQNGCINCCKVL
Xenopus laevis	RhoB	NM_001096461.1	TRAALQKKHGRSGECMSCCKLL
Drosophila mojavensis	uncharacterized	CH933808.1	TRASLQVKKRKKRSGCWSLSCKLL
Schizosaccharomyces pombe	Rho2	NM_001019998.3	TRAALTVRDSENDKSSTKCCIIS
Aspergillus fumigatus	RasA	XM_748433	TRAPEGKMDVSEPGDNAGCCGKCVIM
Aspergillus nidulans	uncharacterized	AN4953	TRAALLTFDKRKSSCCIVL

Table 4. C-terminal sequences of CINCCKVL chimeras, RhoB homologs and related proteins from diverse species.

On top, the C-terminal sequences of GFP-8 and tRFP-T-8 are shown. Below, several RhoB homologs or related proteins along with their PubMed accession numbers and their C-terminal sequences. In red, potential palmitoylation sites. In green, isoprenylation cysteines.

1.3.1 CINCCKVL sorting in amphibian and insect cells

Within the genome of the amphibian *Xenopus laevis*, an endogenous RhoB protein is encoded with a C-terminal sequence that encloses several distinct structural features (Table 4). Though it presents a very similar CAAX box and two cysteines spaced similarly to human RhoB, the two amino acids between the palmitoylatable cysteines differ. Where human RhoB reads “IN”, *Xenopus* RhoB contains the amino acids “MS”, similarly to the H-Ras sequence that elicits binding to the plasma membrane, primarily. Furthermore, *Xenopus* RhoB contains the basic amino acid patch “KKH” upstream of the lipidated cysteines, reminiscent of the human TC10 protein, which is retained at the limiting membrane of endolysosomes. The effect of these unique structural determinants was assessed by transfection of *Xenopus* epithelial A6 cells with GFP tagged *Xenopus* RhoB (GFP-RhoB X), as seen in Figure 25A, left panel. Compared to the typical endolysosomal localization of GFP-8 (Figure 25A, middle panel) and consistent with its H-Ras- and TC10-like motifs, GFP-RhoB X appears mainly at the plasma membrane and scarcely at endolysosomes, as underscored by its low co-localization with LTR (Figure 25A, right panel). However, human GFP-RhoB and tRFP-T-8 are still sorted to endolysosomes, as gathered from their mutual co-localization as well as overlap of the latter with Lamp1-GFP (Figure 25B).

It is thus apparent that the combination of sorting motifs in *Xenopus* RhoB elicits a localization pattern distinct from both human RhoB and CINCCKVL chimeras. Nevertheless, *Xenopus* cells are able to sort proteins derived from the human RhoB C-terminus though they do not code for this sequence endogenously.

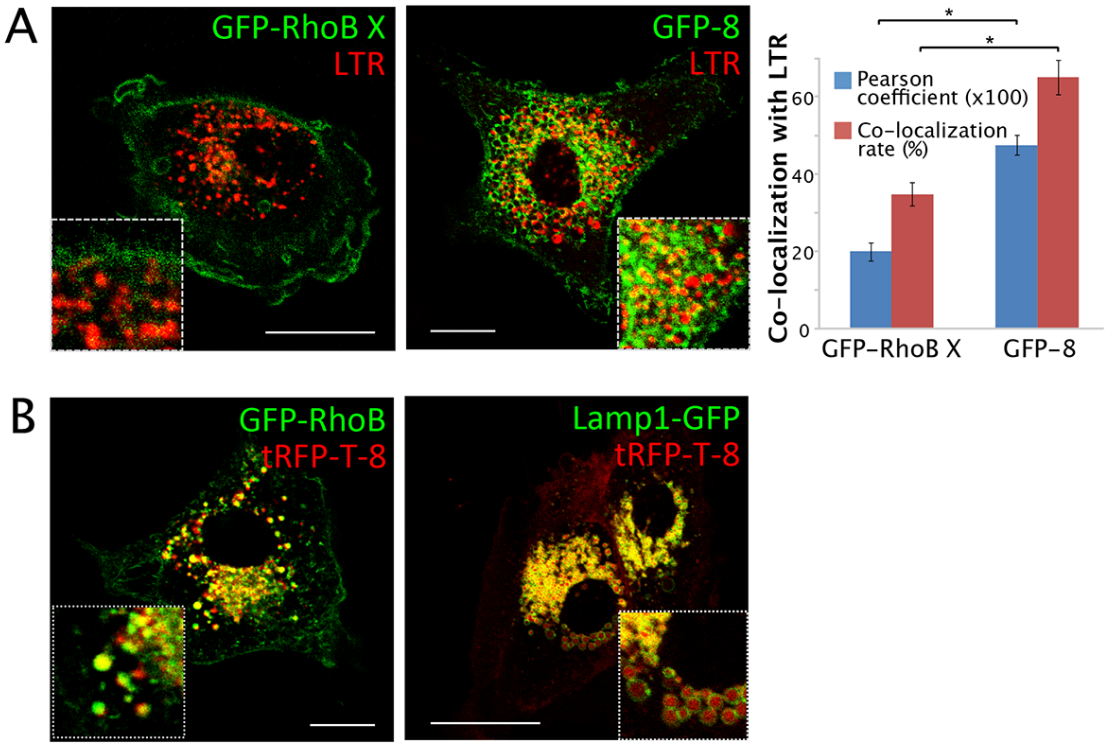

Figure 25. Localization of RhoB-related proteins in amphibian cells.

(A) *Xenopus laevis* A6 cells were transfected with *Xenopus laevis* RhoB (GFP-RhoB X) or GFP-8 and stained with LTR. GFP/LTR co-localization is shown in the right panel as Pearson coefficients (x100) or co-localization rates (in percentages). Asterisks represent $p<1 \times 10^{-6}$ versus GFP-8 (B) A6 cells were co-transfected with human GFP-RhoB or Lamp1-GFP and tRFP-T-8.

Going further down the evolutionary scale to assess the ability of different organisms to sort CINCCKVL chimeras to the late endocytic pathway, cells of the invertebrate *Trichoplusia ni* were transfected with tRFP-T-8. The High Five insect cell line showed tRFP-T-8 sorted into vesicles surrounded by Lamp1-GFP, marking their lysosomal character (Figure 26).

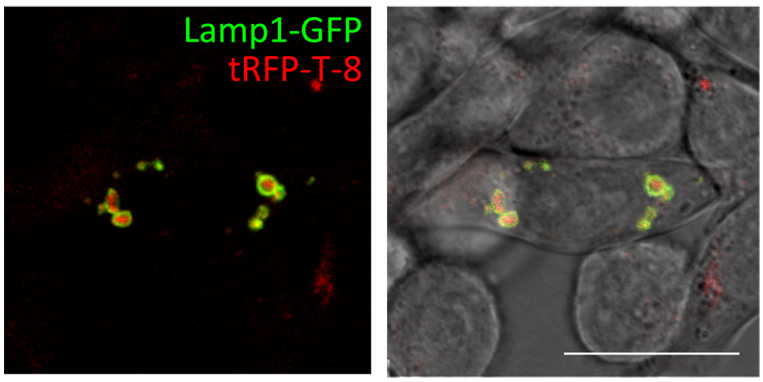

Figure 26. Localization of tRFP-T-8 in High Five insect cells.

High Five cells derived from the cabbage looper *Trichoplusia ni* were co-transfected with Lamp1-GFP and tRFP-T-8 before live observation by confocal microscopy. The left panel shows overlays of single fluorescent channels to which the Differential Interference Contrast (DIC) image has been juxtaposed in the right panel.

In the insect species *Drosophila mojavensis,* an uncharacterized protein containing a CAAX box, an extended basic amino acid patch and only one palmitoylatable cysteine among heterogeneous residues may be found (see Table 4). However, *Trichoplusia ni,* from which High Five cells are derived, does not encode an endogenous RhoB protein. Nonetheless, the structural determinants of the CINCCKVL sequence are robust enough to bestow endolysosomal localization upon its chimeras in this organism, as well.

1.3.2 CINCCKVL localization in *Aspergillus nidulans*

Though palmitoylation occurs on a multitude of proteins and is highly conserved throughout evolution, the mechanisms responsible for this process have remained elusive (Aicart-Ramos et al., 2011). Actually, palmitoyl transferases were discovered roughly a decade ago in yeast (Lobo et al., 2002; Roth et al., 2002), where many crucial proteins undergo this posttranslational modification to regulate their subcellular localization (Roth et al., 2006). A putative Rho-related protein bearing a CAAX box and a possible palmitoylation site is expressed in the fungus *Aspergillus nidulans* (Table 4), but the CINCCKVL motif does not appear in its proteome. To explore whether CINCCKVL sorting can take place in this compelling model organism for vesicular trafficking, *Aspergillus nidulans* strains expressing GFP-8 and its palmitoylation-deficient mutant were established (Figure 27).

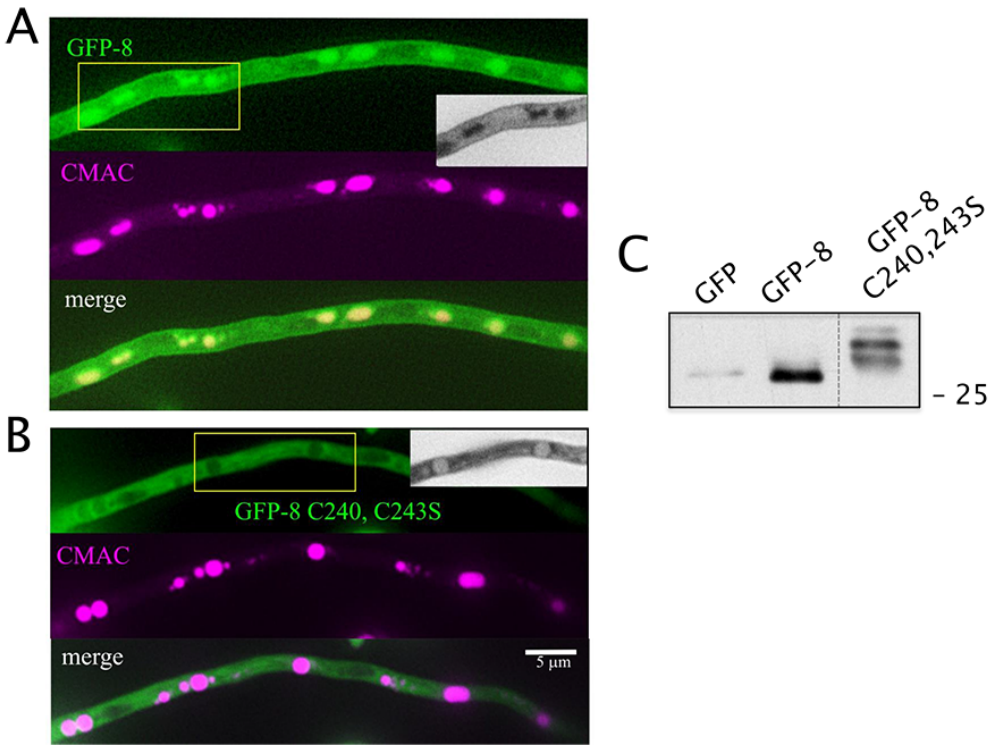

Figure 27. GFP-8 and its palmitoylation mutant in *Aspergillus nidulans*.

Aspergillus nidulans strains established by transformation with GFP-8 (A) or its palmitoylation deficient mutant GFP-8-C240,243S (B) were observed live as described in Methods. Staining with the vacuole marker CMAC is shown in the middle panels and overlays in the bottom panels. Gray scale insets of yellow boxed-in areas are shown for better contrast. (C) *Aspergillus nidulans* strains expressing the indicated constructs were processed for SDS-PAGE and WB using a GFP antibody. Dotted lines indicate a 5-fold shorter exposure time for the last lane than the two preceding ones. The 25 kDa marker is shown for reference.

In the wild-type strain, GFP-8 appears at the plasma membrane as well as in late endosomes and vacuoles stained by the acidic organelle marker CMAC (Figure 27A). In contrast, its palmitoylation-deficient mutant GFP-8-C240,243S is cytosolic and excluded from nuclei, the plasma membrane and CMAC-positive compartments (Figure 27B). Dependence on posttranslational modifications for targeting is similar to that observed in human cells, in which isoprenylation alone is also unable to elicit endolysosomal localization. Lack of GFP-8-C240,243S processing is further evidenced by the appearance of a doublet of slower migrating bands in SDS-PAGE, as described for other Ras superfamily proteins in mammalian cells (Hancock et al., 1989), and shown in Figure 27C. Indeed, levels of the mutant are significantly higher than those of fully lipidated GFP-8, which could be undergoing constitutive vacuolar degradation analogous to its lysosomal degradation in mammalian cells (see Figure 27C, caption).

Moreover, GFP-8 and GFP-8-C240,243S localization patterns are distinct from that of untagged GFP, which appears diffusely throughout the cytoplasm and nucleus, similarly to mammalian cells (not shown).

The filamentous nature of *Aspergillus nidulans* makes it a highly suitable model for tracking the movement of endocytic organelles by time-lapse microscopy (Peñalva et al., 2012). Indeed, GFP-8-positive vesicles could be readily detected travelling within the cell, avoiding nuclei and possibly fusing with large vacuoles also presenting GFP-8 fluorescence (Figure 28A, colored arrows and black arrowhead).

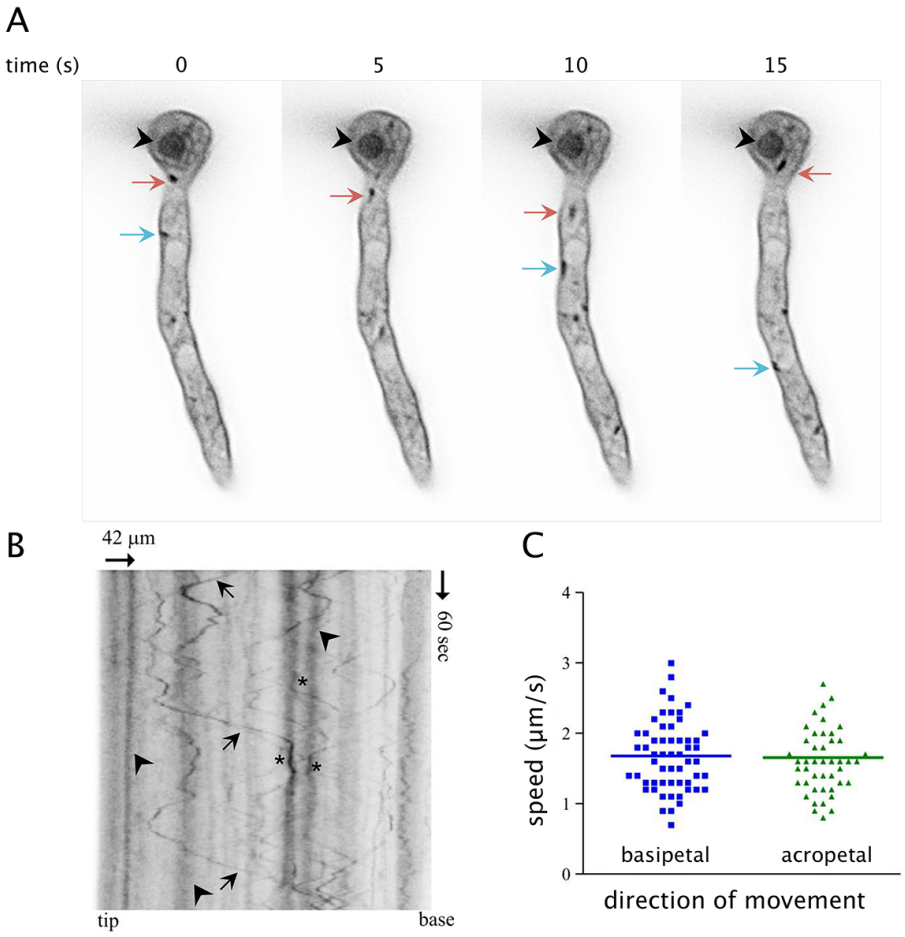

Figure 28. Tracking GFP-8-positive compartments in *Aspergillus nidulans*.

(A) The *Aspergillus nidulans* GFP-8 strain was observed live to follow localization of the construct by time-lapse microscopy. The plasma membrane is marked by GFP-8, as well as a large, sessile vacuole (black arrowhead in all frames). Smaller, motile vesicles also contain GFP-8 (colored arrows). The vesicle marked by a red arrow undergoes both basipetal and acropetal movement, whereas the teal-colored arrow follows a vesicle with acropetal movement only, which is not detectable in the second frame due to movement along the z-axis. (B) Kymograph showing GFP-8-positive compartments in motion from a representative experiment using a GFP-8-expressing strain. Black arrows highlight fast-moving vesicles, whereas black arrowheads mark static vesicles. Asterisks mark possible points of contact or fusion between them. (C) Velocities of individual endosomes travelling in both directions were tracked and are represented in the graph. See text for details.

Fluorescent vesicles can be tracked and their trajectories represented by using kymographs, as shown for GFP-8-positive vesicles of a representative cell in Figure 28B. Thick, straight lines correspond to large, sessile vacuoles (Figure 28B, arrowheads) whereas thin, diagonal lines trace several smaller, fast-moving endosomes (Figure 28B, arrows). Both of these contours come together at certain points that could be indicative of endosome-vacuole fusions (Figure 28B, asterisks). Furthermore, the speed of individual endosomes can be calculated from this type of representation by calculating the slope of their trajectory, be it basipetal or acropetal (Figure 28C). Similar average speeds of approximately 1 to 3 μm per second for GFP-8-containing endosomes in both directions, i.e. fully bidirectional movement, suggests that trafficking of these fast and small vesicles is dependent on microtubules, as has been previously described for other vesicles (Abenza et al., 2012; Abenza et al., 2009). Taken together, these results highlight the presence of GFP-8 along the endocytic pathway in *Aspergillus nidulans* and imply that CINCCKVL sorting occurs through mechanisms conserved in fungi, as well.

2. Mechanisms potentially involved in RhoB sorting

RhoB fluorescent constructs show a very specific subcellular localization at ILV of MVB and lysosomes as well as the plasma membrane, as summarized in Section 1.1.1. This behavior indicates that RhoB follows an endocytic route and accumulates at late compartments to which several sorting machineries escort their cargo, as described in the Introduction (see Figure 9). Therefore, this section comprises studies that attempt to elucidate specific mechanisms involved in driving RhoB constructs and related chimeras to their subcellular destinations, including ILV or the lysosomal lumen, by focusing on protein machineries as well as lipid dynamics.

2.1 Role of the ESCRT machinery in RhoB sorting

The canonical pathway for proteins that enter MVB to be degraded in the lysosome is often represented by ESCRT-mediated internalization of EGFR upon cell stimulation with its agonist. Indeed, RhoB has been shown to be involved in EGFR trafficking in several cell types and its expression is upregulated by EGF stimulation (Canguilhem et al., 2005; Gampel et al., 1999; Lajoie-Mazenc et al., 2008; Tillement et al., 2008). It could be the case that RhoB associates with vesicles on which EGFR travels and therefore follows a similar ESCRT-mediated internalization pathway. Therefore, experiments were carried out in cells in which ESCRT components were altered to study potential ESCRT involvement in sorting of RhoB and its related chimeras.

2.1.1 ESCRT-related processes in sorting of RhoB and related chimeras

ESCRT complexes act sequentially beginning with recognition of ubiquitin by Hrs (the core ESCRT-0 protein) and ending with ESCRT-III disassembly mediated by the ATPase, Vps4. These two major events were approached experimentally in the context of cells expressing RhoB constructs to initially evaluate whether the ESCRT machinery could play a role in their sorting.

There are few studies in which RhoB ubiquitination has been addressed, and those in which RhoB has been found to be ubiquitinated show that this is a cell type- and context-dependent process (Engel et al., 1998; Wang et al., 2014). To establish whether the fluorescent constructs used throughout this study were ubiquitinated, they were expressed in HeLa cells and immunoprecipitated to assay ubiquitin association, as shown in Figure 29. Neither GFP-RhoB nor GFP-8 samples presented signals compatible with ubiquitinated forms of these constructs. Interestingly, the construct GFP-22, which contains a lysine residue potentially susceptible to ubiquitination, was the only sample showing a putative mono-ubiquitinated species, marked by an asterisk in Figure 29A.

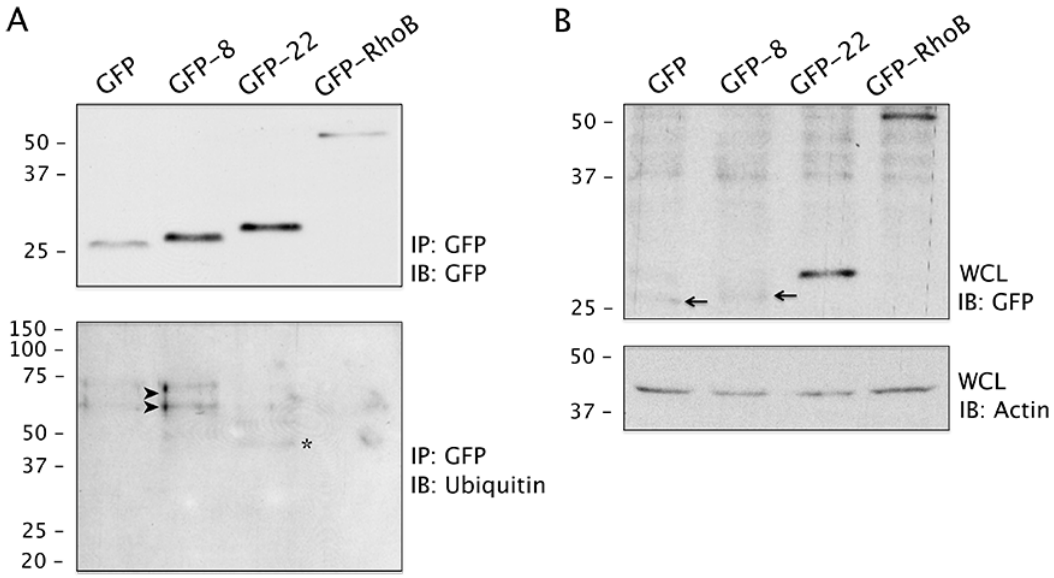

Figure 29. Ubiquitination assays by immunoprecipitation of RhoB constructs.

(A) HeLa cells were transfected with the indicated agents and immunoprecipitated using GFP antibodies conjugated with agarose beads (GFP-Trap) as described in the Methods section. Immunoblots were performed against the indicated proteins. Arrowheads highlight unspecific signals, possibly representing keratin doublets. The asterisk marks faint signals detected consistently in GFP-22 samples. (B) Whole cell lysates (WCL) of samples shown in (A). Arrows mark the GFP and GFP-8 signals.

Therefore, if GFP-RhoB and/or GFP-8 are ubiquitinated, they are so at levels that are undetectable under basal conditions in this type of assay. However, ubiquitin-independent, ESCRT-dependent sorting into ILV of MVB has been previously described (Babst, 2011), as discussed in the Introduction. The ESCRT-associated component, Vps4, was consequently addressed in cells in which the last step of ILV formation was impaired, namely, HeLa cells transfected with a dominant negative form of this protein (Figure 30).

In HeLa cells, transfection of the wild-type GFP-Vps4 construct presents a diffuse pattern throughout the cytosol and does not affect localization at endolysosomes of tRFP-T-RhoB (Figure 30A, top panels) or tRFP-T-8 (not shown), either under control conditions or upon treatment with chloroquine. However, overexpression of dominant negative GFP-Vps4 hinders tRFP-T-RhoB entry into vesicular structures, as shown in the bottom panels of Figure 30A and its profiles. Instead, fluorescent RhoB constructs are mislocalized to the limiting membrane of vesicles formed upon GFP-Vps4 DN expression, defined as aberrant Class E compartments (Bishop and Woodman, 2000), recapitulating the results obtained in BAEC (Pérez-Sala et al., 2009).

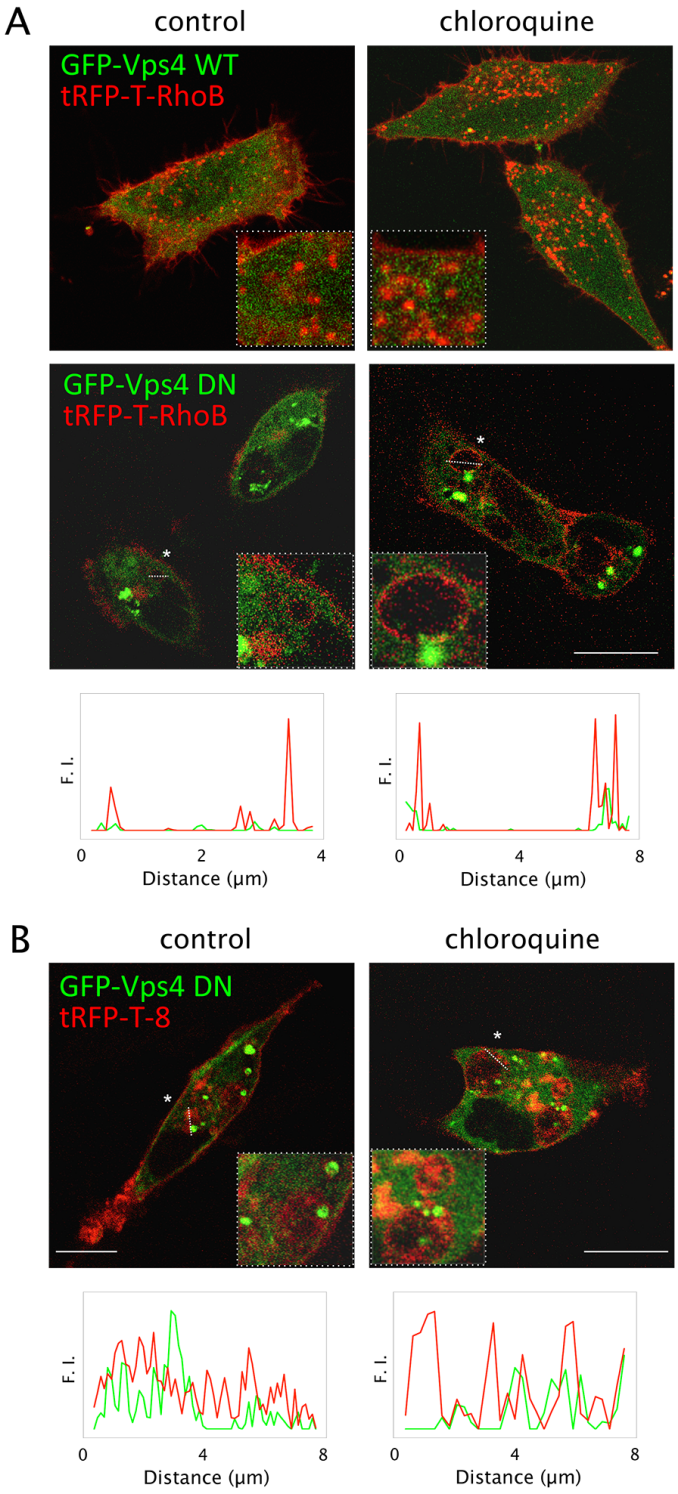

Figure 30. Effect of GFP-Vps4 DN overexpression on RhoB and CINCCKVL chimera localization.

HeLa cells were co-transfected with the indicated constructs and treated with chloroquine for 24 h where specified prior to live confocal microscopy observation. Underneath the panels of cells expressing GFP-Vps4 DN, fluorescence intensity profiles along a section marked by dotted lines and asterisks are shown. F.I., fluorescence intensity.

In contrast, the CINCCKVL construct, tRFP-T-8 is able to enter into the lumen of these compartments in cells expressing the dominant negative mutant of Vps4, as shown in Figure 30B (see profiles). These results point to a possible role for ESCRT proteins in RhoB sorting, so that further studies concerning the ESCRT machinery *per se* were carried out in HeLa cells, as shown below.

2.1.2 ESCRT component depletion in RhoB and –CINCCKVL protein sorting

To further substantiate the role of ESCRT proteins, either control (scr) siRNA or siRNA against either the ESCRT-0 component Hrs or the ESCRT-I protein Tsg101 was transfected into cells to reduce protein levels prior to expression of GFP-RhoB or GFP-8 and chloroquine treatment. The efficiency of ESCRT silencing was analyzed in these cells by SDS-PAGE and WB. As shown in Figure 31A, cells transfected with Hrs-specific siRNA were practically devoid of this ESCRT component as compared to their control (scr). In turn, Tsg101 silencing reduced its protein levels by 72.2 ± 5.3% (Figure 31B).

Figure 31. Depletion of ESCRT components by specific siRNA.

(A) HeLa cells were transfected with scrambled (scr) or Hrs-targeted siRNA. Cell lysis was carried out 48 h later and WB against Hrs is shown. (B) Tsg101 levels were assessed similarly to (A). 50 and 100 kDa markers are shown for reference.

As shown by confocal microscopy analysis in Figure 32A, HeLa cells transfected with control siRNA (scr) were able to sort GFP-RhoB to LTR-positive vesicles, as seen above for several cell types. However, knock-down of the ESCRT-0 component, Hrs or the ESCRT-I component, Tsg101 reduced the appearance of GFP-RhoB at acidic vesicles (Figure 32A, see profiles).

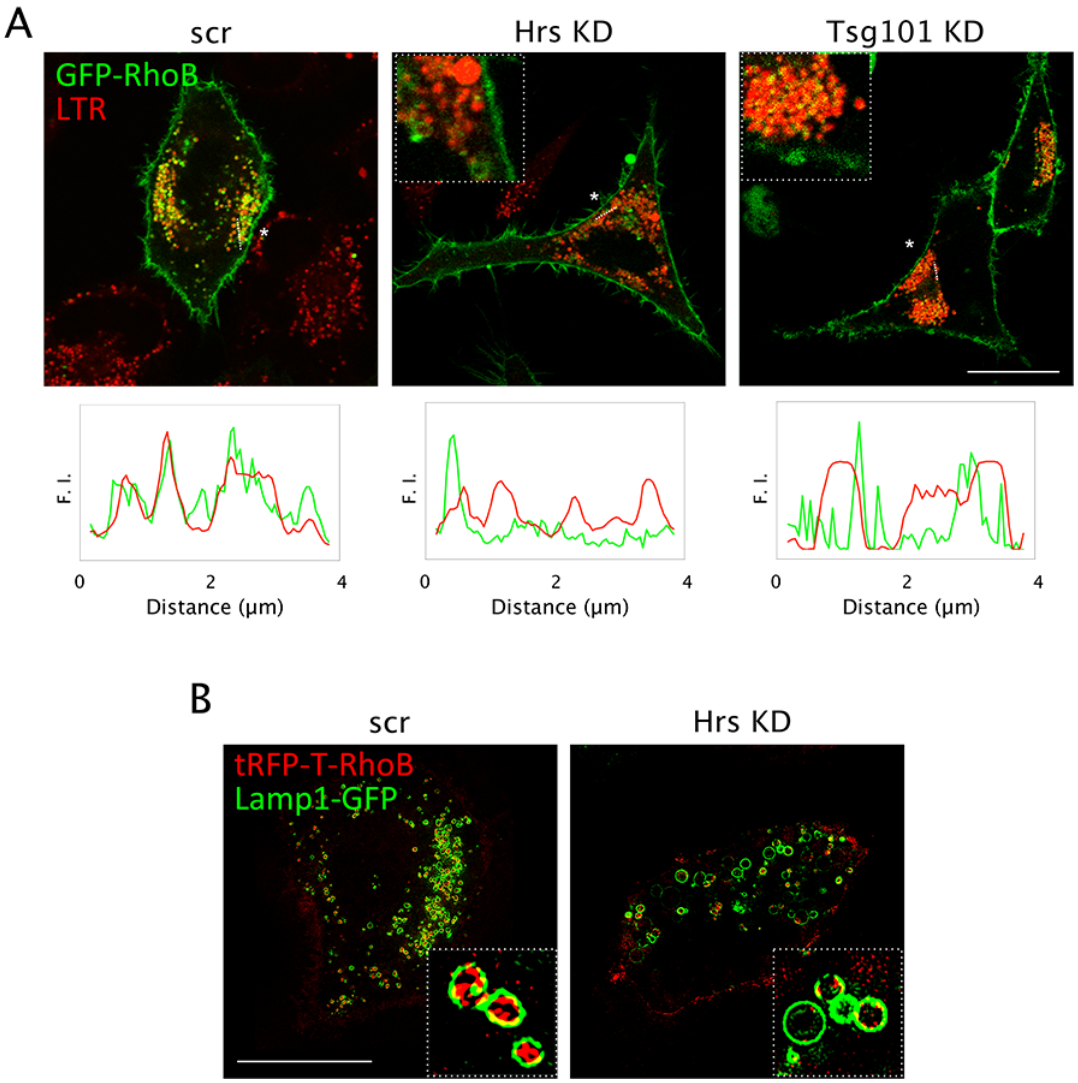

Figure 32. Knock-down of the ESCRT components Hrs or Tsg101 and their effect on localization of RhoB fluorescent constructs.

(A) HeLa cells were transfected with either scrambled siRNA (scr) or siRNA targeting either Hrs or Tsg101 to silence these ESCRT components, replated, and transfected with GFP-RhoB. Cells were treated with chloroquine to induce accumulation at endolysosomes, stained with LTR and observed live by confocal microscopy. Fluorescence intensity profiles along a section (marked by dotted lines and asterisks) appear underneath each condition. KD, knock-down; F.I., fluorescence intensity. (B) HeLa cells transfected with either scrambled siRNA (scr) or siRNA targeting Hrs were further co-transfected with tRFP-T-RhoB and Lamp-GFP. After 24 h of chloroquine treatment, they were visualized live by structured illumination super-resolution microscopy (SIM). Insets show individual MVB and their ILV decorated with RhoB fluorescent protein. The right panel inset highlights the emptier MVB that appear upon Hrs knock-down.

To explore the effect of Hrs knock-down on sorting of RhoB constructs in more detail, the red tRFP-T-RhoB construct was co-transfected with Lamp1-GFP in cells in which Hrs was silenced and observed live under a super-resolution microscope (Figure 32B). Localization of tRFP-T-RhoB at ILV was unmistakably observed in control cells

within MVB surrounded by Lamp1-GFP at their limiting membrane (Figure 32B, left panel). On the other hand, Hrs knock-down cells presented Lamp1-positive structures with a marked reduction of tRFP-T-RhoB inside their lumen, despite treatment with chloroquine that usually causes RhoB construct accumulation inside these vesicles (Figure 32B, right panel inset). Taken together, these results suggest involvement of early ESCRT components in sorting of full-length RhoB constructs.

In order to study the role of the ESCRT machinery on sorting of CINCCKVL constructs, assays analogous to those above were performed on cells transfected with GFP-8. Strikingly, GFP-8 seemed unaffected by either Hrs or Tsg101 knock-down and was still able to enter the lumen of LTR-positive compartments, analogously to its control (Figure 33), in contrast to the marked reduction in endolysosomal localization detected above for GFP-RhoB.

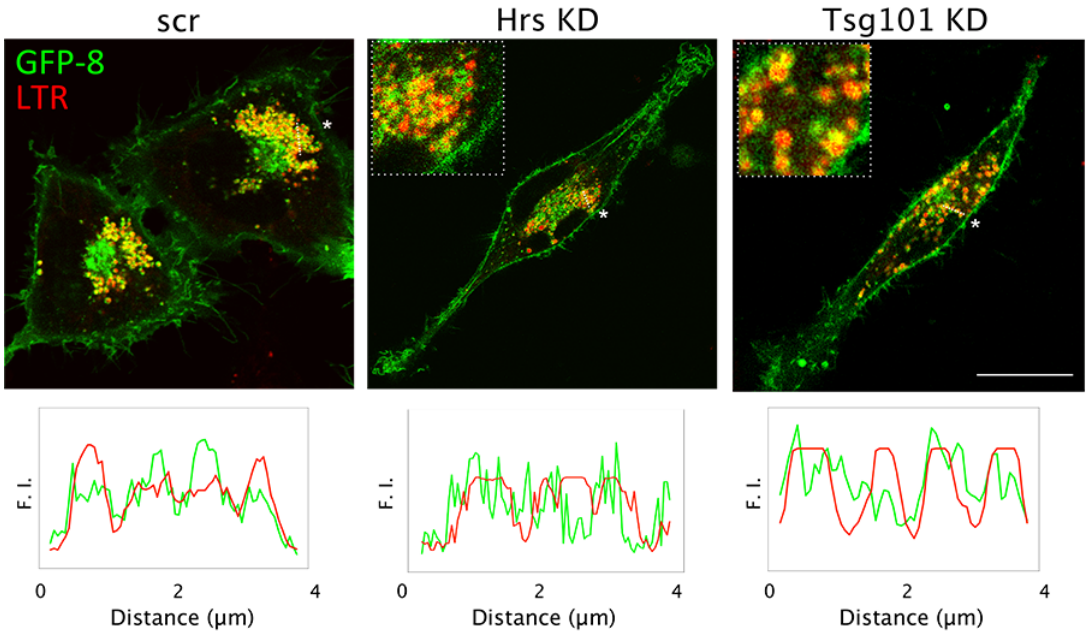

Figure 33. Knock-down of the ESCRT components Hrs or Tsg101 and their effect on GFP-8 localization.

HeLa cells transfected with siRNA targeting ESCRT components, transfected with GFP-8 and treated with chloroquine prior to LTR staining were observed live by confocal microscopy, similarly to Figure 32A. Profiles along a section traced by dotted lines and marked with asterisks show intensity profiles underneath each condition. KD, knock-down. F.I., fluorescence intensity.

In sum, there appears to be a differential effect of ESCRT component knock-down as to the subcellular localization of either full-length RhoB constructs or

CINCCKVL chimeras (compare Figure 32A to Figure 33). These findings are the first studies in which we have encountered dissimilar behavior between full-length RhoB and its sorting motif –CINCCKVL, suggesting that further regulatory determinants in the RhoB protein could be involved in ESCRT interaction, whereas –CINCCKVL bypasses this regulation and enters ILV of MVB independently of ESCRT.

2.2 Lipid-mediated endolysosomal sorting of CINCCKVL

The results above point to ESCRT involvement in full-length RhoB sorting, whereas the C-terminal motif CINCCKVL seems to be targeted to endolysosomes, more specifically ILV of MVB, independently of this protein machinery. Considering that ILV formation can be ESCRT-dependent or –independent (Section 3.2 of the Introduction), other mechanisms possibly involved in CINCCKVL-chimeric protein sorting were assessed. Taking advantage of the fact that inward budding from the limiting membrane of MVB is regulated by its lipid composition (Matsuo et al., 2004; Trajkovic et al., 2008), CINCCKVL chimera subcellular localization was monitored in cells treated with several compounds that modulate late endosomal lipid dynamics.

The precursor mevalonate is used by cells for membrane cholesterol biosynthesis and formation of isoprenoid moieties destined towards protein posttranslational modification, as schematized in Figure 34. The mevalonate pathway can be disrupted at several stages by blocking key enzymes with inhibitors, such as HMG CoA reductase inhibition by statin treatment in cells, which inhibits protein isoprenylation (Figure 34). Furthermore, the lysosomotropic agent U18666A inhibits cholesterol synthesis as well as its trafficking (Figure 34), thus causing its internalization and accumulation into ILV of MVB along with the lipid LBPA, eliciting an NPC-like phenotype (Cenedella, 2009; Kobayashi et al., 1999; Sobo et al., 2007). In turn, the squalene synthase inhibitor zaragozic acid (Figure 34) reduces cellular cholesterol levels and could affect ILV lipid composition significantly, since most of the cholesterol of the endocytic pathway is contained within these vesicles (Möbius et al., 2003).

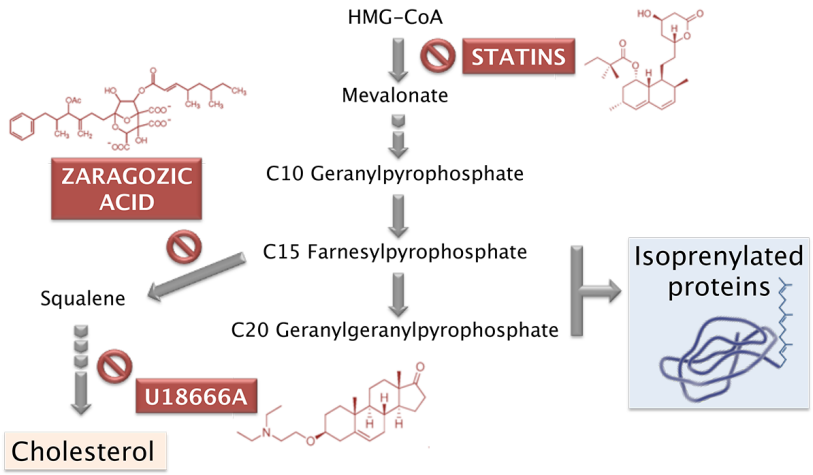

Figure 34. Schematic of the mevalonate pathway and compounds used for its modulation.

Simplified schematic of the mevalonate pathway showing formation of the isoprenylation precursors farnesylpyrophosphate and geranylgeranylpyrophosphate, used in protein modification. The former can be further processed for cholesterol biosynthesis. In red, structures of compounds used in this work to disrupt particular steps of the pathway. Statins such as simvastatin, shown here, inhibit HMG-CoA reductase and therefore halt both protein isoprenylation and cholesterol biosynthesis. In turn, zaragozic acid blocks squalene synthase, blocking subsequent steps of the cholesterol pathway. Similarly, the amphiphilic amino-steroid U18666A hinders cholesterol synthesis and transport. Truncated arrows represent intermediate steps that are not shown here for the sake of clarity.

To assess the effect of lipid alterations in CINCCKVL chimera localization, cells transfected with these constructs were treated with U18666A or ZGA and observed live by confocal microscopy (Figure 35).

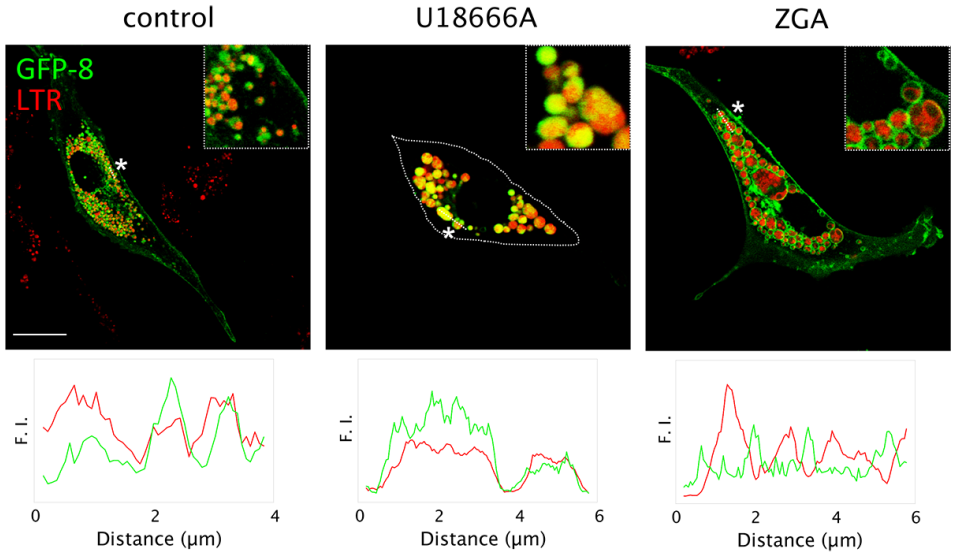

Figure 35. Agents modulating lipid dynamics alter GFP-8 localization.

BAEC transfected with GFP-8 were treated with 10 μM U18666A or 50 μM ZGA for 24 h. Insets show zoom-ins and lower panels represent fluorescence intensity profiles (F.I.) along a section marked by dotted lines and asterisks.

Indeed, these compounds produced drastic phenotypes in several cell types including HeLa cells, BAEC and *Xenopus laevis* cells (Oeste et al., 2014), and the results obtained for BAEC are presented here for clarity. As shown in the middle panel of Figure 35, cells treated with U18666A displayed intensely compact endolysosomes in which GFP-8 accumulated prominently, along with LTR, consistent with results shown in Section 1.1. In sharp contrast, ZGA elicited dilated MVB with either scarce, diffuse staining with GFP-8 or MVB practically devoid of GFP-8, in which GFP-8 was retained at the limiting membranes of MVB and LTR staining was weaker and sometimes patchy (Figure 35, right panel profile). However, ZGA treatment of BAEC transfected with GFP-RhoB showed dilated MVB with patches of LTR in which this construct seemed to enter freely, similarly to its control and conversely to GFP-8, as seen in Figure 36.

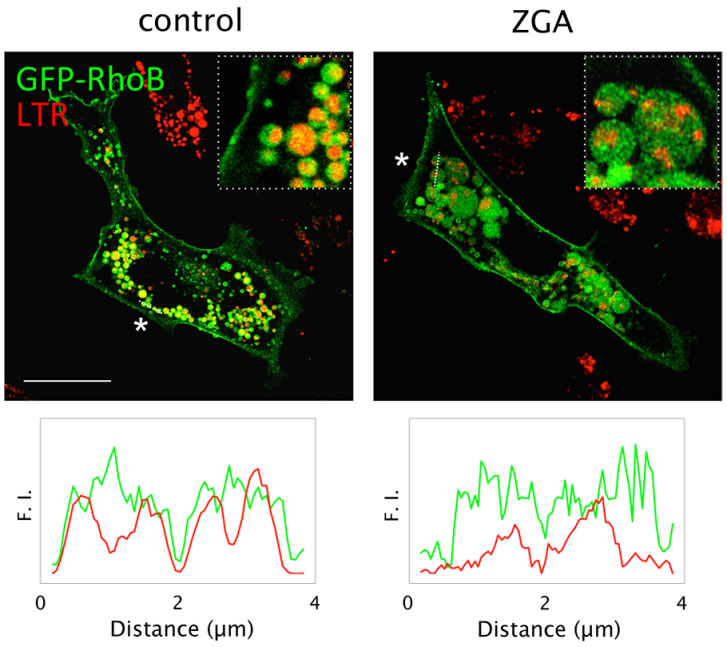

Figure 36. GFP-RhoB appears inside MVB in cells treated with ZGA.

BAEC transfected with GFP-RhoB were treated with ZGA and stained with LTR prior to confocal microscopy observation, as in Figure 35. Insets show details of vesicles and profiles represent fluorescent intensity (F.I.) along sections marked by dotted lines and asterisks.

In order to investigate whether impairment of GFP-8 sorting into the lumen of endolysosomes could be due to a reduction of GFP-8 membrane association, we performed subcellular fractionation studies (Figure 37). For this we used HeLa cells, in which we previously confirmed the inhibitory effect of ZGA on endolysosomal internalization of GFP-8 by confocal microscopy (Oeste et al., 2014). As shown in

Figure 37, cholesterol depletion does not reduce the levels of membrane-associated GFP-8, practically all of which still appears in the particulate (P-100) fraction.

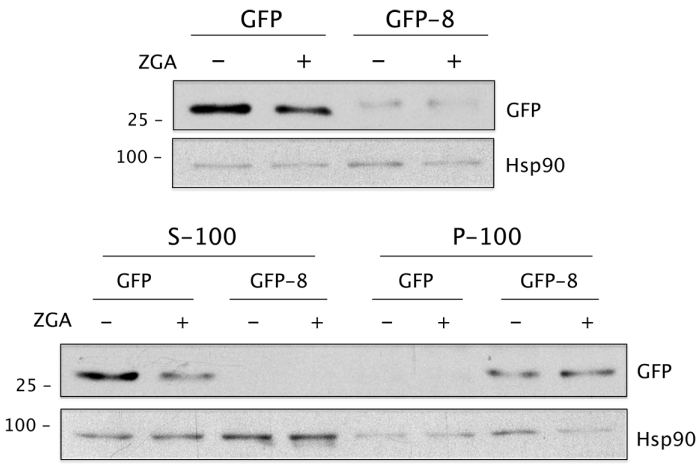

Figure 37. Subcellular fractionation of HeLa cells treated with ZGA.

HeLa cells were transfected with GFP or GFP-8, treated with 100 μM ZGA for 24 h, lysed, and fractionation was performed as described in the Methods section. Upper panels show total cell lysates whereas lower panels correspond to chimeric protein levels in the soluble (S-100) or particulate (P-100) fraction, assessed by WB with an anti-GFP antibody. The 25 kDa marker is shown for electrophoretic reference.

2.3 The tetraspanin CD63 in RhoB and CINCCKVL sorting

The results shown above suggest that sorting of full-length RhoB constructs is mediated partly by the ESCRT machinery, whereas CINCCKVL chimeras seem to enter ILV of MVB regardless of ESCRT disruption. As described in Section 3.1.3 of the Introduction, evidence pointing to ESCRT-independent sorting accumulating in recent years indicates a role for CD63 in trafficking to ILV as well as in biogenesis of ILV destined for release as exosomes (Pols and Klumperman, 2009). Furthermore, the small ILV that still form after Hrs depletion carry CD63 and its cargo (Edgar et al., 2014), so that the internalization of GFP-8 into MVB in cells after Hrs knock-down observed above in Section 2.1.2 could be CD63-mediated. These findings warranted further studies to explore the role of CD63 in sorting of CINCCKVL proteins and full-length RhoB.

2.3.1 Impact of CD63 overexpression on localization of RhoB and CINCCKVL constructs

In HeLa cells, RhoB and CD63 constructs co-localize to a very high degree in their small endolysosomes, as seen in Figure 18. Therefore, co-transfection studies were carried out in BAEC to observe more specific localization inside their larger MVB, particularly after chloroquine treatment (Figure 38). Co-localization was apparent in cells expressing wild-type mCherry-CD63 and GFP-8 (Pearson coefficient = 0.63 ± 0.04), and treatment of these cells with chloroquine further increased co-localization (Pearson coefficient = 0.81 ± 0.03). In contrast, GFP-RhoB and mCherry-CD63 co-localization was significantly lower respect to GFP-8 in control cells (Pearson coefficient = 0.41 ± 0.04). The large vesicles typical of BAEC also presented several GFP-RhoB- or GFP-8-positive structures that did not contain fluorescent CD63 and *vice versa* (Figure 38)..

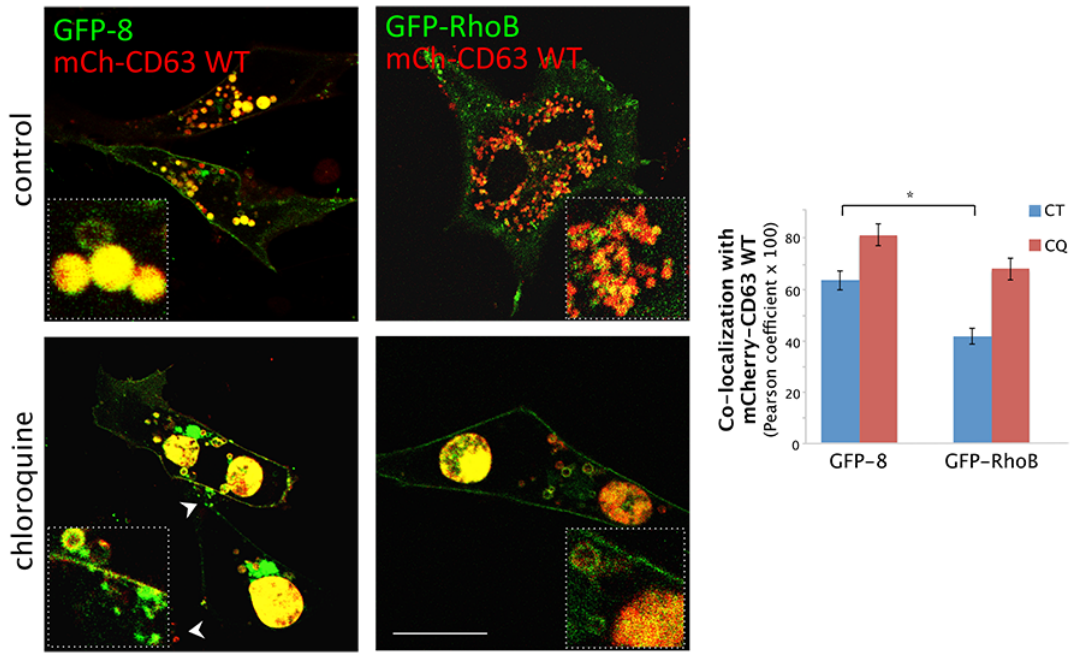

Figure 38. Wild-type mCherry-CD63 co-localization with GFP-8 or GFP-RhoB.

BAEC co-transfected with mCherry-CD63 wild-type (mCh-CD63 WT) and either GFP-RhoB or GFP-8 were visualized by live confocal microscopy after treatment with chloroquine, where indicated. White arrowheads mark the extracellular material in the lower left panel. The graph shows average co-localization between constructs, assessed as described in Methods in the image analysis section. *p < 0.01

In this cell type, whereas co-transfection of CD63 and full-length RhoB constructs was well tolerated under the conditions studied, CD63 in combination with CINCCKVL proteins elicited accumulation of extracellular, vesicular material throughout the culture dish that was positive for GFP-8 and mCherry-CD63 (marked by arrowheads in Figure 38, bottom left panel)

The differential effect of overexpressing CD63 with full-length RhoB constructs versus CINCCKVL proteins could imply that this tetraspanin is involved in sorting, or interacts with, the lipidated RhoB motif. To further explore this possibility, similar studies were carried out with the mCh-CD63 YA construct in which the tyrosine found in the C-terminal lysosomal targeting motif YEVM was mutated to alanine (Figure 39). It has been reported that this mutant is unable to interact with the sorting complex AP-3 and is therefore largely localized to the plasma membrane (Rous et al., 2002).

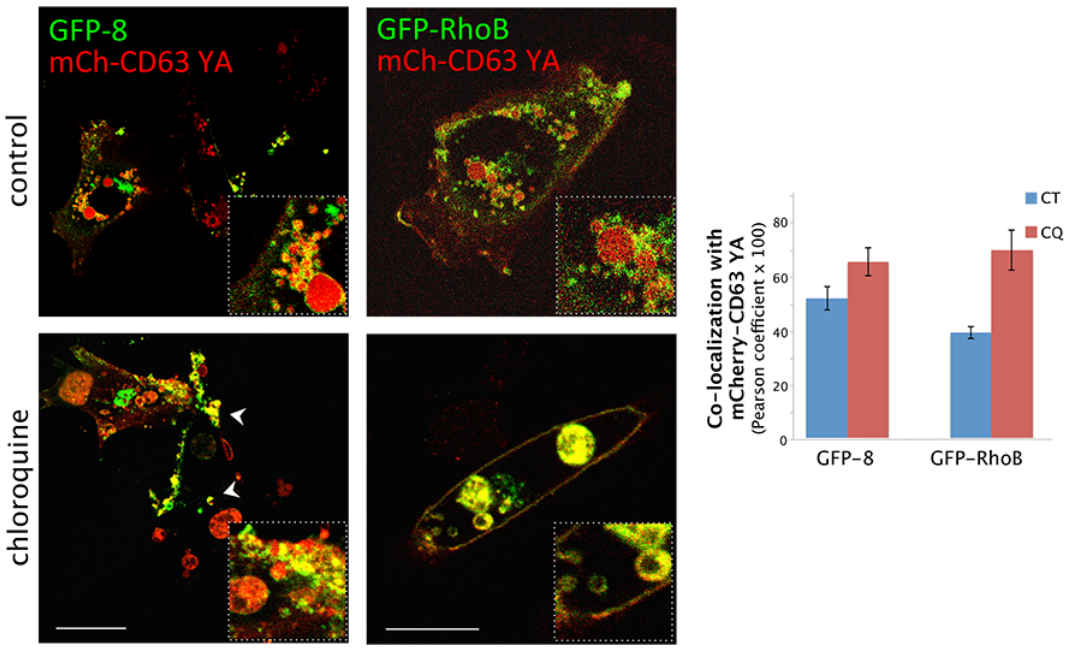

Figure 39. mCherry-CD63 Y235A mutant co-localization with GFP-8 or GFP-RhoB.

BAEC co-transfected with the mCherry-CD63 lysosomal targeting tyrosine mutant (mCh-CD63 YA) and either GFP-RhoB or GFP-8 were visualized by live confocal microscopy after treatment with chloroquine, where indicated. Note the extracellular material marked by arrowheads in the bottom left panel. Co-localization is shown in the graph, as described in Figure 38.

Under the conditions used throughout this work, the proportion of plasma membrane to endolysosomal localization of the CD63 mutant varies in a cell-type dependent manner for, as seen in Figure 39, mCh-CD63 YA is only partially associated

with the plasma membrane in BAEC and is still prominently present at endolysosomes. GFP-8 co-localization with the mCherry-CD63 YA mutant was significantly reduced with respect to the wild-type protein, particularly upon chloroquine treatment (Pearson coefficient = 0.66 ± 0.02 versus 0.81 ± 0.03). Furthermore, large amounts of GFP-8-positive extracellular vesicles were detectable in the medium as well as at the extracellular surface of the plasma membrane in many cells, particularly upon chloroquine treatment (Figure 39, left panels). In contrast, GFP-RhoB co-localization with mCherry-CD63 YA was similar to co-localization with its wild-type form, both for control conditions and after chloroquine treatment (Pearson coefficient = 0.41 ± 0.04 for the YA construct and 0.40 ± 0.05 for the wild-type, control; 0.67 ± 0.04 versus 0.71 ± 0.08, chloroquine treatment). It is therefore possible that the tetraspanin CD63 is involved in CINCCKVL protein sorting, which could potentially result in extracellular localization of the chimera under certain conditions.

2.3.2 Effect of C6 ceramide treatment on RhoB construct localization

Targeting to MVB precedes an important step in protein sorting, for ILV pinched off into the MVB lumen can be sorted to lysosomes for degradation or be secreted into the extracellular milieu by MVB fusion with the plasma membrane, as depicted in Figure 40A. Considering CD63 function in the biogenesis of exosomes and the extracellular destination detected for CINCCKVL proteins in a scenario of aberrant CD63 overexpression, it is possible that this RhoB motif could be preferentially targeted for ILV destined for secretion instead of those destined for degradation in the lysosome, which are usually associated with ESCRT-dependent mechanisms. Furthermore, cell material can be secreted from the cell by direct shedding of microvesicles from the plasma membrane. In fact, a closer look by super-resolution imaging at the plasma membrane of HeLa cells transfected with GFP-8 shows what appear to be discrete compartments possibly corresponding to microvesicles, as well as protruding areas of the plasma membrane budding outwards (Figure 40B). Therefore, it is plausible that CINCCKVL targets its chimeric proteins to be secreted either directly at the plasma membrane or through the late endosomal pathway, into MVB and out of the cell in

exosomes. Nevertheless, it must be taken into account that due to the tight z-sections obtained by super-resolution microscopy, the structures that appear to be vesicles could in fact correspond to undulations still attached to the plasma membrane.

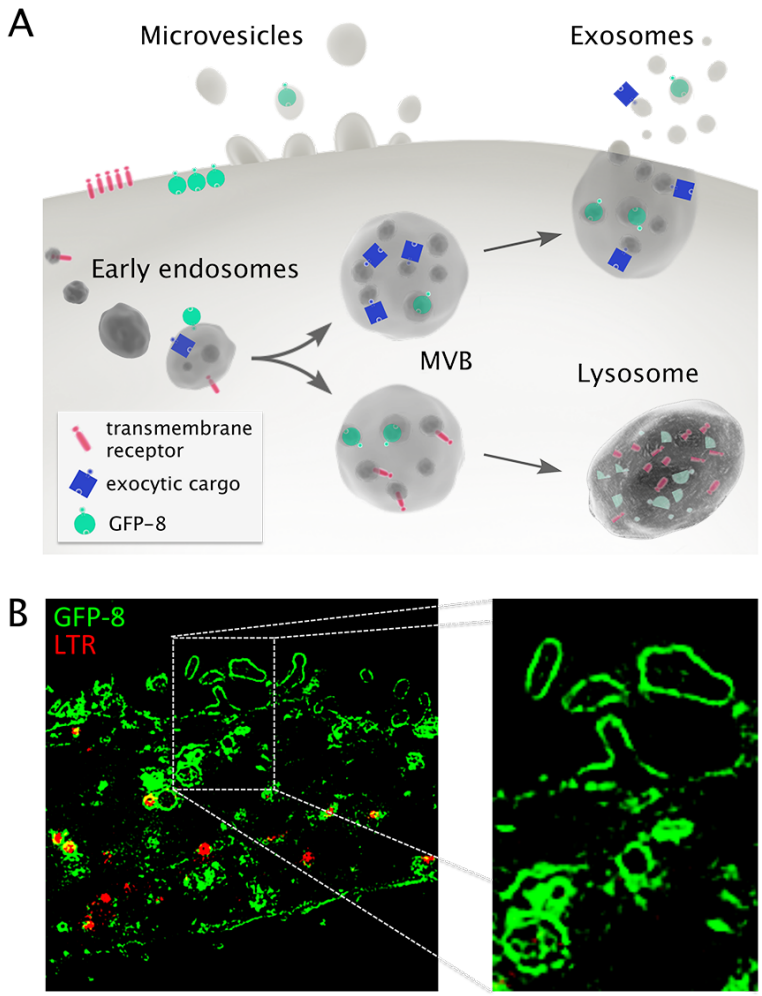

Figure 40. Extracellular vesicle release routes as potential destinations for GFP-8.

(A) Schematic representing pathways for extracellular release of vesicles and their cargo. Whereas microvesicles bud directly from the plasma membrane, exosomes are formed by inward budding of ILV into MVB that can fuse to the plasma membrane, releasing their internal vesicles. MVB can also be destined for fusion with lysosomes for cargo degradation. It has not yet been fully established whether whole MVB are either exocytic or degradative or if ILV destined for either fate can co-exist within the same MVB. Note that budding of small ILV begins at the early endosome stage. Red rods represent transmembrane receptors and blue squares depict proteins destined for secretion. Green circles represent GFP-8 and its possible destinations. Modified from (Raposo and Stoorvogel, 2013). (B) Detailed inspection of the super-resolution image presented in Figure 19 shows GFP-8 at several LTR-positive endolysosomes and MVB (bottom left in inset). The inset further shows structures budding directly from the membrane, morphologically consistent with shed microvesicles.

To approach the possibility of CINCCKVL sorting to extracellular vesicles, cells transfected with either GFP-RhoB or GFP-8 were treated with C6 ceramide (Figure 41), which has been shown to induce ESCRT-independent formation of ILV that are secreted as exosomes (Trajkovic et al., 2008). An inactive form of this compound, dihydroceramide C6, was used as a negative control.

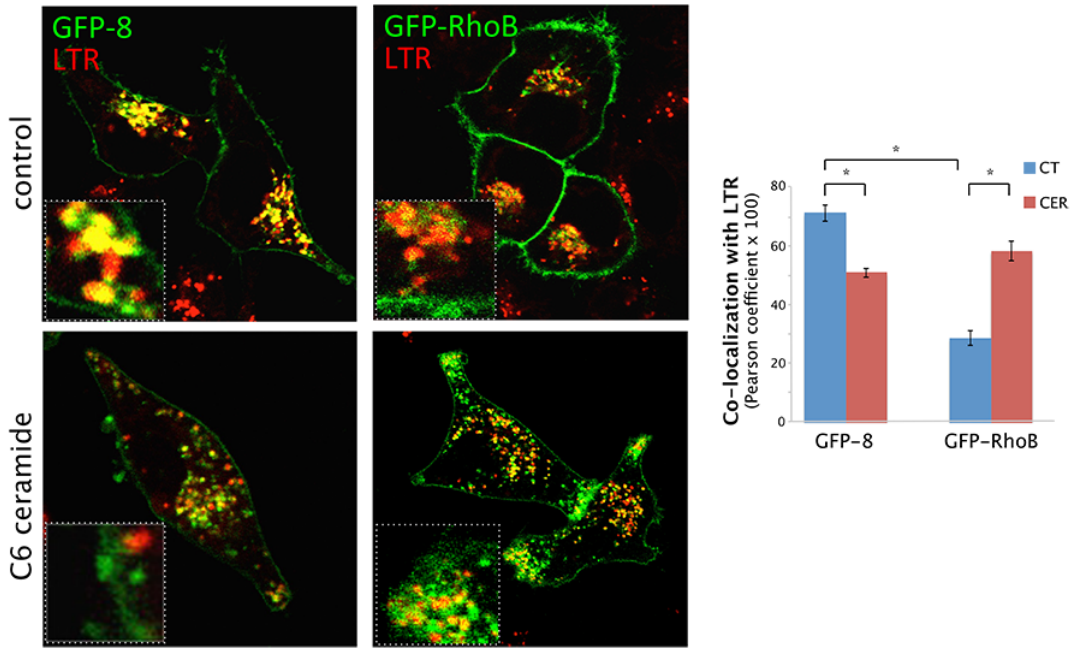

Figure 41. Effect of C6 ceramide on GFP-8 or GFP-RhoB endolysosomal localization.

HeLa cells transfected with the indicated agents were treated with either dihydroceramide C6 (control) or C6 ceramide and stained with LTR prior to live confocal microscopy observation. The graph represents co-localization with LTR of either GFP-8 or GFP-RhoB after the indicated treatments. *$p < 0.001$

As seen in the left panels of Figure 41, upon ceramide treatment, GFP-8 accumulated less at perinuclear, LTR-positive vesicles, its localization at the plasma membrane was in part diminished, and GFP-8-positive material was detected in the proximity of the plasma membrane as well as throughout the culture dish. This behavior was reflected by a significant decrease in co-localization of GFP-8 with LTR upon ceramide treatment (Pearson coefficient = 0.71 ± 0.03 for control compared to 0.51 ± 0.02 after ceramide treatment). However, after treatment with ceramide, GFP-RhoB was retained at the plasma membrane in polarized accumulations that were positive for LTR and did not seem to reach the extracellular space (Figure 41), hence eliciting a significant increase in GFP-RhoB co-localization with LTR (Pearson coefficient = 0.29 ±

0.02 control versus 0.59 ± 0.03). Taken together, these results suggest that CINCCKVL is able to reach the extracellular medium whereas the full-length protein is retained within the cell, possibly due to further sorting signals precluding its secretion or an active role in these processes. These results warrant further studies regarding the extracellular fate of CINCCKVL chimeras and the involvement of the CINCCKVL sequence in this process in the context of full-length RhoB.

3. Small GTPases in pathological scenarios

The plethora of signaling cascades in which small GTPases are involved highlights their importance in maintaining cellular homeostasis. Indeed, as described in the Introduction, members of this protein family have been found to play roles in many pathological processes such as tumorigenesis, inflammation or lysosomal diseases. The experiments described in this section are focused first on exploring GTPase involvement in lysosomal storage diseases, specifically, Chediak-Higashi Syndrome. Secondly, the amenability of several GTPases to be modified by reactive compounds produced during inflammatory or oxidative stress conditions was assessed, for these modifications could alter their subcellular localization and activation, resulting in unfavorable cellular outcomes.

3.1 Endosomal GTPases in cells from patients with lysosomal storage diseases

Cells derived from patients suffering from lysosomal storage disorders are used alongside mouse models not only to study the pathogenesis of these diseases, but also to study the basic processes involved in general trafficking towards the lysosome. Much information about the endocytic route and the trafficking partners involved has been obtained by detection of mutations leading to these pathologies (Ballabio and Gieselmann, 2009). Therefore, GTPase localization was studied in the context of these

models for altered endolysosomal sorting. Several of these cell models have been previously employed in other works from the laboratory (Pérez-Sala et al., 2009; Valero et al., 2010); hence, attention here is focused on Chediak-Higashi Syndrome.

3.1.1 Studies in cells from patients with Chediak-Higashi Syndrome

The enlarged lysosomes found in many cell types of Chediak-Higashi patients were detected by optical microscopy early on and have since been found to accumulate cellular material of different kinds (Oliver et al., 1976). Several lysosomal storage diseases such as NPC present increased cholesterol levels in aberrant compartments as part of their pathogenic scenario. Moreover, a study on the lipid composition of CHS erythrocyte membranes pointed to higher levels of cholesterol (Chico et al., 2000), but to the best of our knowledge, intracellular cholesterol has not been studied in fibroblasts from this disease. Since cholesterol homeostasis can affect sorting of RhoB or CINCCKVL chimeras, unesterified cholesterol levels were assessed in CHS fibroblasts by filipin staining and confocal microscopy observation. As shown in Figure 42, CHS fibroblasts contain significantly higher levels of free cholesterol in their endolysosomes than control cells, quantified to almost double the value of control cells by fluorescence intensity detection.

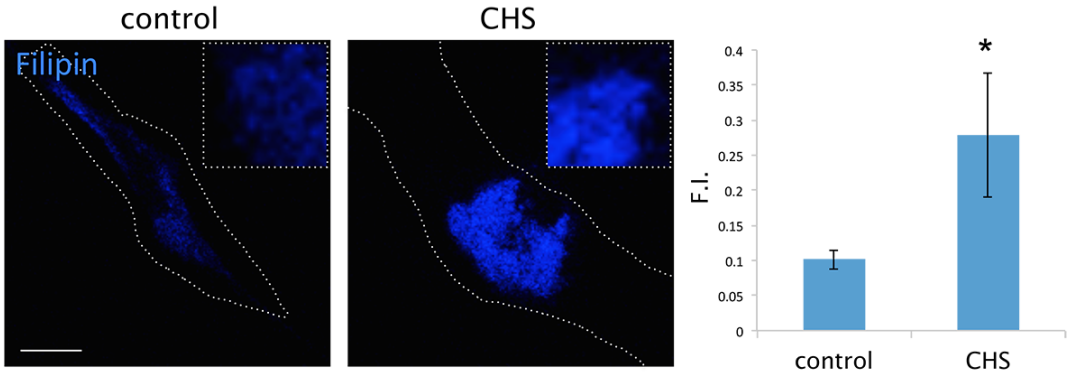

Figure 42. Cholesterol staining in control and Chediak-Higashi fibroblasts.

Confocal imaging of fixed fibroblasts from control subjects versus CHS cells after filipin staining. Images were acquired with identical settings. Quantification of confocal image intensities was performed on wide fields containing several cells and is shown to the right of the images. F.I., fluorescence intensity. *p, 0.05 versus control.

In addition to lipids, several proteins have been found to accumulate at the enlarged endolysosomes of CHS cells, including proteins involved in the endocytic

pathway (Burkhardt et al., 1993). In order to further characterize CHS endolysosomes, a systematic approach was set up whereby the subcellular localization of several endosomal GTPases was compared to endolysosomal markers. Similarly to control fibroblasts, in CHS fibroblasts GFP-Rab7 and Lamp-GFP co-localized with LTR, whereas GFP-Rab5 appeared at smaller, more peripheral vesicles consistent with early endosomes (Oeste et al., unpublished observations). As shown in Figure 43, GFP-RhoB is internalized into the enlarged endolysosomes that appear in CHS cells and co-localizes with LTR at these vesicles. However, GFP-Rab9 elicited an even further enlargement of CHS endolysosomes and was retained at their limiting membrane, in sharp contrast to the normal-sized endolysosomes that contain GFP-Rab9 in control fibroblasts.

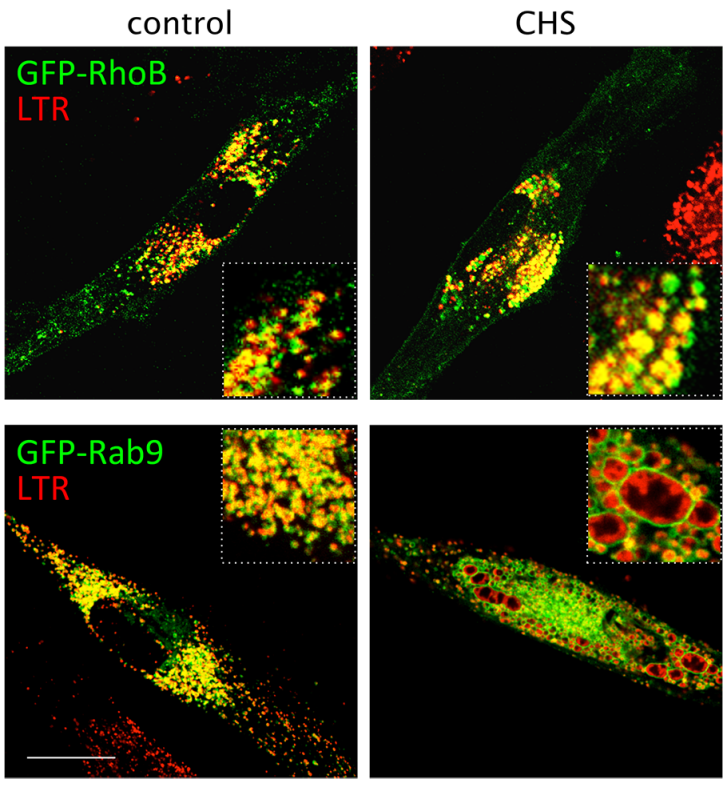

Figure 43. GFP-Rab9 subcellular localization in CHS fibroblasts.

Fibroblasts from control subjects or from CHS patients were transfected with GFP-RhoB or GFP-Rab9 and treated with 25 nM LTR for 15 min prior to live observation by confocal microscopy.

Taken together, these results suggest that the endolysosomal malfunction derived from LYST mutations involves an alteration in lipid composition, as seen by

cholesterol accumulation, that could be responsible for the inadequate localization of Rab9 constructs, as seen in NPC1 cells (Ganley and Pfeffer, 2006).

3.1.2 CINCCKVL localization in cells from lysosomal storage disease patients

Taking into account the aberrant behavior observed in late endolysosomal pathways of lysosomal storage diseases and the results shown above in Chediak-Higashi cells, it was deemed necessary to explore CINCCKVL localization in these lysosomal pathologies. As shown in Figure 44, the distribution of GFP-8 reflected the morphological alterations affecting lysosomal compartments in various diseases.

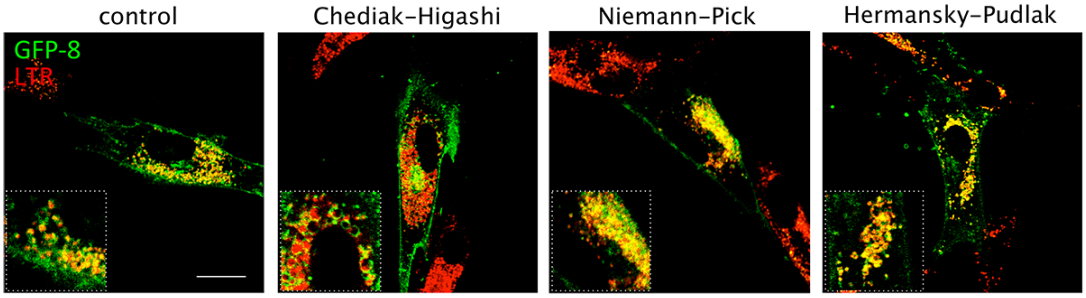

Figure 44. GFP-8 localization in lysosomal storage diseases.

Fibroblasts from control subjects or from patients with the indicated lysosomal diseases were transfected with GFP-8 and treated with 25 nM LTR for 15 min prior to live confocal microscopy observation.

Whereas in control cells, GFP-8 co-localized substantially with lysosomes detected by LTR staining, in fibroblasts from Chediak-Higashi patients, GFP-8 was located at the edge of the abnormally dilated acidic compartments typical of this condition. Interestingly, CHS cells present defects in regulated secretion (Ward et al., 2000). The inset shows that even LTR has difficulty entering the dense lysosomes that accumulate large amounts of ceroid-like material (Figure 44, second panel). On the other hand, as we previously observed (Pérez-Sala et al., 2009), fibroblasts from Niemann Pick type C1 patients, a disease characterized by alterations in intracellular cholesterol traffic, showed increased accumulation of GFP-8 inside lysosomes, probably arising from the altered late endosomal lipid dynamics in this disease. Similarly, fibroblasts from Hermansky-Pudlak Syndrome patients also showed an increase in the

appearance of GFP-8 at LTR-positive compartments. Considering the possible mechanisms responsible for CINCCKVL sorting described in Section 2 of the Results and the altered GFP-8 localization found in CHS cells, further studies could shed light on the sorting mechanisms that are defective in this disease and could find their correlation in other endolysosomal malfunctions.

3.2 Modifications of small GTPase cysteine residues by electrophilic compounds

As described throughout this dissertation, several small GTPases contain cysteine residues at their C-terminal ends that are amenable to palmitoylation and mediate their association with endomembranes of different nature. However, in situations associated with oxidative or electrophilic stress, as occurs in many pathological conditions such as inflammatory processes, diabetes or neurodegeneration, cysteines can suffer non-enzymatic modifications. These include direct oxidation or addition of compounds of electrophilic nature that could preclude palmitoylation and thus proper localization, as previously described for cyPG binding to H-Ras in works from the laboratory (Oeste et al., 2011; Renedo et al., 2007). The assays presented in this section explore whether other small GTPases bearing lipidation cysteines additionally to that of their CAAX box could also be directly modified by cyPG or other small cysteine-reactive compounds, hence eliciting conformation changes in their C-termini that could spread to other areas of the protein, changing their biochemical properties.

3.2.1 Direct binding of cyPG to small GTPases

Previous results from the laboratory established that dienone cyPG such as 15d-PGJ_2 and Δ^{12}-PGJ_2 covalently modify H-Ras at its C-terminal peptide, which bears the palmitoylation cysteines, i.e. C181 and C184 (Renedo et al., 2007). Therefore, binding of biotinylated 15d-PGJ_2 (15d-PGJ_2-B) to other small GTPases containing two palmitoylation cysteines at their C-terminus was assessed. As shown in Figure 45, the

negative control K-Ras4B, which does not have palmitoylatable cysteines in its C-terminus, does not present a detectable biotin signal, as previously reported in cell assays (Renedo et al., 2007). However, binding of 15d-PGJ_2-B was readily observable in the case of H-Ras, RhoB and Rap2B (Figure 45), all of which contain palmitoylation cysteines near the isoprenylation site (see Table 3). Therefore, of the GTPases studied, only those containing cysteine residues that are known to undergo palmitoylation are modified by 15d-PGJ_2-B *in vitro*.

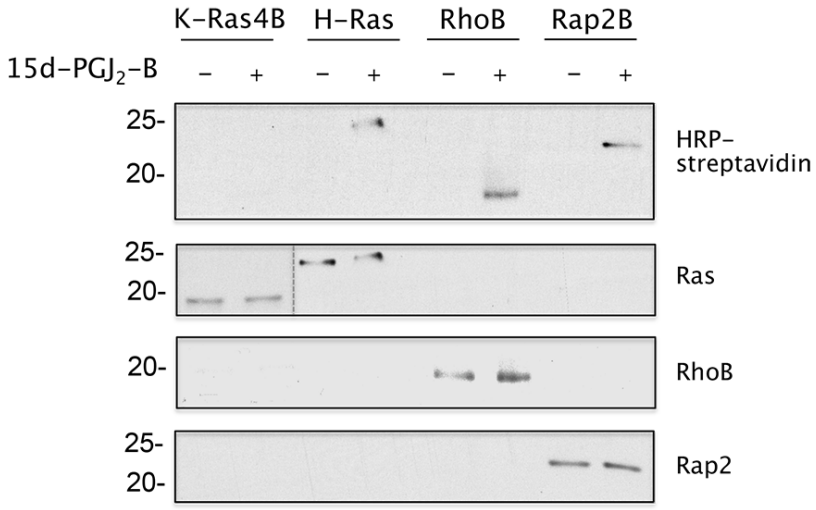

Figure 45. Binding of biotinylated 15d-PGJ_2 to small GTPases.

Human recombinant K-Ras4B, H-Ras, RhoB or His-tagged Rap2B at 5 μM were incubated with 15d-PGJ_2-B at 10 μM for 2 h at room temperature. Incorporation of the biotinylated cyPG was assessed by SDS-PAGE, protein blot and detection with horseradish peroxidase (HRP)-streptavidin (upper panel) or WB with anti-pan Ras, anti-RhoB or anti-Rap2 antibodies. The dashed gray line indicates different exposures due to saturation of the K-Ras4B signal. 20 and 25 kDa markers are shown for reference.

To assess binding of other cyPG to RhoB, *in vitro* studies were carried out with either single enone cyPG or dienone cyPG, as shown in Figure 46. Detection of the biotin signal shows binding of the biotinylated single enones PGA_1 and PGA_2. Interestingly, the *trans* side chain isomer of PGA_2, i.e. the isoprostane 8-iso-PGA_2, displayed a higher biotin signal than its *cis* isomer. Similarly to above, binding of the dienone cyPG 15d-PGJ_2-B was detected, as well. A biotinylated PG devoid of electrophilic carbons, PGE_2, did not bind to RhoB, as expected for this negative control.

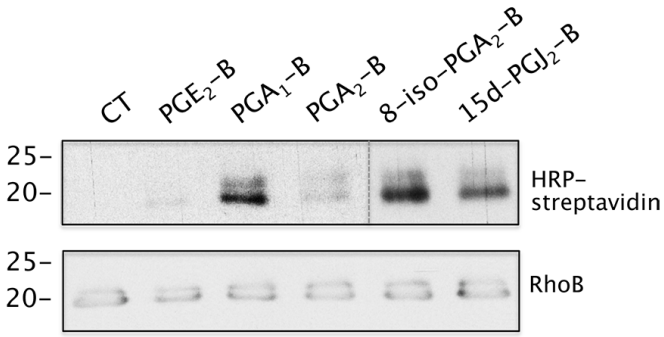

Figure 46. Binding of several cyPG to recombinant RhoB *in vitro*.

Recombinant RhoB at 5 μM was incubated with the indicated biotinylated cyPG at 10 μM for 2 h at room temperature prior to SDS-PAGE analysis, as in Figure 45. The gray dashed line represents two different exposures due to higher biotin levels in the last two lanes.

3.2.2 Binding of small reactive compounds to H-Ras and RhoB

It is possible that other small, bifunctional, thiol-reactive molecules could mimic the behavior of dienone cyPG with respect to binding to GTPases with C-terminal cysteines amenable to palmitoylation. A compound that meets these criteria and is commonly used in cell signaling studies, phenylarsine oxide (PAO, mass 168.02, structure shown in Figure 49B), acts as a tyrosine phosphatase inhibitor that forms adducts with proteins containing sulfhydryl groups close enough to form thioarsine rings (Gerhard et al., 2003; Wang et al., 2003). Indeed, as shown by MALDI-TOF MS in Figure 47A, PAO binding to H-Ras results in a mass increment compatible with addition of a single PAO molecule, which MS-MS analysis detected to be at the C-terminal palmitoylatable cysteines (Oeste et al., 2011). Additionally, since biotinylated 15d-PGJ_2 (15d-PGJ_2-B) binds to full-length H-Ras at its C-terminus, competition assays were performed to determine whether PAO could abrogate dienone cyPG addition. Figure 47B shows that pre-incubation with PAO reduced 15d-PGJ_2-B binding to H-Ras, as reflected by a reduction in biotin detection (28%±7 reduction for PAO versus vehicle-treated Ras). Similarly, the small reactive thiol cross-linker, dibromobimane (DBB, mass 350.01, structure shown in Figure 49B), also elicited a decrease in the biotin signal corresponding to 15d-PGJ_2-B (55% reduction, Figure 47C). The distance between the bromide ions in DBB that are lost upon binding to thiols of cysteines within close range

has been calculated to be approximately 3-6 Å (Sinz and Wang, 2001). Furthermore, DBB is known to undergo a fluorescent shift after bromine loss resulting from cysteine cross-linking (Kim and Raines, 1995), and can indeed be detected directly in gels when incubated with H-Ras (Figure 47C).

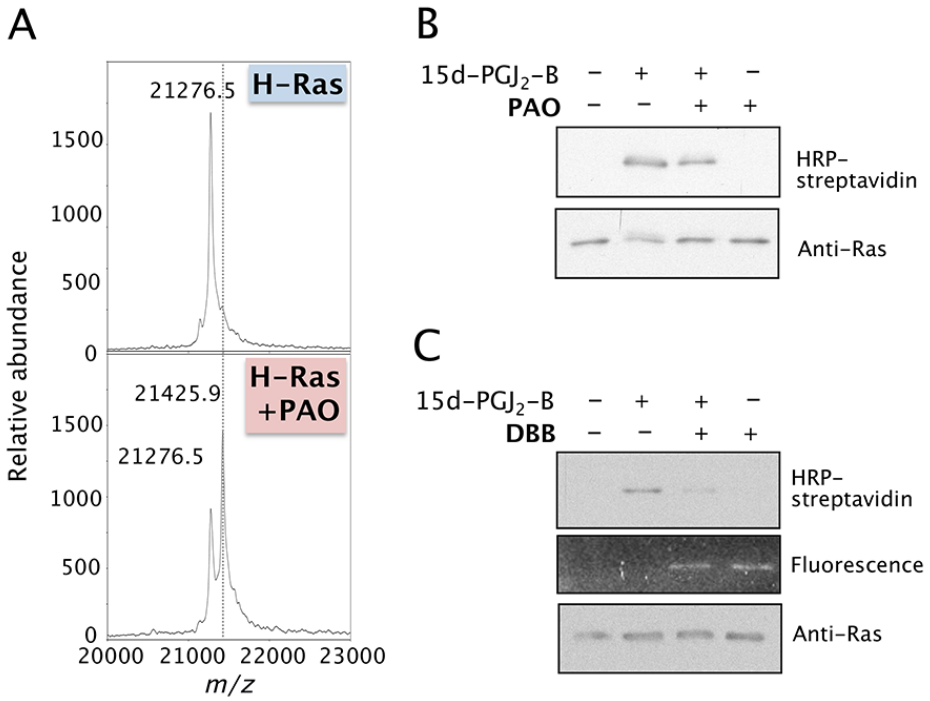

Figure 47. PAO and DBB binding to recombinant H-Ras *in vitro*.

(A) MALDI-TOF MS analysis of human recombinant H-Ras incubated with PAO. (B) Recombinant H-Ras at 5 μM was incubated for 30 min with 50 μM PAO before addition of 1 μM biotinylated 15d-PGJ_2 (15d-PGJ_2-B) for 1 h, where indicated. Incorporation of the biotinylated cyPG was assessed by SDS-PAGE, protein blot and detection with horseradish peroxidase (HRP)-streptavidin (upper panel) or WB with anti-pan Ras antibody (lower panel). (C) Competition of 15d-PGJ_2-B binding to H-Ras by DBB. Full-length H-Ras was incubated similarly to (B) with DBB. Incorporation of DBB was assessed by UV fluorescence detection (middle panel).

In light of the results obtained by SDS-PAGE analysis of RhoB modification by 15d-PGJ_2-B, competition experiments between 15d-PGJ_2-B and PAO or DBB were performed with RhoB, as well. There is a clearly detectable reduction in the biotin signal representing 15d-PGJ_2-B binding when the protein is pre-incubated with either PAO (Figure 48A) or DBB (Figure 48B). Similarly to the results obtained with H-Ras, UV gel fluorescence indicating direct DBB binding was also observed.

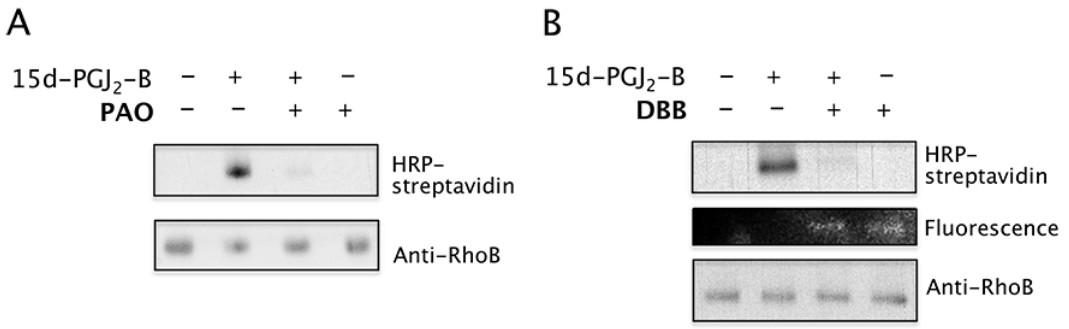

Figure 48. 15d-PGJ_2, PAO and DBB binding to recombinant RhoB *in vitro*.

(A) Recombinant RhoB at 5 μM was incubated for 30 min with 50 μM PAO before addition of 10 μM biotinylated 15d-PGJ_2 (15d-PGJ_2-B) for 1 h, where indicated. Incorporation of the biotinylated cyPG was assessed by SDS-PAGE, protein blot and detection with horseradish peroxidase (HRP)-streptavidin (upper panel) or western blot with anti-RhoB antibody (lower panel). (B) Competition of 15d-PGJ_2-B binding to RhoB by DBB. Full-length RhoB was incubated similarly to (A) with DBB. Incorporation of DBB was assessed by UV fluorescence detection (middle panel).

Several bifunctional reagents have therefore been shown to bind to either full-length H-Ras or RhoB (Figure 47 and Figure 48). Since these proteins contain vicinal cysteines, these compounds could be binding to both cysteine residues simultaneously. Moreover, as mentioned above, direct detection of DBB fluorescence upon incubation of H-Ras or RhoB with this compound indicates that it is bound to two cysteines within 3-6 Å of each other (Kim and Raines, 1995). To directly observe the cross-linking of palmitoylation cysteines elicited by bifunctional compounds, a synthetic peptide corresponding to the H-Ras C-terminus was used as a model in MALDI-TOF MS analyses. This peptide is equivalent to the fragment obtained by tryptic digestion of H-Ras, namely K170-K185 (m/z 1662.7, sequence in Figure 49B), which contains the palmitoylatable cysteines, and presents a more favorable sequence than the equivalent peptide of RhoB, in which the tryptic fragment would include the isoprenylation cysteine in addition to those amenable to palmitoylation. Peptide incubation with 15d-PGJ_2 presents a predominant peak corresponding to the addition of one PG molecule (m/z 1979.80,), as well as two oxidation peaks (m/z 1994.9 and 2010.7), as described in earlier works (Oliva et al., 2003; Renedo et al., 2007).

A

K170–K185: KLNPPDESGPG**C**MS**C**K

	Theoretical *m/z*
Unmodified peptide	1662.73
15d-PGJ_2 adduct (+316.5)	1979.23
PAO adduct (+150)	1812.75
DBB adduct (+188)	1850.73

B

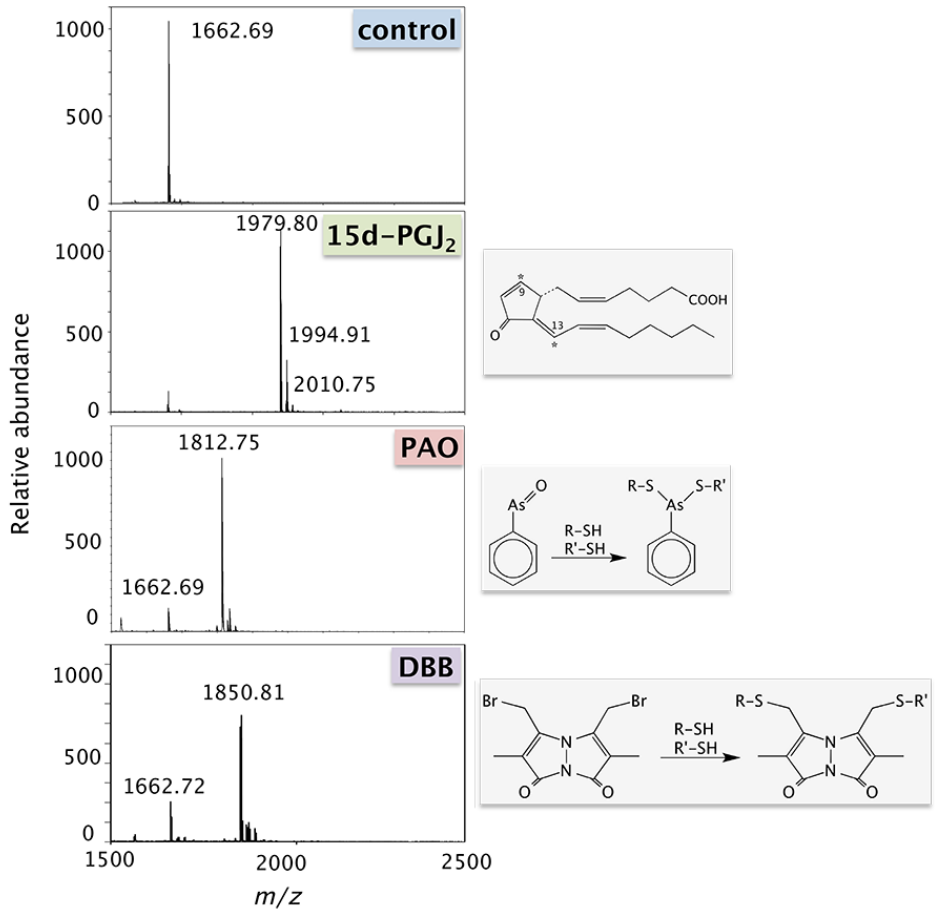

Figure 49. Modification of the K170-K185 H-Ras C-terminal peptide by 15d-PGJ_2, PAO and DBB.

(A) Sequence of the K170-K185 peptide with the modified cysteines in larger, bold font and summary of the theoretical peptide adducts for which compatible peaks were observed by MALDI-TOF mass spectrometry. (B) Incubation of the synthetic H-Ras C-terminal peptide, K170-K185, with either 15d-PGJ_2, PAO or DBB resulted in adducts detected by MALDI-TOF MS. Structures of the compounds employed are shown to the right of the spectra, with a schematic of adduct formation with two thiol groups in the case of PAO and DBB.

Incubation of the K170-K185 peptide with PAO gave rise to a single peak with m/z 1812.7 that represents the simultaneous binding to both cysteines, as depicted to the right of the PAO spectrum (Figure 49B). Likewise, DBB bound to the K170-K185

peptide, resulting in the appearance of a single peak of m/z 1850.81, compatible with a 1:1 adduct of peptide:DBB (Figure 49B). The small span of the DBB reactive groups and the fact that peptide dimers were not detected upon DBB incubation (Oeste et al., 2011) suggest that C181 and C184 are within close range of each other and hence amenable to intramolecular cross-linking by DBB (Figure 49B, bottom).

It should be noted that the H-Ras hypervariable domain does not present a well-defined structure in solution (Thapar et al., 2004), whereas membrane binding induces a more rigid conformation (Gorfe et al., 2007). Therefore, cross-linking of C181 and C184 by 15d-PGJ_2, PAO or DBB binding could potentially stabilize a fixed conformation and disturb H-Ras membrane interactions. These results pave the way for studies in cells to determine the functional repercussion of direct modification by small electrophilic moieties. Assays performed on cells transfected with H-Ras constructs have shown that, indeed, its localization and activation shift from the plasma membrane to endomembranes upon treatment with PAO or DBB (Oeste et al., 2011). Preliminary assays using RhoB have proven unfruitful due to its rapid degradation and low basal levels in cells, though further studies are warranted to determine the cellular effect of binding of these compounds to RhoB.

DISCUSSION

1. Role of the hypervariable motif in small GTPase subcellular localization

Many small GTPases are singly or doubly isoprenylated and some of them undergo further post-translational modifications by palmitoylation. In addition to C-terminal lipidation, the hypervariable region of some Ras superfamily proteins contain basic residue patches that interact with anionic phospholipids that accumulate at particular subcellular membranes and others include further sorting elements such as motifs recognized by adaptors (Bonifacino and Traub, 2003). Significantly, these structural motifs determine subcellular localization patterns that derive from or elicit conformational changes extending to the totality of the protein, which ultimately govern GTPase activation states and signaling functions. In fact, hypervariable regions containing very similar motifs can give rise to different endomembrane sorting on the basis of distinct lipid moiety spacing or even the nature of a few neighboring amino acids.

1.1 Endosomal GTPases appear at distinct subcellular membranes

Studies regarding the hypervariable region sequences of several small GTPases were carried out to assess the structural determinants involved in subcellular localization. Previous studies from the laboratory established the RhoB C-terminal sequence as a motif for sorting to endolysosomes and lysosomal degradation (Pérez-Sala et al., 2009). This behavior depends on its isoprenylation and double palmitoylation, which begged the question of whether other similarly lipidated small GTPases such as H-Ras, Rap2A and B, or TC10 presented similar subcellular localization. As has been performed in detail for H-Ras (Gorfe et al., 2007), short constructs bearing sequences pertaining only to the isoprenylation and palmitoylation motifs of these proteins aided in determining the impact on sorting and degradation of their full-length counterparts.

The results shown in Section 1.1 of the Results indicate that sorting into MVB and subsequent lysosomal degradation is highly specific for RhoB. Though the TC10 C-terminus is very similar to that of RhoB, a basic amino acid patch upstream of the palmitoylation cysteines is responsible for retention at limiting membranes of MVB and

hampers inclusion into ILV (Valero et al., 2010). Indeed, this basic residue motif could mediate an electrostatic interaction of TC10 with the most abundant negatively charged phospholipid, i.e. phosphatidylserine, which is found mainly on the cytosolic surface of endosomes and the plasma membrane (Leventis and Grinstein, 2010; Urade et al., 1988; Yeung et al., 2008), hence obstructing entry into the lumen of MVB and subsequent degradation. Other bipalmitoylated proteins were found similarly retained at the limiting membranes of endolysosomes, such as the Rap2 isoforms (Valero et al., 2010). In this case, the alternate spacing between lipidated residues could confer a distinct overall three-dimensional conformation at the C-terminus of Rap2 proteins that promotes association with membrane microdomains of singular properties. Short constructs derived from the H-Ras C-terminal sequence were mainly present at the plasma membrane, as previously described (Gorfe et al., 2007). It could therefore be postulated that combinations of electrostatic interactions and reversible palmitoylation are responsible for endowing C-termini with conformations that allow binding to membrane regions of well-defined characteristics. Taken together, these results indicate that the isoprenylation and palmitoylation motif of RhoB constitutes a precise structure with affinity for particular membrane domains that determines its selective sorting through the endolysosomal pathway into the lumen of MVB.

1.2 The RhoB C-terminus CINCCKVL is an MVB and endolysosomal marker

Several studies from our laboratory have shown that the fully processed RhoB C-terminal sequence CINCCKVL co-localizes with endolysosomal probes such as LTR, Lamp1, Rab7, Rab9 and CD63 constructs, or LBPA, as well as appearing directly at ILV of MVB (Oeste et al., 2014; Pérez-Sala et al., 2009; Valero et al., 2010). These results were confirmed through the use of several fusion proteins containing this sequence, including varied fluorescent constructs such as GFP, RFP and its photostable forms (tagRFP, tagRFP-T), mCherry, or photoswitchable Dendra2. Intracellular live markers are not devoid of pitfalls, such as endosome enlargement induced by overexpression of Lamp1 or Rab7 constructs and induction of stress fibers by transfecting with full-length RhoB fusion proteins (unpublished observations). In the case of CINCCKVL chimeras, no detectable morphological abnormalities have been encountered during its use, so far.

Furthermore, work from the laboratory in live BAEC and HeLa reported a lack of overlap with several autophagy probes after induction of autophagy such that independent GFP-8-positive structures were clearly distinct from RFP-LC3 autophagosomes (Oeste et al., 2013). CINCCKVL localization to Golgi compartments is also negligible when full modification is allowed (Oeste et al., 2014). As will be discussed below, lipidation status is crucial to CINCCKVL sorting through the endocytic pathway, and can hence be regulated to track subcellular organelles or detect overall isoprenylation precursor status through statin switch assays. Therefore, CINCCKVL fusion proteins may be used as markers amenable to pharmacological modulation for dynamic tracking of MVB and endolysosomes in live cells.

1.3 CINCCKVL localization at endolysosomes depends on lipid modifications

The presence of CINCCKVL proteins at endolysosomes is completely dependent on full post-translational processing by lipids. It is shown in this work that isoprenylated but non-palmitoylated constructs are diffuse within the cytoplasm but exclude the nucleus and are in part retained at the Golgi apparatus, where palmitoyl transferases are usually accumulated, which could represent species that are awaiting palmitoylation, (Aicart-Ramos et al., 2011). In contrast, non-lipidated forms spread throughout the cell, leaving some small, LTR-positive vesicles empty. It therefore becomes apparent that palmitoylation is a *sine qua non* for CINCCKVL entry into endolysosomes, as shown schematically in Figure 50. Similarly, studies involving the Ca^{2+} sensor synaptotagmin 7 described that its palmitoylation elicits association with CD63 and subsequent sorting to lysosomes, whereas non-palmitoylated forms are retained in the Golgi (Flannery et al., 2010). However, these instances are in contrast with the more numerous cases of proteins in which palmitoylation precludes access to lysosomes, as seen in (McCormick et al., 2008; Pérez-Sala et al., 2009). For example, recycling of the M6P receptor from lysosomes to the Golgi is dependent on its N-terminal palmitoylation, for palmitoylation-defective mutants accumulate into dense lysosomes (Schweizer et al., 1996).

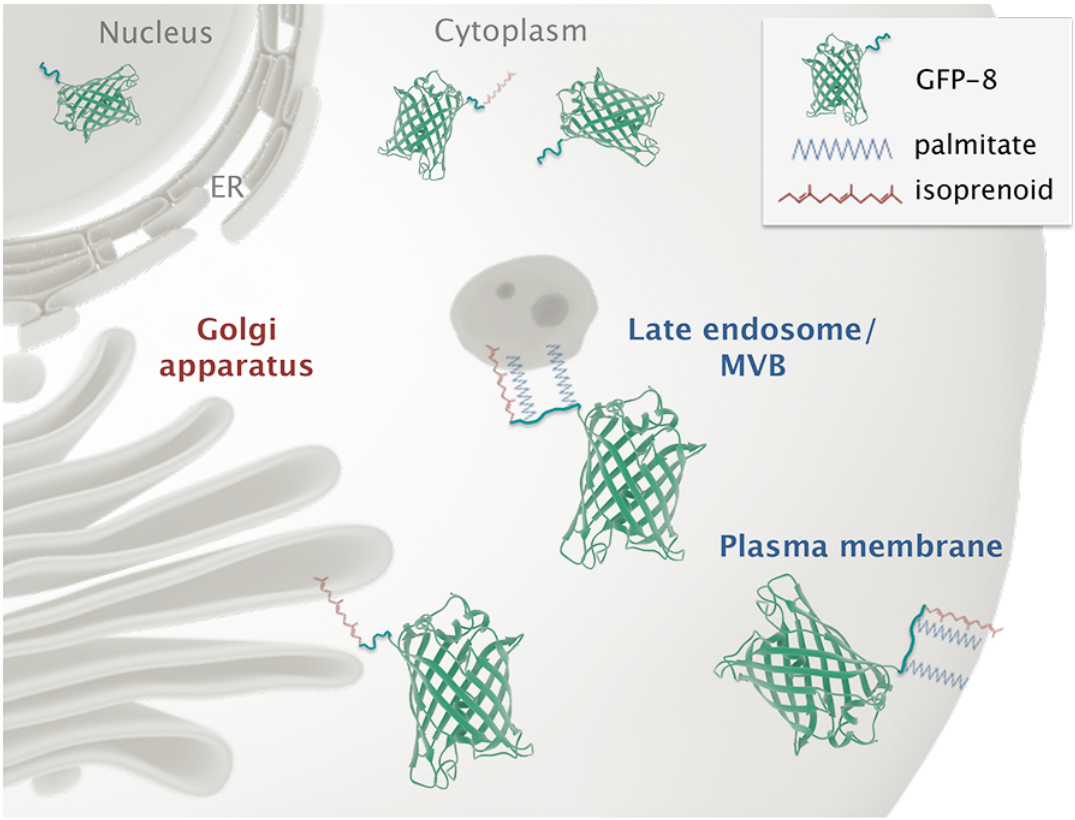

Figure 50. GFP-8 subcellular localization depends on its lipid modifications.

The GFP structure appears as a ribbon diagram in green, with the CINCCKVL motif represented as a green squiggle attached to it. Totally unlipidated forms are completely diffuse throughout the cytoplasm and the nucleus (gray font), whereas isoprenylated forms exclude the nucleus, are predominantly cytosolic and are sometimes associated with the Golgi apparatus (red font). However, isoprenylated and bipalmitoylated GFP-8 appears at late endosomes/MVB and the plasma membrane (blue font). See text for details.

Concerning the GPCR, PAR-1 (protease-activated receptor 1), there seems to be an interplay between its YXXΦ sorting motifs and palmitoylation, such that correct sorting mediated by the tyrosine motif requires correct modification by palmitate and PAR-1 mutants lacking palmitoylation cysteines are degraded in lysosomes to a higher extent (Canto and Trejo, 2013). The yeast protein Vac8 is localized at the vacuolar membrane in yeast, though internalization into this compartment has not been described (Peng et al., 2006). Hence, a general role for palmitoylation in protein sorting is lacking, since the consequences of modification by this lipid seem to be protein-specific and cell-type dependent. Additionally, palmitoylation of RhoB constructs is probably accountable for the lack of interaction between either GFP-8 or GFP-RhoB with RhoGDIα as compared to that detected for GFP-RhoA (Oeste et al., unpublished observations), as previously hypothesized (Michaelson et al., 2001). Nevertheless, it still

remains to be established whether non-palmitoylated RhoB constructs interact with RhoGDI in the cytosol (Ho et al., 2008).

Upon isoprenylation inhibition, full-length RhoB-derived constructs behave as cytosolic proteins, similarly to unprenylated GFP-8 (see Figure 50). Therefore, both membrane and RhoGDI binding cannot occur and RhoB could be degraded through the expected proteasomal pathway followed by soluble proteins. In fact, excessive overexpression of fluorescent RhoB constructs elicits diffuse accumulation in the cytosol, most likely due to saturation of the lipidation machinery and subsequent lack of precursors. Such "extra" proteins could become ubiquitinated and degraded through the proteasome, which is a putative scenario for a study detecting RhoB ubiquitination upon overexpression of RhoB and ubiquitin in cells treated with proteasomal inhibitors (Engel et al., 1998). Indeed, RhoB is an early response gene and its levels can rise quickly within the cell to overcome damage by UV exposure (Canguilhem et al., 2005). It would be interesting to detect whether, following this stimulus, the newly synthesized proteins are capable of becoming isoprenylated and bipalmitoylated to follow the endolysosomal pathway described herein, or whether full lipidation occurs to maintain low RhoB levels principally in resting state conditions.

Pharmacological statin treatment, which is widely prescribed for hypercholesterolemia, greatly increases levels of unprocessed RhoB in the cytosol (Stamatakis et al., 2002). Another report determined that an increase in non-prenylated Rho protein translates into overall elevated levels of GTP-bound Rho as compared to untreated cells expressing normal levels, suggesting that Rho-dependent signaling pathways are more active in statin-treated cells (Turner et al., 2008). Furthermore, it has been previously described that accumulation of unprocessed, soluble forms of Rho proteins (mostly RhoA) are partly responsible for the serious side effects resulting from abrupt statin withdrawal, which implies a sudden lift of the blockade on isoprenoid precursor formation. The accumulated Rho protein is rapidly modified by newly synthesized geranylgeranyl moieties and translocates to the plasma membrane, strongly activating its signaling cascades, including repression of endothelial nitric oxide synthase (eNOS). This phenomenon causes a dangerously abrupt drop in nitric oxide production in cardiac endothelial cells, hence impairing vascular function (Laufs et al., 2000). These effects were studied in detail in the context of RhoA, but the concomitant

increase in unprocessed RhoB concentration in cells from patients undergoing statin treatment warrants further investigation.

1.4 CINCCKVL sorting is conserved from fungi to human cell models

Cells from very diverse species including ascomycetous fungi, insects, amphibians and several mammals are all able to sort RhoB C-terminus constructs to the vacuole or endolysosomes. However, they endogenously express different sets of Ras superfamily proteins, and in some cases a clear RhoB homolog has not been identified or is not localized to endosomes. Mammals and birds express identical RhoB proteins, but organisms studied in this work that are lower on the evolutionary scale differ in their C-terminal RhoB sequence or do not encode a RhoB homolog, as seen in insect cells. In the case of *Schizosaccharomyces pombe,* there is a RhoB homolog termed Rho2 that appears at the plasma membrane, the septation site and growing ends (Hirata et al., 1998). However, this protein contains only one palmitoylated cysteine close to the isoprenylation site (Roth et al., 2006), which is modified by a farnesyl moiety (Ma et al., 2006) in *lieu* of the preferential geranylgeranylation that takes place on RhoB in cells (Roberts et al., 2008). RhoB can become alternatively isoprenylated, though studies with constructs containing CAAX boxes more inclined to either modification, namely GFP-CINCCKVL and GFP-CINCCLVM (geranylgeranylated or farnesylated, respectively), did not present detectable differences as to their endolysosomal localization, so that a crucial role for the length of the C-terminal isoprenoid is not likely (Oeste et al., unpublished observations). Another yeast protein, RasA, is indeed bipalmitoylated, but it accumulates at the plasma membrane and disrupting its palmitoylation elicits a patchy intracellular distribution (Fortwendel et al., 2012). *Aspergillus nidulans* codes for a putative Rho2-like protein expected to be geranylgeranylated and palmitoylated, though a homolog for GGTase I has not yet been biochemically identified in this species.

The instances of lipidated proteins in lower organisms described above highlight the fact that, though these species are able to sort CINCCKVL to endolysosomes, none of their endogenous proteins have been described to follow this route directly. It is therefore worth examining whether the sorting machineries potentially responsible for

RhoB construct sorting in mammals, i.e. Rabs, ESCRT or the tetraspanin CD63, are conserved from fungi to human cells. Indeed, the basic Rab components of the endocytic route are conserved throughout metazoan evolution. In-depth phylogenetic studies on Rab family proteins highlight the existence of a large number of Rabs early on in evolution (Elias et al., 2012; Klöpper et al., 2012). Moreover, it has been proposed that the latest eukaryotic common ancestor (LECA) contained more than 20 core Rab proteins that have suffered expansions by gene duplication or losses throughout eukaryotic evolution (Klöpper et al., 2012). Further human Rabs have arisen from gene duplication of the fundamental Rabs associated either to early endosomes (Rab5), late endosomes (Rab7 and Rab9) recycling endosomes (Rab11) and so on, up to the ten subfamilies identified through phylogenetic studies of mammalian Rabs (Pereira-Leal and Seabra, 2000). Interestingly, CINCCKVL chimeras are present inside vesicles that are marked at their limiting membranes by proteins included in a category containing late endosomal LECA Rabs (group III), such as Rab7.

As is the case for Rab proteins, at least one component from each of the ESCRT-I, -II or –III complexes is present in fungi and metazoans (Wideman et al., 2014). However, outside Ophisthokonta, ESCRT-0 is completely absent, so that other mechanisms for ubiquitin recognition must exist in organisms present before the LECA branched off from other life forms (Leung et al., 2008). Considering the role of ESCRT proteins in MVB biogenesis, it would be expected that organisms with defined intracellular compartments would require their action for correct endosomal sorting. However, *Archaea* have also been shown to contain ESCRT components, though only ESCRT-III and Vps4 (Samson et al., 2008). Such is the case due to the vital role of several ESCRT proteins in membrane abscission during cytokinesis (Rusten et al., 2012). Furthermore, ESCRT proteins are also involved in virus budding, such as human immunodeficiency virus-1 (HIV-1) egress from the plasma membrane, which follows an "inside-out" route from the cytoplasm that is topologically similar to ILV formation (Garrus et al., 2001; Morita and Sundquist, 2004).

Therefore, the Rab and ESCRT proteins found to co-localize with CINCCKVL and RhoB constructs or involved in their sorting could potentially be present in the diverse species studied. In the case of tetraspanin proteins, fungi have been found to contain homologs, though in *Aspergillus nidulans* only a tetraspanin-like protein has

been proposed by sequence homology but has not been characterized (Lambou et al., 2008).

2. RhoB subcellular sorting mechanisms

The structural determinants guiding endosomal small GTPase sorting include lipidation motifs and amino acids of specific characteristics. In the case of RhoB, its C-terminus CINCCKVL represents a unique structure upon lipidation that attaches to the very specific subcellular localization of late endosomal pathway vesicle lumina that is conserved in cells from many organisms. In human cells, targeting to ILV of MVB such as occurs for RhoB does not necessarily mean degradation at lysosomes, though RhoB constructs are indeed degraded mainly through this pathway (Pérez-Sala et al., 2009). As described previously, proteins present at MVB can also be exocytosed by fusing with the plasma membrane or recycled back to the Golgi apparatus as well as being delivered to the lysosome (Futter et al., 1996; Lu and Hong, 2014; Murk et al., 2002; Vlassov et al., 2012). However, there is still debate as to whether the same MVB contains ILV directed towards different sites or if there are specialized MVB that deliver all their ILV to the same subcellular destination (Edgar et al., 2014; van Niel et al., 2011; Vlassov et al., 2012). Therefore, it was crucial to investigate some of the trafficking pathways that lead proteins to and from MVB in eukaryotic cells to determine their role in sorting of RhoB and its last eight amino acids. The interplay between protein sequence and lipid modifications in sorting of these proteins warranted the study not only of protein complexes involved in shuttling material within the cell, but also of the lipid features of the membranes to which they attach.

2.1 Differential role of the ESCRT machinery in sorting of RhoB versus CINCCKVL constructs

Protein sorting into MVB is at the convergence of several endocytic routes, as well as a hub towards other intracellular destinations. ESCRT proteins regulate the canonical pathway described for entry into MVB of many proteins, such as the EGF

receptor. Previous work from the laboratory suggested the involvement of this machinery in RhoB sorting through the use of Vps4 dominant negative constructs in BAEC (Pérez-Sala et al., 2009). Furthermore, other routes to the MVB such as autophagy, microautophagy or chaperone-mediated autophagy are highly unlikely routes for trafficking this GTPase, as discussed in (Oeste et al., 2014). It was therefore possible that the ESCRT machinery played a role in RhoB sorting.

ESCRT-mediated sorting into MVB, when dependent on the whole machinery, begins by ubiquitination of cargo such as EGFR. Ubiquitin-independent mechanisms also exist, but these usually involve only late ESCRT components and ESCRT-III-associated proteins such as Alix. Many attempts at detecting ubiquitination of RhoB constructs were undertaken for this work, including stimulation with EGF, treatment with proteasomal or lysosomal degradation inhibitors, or simvastatin treatment to accumulate RhoB, though none of them resulted in a clear signal of ubiquitinated full-length RhoB or CINCCKVL proteins, rendering these results inconclusive (not shown). Interestingly, the GFP-22 construct that showed a faint ubiquitin signal contains a lysine residue that could become ubiquitinated, but might be less exposed in full-length RhoB, such that regulated processes could mediate its amenability to ubiquitination. However, use of ESCRT siRNA to silence some components of the machinery and observation of GFP-RhoB and GFP-8 by live microscopy revealed differential phenotypes, so that ESCRT could be involved regardless of ubiquitination. Strikingly, by using these constructs in parallel, a distinctive subcellular localization was observed upon depletion of the ESCRT components Hrs and Tsg101. These were the first studies to show differential behavior between full-length RhoB, which showed impaired sorting in cells depleted of these ESCRT, and its chimera, GFP-8, which was sorted into endolysosomes in these cells. It is possible that RhoB is in fact ubiquitinated but we have not achieved its detection, either because its ubiquitination is fast and transient or because it is rapidly degraded in the lysosome upon ubiquitination, or both. In any case, our results suggest that GFP-RhoB would follow an ESCRT-mediated pathway into the lumen of endolysosomes, be it ubiquitin-dependent or -independent. In contrast, GFP-8 would not become ubiquitinated and could therefore follow ceramide and CD63-driven budding into MVB and pinch off to become ILV regardless of alterations in the ESCRT machinery.

Differences encountered between GFP-8 and GFP-RhoB give rise to a working hypothesis for the molecular players involved in RhoB and CINCCKVL localization and sorting. This view is schematized in Figure 51 and will aid in discussing the possible sorting mechanisms throughout the following sections, as well as in future studies.

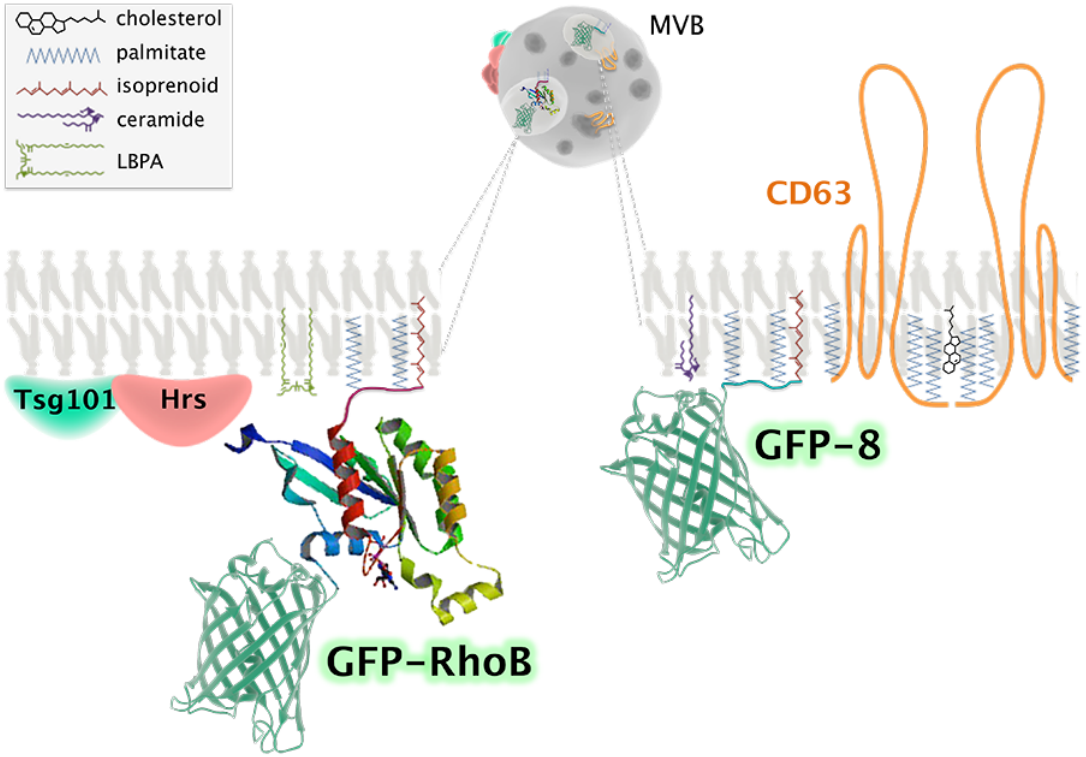

Figure 51. Schematic of possible membrane platforms for GFP-RhoB and GFP-8.

Zoom-in on putative differential ILV of MVB containing either GFP-RhoB or GFP-8. The results shown in this work point to a possible role for the ESCRT proteins Hrs and Tsg101 in GFP-RhoB sorting (left membrane), but not for that of GFP-8. The larger ILV into which GFP-RhoB enters would contain the late endosome lipid, LBPA (light green). In contrast, CD63 could be involved in GFP-8 sorting, as well as cholesterol dynamics (right membrane). Furthermore, ceramide treatment could induce the appearance of GFP-8 in small ILV containing CD63, which could putatively be secreted to the extracellular space.

2.2 Effects of agents altering cellular lipid dynamics on CINCCKVL and full-length RhoB sorting

Apart from the protein machineries involved in intracellular sorting, the lipid composition of endosomal membranes plays a key role in cargo trafficking and MVB biogenesis (Bissig and Gruenberg, 2013; Bissig et al., 2012). In fact, lipid microdomains in the *Saccharomyces cerevisiae* vacuole were recently found to mediate protein

segregation (Toulmay and Prinz, 2013). On one hand, bulk lipids can convey specific conformations to membranes according to their three-dimensional properties, so that conical lipids induce curvature and straight molecules increase membrane order, i.e. diacylglycerol and cholesterol, respectively (Bigay and Antonny, 2012). Altering cholesterol dynamics in several cell types by pharmacological treatment indeed disrupts the association of CINCCKVL constructs to endolysosomes. On one hand, treatment with U18666A, which increases membrane invagination into MVB (Marchetti et al., 2004), gives rise to prominent accumulations of CINCCKVL chimeras within endolysosomes containing LBPA, cholesterol and delimited by markers such as Lamp1-GFP, GFP-Rab7 or -Rab9 (Valero et al., 2010), reflecting their specific association with ILV. On the other hand, inhibiting cholesterol biosynthesis by ZGA treatment induced MVB dilation and a striking retention of proteins at MVB limiting membranes, i.e. GFP-8 or CD63 constructs, which normally internalize into ILV in control cells (Oeste et al., 2014), though this retention was not observed for GFP-RhoB, which still entered endolysosomes upon ZGA treatment (Figure 36).

The results observed for GFP-8 agree with previous reports describing ILV as the major cholesterol-containing vesicles in the endosomal pathway (Möbius et al., 2003). It is possible that overall cholesterol depletion would therefore affect these structures more markedly, hampering the route followed by GFP-8 for invagination into MVB (see Figure 51). In fact, endothelial cells have been shown to contain cholesterol-rich membrane domains in their MVB (Amiya et al., 2013). Moreover, mice deficient in the last enzyme of the cholesterol biosynthetic pathway (Δ24 sterol reductase) present reduced ILV material within their MVB, which follows the same pattern as the reduction of GFP-8 and CD63 constructs in the lumen of MVB upon ZGA treatment (Gilk et al., 2013). Cholesterol has also been found to stabilize particular microdomains containing specialized phosphoinositides (Jiang et al., 2014), so that altering its dynamics could affect these small signaling platforms, as well. Furthermore, specific lipids exist at defined membrane microdomains, as is the case for the curvature-inducing lipid LBPA in endolysosomes (Matsuo et al., 2004), or particular phosphoinositides along the endocytic pathway (Di Paolo and De Camilli, 2006). In this regard, full-length RhoB constructs co-localize to a large extent with LBPA in the endolysosomal lumen (Pérez-Sala et al., 2009), whereas the PI(3)P marker 2xFYVE

appears at small, dispersed vesicles that do not overlap with RhoB or CINCCKVL constructs (Oeste et al., unpublished observations). Therefore, sorting of RhoB constructs is dependent on lipid-mediated mechanisms of ILV formation for which cholesterol and LBPA are essential.

2.3 CD63 overexpression has differential effects on full-length RhoB and CINCCKVL localization

Sorting mediated by tetraspanins and TEM are a telling example of the intrinsic relationship between protein sequence, lipid modifications and membrane organization. In the case of CD63, its four transmembrane domains direct insertion into membranes, its YXXΦ motif guides intracellular trafficking, and palmitoylation at cysteine residues determines attachment to membranes of specific characteristics in a cholesterol-dependent manner (Charrin et al., 2003; Israels and McMillan-Ward, 2010; Pols and Klumperman, 2009; Yang et al., 2002). These features give rise to CD63 sorting to specific membrane microdomains, which are also the destination for RhoB chimeras, i.e. ILV of MVB and the plasma membrane, to a varying extent. In fact, co-localization studies in resting cells show almost total overlap between wild-type CD63 constructs and CINCCKVL chimeras, and to a lesser degree with full-length RhoB constructs. As depicted in Figure 51, it could be hypothesized that GFP-8 is intimately connected to TEM through its palmitate residues by a similar cholesterol-dependent mechanism that keeps CD proteins together (Charrin et al., 2003). The lack of further sorting determinants in GFP-8 would render the protein quite dependent on TEM dynamics. Therefore, disruption of CD63 intracellular trafficking such as that which could take place upon overexpression of CD63 constructs, particularly the Y235A mutant, would hinder binding to AP-3 complexes, which could alter CD63 sorting to TEM at MVB and therefore result in a concomitant misplacement of GFP-8. AP-3 has been shown to contribute to the regulated secretory pathway, as AP-3 depletion reduces regulated secretion of secretogranin II, though it elicits an increase in its constitutive secretion as a compensatory mechanism (Asensio et al., 2010). Therefore, a putative indirect association of GFP-8 to AP-3 via CD63 could be abolished in a scenario of altered CD63 sorting such as cells overexpressing CD63 constructs, sending CINCCKVL proteins

towards constitutive exocytosis. In contrast, additional sorting motifs, interactions with effectors, or an active role in endosomal dynamics could be responsible for full-length RhoB localization at endolysosomes without partaking in secretion mechanisms, regardless of changes in CD63 sorting. In any case, these results set forth the possibility that CINCCKVL chimeras could also appear in the extracellular space, which is congruent with their localization at ILV of MVB containing CD63 and possibly destined for exocytosis.

Biogenesis of ILV destined towards exocytosis, which contain CD63, can occur independently of the ESCRT machinery; instead, the curvature-inducing lipid, ceramide, mediates inward budding from the MVB limiting membrane (Trajkovic et al., 2008). Follow-up studies to determine whether CINCCKVL proteins can be delivered to the extracellular space were performed by exogenous treatment with C6 ceramide. These studies revealed that this lipid elicits an "emptying out" of cells co-transfected with GFP-8 and CD63, with a concomitant appearance of fluorescent extracellular material and reduction of GFP-8/mCherry-CD63 co-localization. On the other hand, GFP-RhoB was retained at several subcortical sites below the plasma membrane and did not appear in secreted membranous structures. Full-length RhoB could therefore contain a motif(s) upstream from the CINCCKVL sequence acting as a retention signal to bar its exit from the cell. Indeed, very few instances of human extracellular vesicle-associated RhoB have been described, including one report in exosomes of colorectal cancer cells, another report describing RhoB in exosomes from urine, and three studies in which microvesicles were found to contain RhoB (www.microvesicles.org). Furthermore, under the conditions employed in preliminary assays for isolating an extracellular vesicle fraction by sequential ultracentrifugation, we were unable to detect RhoB (unpublished observations).

It is worth noting that a study using numerous chimeric proteins postulates that cytosolic proteins with a tendency to oligomerize, when attached to a lipid anchor, become secreted into the extracellular medium. Indeed, a GFP-tagged, oligomeric, cytosolic protein with a RhoB-related isoprenylation and mono-palmitoylation sequence attached (CCKVL) is detectable in an exosome/microvesicle fraction, albeit to a much lesser degree than the positive controls containing either an N-myristoylation tag or a PIP_2-binding domain (Shen et al., 2011). However, throughout this work we

have used different fluorescent proteins besides GFP, some of which are theoretically expressed as monomers and therefore would not necessarily follow this oligomerization trend *per se*, e.g. mCherry, which stands for *m*onomeric Cherry (Shaner et al., 2004). Interestingly, the Hrs domain 2xFYVE is practically incapable of eliciting a secretory phenotype in the study mentioned above. It could be hypothesized that the potential RhoB-Hrs interaction hinted at by Hrs KD cells guides RhoB constructs into ILV destined towards degradation at the lysosome, hindering its entry into exocytic ILV into which GFP-8 is sorted and retaining GFP-RhoB within the cell, as described above. These distinct phenotypes only appear upon altering cellular homeostasis, such as ESCRT depletion or C6 ceramide treatment, but not under resting conditions. Whether these distinct ILV subpopulations exist within the same MVB will be the subject of further studies, though co-transfection of CINCCKVL and RhoB constructs has proven highly toxic, perhaps due to lipid precursor depletion (results not shown).

Considering that lipidated CINCCKVL constructs are fused directly to GFP and have no other RhoB-derived sequences, the differences encountered between these proteins and full-length RhoB constructs point to other sorting, signaling, or interaction sequences upstream of the lipidation sites. A close look at the RhoB sequence does indeed bring up interesting sequences and residues as hypothetical recognition motifs, as shown in Figure 52.

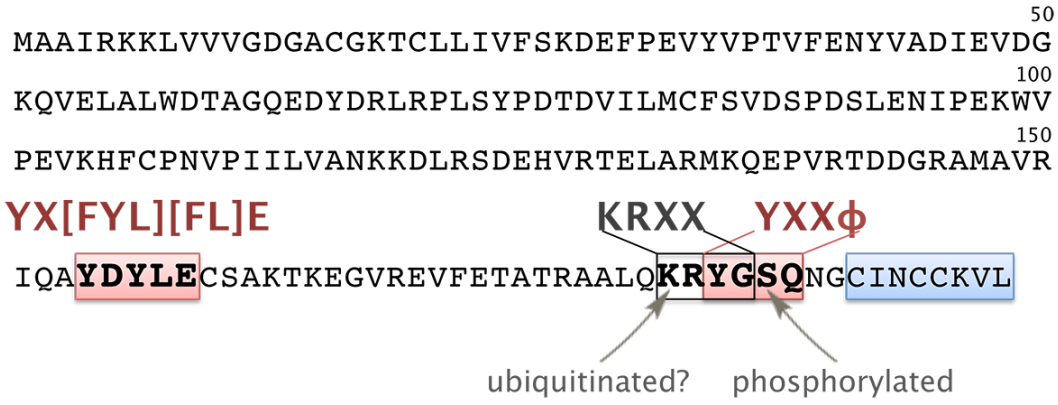

Figure 52. RhoB sequence and possible sorting motifs upstream of its lipidation region.

The full-length human RhoB sequence is shown. The lipidation motif, CINCCKVL is highlighted in blue, while possible AP-interaction motifs are boxed in red or black. The YDYLE sequence fits with a putative motif recognized by AP-4, namely "YX[FYL][FL]E". The second is a putative YXXΦ motif that is recognized by several AP complexes. The "KRXX" sequence is a hypothetical AP-3 binding motif. Arrows mark a possibly ubiquitinated lysine residue and a serine that becomes phosphorylated. See text for details.

Indeed, it has been reported that serine 185 of RhoB, close to its palmitoylation cysteines (see Figure 52), is phosphorylated by casein kinase-1, which hampers stress fiber formation and EGF receptor stabilization (Tillement et al., 2008). As discussed above, a few amino acids upstream, there is a lysine residue included in the GFP-22 construct that could be amenable to ubiquitination. RhoB also possesses a sequence matching a recently described, non-canonical AP-3 interaction motif of interferon-induced transmembrane (IFITM) protein 1, i.e. the dibasic patch "KRXX", as shown in Figure 52. Interestingly, two possible YXXΦ motifs appear in regions upstream of the CAAX box that are unique to RhoB. As seen in Figure 52, that which is closest to the C-terminus, "YGSQ", follows a rather canonical pattern and could hence be recognized by several AP complexes (Bonifacino and Traub, 2003). Furthermore, this sequence includes the phosphorylatable serine and its recognition by AP complexes could therefore depend on its phosphorylation state. The other YXXΦ motif, "YDYLE", appears further upstream (Figure 52), beginning with Tyr154, and is a striking match to the motif that mediates AP-4 binding for trans-Golgi to endosome sorting of the amyloid precursor protein, namely YX[FYL][FL]E (Burgos et al., 2010; Park and Guo, 2014). RhoB interaction with AP-4 would hypothetically be consistent with exit from the Golgi after palmitoylation, *en route* towards its endosomal localization.

Preliminary localization studies were carried out with mutants of tyrosines belonging to these hypothetical YXXΦ motifs, namely, GFP-RhoB-Y154A and GFP-RhoB-Y183A. However, there were no apparent changes in subcellular localization in basal conditions compared to wild-type GFP-RhoB by live confocal microscopy observation. Further studies are needed to address the possibility that response to stimuli such as EGF or alteration of endocytic components such as those used throughout this work would yield discrete phenotypes, or to assess the behavior of these mutants at different time points to detect whether their trafficking is delayed or expedited due to hypothetical disruption with AP complexes.

3. Small GTPases in pathological scenarios

3.1 RhoB constructs appear at endolysosomes in cell models with impaired endolysosomal dynamics

Mutations in several proteins involved in intracellular sorting or lipid homeostasis give rise to an array of lysosomal storage diseases characterized by oculocutaneous albinism, deficiencies in immune processes and neurodegenerative defects (Ballabio and Gieselmann, 2009). These cell models have been widely studied to elucidate intracellular sorting machineries and the routes followed by particular proteins, so that it was deemed necessary to benefit from this approach in the context of RhoB trafficking. Among these disorders, Niemann-Pick Type C Disease is clearly linked to altered cholesterol dynamics, since the mutated protein NPC-1 is responsible for shuttling cholesterol at endolysosomes (Mukherjee and Maxfield, 2004). In turn, Hermansky-Pudlak Syndrome patients develop this disease due to mutation of several proteins, including AP-3 or Rab27, both involved in LRO biogenesis and transport (Wei, 2006). In both of these diseases, GFP-8 appears at intra-endolysosomal accumulations co-localizing with LTR. However, Chediak-Higashi cells, which contain enlarged endolysosomes, show GFP-8 accumulation at their limiting membrane instead of inside the lumen, in spite of the elevated intraluminal cholesterol and LBPA content of these compartments in CHS. Point mutations responsible for CHS occur on the very large scaffolding protein LYST (Karim et al., 2002), of mostly unknown function, though recent studies suggest it could regulate lysosomal size and quantity but not trafficking (Holland et al., 2014). Interestingly, reports using expression constructs of LYST fragments have detected a direct interaction of LYST and the ESCRT component Hrs (Tchernev et al., 2002), further substantiating its involvement in late endosomal dynamics. Considering the results presented in this work with respect to the possible dependence of RhoB sorting on Hrs function, retention of CINCCKVL constructs at the periphery of CHS vesicles could also be due to indirect LYST-mediated mechanisms. However, full-length RhoB constructs do internalize into enlarged CHS endolysosomes, which questions this interpretation.

Another striking phenotype found in CHS fibroblasts was the endolysosomal dilation caused by GFP-Rab9 overexpression, indicating a potential impairment of Rab9-mediated shuttling of material from the trans Golgi network to late endosomes and *vice versa*. In fact, there seems to be an overall entrapment of many small GTPases, i.e. RhoB, Rab7, TC10 and Rab9, co-localizing in endolysosomal compartments, hinting at impaired traffic from that point onwards, be it towards the plasma membrane by exocytosis or endocytic recycling, or towards the Golgi apparatus in biosynthetic recycling (Huynh et al., 2004; Zhang et al., 2007). Another possibility would be that CHS lysosomes possess inefficient degradation mechanisms, though studies with EGFR or RhoB argue against this hypothesis. Recently, degradation of EGFR was found to occur normally in LYST knock-down HeLa cells (Holland et al., 2014). These findings are in line with preliminary studies from the laboratory that showed similar degradation rates for several GTPase constructs in CHS and control fibroblasts (results not shown). These results merit further studies regarding the subcellular functions of the large LYST protein in the context of GTPase involvement in subcellular traffic, ultimately aiming at new therapeutic opportunities for CHS patients.

3.2 Small GTPases as targets for electrophilic lipids

The plethora of posttranslational modifications that can occur on Ras proteins is largely responsible for their ability to act as stimulus sensors from different sites in the cell. In addition to CAAX processing, isoprenylation, palmitoylation or phosphorylation (Hancock et al., 1989; Kim et al., 2009), it has also been established that Ras family proteins (H-Ras, N-Ras or K-Ras) undergo non-enzymatic modifications including nitrosylation, thiolation or addition of lipid electrophiles (Mallis et al., 2001; Oliva et al., 2003). However, the results presented in this work are the first to detect modification by cyPG of RhoB and Rap2B.

Previous results from the laboratory have reported that H-Ras is a target for modification by cyPG and isoprostanes (Oliva et al., 2003; Renedo et al., 2007). Specifically, single enone compounds preferentially modified C118, whereas the dienone compound, 15d-PGJ_2, bound preferentially to C181 and 184 of its C-terminal peptide. Since these latter cysteine residues represent the palmitoylation sites of H-Ras,

binding of 15d-PGJ_2 to RhoB and Rap2B, which also contain palmitoylatable cysteines close to each other at their C-termini, could represent cross-linking of these two residues, similarly to that detected for H-Ras and its synthetic C-terminal peptide (Oeste et al., 2011). In assays addressing modification of RhoB by other cyPG, results showed that biotinylated 15d-PGJ_2 bound to a great extent, as determined by WB. Furthermore, incubation with biotinylated 8-iso-PGA_2 elicited a stronger signal than that of its *cis* isoform, PGA_2. These results suggest that single enones can also bind to RhoB cysteines and that the isoprostane form of PGA_2 is more easily accessible to the cysteine to which it binds. Further experiments are required to ascertain the binding sites of these cyPG and the molecular characteristics responsible for the different signal intensities detected for each cyPG.

As has been described in detail for H-Ras (Oeste et al., 2011), if it is the case in cells that these bipalmitoylated and prenylated proteins are modified by dienone cyPG at the cysteines in their C-termini, their subcellular localization and signaling properties could become significantly altered. The half-life of H-Ras palmitoylation has been estimated as approximately 20 min, which is a small timeframe compared to its 20 h half-life or even the 2-3 h half-life of RhoB, if its palmitoylation dynamics are assumed to be of a similar magnitude (Pérez-Sala et al., 2009; Rocks et al., 2005). Furthermore, Ras activation can induce its depalmitoylation (Omerovic et al., 2007), so that during the palmitoylation-depalmitoylation cycle of H-Ras, it could be that C181 and C184 become available for chemical modification by cyPG or other agents. These modifications could obstruct subsequent rounds of palmitoylation and the microdomain partitioning or subcellular localization prompted by palmitate binding to H-Ras. As will be discussed below, modification of H-Ras by several agents does indeed disrupt its activation patterns and subcellular localization (Oeste et al., 2011). However, whether this is also the case for the other bipalmitoylated and isoprenylated GTPases explored in this work will be the subject of further investigations.

cyPG production is significantly increased upon oxidative stress, suggesting that GTPases that can be modified by these compounds *in vitro* could do so in cells in an oxidative scenario. Furthermore, increased generation of reactive oxygen or nitrogen species that takes place within cells in situations such as inflammation affects unsaturated lipids with a tendency for oxidation (Koenitzer and Freeman, 2010). This is

the case for polyunsaturated fatty acids at membranes, which suffer non-enzymatic oxidations to produce compounds of diverse structure that can modify proteins and affect their subcellular functions (Ceaser et al., 2004). Since the structures and electrophilic groups of these reactive endogenous compounds are similar to those of cyPG, the possibility is set forth that the GTPases studied in this work could become targets for species such as nitrated fatty acids or oxidized phospholipids, which could have a profound impact on their biological actions.

3.3 Electrophilic reagents bind to C-terminal cysteines in H-Ras and RhoB

Additionally to reactive lipids that can be found in biological systems, we have used exogenous, small, bifunctional cysteine reagents as biochemical tools to characterize the structural requirements and functional consequences of C-terminal modification of H-Ras and RhoB. Binding of DBB to two cysteines is only feasible if these are within 3-6 Å of each other, so that the results shown in this work place the palmitoylation cysteines within that range. As addressed above, cyPG could interfere with palmitoylation cycles of H-Ras and hence elicit changes in its subcellular behavior. Similarly, binding of small reactive compounds such as PAO and DBB to C-terminal cysteines can abrogate palmitoylation, though their effects on GTPase activation and localization need not match those of cyPG. Indeed, cells transfected with a fluorescent construct of the Ras binding domain (RBD) of the Ras effector, Raf, and treated with PAO or DBB show that active Ras is recruited to endomembranes. Treatment with these compounds also hampers Ras translocation to the plasma membrane upon EGF stimulation (Oeste et al., 2011). Interestingly, depalmitoylated H-Ras has been shown to travel back to the Golgi complex for addition of new palmitate moieties, and palmitoylation cysteine mutants signal from this localization upon stimulation with growth factors (Chiu et al., 2002). It is therefore possible that PAO or DBB bind to depalmitoylated H-Ras at the Golgi and induce its activation at this site, as summarized in Figure 53. Another approach resulting in alteration of the H-Ras hypervariable region structure is the mutation of C184 for a leucine residue, as appears naturally in N-Ras, which was suggested to replace the palmitate chain that is usually present and results in H-Ras association with the plasma membrane and recycling endosomes (Misaki et al.,

2010). Taken together, cyPG and bifunctional cysteine reagent modification of H-Ras highlights the relevance of hypervariable cysteines and the proximity between them as crucial structural determinants for selectivity of posttranslational modifications.

Modification	Schematic structure	Functional outcome	Reference
Palmitoylation	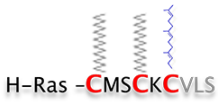	Cycle of palmitoyation/ depalmitoylation and traffic between Golgi and plasma membrane	Hancock, 1989 Rocks, 2005
Lipoxidation (15d-PGJ_2)	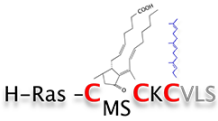	Activation	Oliva, 2003 Renedo, 2007 Oeste, 2011
PAO	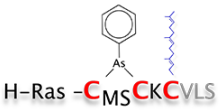	Activation on endomembranes	Oeste, 2011
DBB	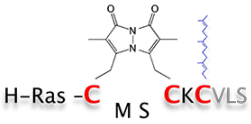	Activation on endomembranes	Oeste, 2011
Guanylation	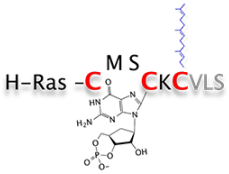	Activation at plasma membrane	Nishida, 2012
Glutathionylation	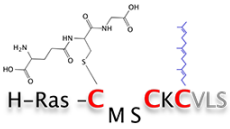	Inhibition of palmitoylation and plasma membrane association	Mallis, 2001 Burgoyne, 2012

Figure 53. H-Ras C-terminal modifications and their functional outcomes.

The three C-terminal H-Ras cysteine residues are shown in red, the last of which becomes irreversibly farnesylated (blue chain). The "-AAX" amino acids removed upon CAAX box processing are shown in gray. Palmitoylation cysteines, i.e. C181 and 184, can undergo modification by electrophilic compounds with varying structures (shown in black), resulting in diverse functional outcomes.

Modification of H-Ras at its C-terminus by compounds with distinct structural features and the functional outcomes that result from them have been explored by our laboratory and others (Figure 53). As described above, binding of several cyPG, including 15d-PGJ_2, elicits H-Ras activation at the plasma membrane, whereas addition of PAO or DBB molecules to the C-terminal cysteines results in activation at endomembranes. Similarly, guanylation of C184 induces Ras activation at the plasma membrane (Nishida et al., 2012). In contrast, glutathionylation of the H-Ras C-terminus in cells hinders palmitoylation and concomitant plasma membrane binding, as well as

inducing apoptosis (Burgoyne et al., 2012). Additionally, this study showed that metabolic stress induces oxidation of reactive cysteine thiolates, which also alters H-Ras palmitoylation, both in cells and mouse models (Burgoyne et al., 2012). Hence a scenario is set forth in which the physicochemical characteristics of the agents that modify palmitoylation cysteines determine the specificity of GTPase subcellular localization or activation.

As seen in this work, small differences in amino acid sequences can have a profound impact on binding to membranes of distinct nature, illustrated by TC10 and RhoB. Furthermore, processed lipidation motifs endow each of these proteins with a defined structural membrane-binding unit. Modification with reactive lipids occurring in pathological settings adds another layer of complexity to the determinants driving intracellular localization of small GTPases such as RhoB. Binding of cyPG or reactive compounds with varied structures to RhoB *in vitro* paves the way for studies in cells to define putative impediments in RhoB palmitoylation due to these modifications, which could alter its subcellular localization pattern and hence its biological actions.

CONCLUSIONS

As a result of the work presented in this dissertation, in which localization and subcellular trafficking of endosomal GTPases have been assessed in the context of their posttranslational modifications, the following conclusions have been arrived at:

1.1. Structural determinants present at the hypervariable region of the endosomal GTPases RhoB and TC10, when exchanged, interconvert their behavior regarding association with distinct subcellular membranes.

1.2. Endolysosomal targeting of RhoB and chimeras of its lipidation motif (CINCCKVL) depends on isoprenylation and palmitoylation at C-terminal cysteines.

1.3. RhoB and CINCCKVL chimeras appear inside endolysosomes and are detected at intraluminal vesicles of multivesicular bodies by super-resolution microscopy.

1.4. CINCCKVL sorting is conserved in cells from diverse model organisms, including fungi, insects, amphibians, and mammals.

These results shed light on the interplay between lipidated residues and other structural determinants in subcellular targeting of GTPases.

2.1 In cells depleted of the ESCRT components Hrs and Tsg101, sorting of full-length RhoB into endolysosomal compartments is impaired, but not that of CINCCKVL chimeras.

2.2 Agents altering late endosomal lipid dynamics differentially disturb RhoB and CINCCKVL chimera localization inside endolysosomes.

2.3 Overexpression of CD63 constructs alters CINCCKVL chimera localization, but not that of full-length RhoB.

Taken together, these results imply that sorting of full-length RhoB and CINCCKVL constructs could be regulated by distinct subcellular trafficking machineries.

3.1 RhoB or CINCCKVL constructs recapitulate endolysosomal defects in cells of patients with lysosomal storage diseases.

3.2 The palmitoylation cysteines of the small GTPases RhoB and H-Ras are targets for modification by structurally diverse electrophilic lipids *in vitro*.

These results suggest that subcellular localization of endosomal GTPases could become altered in pathological scenarios such as genetic diseases or processes involving the generation of reactive species.

SUMMARY IN ENGLISH

Small GTPases of the Ras superfamily are key to cellular processes such as differentiation, proliferation or regulation of the cytoskeleton (Takai et al., 2001). These proteins undergo lipid modifications that elicit their attachment to membranes and are crucial to their activity. Specifically, Ras protein isoprenylation serves as an anchor to the membrane, and Ras proteins are further amenable to reversible palmitoylation, which contributes to their dynamic localization at distinct subcellular compartments (Hancock et al., 1989). Lipid modifications take place at cysteine residues in the C-terminal region. Furthermore, these cysteines can undergo oxidation or addition of electrophilic compounds, e.g. cyclopentenone prostaglandin binding. These compounds are formed by non-enzymatic oxidation of arachidonic acid or from dehydration of other prostaglandins, which endows them with electrophilic carbons (Funk, 2001).

Rho proteins are a group of Ras superfamily proteins that are crucial to cell adhesion and migration, hence modulating cardiovascular pathophysiology and tumorigenic processes (Ridley, 2001). RhoB is a member of this family with roles in vesicular trafficking, tumor suppression and localization of signaling proteins. RhoB lipid modifications (isoprenylation and double palmitoylation) are necessary for its localization to endolysosomes and its degradation through this pathway (Pérez-Sala et al., 2009; Stamatakis et al., 2002). The last eight amino acids of RhoB, which correspond to the lipidation motif, constitute an endolysosomal localization and degradation sequence for chimeric proteins to which this extension is added at their C-terminal end (Pérez-Sala et al., 2009).

In the context of this dissertation, *in vitro* and cell models have been used to study mechanistic and structural aspects of Ras and Rho protein modification, particularly that of RhoB, and its influence on localization and trafficking of these proteins or their chimeras modified by lipids and other compounds. Though lipid modifications of Ras proteins have been described as important regulatory factors, the involvement of lipidation and its interplay with other structural determinants in subcellular targeting of GTPases has not been fully elucidated. Therefore, the role of lipid modifications of RhoB cysteine residues and other important residues at the

hypervariable region on its intracellular sorting has been analyzed. Furthermore, studies were carried out to determine whether the RhoB lipidation motif *per se* (CINCCKVL) is able to mimic the full-length protein. Cell models from different species were used to evaluate whether the latent sorting mechanisms for CINCCKVL proteins are conserved in these model organisms. Using this C-terminal construct in parallel to the full-length protein, the potential involvement of key molecular machineries, i.e. ESCRT complexes, CD63 or lipid dynamics, in their sorting was assessed. Considering the potential alteration of subcellular localization of Ras proteins by modification, targeting of lipidation sequences by other structurally diverse moieties, including reactive species arising in pathological scenarios, was also explored. In addition, assays were carried out to study the potential alteration of endosomal GTPase localization in genetic models of lysosomal disease.

In order to characterize the precise subcellular localization of RhoB, constructs of fluorescent proteins fused to this protein were compared to those of other small GTPases used as markers of endocytic vesicles. Co-localization with fusion proteins of Rab7, Rab9 or Lamp and negligible overlap with early endosome markers, i.e. Rab5 fusion proteins, or the Golgi marker, giantin, underscore RhoB localization within the endolysosomal lumen. These studies also include assays with autophagy probes, with which RhoB or its chimeras show negligible co-localization. The small GTPase, TC10, contains a C-terminal sequence that is very similar to that of RhoB, though a basic amino acid patch upstream of the lipidation sequence elicits retention at the limiting membrane of endolysosomes. Insertion of this basic patch into the RhoB sequence hinders its entry into endolysosomes, highlighting that exchange of structural determinants between these proteins elicits interconversion of their subcellular localization patterns. Furthermore, it has been determined that chimeras bearing the RhoB C-terminal sequence, CINCCKVL, are also internalized into endolysosomes.

It was also described that chimeric proteins fused to the C-terminal sequence of RhoB (CINCCKVL) enter into the endolysosomal lumen. Therefore, studies were carried out to assess whether the CINCCKVL sequence can travel to endolysosomes in cells from diverse species, which in some cases lack an endogenous RhoB homolog sequence. The universality of endolysosomal localization of chimeras bearing the RhoB

C-terminus was set forth by detection of these proteins in endolysosomes of cells as phylogenetically distant as amphibians, insects and fungi.

In order to explore the possible localization mechanisms of RhoB, advanced confocal and super-resolution techniques were employed. By means of these tools, RhoB and CINCCKVL chimeras were unequivocally detected at intraluminal vesicles of multivesicular bodies. Cells were transfected with small interfering RNA to silence components of the ESCRT machinery, which is responsible for endolysosomal trafficking and formation of multivesicular bodies (Raiborg and Stenmark, 2009). By blocking the function of some of these components, RhoB is not internalized into endolysosomes, which reflects a possible role of ESCRT proteins in RhoB endosomal trafficking. However, CINCCKVL chimeras are not similarly affected by ESCRT knock-down. Therefore, other protein and lipid components of multivesicular bodies could play a role in localization of these chimeras, e.g. the tetraspanin CD63. This protein presents a high degree of co-localization with RhoB and related chimeras at multivesicular bodies. Interestingly, it was shown that overexpression of fluorescent constructs of CD63 alter the subcellular localization pattern of CINCCKVL proteins, possibly towards extracellular destinations, but not that of RhoB. To explore the role of lipid dynamics in localization of these proteins, cells were treated with compounds that alter cholesterol dynamics at membranes. In these cells, internalization of C-terminal RhoB chimeras into endolysosomes was reduced, whereas the full-length protein was able to access these compartments. Furthermore, ceramide treatment induced changes in cell morphology that affect RhoB and related protein localization. Taken together, these results suggest that CINCCKVL chimeras can follow a subcellular destination mediated by machineries that are different to those responsible for sorting of full-length RhoB, which implies that RhoB contains further structural determinants for localization or interaction, beyond those that appear at its lipidation sequence.

It has been previously described that RhoB is involved in diverse pathologies such as tumorigenic processes and cardiovascular malfunction (Prendergast, 2001). The results obtained showing RhoB localization to endolysosomal membranes warranted studies in models of lysosomal diseases such as Chediak-Higashi or Niemann-Pick. These disorders result in oculocutaneous albinism, immunodeficiency and cognitive impairment of varying degree (Huizing et al., 2008). Comparing RhoB to other

endosomal GTPases in cells of patients suffering from these diseases, confocal laser microscopy shows that RhoB is localized to the dilated endolysosomes typical of these diseases.

In many pathological scenarios, proteins suffer modifications due to alterations in overall cellular redox status. By means of electrophoretic assays (SDS-PAGE) or proteomic approaches (MALDI-TOF), it was shown that proteins of the Ras superfamily, particularly H-Ras and RhoB, could be modified in vitro at their C-terminal cysteine residues by structurally diverse electrophilic lipids. Specifically, dienone cyclopentenone prostaglandins, derived from non-enzymatic oxidation of arachidonic acid or dehydration of other prostaglandins, bind to these residues. Recombinant RhoB protein is also selectively modified by biotinylated dienone cyclopentenone prostaglandins, as well as by other bifunctional cysteine reagents such as phenylarsine oxide and dibromobimane. It is therefore possible that regulation of small GTPases can occur through processes related to cellular redox status that can have implications beyond the canonical signaling pathways that are mediated by these proteins.

As a result of the work presented in this dissertation, in which localization and subcellular trafficking of endosomal GTPases have been assessed in the context of their posttranslational modifications, several conclusions have been arrived at. Regarding localization sequences at the hypervariable regions of small GTPases, these studies have shown that interplay between lipidated residues and other structural determinants such as basic residue patches elicits specific patterns of subcellular targeting. Furthermore, in the case or RhoB, endolysosomal targeting of full-length or CINCCKVL chimeras depends on isoprenylation and palmitoylation at C-terminal cysteines. These proteins, when fully lipidated, appear inside endolysosomes and are detected at intraluminal vesicles of multivesicular bodies by super-resolution microscopy. Endolysosomal or vacuolar sorting of CINCCKVL chimeras was shown to be conserved in cells from diverse model organisms, including fungi, insects, amphibians, and mammals. As referred to the molecular mechanisms involved in sorting, results imply that sorting of full-length RhoB and CINCCKVL constructs could be regulated by distinct subcellular trafficking machineries, for full-length RhoB sorting is impaired upon ESCRT component depletion, whereas CINCCKVL construct localization is altered in cells

overexpressing CD63 constructs or after treatment with cholesterol-reducing agents. Experiments performed in pathological scenarios such as genetic models of endolysosomal malfunction or processes involving the generation of reactive species show that RhoB or CINCCKVL constructs recapitulate endolysosomal defects in cells of patients with lysosomal storage diseases and that the palmitoylation cysteines of the small GTPases RhoB and H-Ras are targets for modification by structurally diverse electrophilic lipids *in vitro*. These results pave the way for exploring the extent to which diverse modifications of Ras proteins at C-terminal cysteines can disturb their subcellular localization and consequently alter their functional outcomes.

SUMMARY IN SPANISH

1. Introducción

Las GTPasas de bajo peso molecular comprendidas en la superfamilia Ras son proteínas fundamentales para procesos celulares como la diferenciación celular, la regulación del citoesqueleto y la proliferación (Takai et al., 2001). Estas proteínas sufren modificaciones lipídicas que les permiten asociarse con las membranas celulares y son clave para su actividad. En concreto, las proteínas Ras están isopreniladas para anclarse a la membrana, además de ser susceptibles de palmitoilación reversible, lo cual contribuye a su localización dinámica en distintos compartimentos subcelulares (Hancock et al., 1989). Estas modificaciones lipídicas tienen lugar sobre residuos de cisteína en la región carboxilo-terminal (C-terminal). Además, estas cisteínas pueden sufrir oxidaciones o adición de compuestos de naturaleza electrofílica, como por ejemplo, la unión de prostaglandinas ciclopentenonas (Oeste and Pérez-Sala, 2014). Estos compuestos se forman por oxidación no enzimática del ácido araquidónico o por deshidratación de otras prostaglandinas, lo cual las dota de carbonos electrófilos (Funk, 2001).

Las proteínas Rho juegan papeles cruciales en la adhesión y migración celular que repercuten sobre la fisiopatología cardiovascular y procesos tumorigénicos (Ridley, 2001). RhoB es un miembro de esta familia con funciones reguladoras del tráfico vesicular, la supresión de tumores y la localización de proteínas señalizadoras. Las modificaciones lipídicas de RhoB (isoprenilación y doble palmitoilación) son necesarias para su localización endolisosomal y posterior degradación por esta vía (Pérez-Sala et al., 2009; Stamatakis et al., 2002). Los últimos ocho amino ácidos de RhoB, zona donde se encuentran las cisteínas que se lipidan, comprenden una secuencia de localización y degradación endolisosomal para proteínas quiméricas a las que se les añade esta extensión en su extremo carboxilo-terminal (Pérez-Sala et al., 2009).

En el contexto de esta tesis se han estudiado, tanto *in vitro* como en modelos celulares, aspectos mecanísticos y estructurales de la modificación de proteínas Ras y Rho, en concreto RhoB, y su repercusión sobre la localización y tráfico de estas proteínas o sus quimeras modificadas por lípidos y otros compuestos.

2. Objetivos

Las GTPasas de bajo peso molecular ejercen diversas funciones celulares desde localizaciones de membrana específicas. Entre los factores que las regulan, la modificación en secuencias C-terminales juegan un papel crucial, aunque la participación de la lipidación y su interacción con otros determinantes estructurales en la localización subcelular de las GTPasas no ha sido completamente dilucidado. Por ello, el trabajo presentado en esta tesis se centra en analizar el papel de las modificaciones lipídicas en residuos de cisteína de RhoB sobre su tráfico intracelular y determinar si el motivo de lipidación per se es capaz de reproducir el comportamiento de la proteína completa. Además, la posibilidad de que las secuencias de lipidación puedan ser dianas de modificación por otros compuestos de estructura diversa, incluidas especies reactivas que se producen en situaciones patológicas, no se ha explorado. Por tanto, los siguientes objetivos fueron planteados:

- Estudiar el papel de las secuencias C-terminales de GTPasas endosomales en su localización subcelular.
- Valorar la importancia de la isoprenilación y la palmitoilación en la asociación de estas proteínas a vesículas intracelulares.
- Determinar la localización subcelular de quimeras que contienen la secuencia de lipidación del C-terminal de RhoB.
- Evaluar si los mecanismos latentes de localización del C-terminal de RhoB están conservados en células de diversas especies.
- Explorar el posible rol de maquinarias moleculares clave, tales como los complejos ESCRT, CD63 o la dinámica lipídica, en la localización de RhoB y quimeras relacionadas.
- Asentar las bases para estudiar posibles alteraciones en la localización y modificación de GTPasas endosomales en modelos experimentales de enfermedad.

3. Resultados

Se ha llevado a cabo una caracterización de RhoB fusionada a proteínas fluorescentes en el contexto de las endomembranas al comparar su localización y degradación con las de otras GTPasas pequeñas. Su colocalización con proteínas fluorescentes fusionadas a Rab7, Rab9 o Lamp y falta de coincidencia con marcadores de endosomas tempranos (GFP-Rab5) o aparato de Golgi (giantin) atestiguan su localización en el lumen endolisosomal. Los estudios aquí presentados incluyen también la utilización de sondas de la vía autofagocítica, con las cuales ni RhoB ni sus proteínas quimera colocalizan de forma detectable. La GTPasa de bajo peso molecular, TC10, cuya secuencia C-terminal es muy similar a la de RhoB, contiene unos amino ácidos básicos que sin embargo la retienen en la membrana limitante de dichas vesículas. La inserción de la secuencia polibásica de TC10 en la secuencia de RhoB impide su entrada a endolisosomas, lo cual pone de manifiesto que hay determinantes estructurales que al intercambiarse entre estas proteínas dan lugar a patrones subcelulares específicos.

Se describió además que las proteínas quimera fusionadas a la secuencia C-terminal de RhoB (CINCCKVL) también acceden al lumen endolisosomal. Por lo tanto, se exploró si la secuencia CINCCKVL accede a los endolisosomas no sólo en células de mamíferos, sino en células de organismos que pueden contener o no una secuencia endógena para proteínas homólogas a RhoB. La universalidad de la localización endolisosomal de quimeras con el C-terminal de RhoB se pone de manifiesto al detectarse en endolisosomas de células de organismos muy alejados entre sí en la escala filogenética, tales como anfibios, insectos y hongos.

Para explorar los posibles mecanismos de localización de RhoB, se emplearon técnicas de microscopía láser avanzada confocal y de superresolución. Por medio de estas potentes herramientas se ha podido establecer la localización inequívoca de RhoB y quimeras CINCCKVL en vesículas intraluminales de cuerpos multivesiculares. Se transfectaron células con RNA de interferencia para así silenciar componentes de la maquinaria ESCRT, responsable del tráfico endolisosomal y la formación de cuerpos multivesiculares (Raiborg and Stenmark, 2009). Al bloquear la función de algunos de

estos componentes, RhoB no se internaliza en los endolisosomas, lo cual refleja un posible papel de las proteínas ESCRT en el tráfico endosomal de RhoB. Sin embargo, las quimeras CINCCKVL no se ven igualmente afectadas por el bloqueo de componentes ESCRT. Se estudiaron pues otros componentes proteicos y lipídicos de los cuerpos multivesiculares que podrían jugar también un papel en la localización de proteínas CINCCKVL, como por ejemplo la tetraspanina CD63. Esta proteína presenta una alta colocalización con RhoB y quimeras relacionadas en cuerpos multivesiculares. Curiosamente, se observó que la sobreexpresión de construcciones fluorescentes de CD63 cambian el patrón de localización subcelular de quimeras CINCCKVL, posiblemente hacia destinos extracelulares, pero no así el de RhoB. Para explorar el papel de la dinámica lipídica en la localización de estas proteínas, se realizaron ensayos de tratamiento celular con compuestos que alteran la dinámica de colesterol en las membranas. En estas células, se redujo la internalización de quimeras del C-terminal de RhoB hacia el lumen de cuerpos multivesiculares, mientras que la proteína completa siguió su camino hacia el interior de estos compartimentos. Además, el tratamiento con ceramida indujo cambios en la morfología celular que afectan la localización de RhoB y proteínas relacionadas. En conjunto, estos resultados sugieren que las quimeras CINCCKVL pueden seguir un destino subcelular mediado por maquinarias distintas a las responsables del transporte de RhoB completa, lo cual sugiere que RhoB contiene determinantes estructurales de localización o interacción más allá de los que aparecen en su secuencia de lipidación.

Se ha descrito que RhoB interviene en diversas patologías como procesos tumorigénicos y afecciones cardiovasculares (Prendergast, 2001). Debido a los resultados obtenidos sobre la localización de RhoB en membranas endolisosomales, se quiso estudiar su papel en modelos de enfermedades lisosomales como Chediak-Higashi o Niemann-Pick. Estas patologías cursan con albinismo oculocutáneo, inmunodeficiencias y retrasos cognitivos de severidad variada (Huizing et al., 2008). Al comparar RhoB con otras GTPasas endosomales en células de pacientes que sufren estas enfermedades, se detectó por microscopía láser confocal la localización de RhoB en los endolisosomas dilatados típicos de estas patologías.

En muchos escenarios patológicos, las proteínas sufren modificaciones al verse alterado el estado redox global de las células. Se determinó que proteínas de la

superfamilia Ras, en concreto H-Ras y RhoB, se pueden modificar *in vitro* en sus residuos de cisteína del extremo carboxilo-terminal por compuestos electrófilos de diversa índole utilizando ensayos de electroforesis (SDS-PAGE) o métodos proteómicos (MALDI-TOF). En concreto, las prostaglandinas ciclopentenonas dienonas, derivadas de la oxidación no enzimática del ácido araquidónico o deshidratación de otras prostaglandinas, se unen a estos residuos. La proteína recombinante RhoB también se modifica por derivados biotinilados de prostaglandinas ciclopentenonas dienonas de manera selectiva, además de por otros reactivos bifuncionales de unión a cisteínas, como el óxido de fenilo arsénico o el dibromobimano. Se establece así una capacidad reguladora de GTPasas pequeñas por medio de procesos relacionados con el estado redox de la célula que puede tener implicaciones más allá de las vías de señalización canónicas mediadas por estas proteínas.

4. Conclusiones

Como resultado del trabajo presentado en esta tesis, en la que la localización y tráfico subcelular de GTPasas endosomales se han evaluado en el contexto de sus modificaciones postraduccionales, se ha llegado a las siguientes conclusiones:

1.1. Ciertos determinantes estructurales de la región hipervariable de las GTPasas endosomales RhoB y TC10, al intercambiarse, permutan su comportamiento en cuanto a la asociación con membranas subcelulares concretas.

1.2. La localización endolisosomal de RhoB y quimeras de su secuencia de lipidación (CINCCKVL) depende de la isoprenilación y palmitoilación en las cisteínas C-terminales.

1.3. Quimeras de RhoB y CINCCKVL aparecen en el interior de endolisosomas y se detectan en vesículas intraluminales de cuerpos multivesiculares mediante microscopía de superresolución.

1.4. La localización de proteínas CINCCKVL está conservada en células de diversos organismos modelos, incluidos modelos de hongo, insecto, anfibio y mamíferos.

Estos resultados ponen de manifiesto la interacción entre residuos modificados por lípidos y otros determinantes estructurales a la hora de guiar la localización subcelular de GTPasas.

2.1. En células en las que componentes ESCRT (Hrs y Tsg101) han sido silenciados mediante RNA de interferencia, disminuye la localización de la proteína RhoB completa en endolisosomas, pero no así la de quimeras CINCCKVL.

2.2. El uso de compuestos que perturban la dinámica lipídica de endosomas tardíos altera diferencialmente la localización de quimeras de RhoB o CINCCKVL dentro de los endolisosomas.

2.3. La sobreexpresión de construcciones de CD63 altera la localización de quimeras CINCCKVL, pero no así la de RhoB completa.

En conjunto, estos resultados sugieren que la localización de RhoB completa y de construcciones de CINCCKVL podría verse regulada por diferentes maquinarias de tráfico subcelular.

3.1. Las quimeras de RhoB o CINCCKVL recapitulan los defectos endolisosomales en células de pacientes con enfermedades por almacenamiento lisosomal.

3.2. Las cisteínas de palmitoilación de las GTPasas pequeñas RhoB y H-Ras son dianas de modificación *in vitro* por lípidos electrófilos de estructura variada.

Estos resultados sugieren que la localización subcelular de GTPasas endosomales podría verse alterada en situaciones patológicas como enfermedades genéticas o procesos que cursan con generación de especies reactivas.

5. Aportaciones fundamentales

Este trabajo muestra resultados obtenidos mediante técnicas de microscopía avanzada como la microscopía láser confocal y de superresolución, para determinar las localizaciones subcelulares concretas de la proteína RhoB fusionada a diversas proteínas fluorescentes, además de quimeras fluorescentes fusionadas a una secuencia corta derivada del C-terminal de RhoB. Además, se ha determinado la importancia de la lipidación de los residuos de cisteína para la localización endolisosomal de las proteínas de fusión mediante la generación de mutantes no susceptibles de modificación. Por

primera vez, se ha llevado a cabo el estudio de la distribución de la proteína RhoB y quimeras relacionadas en células con alteraciones de la función lisosomal (síndromes de Chediak-Higashi, Niemann-Pick y Hermansky-Pudlak). Por medio de las quimeras fluorescentes del C-terminal de RhoB, se ha caracterizado la especificidad de la localización de dicha secuencia en varias líneas celulares humanas y de especies diversas, incluidos insectos y hongos. Además, estos estudios son los primeros en analizar el papel de mediadores del tráfico intracelular como los complejos ESCRT, la tetraspanina CD63 o la dinámica lipídica en la localización subcelular de RhoB o su secuencia C-terminal.

Se han realizado estudios sobre la modificación de GTPasas de bajo peso molecular, particularmente H-Ras y RhoB, por compuestos que se unen a cisteínas por mecanismos no enzimáticos. Se ha detectado la unión de prostaglandinas ciclopentenonas dienonas a dos residuos del C-terminal de H-Ras. Las diversas técnicas empleadas han servido para caracterizar los motivos estructurales de GTPasas pequeñas que son susceptibles de modificaciones y que pueden repercutir en la actividad o localización de dichas proteínas.

REFERENCES

Abenza JF, Galindo A, Pinar M, Pantazopoulou A, de los Ríos V and Peñalva MA (2012) Endosomal maturation by Rab conversion in *Aspergillus nidulans* is coupled to dynein-mediated basipetal movement. *Mol. Biol. Cell* **23**(10): 1889-1901.

Abenza JF, Pantazopoulou A, Rodríguez JM, Galindo A and Peñalva MA (2009) Long-distance movement of *Aspergillus nidulans* early endosomes on microtubule tracks. *Traffic* **10**(1): 57-75.

Adamson P, Marshall CJ, Hall A and Tilbrook PA (1992) Post-translational modifications of p21rho proteins. *J. Biol. Chem.* **267**(28): 20033-20038.

Adini I, Rabinovitz I, Sun JF, Prendergast GC and Benjamin LE (2003) RhoB controls Akt trafficking and stage-specific survival of endothelial cells during vascular development. *Genes Dev.* **17**(21): 2721-2732.

Ahearn IM, Haigis K, Bar-Sagi D and Philips MR (2012) Regulating the regulator: post-translational modification of RAS. *Nat. Rev. Mol. Cell Biol.* **13**(1): 39-51.

Aicart-Ramos C, Valero RA and Rodríguez-Crespo I (2011) Protein palmitoylation and subcellular trafficking. *Biochim. Biophys. Acta* **1808**(12): 2981-2994.

Amano Y, Yamashita Y, Kojima K, Yoshino K, Tanaka N, Sugamura K and Takeshita T (2011) Hrs recognizes a hydrophobic amino acid cluster in cytokine receptors during ubiquitin-independent endosomal sorting. *J. Biol. Chem.* **286**(17): 15458-15472.

Amiya E, Watanabe M, Takeda N, Saito T, Shiga T, Hosoya Y, Nakao T, Imai Y, Manabe I, Nagai R, Komuro I and Maemura K (2013) Angiotensin II impairs endothelial nitric-oxide synthase bioavailability under free cholesterol-enriched conditions via intracellular free cholesterol-rich membrane microdomains. *J. Biol. Chem.* **288**(20): 14497-14509.

Andreu Z and Yáñez-Mo M (2014) Tetraspanins in extracellular vesicle formation and function. *Front. Immunol.* **5**: 442.

Asensio CS, Sirkis DW and Edwards RH (2010) RNAi screen identifies a role for adaptor protein AP-3 in sorting to the regulated secretory pathway. *J. Cell Biol.* **191**(6): 1173-1187.

Aspenström P, Fransson A and Saras J (2004) Rho GTPases have diverse effects on the organization of the actin filament system. *Biochem. J.* **377**(Pt 2): 327-337.

Babst M (2011) MVB vesicle formation: ESCRT-dependent, ESCRT-independent and everything in between. *Curr. Opin. Cell Biol.* **23**(4): 452-457.

Babst M, Katzmann DJ, Estepa-Sabal EJ, Meerloo T and Emr SD (2002a) ESCRT-III: an endosome-associated heterooligomeric protein complex required for MVB sorting. *Dev. Cell* **3**(2): 271-282.

Babst M, Katzmann DJ, Snyder WB, Wendland B and Emr SD (2002b) Endosome-associated complex, ESCRT-II, recruits transport machinery for protein sorting at the multivesicular body. *Dev. Cell* **3**(2): 283-289.

Babst M, Wendland B, Estepa EJ and Emr SD (1998) The Vps4p AAA ATPase regulates membrane association of a Vps protein complex required for normal endosome function. *EMBO J.* **17**(11): 2982-2993.

Baietti MF, Zhang Z, Mortier E, Melchior A, Degeest G, Geeraerts A, Ivarsson Y, Depoortere F, Coomans C, Vermeiren E, Zimmermann P and David G (2012) Syndecan-syntenin-ALIX regulates the biogenesis of exosomes. *Nat. Cell Biol.* **14**(7): 677-685.

Baixauli F, López-Otín C and Mittelbrunn M (2014) Exosomes and autophagy: coordinated mechanisms for the maintenance of cellular fitness. *Front. Immunol.* **5**: 403.

Ballabio A and Gieselmann V (2009) Lysosomal disorders: from storage to cellular damage. *Biochim. Biophys. Acta* **1793**(4): 684-696.

Bampton ET, Goemans CG, Niranjan D, Mizushima N and Tolkovsky AM (2005) The dynamics of autophagy visualized in live cells: from autophagosome formation to fusion with endolysosomes. *Autophagy* **1**(1): 23-36.

Barbacid M (1987) Ras genes. *Annu. Rev. Biochem.* **56**: 779-827.

Barth S, Glick D and Macleod KF (2010) Autophagy: assays and artifacts. *J. Pathol.* **221**(2): 117-124.

Berg TO, Fengsrud M, Stromhaug PE, Berg T and Seglen PO (1998) Isolation and characterization of rat liver amphisomes. Evidence for fusion of autophagosomes with both early and late endosomes. *J. Biol. Chem.* **273**(34): 21883-21892.

Bigay J and Antonny B (2012) Curvature, lipid packing, and electrostatics of membrane organelles: defining cellular territories in determining specificity. *Dev. Cell* **23**(5): 886-895.

Bishop N and Woodman P (2000) ATPase-defective mammalian Vps4 localizes to aberrant endosomes and impairs cholesterol trafficking. *Mol. Biol. Cell* **11**(1): 227-239.

Bishop NE (2003) Dynamics of endosomal sorting. *Int. Rev. Cytol.* **232**: 1-57.

Bissig C and Gruenberg J (2013) Lipid sorting and multivesicular endosome biogenesis. *Cold Spring Harb. Perspect. Biol.* **5**(10): a016816.

Bissig C, Johnson S and Gruenberg J (2012) Studying lipids involved in the endosomal pathway. *Methods Cell Biol.* **108**: 19-46.

Bogatcheva NV, Sergeeva MG, Dudek SM and Verin AD (2005) Arachidonic acid cascade in endothelial pathobiology. *Microvasc. Res.* **69**(3): 107-127.

Bonifacino JS and Traub LM (2003) Signals for sorting of transmembrane proteins to endosomes and lysosomes. *Annu. Rev. Biochem.* **72**: 395-447.

Boya P, Reggiori F and Codogno P (2013) Emerging regulation and functions of autophagy. *Nat. Cell Biol.* **15**(7): 713-720.

Bucci C, Parton RG, Mather IH, Stunnenberg H, Simons K, Hoflack B and Zerial M (1992) The small GTPase Rab5 functions as a regulatory factor in the early endocytic pathway. *Cell* **70**(5): 715-728.

Bucci C, Thomsen P, Nicoziani P, McCarthy J and van Deurs B (2000) Rab7: a key to lysosome biogenesis. *Mol. Biol. Cell* **11**(2): 467-480.

Burgos PV, Mardones GA, Rojas AL, daSilva LL, Prabhu Y, Hurley JH and Bonifacino JS (2010) Sorting of the Alzheimer's disease amyloid precursor protein mediated by the AP-4 complex. *Dev. Cell* **18**(3): 425-436.

Burgoyne JR, Haeussler DJ, Kumar V, Ji Y, Pimental DR, Zee RS, Costello CE, Lin C, McComb ME, Cohen RA and Bachschmid MM (2012) Oxidation of H-Ras cysteine thiols by metabolic stress prevents palmitoylation in vivo and contributes to endothelial cell apoptosis. *FASEB J.* **26**(2): 832-841.

Burkhardt JK, Wiebel FA, Hester S and Argon Y (1993) The giant organelles in *beige* and Chediak-Higashi fibroblasts are derived from late endosomes and mature lysosomes. *J. Exp. Med.* **178**(6): 1845-1856.

Buschow SI, Nolte-'t Hoen EN, van Niel G, Pols MS, ten Broeke T, Lauwen M, Ossendorp F, Melief CJ, Raposo G, Wubbolts R, Wauben MH and Stoorvogel W (2009) MHC II in dendritic cells is targeted to lysosomes or T cell-induced exosomes via distinct multivesicular body pathways. *Traffic* **10**(10): 1528-1542.

Bustelo XR, Sauzeau V and Berenjeno IM (2007) GTP-binding proteins of the Rho/Rac family: regulation, effectors and functions in vivo. *Bioessays* **29**(4): 356-370.

Callahan JW, Bagshaw RD and Mahuran DJ (2009) The integral membrane of lysosomes: its proteins and their roles in disease. *J. Proteomics* **72**(1): 23-33.

Canguilhem B, Pradines A, Baudouin C, Boby C, Lajoie-Mazenc I, Charveron M and Favre G (2005) RhoB protects human keratinocytes from UVB-induced apoptosis through epidermal growth factor receptor signaling. *J. Biol. Chem.* **280**(52): 43257-43263.

Canto I and Trejo J (2013) Palmitoylation of protease-activated receptor-1 regulates adaptor protein complex-2 and -3 interaction with tyrosine-based motifs and endocytic sorting. *J. Biol. Chem.* **288**(22): 15900-15912.

Carstea ED, Morris JA, Coleman KG, Loftus SK, Zhang D, Cummings C, Gu J, Rosenfeld MA, Pavan WJ, Krizman DB, Nagle J, Polymeropoulos MH, Sturley SL, Ioannou YA, Higgins ME, Comly M, Cooney A, Brown A, Kaneski CR, Blanchette-Mackie EJ, Dwyer NK, Neufeld EB, Chang TY, Liscum L, Strauss JF, 3rd, Ohno K, Zeigler M, Carmi R, Sokol J, Markie D, O'Neill RR, van Diggelen OP, Elleder M, Patterson MC, Brady RO, Vanier MT, Pentchev PG and Tagle DA (1997) Niemann-Pick C1 disease gene: homology to mediators of cholesterol homeostasis. *Science* **277**(5323): 228-231.

Ceaser EK, Moellering DR, Shiva S, Ramachandran A, Landar A, Venkartraman A, Crawford J, Patel R, Dickinson DA, Ulasova E, Ji S and Darley-Usmar VM (2004) Mechanisms of signal transduction mediated by oxidized lipids: the role of the electrophile-responsive proteome. *Biochem. Soc. Trans.* **32**(Pt 1): 151-155.

Cenedella RJ (2009) Cholesterol synthesis inhibitor U18666A and the role of sterol metabolism and trafficking in numerous pathophysiological processes. *Lipids* **44**(6): 477-487.

Cernuda-Morollón E, Pineda-Molina E, Cañada FJ and Pérez-Sala D (2001) 15-Deoxy-Delta 12,14-prostaglandin J2 inhibition of NF-kappaB-DNA binding through covalent modification of the p50 subunit. *J. Biol. Chem.* **276**(38): 35530-35536.

Charrin S, Manie S, Thiele C, Billard M, Gerlier D, Boucheix C and Rubinstein E (2003) A physical and functional link between cholesterol and tetraspanins. *Eur. J. Immunol.* **33**(9): 2479-2489.

Chavrier P, Gorvel JP, Stelzer E, Simons K, Gruenberg J and Zerial M (1991) Hypervariable C-terminal domain of Rab proteins acts as a targeting signal. *Nature* **353**(6346): 769-772.

Chazotte B (2011) Labeling lysosomes in live cells with LysoTracker. *Cold Spring Harb Protoc* **2011**(2): pdb prot5571.

Cherezov V, Rosenbaum DM, Hanson MA, Rasmussen SG, Thian FS, Kobilka TS, Choi HJ, Kuhn P, Weis WI, Kobilka BK and Stevens RC (2007) High-resolution crystal structure of an engineered human beta2-adrenergic G protein-coupled receptor. *Science* **318**(5854): 1258-1265.

Cherfils J and Zeghouf M (2013) Regulation of small GTPases by GEFs, GAPs, and GDIs. *Physiol. Rev.* **93**(1): 269-309.

Chico Y, Lafita M, Ramírez-Duque P, Merino F and Ochoa B (2000) Alterations in erythrocyte membrane lipid and fatty acid composition in Chediak-Higashi syndrome. *Biochim. Biophys. Acta* **1502**(3): 380-390.

Chiu VK, Bivona T, Hach A, Sajous JB, Silletti J, Wiener H, Johnson RL, 2nd, Cox AD and Philips MR (2002) Ras signalling on the endoplasmic reticulum and the Golgi. *Nat. Cell Biol.* **4**(5): 343-350.

Chua CE, Gan BQ and Tang BL (2011) Involvement of members of the Rab family and related small GTPases in autophagosome formation and maturation. *Cell. Mol. Life Sci.* **68**(20): 3349-3358.

Clague MJ and Urbe S (2006) Endocytosis: the DUB version. *Trends Cell Biol.* **16**(11): 551-559.

Colombo M, Moita C, van Niel G, Kowal J, Vigneron J, Benaroch P, Manel N, Moita LF, Thery C and Raposo G (2013) Analysis of ESCRT functions in exosome biogenesis, composition and secretion highlights the heterogeneity of extracellular vesicles. *J. Cell Sci.* **126**(Pt 24): 5553-5565.

Coutinho MF, Prata MJ and Alves S (2012) A shortcut to the lysosome: the mannose-6-phosphate-independent pathway. *Mol. Genet. Metab.* **107**(3): 257-266.

Coyne CB, Shen L, Turner JR and Bergelson JM (2007) Coxsackievirus entry across epithelial tight junctions requires occludin and the small GTPases Rab34 and Rab5. *Cell Host Microbe* **2**(3): 181-192.

Cuervo AM and Dice JF (1996) A receptor for the selective uptake and degradation of proteins by lysosomes. *Science* **273**(5274): 501-503.

Cullen PJ and Korswagen HC (2012) Sorting nexins provide diversity for retromer-dependent trafficking events. *Nat. Cell Biol.* **14**(1): 29-37.

D'Adamo P, Menegon A, Lo Nigro C, Grasso M, Gulisano M, Tamanini F, Bienvenu T, Gedeon AK, Oostra B, Wu SK, Tandon A, Valtorta F, Balch WE, Chelly J and Toniolo D (1998) Mutations in GDI1 are responsible for X-linked non-specific mental retardation. *Nat. Genet.* **19**(2): 134-139.

de Duve D (1969) The peroxisome: a new cytoplasmic organelle. *Proc. R. Soc. Lond. B. Biol. Sci.* **173**(1030): 71-83.

Dell'Angelica EC (2004) The building BLOC(k)s of lysosomes and related organelles. *Curr. Opin. Cell Biol.* **16**(4): 458-464.

Dell'Angelica EC, Mullins C, Caplan S and Bonifacino JS (2000) Lysosome-related organelles. *FASEB J.* **14**(10): 1265-1278.

Desnoyers L, Anant JS and Seabra MC (1996) Geranylgeranylation of Rab proteins. *Biochem. Soc. Trans.* **24**(3): 699-703.

Dessinioti C, Stratigos AJ, Rigopoulos D and Katsambas AD (2009) A review of genetic disorders of hypopigmentation: lessons learned from the biology of melanocytes. *Exp. Dermatol.* **18**(9): 741-749.

Di Paolo G and De Camilli P (2006) Phosphoinositides in cell regulation and membrane dynamics. *Nature* **443**(7112): 651-657.

Dianzani MU (2003) 4-hydroxynonenal from pathology to physiology. *Mol. Aspects Med.* **24**(4-5): 263-272.

Dietrich LE and Ungermann C (2004) On the mechanism of protein palmitoylation. *EMBO Rep* **5**(11): 1053-1057.

Díez-Dacal B and Pérez-Sala D (2010) Anti-inflammatory prostanoids: focus on the interactions between electrophile signaling and resolution of inflammation. *ScientificWorldJournal* **10**: 655-675.

Dirac-Svejstrup AB, Sumizawa T and Pfeffer SR (1997) Identification of a GDI displacement factor that releases endosomal Rab GTPases from Rab-GDI. *EMBO J.* **16**(3): 465-472.

Dores MR, Chen B, Lin H, Soh UJ, Paing MM, Montagne WA, Meerloo T and Trejo J (2012) ALIX binds a YPX(3)L motif of the GPCR PAR1 and mediates ubiquitin-independent ESCRT-III/MVB sorting. *J. Cell Biol.* **197**(3): 407-419.

Dransart E, Olofsson B and Cherfils J (2005) RhoGDIs revisited: novel roles in Rho regulation. *Traffic* **6**(11): 957-966.

Duffield A, Kamsteeg EJ, Brown AN, Pagel P and Caplan MJ (2003) The tetraspanin CD63 enhances the internalization of the H,K-ATPase beta-subunit. *Proc. Natl. Acad. Sci. U. S. A.* **100**(26): 15560-15565.

Dunn WA, Jr. (1994) Autophagy and related mechanisms of lysosome-mediated protein degradation. *Trends Cell Biol.* **4**(4): 139-143.

Dunphy JT, Greentree WK, Manahan CL and Linder ME (1996) G-protein palmitoyltransferase activity is enriched in plasma membranes. *J. Biol. Chem.* **271**(12): 7154-7159.

Durchfort N, Verhoef S, Vaughn MB, Shrestha R, Adam D, Kaplan J and Ward DM (2012) The enlarged lysosomes in *beige j* cells result from decreased lysosome fission and not increased lysosome fusion. *Traffic* **13**(1): 108-119.

Edgar JR, Eden ER and Futter CE (2014) Hrs- and CD63-dependent competing mechanisms make different sized endosomal intraluminal vesicles. *Traffic* **15**(2): 197-211.

Elias M, Brighouse A, Gabernet-Castello C, Field MC and Dacks JB (2012) Sculpting the endomembrane system in deep time: high resolution phylogenetics of Rab GTPases. *J. Cell Sci.* **125**(Pt 10): 2500-2508.

Engel ME, Datta PK and Moses HL (1998) RhoB is stabilized by transforming growth factor beta and antagonizes transcriptional activation. *J. Biol. Chem.* **273**(16): 9921-9926.

Epp N, Rethmeier R, Kramer L and Ungermann C (2011) Membrane dynamics and fusion at late endosomes and vacuoles- Rab regulation, multisubunit tethering complexes and SNAREs. *Eur. J. Cell Biol.* **90**(9): 779-785.

Escola JM, Kleijmeer MJ, Stoorvogel W, Griffith JM, Yoshie O and Geuze HJ (1998) Selective enrichment of tetraspan proteins on the internal vesicles of multivesicular endosomes and on exosomes secreted by human B-lymphocytes. *J. Biol. Chem.* **273**(32): 20121-20127.

Eskelinen EL (2005) Maturation of autophagic vacuoles in mammalian cells. *Autophagy* **1**(1): 1-10.

Fader CM and Colombo MI (2009) Autophagy and multivesicular bodies: two closely related partners. *Cell Death Differ.* **16**(1): 70-78.

Faigle W, Raposo G, Tenza D, Pinet V, Vogt AB, Kropshofer H, Fischer A, de Saint-Basile G and Amigorena S (1998) Deficient peptide loading and MHC class II endosomal sorting in a human genetic immunodeficiency disease: the Chediak-Higashi syndrome. *J. Cell Biol.* **141**(5): 1121-1134.

Falguières T, Luyet PP and Gruenberg J (2009) Molecular assemblies and membrane domains in multivesicular endosome dynamics. *Exp. Cell Res.* **315**(9): 1567-1573.

Falkenstein K and De Lozanne A (2014) Dictyostelium LvsB has a regulatory role in endosomal vesicle fusion. *J. Cell Sci.* **127**(Pt 20): 4356-4367.

Fernández-Borja M, Janssen L, Verwoerd D, Hordijk P and Neefjes J (2005) RhoB regulates endosome transport by promoting actin assembly on endosomal membranes through Dia1. *J. Cell Sci.* **118**(Pt 12): 2661-2670.

Flannery AR, Czibener C and Andrews NW (2010) Palmitoylation-dependent association with CD63 targets the Ca2+ sensor synaptotagmin VII to lysosomes. *J. Cell Biol.* **191**(3): 599-613.

Fortwendel JR, Juvvadi PR, Rogg LE, Asfaw YG, Burns KA, Randell SH and Steinbach WJ (2012) Plasma membrane localization is required for RasA-mediated polarized morphogenesis and virulence of *Aspergillus fumigatus*. *Eukaryot. Cell* **11**(8): 966-977.

Fritz G and Kaina B (1997) RhoB encoding a UV-inducible Ras-related small GTP-binding protein is regulated by GTPases of the Rho family and independent of JNK, ERK, and p38 MAP kinase. *J. Biol. Chem.* **272**(49): 30637-30644.

Fritz G and Kaina B (2000) Ras-related GTPase RhoB forces alkylation-induced apoptotic cell death. *Biochem. Biophys. Res. Commun.* **268**(3): 784-789.

Fuller M, Meikle PJ and Hopwood JJ (2006) Epidemiology of lysosomal storage diseases: an overview, in *Fabry Disease: Perspectives from 5 Years of FOS* (Mehta A, Beck M and Sunder-Plassmann G eds), Oxford.

Funk CD (2001) Prostaglandins and leukotrienes: advances in eicosanoid biology. *Science* **294**(5548): 1871-1875.

Futter CE, Pearse A, Hewlett LJ and Hopkins CR (1996) Multivesicular endosomes containing internalized EGF-EGF receptor complexes mature and then fuse directly with lysosomes. *J. Cell Biol.* **132**(6): 1011-1023.

Gampel A, Parker PJ and Mellor H (1999) Regulation of epidermal growth factor receptor traffic by the small GTPase RhoB. *Curr. Biol.* **9**(17): 955-958.

Ganley IG and Pfeffer SR (2006) Cholesterol accumulation sequesters Rab9 and disrupts late endosome function in NPC1-deficient cells. *J. Biol. Chem.* **281**(26): 17890-17899.

Gao L, Zackert WE, Hasford JJ, Danekis ME, Milne GL, Remmert C, Reese J, Yin H, Tai HH, Dey SK, Porter NA and Morrow JD (2003) Formation of prostaglandins E2 and D2 via the isoprostane pathway: a mechanism for the generation of bioactive prostaglandins independent of cyclooxygenase. *J. Biol. Chem.* **278**(31): 28479-28489.

Garrus JE, von Schwedler UK, Pornillos OW, Morham SG, Zavitz KH, Wang HE, Wettstein DA, Stray KM, Cote M, Rich RL, Myszka DG and Sundquist WI (2001) Tsg101 and the vacuolar protein sorting pathway are essential for HIV-1 budding. *Cell* **107**(1): 55-65.

Garzón B, Oeste CL, Díez-Dacal B and Pérez-Sala D (2011) Proteomic studies on protein modification by cyclopentenone prostaglandins: expanding our view on electrophile actions. *J. Proteomics* **74**(11): 2243-2263.

Gerald D, Adini I, Shechter S, Perruzzi C, Varnau J, Hopkins B, Kazerounian S, Kurschat P, Blachon S, Khedkar S, Bagchi M, Sherris D, Prendergast GC, Klagsbrun M, Stuhlmann H, Rigby AC, Nagy JA and Benjamin LE (2013) RhoB controls coordination of adult angiogenesis and lymphangiogenesis following injury by regulating VEZF1-mediated transcription. *Nat Commun* **4**: 2824.

Gerhard R, John H, Aktories K and Just I (2003) Thiol-modifying phenylarsine oxide inhibits guanine nucleotide binding of Rho but not of Rac GTPases. *Mol. Pharmacol.* **63**(6): 1349-1355.

Geyer M and Wittinghofer A (1997) GEFs, GAPs, GDIs and effectors: taking a closer (3D) look at the regulation of Ras-related GTP-binding proteins. *Curr. Opin. Struct. Biol.* **7**(6): 786-792.

Ghosh P, Dahms NM and Kornfeld S (2003) Mannose 6-phosphate receptors: new twists in the tale. *Nat. Rev. Mol. Cell Biol.* **4**(3): 202-212.

Gibbings DJ, Ciaudo C, Erhardt M and Voinnet O (2009) Multivesicular bodies associate with components of miRNA effector complexes and modulate miRNA activity. *Nat. Cell Biol.* **11**(9): 1143-1149.

Gilk SD, Cockrell DC, Luterbach C, Hansen B, Knodler LA, Ibarra JA, Steele-Mortimer O and Heinzen RA (2013) Bacterial colonization of host cells in the absence of cholesterol. *PLoS Pathog.* **9**(1): e1003107.

Gillooly DJ, Morrow IC, Lindsay M, Gould R, Bryant NJ, Gaullier JM, Parton RG and Stenmark H (2000) Localization of phosphatidylinositol 3-phosphate in yeast and mammalian cells. *EMBO J.* **19**(17): 4577-4588.

Gómez GA and Daniotti JL (2005) H-Ras dynamically interacts with recycling endosomes in CHO-K1 cells: involvement of Rab5 and Rab11 in the trafficking of H-Ras to this pericentriolar endocytic compartment. *J. Biol. Chem.* **280**(41): 34997-35010.

Gorfe AA, Babakhani A and McCammon JA (2007) H-Ras protein in a bilayer: interaction and structure perturbation. *J. Am. Chem. Soc.* **129**(40): 12280-12286.

Hall A (2005) Rho GTPases and the control of cell behaviour. *Biochem. Soc. Trans.* **33**(Pt 5): 891-895.

Hancock JF, Magee AI, Childs JE and Marshall CJ (1989) All Ras proteins are polyisoprenylated but only some are palmitoylated. *Cell* **57**(7): 1167-1177.

Hancock JF and Parton RG (2005) Ras plasma membrane signalling platforms. *Biochem. J.* **389**(Pt 1): 1-11.

Hanson PI, Roth R, Lin Y and Heuser JE (2008) Plasma membrane deformation by circular arrays of ESCRT-III protein filaments. *J. Cell Biol.* **180**(2): 389-402.

Hartman HL, Hicks KA and Fierke CA (2005) Peptide specificity of protein prenyltransferases is determined mainly by reactivity rather than binding affinity. *Biochemistry* **44**(46): 15314-15324.

Hemler ME (2005) Tetraspanin functions and associated microdomains. *Nat. Rev. Mol. Cell Biol.* **6**(10): 801-811.

Henne WM, Stenmark H and Emr SD (2013) Molecular mechanisms of the membrane sculpting ESCRT pathway. *Cold Spring Harb. Perspect. Biol.* **5**(9).

Hirata D, Nakano K, Fukui M, Takenaka H, Miyakawa T and Mabuchi I (1998) Genes that cause aberrant cell morphology by overexpression in fission yeast: a role of a small GTP-binding protein Rho2 in cell morphogenesis. *J. Cell Sci.* **111 (Pt 2)**: 149-159.

Hislop JN, Marley A and Von Zastrow M (2004) Role of mammalian vacuolar protein-sorting proteins in endocytic trafficking of a non-ubiquitinated G protein-coupled receptor to lysosomes. *J. Biol. Chem.* **279**(21): 22522-22531.

Ho TT, Merajver SD, Lapiere CM, Nusgens BV and Deroanne CF (2008) RhoA-GDP regulates RhoB protein stability. Potential involvement of RhoGDIalpha. *J. Biol. Chem.* **283**(31): 21588-21598.

Holland P, Torgersen ML, Sandvig K and Simonsen A (2014) LYST affects lysosome size and quantity, but not trafficking or degradation through autophagy or endocytosis. *Traffic*.

Huang J, Reggiori F and Klionsky DJ (2007a) The transmembrane domain of acid trehalase mediates ubiquitin-independent multivesicular body pathway sorting. *Mol. Biol. Cell* **18**(7): 2511-2524.

Huang M, Duhadaway JB, Prendergast GC and Laury-Kleintop LD (2007b) RhoB regulates PDGFR-beta trafficking and signaling in vascular smooth muscle cells. *Arterioscler. Thromb. Vasc. Biol.* **27**(12): 2597-2605.

Huang M, Kamasani U and Prendergast GC (2006) RhoB facilitates c-Myc turnover by supporting efficient nuclear accumulation of GSK-3. *Oncogene* **25**(9): 1281-1289.

Huizing M, Anikster Y and Gahl WA (2001) Hermansky-Pudlak syndrome and Chediak-Higashi syndrome: disorders of vesicle formation and trafficking. *Thromb. Haemost.* **86**(1): 233-245.

Huizing M, Helip-Wooley A, Westbroek W, Gunay-Aygun M and Gahl WA (2008) Disorders of lysosome-related organelle biogenesis: clinical and molecular genetics. *Annu Rev Genomics Hum Genet* **9**: 359-386.

Huotari J and Helenius A (2011) Endosome maturation. *EMBO J.* **30**(17): 3481-3500.

Huynh C, Roth D, Ward DM, Kaplan J and Andrews NW (2004) Defective lysosomal exocytosis and plasma membrane repair in Chediak-Higashi/*beige* cells. *Proc. Natl. Acad. Sci. U. S. A.* **101**(48): 16795-16800.

Israels SJ and McMillan-Ward EM (2010) Palmitoylation supports the association of tetraspanin CD63 with CD9 and integrin alphaIIbbeta3 in activated platelets. *Thromb. Res.* **125**(2): 152-158.

Janosi L, Li Z, Hancock JF and Gorfe AA (2012) Organization, dynamics, and segregation of Ras nanoclusters in membrane domains. *Proc. Natl. Acad. Sci. U. S. A.* **109**(21): 8097-8102.

Jiang Z, Redfern RE, Isler Y, Ross AH and Gericke A (2014) Cholesterol stabilizes fluid phosphoinositide domains. *Chem. Phys. Lipids* **182**: 52-61.

Kabeya Y, Mizushima N, Ueno T, Yamamoto A, Kirisako T, Noda T, Kominami E, Ohsumi Y and Yoshimori T (2000) LC3, a mammalian homologue of yeast Apg8p, is localized in autophagosome membranes after processing. *EMBO J.* **19**(21): 5720-5728.

Kamasani U, Huang M, Duhadaway JB, Prochownik EV, Donover PS and Prendergast GC (2004) Cyclin B1 is a critical target of RhoB in the cell suicide program triggered by farnesyl transferase inhibition. *Cancer Res.* **64**(22): 8389-8396.

Karim MA, Suzuki K, Fukai K, Oh J, Nagle DL, Moore KJ, Barbosa E, Falik-Borenstein T, Filipovich A, Ishida Y, Kivrikko S, Klein C, Kreuz F, Levin A, Miyajima H, Regueiro J, Russo C, Uyama E, Vierimaa O and Spritz RA (2002) Apparent genotype-phenotype correlation in childhood, adolescent, and adult Chediak-Higashi syndrome. *Am. J. Med. Genet.* **108**(1): 16-22.

Katzmann DJ, Babst M and Emr SD (2001) Ubiquitin-dependent sorting into the multivesicular body pathway requires the function of a conserved endosomal protein sorting complex, ESCRT-I. *Cell* **106**(2): 145-155.

Kim EH and Surh YJ (2006) 15-deoxy-Delta12,14-prostaglandin J2 as a potential endogenous regulator of redox-sensitive transcription factors. *Biochem. Pharmacol.* **72**(11): 1516-1528.

Kim JS and Raines RT (1995) Dibromobimane as a fluorescent cross-linking reagent. *Anal. Biochem.* **225**(1): 174-176.

Kim SE, Yoon JY, Jeong WJ, Jeon SH, Park Y, Yoon JB, Park YN, Kim H and Choi KY (2009) H-Ras is degraded by Wnt/beta-catenin signaling via beta-TrCP-mediated polyubiquitylation. *J. Cell Sci.* **122**(Pt 6): 842-848.

Klöpper TH, Kienle N, Fasshauer D and Munro S (2012) Untangling the evolution of Rab G proteins: implications of a comprehensive genomic analysis. *BMC Biol.* **10**: 71.

Kneen M, Farinas J, Li Y and Verkman AS (1998) Green fluorescent protein as a noninvasive intracellular pH indicator. *Biophys. J.* **74**(3): 1591-1599.

Kobayashi T, Beuchat MH, Lindsay M, Frias S, Palmiter RD, Sakuraba H, Parton RG and Gruenberg J (1999) Late endosomal membranes rich in lysobisphosphatidic acid regulate cholesterol transport. *Nat. Cell Biol.* **1**(2): 113-118.

Koenitzer JR and Freeman BA (2010) Redox signaling in inflammation: interactions of endogenous electrophiles and mitochondria in cardiovascular disease. *Ann. N. Y. Acad. Sci.* **1203**: 45-52.

Kolter T and Sandhoff K (2005) Principles of lysosomal membrane digestion: stimulation of sphingolipid degradation by sphingolipid activator proteins and anionic lysosomal lipids. *Annu. Rev. Cell. Dev. Biol.* **21**: 81-103.

Krzewski K and Cullinane AR (2013) Evidence for defective Rab GTPase-dependent cargo traffic in immune disorders. *Exp. Cell Res.* **319**(15): 2360-2367.

Kypri E, Falkenstein K and De Lozanne A (2013) Antagonistic control of lysosomal fusion by Rab14 and the Lyst-related protein LvsB. *Traffic* **14**(5): 599-609.

Lajoie-Mazenc I, Tovar D, Penary M, Lortal B, Allart S, Favard C, Brihoum M, Pradines A and Favre G (2008) MAP1A light chain-2 interacts with GTP-RhoB to control epidermal growth factor (EGF)-dependent EGF receptor signaling. *J. Biol. Chem.* **283**(7): 4155-4164.

Lambou K, Tharreau D, Kohler A, Sirven C, Marguerettaz M, Barbisan C, Sexton AC, Kellner EM, Martín F, Howlett BJ, Orbach MJ and Lebrun MH (2008) Fungi have three tetraspanin families with distinct functions. *BMC Genomics* **9**: 63.

Laufs U, Endres M, Custodis F, Gertz K, Nickenig G, Liao JK and Bohm M (2000) Suppression of endothelial nitric oxide production after withdrawal of statin treatment is mediated by negative feedback regulation of rho GTPase gene transcription. *Circulation* **102**(25): 3104-3110.

Laulagnier K, Motta C, Hamdi S, Roy S, Fauvelle F, Pageaux JF, Kobayashi T, Salles JP, Perret B, Bonnerot C and Record M (2004) Mast cell- and dendritic cell-derived exosomes display a specific lipid composition and an unusual membrane organization. *Biochem. J.* **380**(Pt 1): 161-171.

Lee J, Giordano S and Zhang J (2012) Autophagy, mitochondria and oxidative stress: cross-talk and redox signalling. *Biochem. J.* **441**(2): 523-540.

Lee SE and Park YS (2013) Role of lipid peroxidation-derived alpha, beta-unsaturated aldehydes in vascular dysfunction. *Oxid. Med. Cell. Longev.* **2013**: 629028.

Leung KF, Baron R and Seabra MC (2006) Thematic review series: lipid posttranslational modifications. geranylgeranylation of Rab GTPases. *J. Lipid Res.* **47**(3): 467-475.

Leung KF, Dacks JB and Field MC (2008) Evolution of the multivesicular body ESCRT machinery; retention across the eukaryotic lineage. *Traffic* **9**(10): 1698-1716.

Leventis PA and Grinstein S (2010) The distribution and function of phosphatidylserine in cellular membranes. *Annu Rev Biophys* **39**: 407-427.

Levonen AL, Landar A, Ramachandran A, Ceaser EK, Dickinson DA, Zanoni G, Morrow JD and Darley-Usmar VM (2004) Cellular mechanisms of redox cell signalling: role of cysteine modification in controlling antioxidant defences in response to electrophilic lipid oxidation products. *Biochem. J.* **378**(Pt 2): 373-382.

Liou W, Geuze HJ, Geelen MJ and Slot JW (1997) The autophagic and endocytic pathways converge at the nascent autophagic vacuoles. *J. Cell Biol.* **136**(1): 61-70.

Lippincott-Schwartz J and Phair RD (2010) Lipids and cholesterol as regulators of traffic in the endomembrane system. *Annu Rev Biophys* **39**: 559-578.

Liu AX, Rane N, Liu JP and Prendergast GC (2001) RhoB is dispensable for mouse development, but it modifies susceptibility to tumor formation as well as cell adhesion and growth factor signaling in transformed cells. *Mol. Cell. Biol.* **21**(20): 6906-6912.

Lobo S, Greentree WK, Linder ME and Deschenes RJ (2002) Identification of a Ras palmitoyltransferase in Saccharomyces cerevisiae. *J. Biol. Chem.* **277**(43): 41268-41273.

Lu L and Hong W (2014) From endosomes to the trans-Golgi network. *Semin. Cell Dev. Biol.* **31**: 30-39.

Ma Y, Kuno T, Kita A, Asayama Y and Sugiura R (2006) Rho2 is a target of the farnesyltransferase Cpp1 and acts upstream of Pmk1 mitogen-activated protein kinase signaling in fission yeast. *Mol. Biol. Cell* **17**(12): 5028-5037.

Madaule P and Axel R (1985) A novel Ras-related gene family. *Cell* **41**(1): 31-40.

Mageswaran SK, Dixon MG, Curtiss M, Keener JP and Babst M (2014) Binding to any ESCRT can mediate ubiquitin-independent cargo sorting. *Traffic* **15**(2): 212-229.

Malcolm T, Ettehadieh E and Sadowski I (2003) Mitogen-responsive expression of RhoB is regulated by RNA stability. *Oncogene* **22**(40): 6142-6150.

Mallis RJ, Buss JE and Thomas JA (2001) Oxidative modification of H-Ras: S-thiolation and S-nitrosylation of reactive cysteines. *Biochem. J.* **355**(Pt 1): 145-153.

Marchetti A, Mercanti V, Cornillon S, Alibaud L, Charette SJ and Cosson P (2004) Formation of multivesicular endosomes in Dictyostelium. *J. Cell Sci.* **117**(Pt 25): 6053-6059.

Matozaki T, Nakanishi H and Takai Y (2000) Small G-protein networks: their crosstalk and signal cascades. *Cell. Signal.* **12**(8): 515-524.

Matsuo H, Chevallier J, Mayran N, Le Blanc I, Ferguson C, Faure J, Blanc NS, Matile S, Dubochet J, Sadoul R, Parton RG, Vilbois F and Gruenberg J (2004) Role of LBPA and Alix in multivesicular liposome formation and endosome organization. *Science* **303**(5657): 531-534.

Maurer-Stroh S, Washietl S and Eisenhaber F (2003) Protein prenyltransferases: anchor size, pseudogenes and parasites. *Biol. Chem.* **384**(7): 977-989.

Maxfield FR and van Meer G (2010) Cholesterol, the central lipid of mammalian cells. *Curr. Opin. Cell Biol.* **22**(4): 422-429.

McCormick PJ, Dumaresq-Doiron K, Pluviose AS, Pichette V, Tosato G and Lefrancois S (2008) Palmitoylation controls recycling in lysosomal sorting and trafficking. *Traffic* **9**(11): 1984-1997.

McMahon HT and Gallop JL (2005) Membrane curvature and mechanisms of dynamic cell membrane remodelling. *Nature* **438**(7068): 590-596.

McTaggart SJ (2006) Isoprenylated proteins. *Cell. Mol. Life Sci.* **63**(3): 255-267.

Mellor H, Flynn P, Nobes CD, Hall A and Parker PJ (1998) PRK1 is targeted to endosomes by the small GTPase, RhoB. *J. Biol. Chem.* **273**(9): 4811-4814.

Menasche G, Feldmann J, Houdusse A, Desaymard C, Fischer A, Goud B and de Saint Basile G (2003) Biochemical and functional characterization of Rab27a mutations occurring in Griscelli syndrome patients. *Blood* **101**(7): 2736-2742.

Michaelson D, Silletti J, Murphy G, D'Eustachio P, Rush M and Philips MR (2001) Differential localization of Rho GTPases in live cells: regulation by hypervariable regions and RhoGDI binding. *J. Cell Biol.* **152**(1): 111-126.

Misaki R, Morimatsu M, Uemura T, Waguri S, Miyoshi E, Taniguchi N, Matsuda M and Taguchi T (2010) Palmitoylated Ras proteins traffic through recycling endosomes to the plasma membrane during exocytosis. *J. Cell Biol.* **191**(1): 23-29.

Mitra S, Cheng KW and Mills GB (2011) Rab GTPases implicated in inherited and acquired disorders. *Semin. Cell Dev. Biol.* **22**(1): 57-68.

Mizushima N, Levine B, Cuervo AM and Klionsky DJ (2008) Autophagy fights disease through cellular self-digestion. *Nature* **451**(7182): 1069-1075.

Mizushima N and Yoshimori T (2007) How to interpret LC3 immunoblotting. *Autophagy* **3**(6): 542-545.

Mizushima N, Yoshimori T and Levine B (2010) Methods in mammalian autophagy research. *Cell* **140**(3): 313-326.

Mizushima N, Yoshimori T and Ohsumi Y (2011) The role of Atg proteins in autophagosome formation. *Annu. Rev. Cell. Dev. Biol.* **27**: 107-132.

Möbius W, van Donselaar E, Ohno-Iwashita Y, Shimada Y, Heijnen HF, Slot JW and Geuze HJ (2003) Recycling compartments and the internal vesicles of multivesicular bodies harbor most of the cholesterol found in the endocytic pathway. *Traffic* **4**(4): 222-231.

Mollinedo F, Pérez-Sala D, Gajate C, Jiménez B, Rodríguez P and Lacal JC (1993) Localization of Rap1 and Rap2 proteins in the gelatinase-containing granules of human neutrophils. *FEBS Lett.* **326**(1-3): 209-214.

Morita E and Sundquist WI (2004) Retrovirus budding. *Annu. Rev. Cell. Dev. Biol.* **20**: 395-425.

Mukherjee S and Maxfield FR (2004) Lipid and cholesterol trafficking in NPC. *Biochim. Biophys. Acta* **1685**(1-3): 28-37.

Murk JL, Stoorvogel W, Kleijmeer MJ and Geuze HJ (2002) The plasticity of multivesicular bodies and the regulation of antigen presentation. *Semin. Cell Dev. Biol.* **13**(4): 303-311.

Narumiya S and Fukushima M (1985) Delta 12-prostaglandin J2, an ultimate metabolite of prostaglandin D2 exerting cell growth inhibition. *Biochem. Biophys. Res. Commun.* **127**(3): 739-745.

Nguyen UT, Goody RS and Alexandrov K (2010) Understanding and exploiting protein prenyltransferases. *ChemBioChem* **11**(9): 1194-1201.

Nishida M, Sawa T, Kitajima N, Ono K, Inoue H, Ihara H, Motohashi H, Yamamoto M, Suematsu M, Kurose H, van der Vliet A, Freeman BA, Shibata T, Uchida K, Kumagai Y and Akaike T (2012) Hydrogen sulfide anion regulates redox signaling via electrophile sulfhydration. *Nat. Chem. Biol.* **8**(8): 714-724.

Oeste CL, Díez-Dacal B, Bray F, García de Lacoba M, de la Torre BG, Andreu D, Ruiz-Sánchez AJ, Pérez-Inestrosa E, García-Domínguez CA, Rojas JM and Pérez-Sala D (2011) The C-terminus of H-Ras as a target for the covalent binding of

reactive compounds modulating Ras-dependent pathways. *PLoS One* **6**(1): e15866.

Oeste CL and Pérez-Sala D (2014) Modification of cysteine residues by cyclopentenone prostaglandins: interplay with redox regulation of protein function. *Mass Spectrom. Rev.* **33**(2): 110-125.

Oeste CL, Pinar M, Schink KO, Martínez-Turrion J, Stenmark H, Peñalva MA and Pérez-Sala D (2014) An isoprenylation and palmitoylation motif promotes intraluminal vesicle delivery of proteins in cells from distant species. *PLoS One* **9**(9): e107190.

Oeste CL, Seco E, Patton WF, Boya P and Pérez-Sala D (2013) Interactions between autophagic and endolysosomal markers in endothelial cells. *Histochem. Cell Biol.* **139**(5): 659-670.

Ohno K, Fujiwara M, Fukushima M and Narumiya S (1986) Metabolic dehydration of prostaglandin E2 and cellular uptake of the dehydration product: correlation with prostaglandin E2-induced growth inhibition. *Biochem. Biophys. Res. Commun.* **139**(2): 808-815.

Oliva JL, Pérez-Sala D, Castrillo A, Martínez N, Cañada FJ, Bosca L and Rojas JM (2003) The cyclopentenone 15-deoxy-delta 12,14-prostaglandin J2 binds to and activates H-Ras. *Proc. Natl. Acad. Sci. U. S. A.* **100**(8): 4772-4777.

Oliver C, Essner E, Zimring A and Haimes H (1976) Age-related accumulation of ceroid-like pigment in mice with Chediak-Higashi syndrome. *Am. J. Pathol.* **84**(2): 225-238.

Omerovic J, Laude AJ and Prior IA (2007) Ras proteins: paradigms for compartmentalised and isoform-specific signalling. *Cell. Mol. Life Sci.* **64**(19-20): 2575-2589.

Pantazopoulou A and Peñalva MA (2009) Organization and dynamics of the *Aspergillus nidulans* Golgi during apical extension and mitosis. *Mol. Biol. Cell* **20**(20): 4335-4347.

Park SY and Guo X (2014) Adaptor protein complexes and intracellular transport. *Biosci. Rep.* **34**(4).

Patterson GH and Lippincott-Schwartz J (2002) A photoactivatable GFP for selective photolabeling of proteins and cells. *Science* **297**(5588): 1873-1877.

Peñalva MA, Galindo A, Abenza JF, Pinar M, Calcagno-Pizarelli AM, Arst HN and Pantazopoulou A (2012) Searching for gold beyond mitosis: Mining intracellular membrane traffic in *Aspergillus nidulans*. *Cell Logist* **2**(1): 2-14.

Peng Y, Tang F and Weisman LS (2006) Palmitoylation plays a role in targeting Vac8p to specific membrane subdomains. *Traffic* **7**(10): 1378-1387.

Peplowska K, Markgraf DF, Ostrowicz CW, Bange G and Ungermann C (2007) The CORVET tethering complex interacts with the yeast Rab5 homolog Vps21 and is involved in endolysosomal biogenesis. *Dev. Cell* **12**(5): 739-750.

Pereira-Leal JB and Seabra MC (2000) The mammalian Rab family of small GTPases: definition of family and subfamily sequence motifs suggests a mechanism for functional specificity in the Ras superfamily. *J. Mol. Biol.* **301**(4): 1077-1087.

Pérez-Hernández D, Gutiérrez-Vázquez C, Jorge I, López-Martín S, Ursa A, Sánchez-Madrid F, Vázquez J and Yáñez-Mo M (2013) The intracellular interactome of tetraspanin-enriched microdomains reveals their function as sorting machineries toward exosomes. *J. Biol. Chem.* **288**(17): 11649-11661.

Pérez-Sala D (2007) Protein isoprenylation in biology and disease: general overview and perspectives from studies with genetically engineered animals. *Front. Biosci.* **12**: 4456-4472.

Pérez-Sala D, Boya P, Ramos I, Herrera M and Stamatakis K (2009) The C-terminal sequence of RhoB directs protein degradation through an endo-lysosomal pathway. *PLoS One* **4**(12): e8117.

Pérez-Sala D, Tan EW, Cañada FJ and Rando RR (1991) Methylation and demethylation reactions of guanine nucleotide-binding proteins of retinal rod outer segments. *Proc. Natl. Acad. Sci. U. S. A.* **88**(8): 3043-3046.

Platt FM, Boland B and van der Spoel AC (2012) The cell biology of disease: lysosomal storage disorders: the cellular impact of lysosomal dysfunction. *J. Cell Biol.* **199**(5): 723-734.

Platta HW and Stenmark H (2011) Endocytosis and signaling. *Curr. Opin. Cell Biol.* **23**(4): 393-403.

Pols MS and Klumperman J (2009) Trafficking and function of the tetraspanin CD63. *Exp. Cell Res.* **315**(9): 1584-1592.

Poteryaev D, Datta S, Ackema K, Zerial M and Spang A (2010) Identification of the switch in early-to-late endosome transition. *Cell* **141**(3): 497-508.

Prada-Delgado A, Carrasco-Marín E, Peña-Macarro C, Del Cerro-Vadillo E, Fresno-Escudero M, Leyva-Cobián F and Álvarez-Domínguez C (2005) Inhibition of Rab5a exchange activity is a key step for *Listeria monocytogenes* survival. *Traffic* **6**(3): 252-265.

Prendergast GC (2001) Actin' up: RhoB in cancer and apoptosis. *Nat. Rev. Cancer* **1**(2): 162-168.

Prior IA, Harding A, Yan J, Sluimer J, Parton RG and Hancock JF (2001) GTP-dependent segregation of H-Ras from lipid rafts is required for biological activity. *Nat. Cell Biol.* **3**(4): 368-375.

Raiborg C, Bache KG, Mehlum A, Stang E and Stenmark H (2001) Hrs recruits clathrin to early endosomes. *EMBO J.* **20**(17): 5008-5021.

Raiborg C and Stenmark H (2009) The ESCRT machinery in endosomal sorting of ubiquitylated membrane proteins. *Nature* **458**(7237): 445-452.

Raposo G and Stoorvogel W (2013) Extracellular vesicles: exosomes, microvesicles, and friends. *J. Cell Biol.* **200**(4): 373-383.

Raymond CK, Howald-Stevenson I, Vater CA and Stevens TH (1992) Morphological classification of the yeast vacuolar protein sorting mutants: evidence for a prevacuolar compartment in class E vps mutants. *Mol. Biol. Cell* **3**(12): 1389-1402.

Recchi C and Seabra MC (2012) Novel functions for Rab GTPases in multiple aspects of tumour progression. *Biochem. Soc. Trans.* **40**(6): 1398-1403.

Reddy A, Caler EV and Andrews NW (2001) Plasma membrane repair is mediated by Ca(2+)-regulated exocytosis of lysosomes. *Cell* **106**(2): 157-169.

Renedo M, Gayarre J, García-Domínguez CA, Pérez-Rodríguez A, Prieto A, Cañada FJ, Rojas JM and Pérez-Sala D (2007) Modification and activation of Ras proteins by electrophilic prostanoids with different structure are site-selective. *Biochemistry* **46**(22): 6607-6616.

Ridley AJ (2001) Rho proteins: linking signaling with membrane trafficking. *Traffic* **2**(5): 303-310.

Rink J, Ghigo E, Kalaidzidis Y and Zerial M (2005) Rab conversion as a mechanism of progression from early to late endosomes. *Cell* **122**(5): 735-749.

Roberts PJ, Mitin N, Keller PJ, Chenette EJ, Madigan JP, Currin RO, Cox AD, Wilson O, Kirschmeier P and Der CJ (2008) Rho Family GTPase modification and dependence on CAAX motif-signaled posttranslational modification. *J. Biol. Chem.* **283**(37): 25150-25163.

Rocks O, Peyker A, Kahms M, Verveer PJ, Koerner C, Lumbierres M, Kuhlmann J, Waldmann H, Wittinghofer A and Bastiaens PI (2005) An acylation cycle regulates localization and activity of palmitoylated Ras isoforms. *Science* **307**(5716): 1746-1752.

Rojas AM, Fuentes G, Rausell A and Valencia A (2012) The Ras protein superfamily: evolutionary tree and role of conserved amino acids. *J. Cell Biol.* **196**(2): 189-201.

Rondanino C, Rojas R, Ruiz WG, Wang E, Hughey RP, Dunn KW and Apodaca G (2007) RhoB-dependent modulation of postendocytic traffic in polarized Madin-Darby canine kidney cells. *Traffic* **8**(7): 932-949.

Rotblat B, Yizhar O, Haklai R, Ashery U and Kloog Y (2006) Ras and its signals diffuse through the cell on randomly moving nanoparticles. *Cancer Res.* **66**(4): 1974-1981.

Roth AF, Feng Y, Chen L and Davis NG (2002) The yeast DHHC cysteine-rich domain protein Akr1p is a palmitoyl transferase. *J. Cell Biol.* **159**(1): 23-28.

Roth AF, Wan J, Bailey AO, Sun B, Kuchar JA, Green WN, Phinney BS, Yates JR, 3rd and Davis NG (2006) Global analysis of protein palmitoylation in yeast. *Cell* **125**(5): 1003-1013.

Rous BA, Reaves BJ, Ihrke G, Briggs JA, Gray SR, Stephens DJ, Banting G and Luzio JP (2002) Role of adaptor complex AP-3 in targeting wild-type and mutated CD63 to lysosomes. *Mol. Biol. Cell* **13**(3): 1071-1082.

Rusten TE and Simonsen A (2008) ESCRT functions in autophagy and associated disease. *Cell Cycle* **7**(9): 1166-1172.

Rusten TE, Vaccari T and Stenmark H (2012) Shaping development with ESCRTs. *Nat. Cell Biol.* **14**(1): 38-45.

Sadowski L, Pilecka I and Miaczynska M (2009) Signaling from endosomes: location makes a difference. *Exp. Cell Res.* **315**(9): 1601-1609.

Sadowski M, Suryadinata R, Tan AR, Roesley SN and Sarcevic B (2012) Protein monoubiquitination and polyubiquitination generate structural diversity to control distinct biological processes. *IUBMB Life* **64**(2): 136-142.

Saftig P and Klumperman J (2009) Lysosome biogenesis and lysosomal membrane proteins: trafficking meets function. *Nat. Rev. Mol. Cell Biol.* **10**(9): 623-635.

Sagne C and Gasnier B (2008) Molecular physiology and pathophysiology of lysosomal membrane transporters. *J. Inherit. Metab. Dis.* **31**(2): 258-266.

Samson RY, Obita T, Freund SM, Williams RL and Bell SD (2008) A role for the ESCRT system in cell division in archaea. *Science* **322**(5908): 1710-1713.

Sánchez-Gómez FJ, Cernuda-Morollón E, Stamatakis K and Pérez-Sala D (2004) Protein thiol modification by 15-deoxy-Delta12,14-prostaglandin J2 addition in mesangial cells: role in the inhibition of pro-inflammatory genes. *Mol. Pharmacol.* **66**(5): 1349-1358.

Sánchez-Gómez FJ, Gayarre J, Avellano MI and Pérez-Sala D (2007) Direct evidence for the covalent modification of glutathione-S-transferase P1-1 by electrophilic

prostaglandins: implications for enzyme inactivation and cell survival. *Arch. Biochem. Biophys.* **457**(2): 150-159.

Sandilands E, Cans C, Fincham VJ, Brunton VG, Mellor H, Prendergast GC, Norman JC, Superti-Furga G and Frame MC (2004) RhoB and actin polymerization coordinate Src activation with endosome-mediated delivery to the membrane. *Dev. Cell* **7**(6): 855-869.

Schink KO, Raiborg C and Stenmark H (2013) Phosphatidylinositol 3-phosphate, a lipid that regulates membrane dynamics, protein sorting and cell signalling. *Bioessays* **35**(10): 900-912.

Schmidt-Glenewinkel H, Vacheva I, Hoeller D, Dikic I and Eils R (2008) An ultrasensitive sorting mechanism for EGF receptor endocytosis. *BMC Syst. Biol.* **2**: 32.

Schmitz AA, Govek EE, Bottner B and Van Aelst L (2000) Rho GTPases: signaling, migration, and invasion. *Exp. Cell Res.* **261**(1): 1-12.

Schröder J, Lullmann-Rauch R, Himmerkus N, Pleines I, Nieswandt B, Orinska Z, Koch-Nolte F, Schröder B, Bleich M and Saftig P (2009) Deficiency of the tetraspanin CD63 associated with kidney pathology but normal lysosomal function. *Mol. Cell. Biol.* **29**(4): 1083-1094.

Schwartz AL and Ciechanover A (2009) Targeting proteins for destruction by the ubiquitin system: implications for human pathobiology. *Annu. Rev. Pharmacol. Toxicol.* **49**: 73-96.

Schweizer A, Kornfeld S and Rohrer J (1996) Cysteine34 of the cytoplasmic tail of the cation-dependent mannose 6-phosphate receptor is reversibly palmitoylated and required for normal trafficking and lysosomal enzyme sorting. *J. Cell Biol.* **132**(4): 577-584.

Seabra MC, Brown MS and Goldstein JL (1993) Retinal degeneration in choroideremia: deficiency of Rab geranylgeranyl transferase. *Science* **259**(5093): 377-381.

Seabra MC, Ho YK and Anant JS (1995) Deficient geranylgeranylation of Ram/Rab27 in choroideremia. *J. Biol. Chem.* **270**(41): 24420-24427.

Seals DF, Eitzen G, Margolis N, Wickner WT and Price A (2000) A Ypt/Rab effector complex containing the Sec1 homolog Vps33p is required for homotypic vacuole fusion. *Proc. Natl. Acad. Sci. U. S. A.* **97**(17): 9402-9407.

Shaner NC, Campbell RE, Steinbach PA, Giepmans BN, Palmer AE and Tsien RY (2004) Improved monomeric red, orange and yellow fluorescent proteins derived from *Discosoma sp.* red fluorescent protein. *Nat. Biotechnol.* **22**(12): 1567-1572.

Shaner NC, Lin MZ, McKeown MR, Steinbach PA, Hazelwood KL, Davidson MW and Tsien RY (2008) Improving the photostability of bright monomeric orange and red fluorescent proteins. *Nat. Methods* **5**(6): 545-551.

Sharpe HJ, Stevens TJ and Munro S (2010) A comprehensive comparison of transmembrane domains reveals organelle-specific properties. *Cell* **142**(1): 158-169.

Shen B, Wu N, Yang JM and Gould SJ (2011) Protein targeting to exosomes/microvesicles by plasma membrane anchors. *J. Biol. Chem.* **286**(16): 14383-14395.

Shibata T, Kondo M, Osawa T, Shibata N, Kobayashi M and Uchida K (2002) 15-deoxy-delta 12,14-prostaglandin J2. A prostaglandin D2 metabolite generated during inflammatory processes. *J. Biol. Chem.* **277**(12): 10459-10466.

Shim S, Merrill SA and Hanson PI (2008) Novel interactions of ESCRT-III with LIP5 and Vps4 and their implications for ESCRT-III disassembly. *Mol. Biol. Cell* **19**(6): 2661-2672.

Shiraki T, Kamiya N, Shiki S, Kodama TS, Kakizuka A and Jingami H (2005) Alpha,beta-unsaturated ketone is a core moiety of natural ligands for covalent binding to peroxisome proliferator-activated receptor gamma. *J. Biol. Chem.* **280**(14): 14145-14153.

Simons M and Raposo G (2009) Exosomes-vesicular carriers for intercellular communication. *Curr. Opin. Cell Biol.* **21**(4): 575-581.

Sinensky M (2000) Recent advances in the study of prenylated proteins. *Biochim. Biophys. Acta* **1484**(2-3): 93-106.

Sinz A and Wang K (2001) Mapping protein interfaces with a fluorogenic cross-linker and mass spectrometry: application to nebulin-calmodulin complexes. *Biochemistry* **40**(26): 7903-7913.

Smith AC, Heo WD, Braun V, Jiang X, Macrae C, Casanova JE, Scidmore MA, Grinstein S, Meyer T and Brumell JH (2007) A network of Rab GTPases controls phagosome maturation and is modulated by *Salmonella enterica* serovar *Typhimurium*. *J. Cell Biol.* **176**(3): 263-268.

Smotrys JE and Linder ME (2004) Palmitoylation of intracellular signaling proteins: regulation and function. *Annu. Rev. Biochem.* **73**: 559-587.

Smotrys JE, Schoenfish MJ, Stutz MA and Linder ME (2005) The vacuolar DHHC-CRD protein Pfa3p is a protein acyltransferase for Vac8p. *J. Cell Biol.* **170**(7): 1091-1099.

Sobo K, Le Blanc I, Luyet PP, Fivaz M, Ferguson C, Parton RG, Gruenberg J and van der Goot FG (2007) Late endosomal cholesterol accumulation leads to impaired intra-endosomal trafficking. *PLoS One* **2**(9): e851.

Solinger JA and Spang A (2013) Tethering complexes in the endocytic pathway: CORVET and HOPS. *FEBS J.* **280**(12): 2743-2757.

Stachowiak JC, Brodsky FM and Miller EA (2013) A cost-benefit analysis of the physical mechanisms of membrane curvature. *Nat. Cell Biol.* **15**(9): 1019-1027.

Stamatakis K, Cernuda-Morollón E, Hernández-Perera O and Pérez-Sala D (2002) Isoprenylation of RhoB is necessary for its degradation. A novel determinant in the complex regulation of RhoB expression by the mevalonate pathway. *J. Biol. Chem.* **277**(51): 49389-49396.

Stamatakis K and Pérez-Sala D (2006) Prostanoids with cyclopentenone structure as tools for the characterization of electrophilic lipid-protein interactomes. *Ann. N. Y. Acad. Sci.* **1091**: 548-570.

Stamatakis K, Sánchez-Gómez FJ and Pérez-Sala D (2006) Identification of novel protein targets for modification by 15-deoxy-Delta12,14-prostaglandin J2 in mesangial cells reveals multiple interactions with the cytoskeleton. *J. Am. Soc. Nephrol.* **17**(1): 89-98.

Stenmark H (2009) Rab GTPases as coordinators of vesicle traffic. *Nat. Rev. Mol. Cell Biol.* **10**(8): 513-525.

Stepanek O, Draber P and Horejsi V (2014) Palmitoylated transmembrane adaptor proteins in leukocyte signaling. *Cell. Signal.* **26**(5): 895-902.

Stinchcombe J, Bossi G and Griffiths GM (2004) Linking albinism and immunity: the secrets of secretory lysosomes. *Science* **305**(5680): 55-59.

Stinchcombe JC, Page LJ and Griffiths GM (2000) Secretory lysosome biogenesis in cytotoxic T lymphocytes from normal and Chediak Higashi syndrome patients. *Traffic* **1**(5): 435-444.

Stipp CS, Kolesnikova TV and Hemler ME (2003) Functional domains in tetraspanin proteins. *Trends Biochem. Sci.* **28**(2): 106-112.

Straus DS and Glass CK (2001) Cyclopentenone prostaglandins: new insights on biological activities and cellular targets. *Med. Res. Rev.* **21**(3): 185-210.

Strauss K, Goebel C, Runz H, Möbius W, Weiss S, Feussner I, Simons M and Schneider A (2010) Exosome secretion ameliorates lysosomal storage of cholesterol in Niemann-Pick type C disease. *J. Biol. Chem.* **285**(34): 26279-26288.

Stuffers S, Sem Wegner C, Stenmark H and Brech A (2009) Multivesicular endosome biogenesis in the absence of ESCRTs. *Traffic* **10**(7): 925-937.

Takai Y, Sasaki T and Matozaki T (2001) Small GTP-Binding Proteins. *Physiol. Rev.* **81**(1): 153-208.

Tan EW, Pérez-Sala D, Cañada FJ and Rando RR (1991) Identifying the recognition unit for G protein methylation. *J. Biol. Chem.* **266**(17): 10719-10722.

Tchernev VT, Mansfield TA, Giot L, Kumar AM, Nandabalan K, Li Y, Mishra VS, Detter JC, Rothberg JM, Wallace MR, Southwick FS and Kingsmore SF (2002) The Chediak-Higashi protein interacts with SNARE complex and signal transduction proteins. *Mol. Med.* **8**(1): 56-64.

Terebiznik MR, Vázquez CL, Torbicki K, Banks D, Wang T, Hong W, Blanke SR, Colombo MI and Jones NL (2006) *Helicobacter pylori* VacA toxin promotes bacterial intracellular survival in gastric epithelial cells. *Infect. Immun.* **74**(12): 6599-6614.

Thapar R, Williams JG and Campbell SL (2004) NMR characterization of full-length farnesylated and non-farnesylated H-Ras and its implications for Raf activation. *J. Mol. Biol.* **343**(5): 1391-1408.

Theos AC, Truschel ST, Tenza D, Hurbain I, Harper DC, Berson JF, Thomas PC, Raposo G and Marks MS (2006) A lumenal domain-dependent pathway for sorting to intralumenal vesicles of multivesicular endosomes involved in organelle morphogenesis. *Dev. Cell* **10**(3): 343-354.

Tillement V, Lajoie-Mazenc I, Casanova A, Froment C, Penary M, Tovar D, Marquez R, Monsarrat B, Favre G and Pradines A (2008) Phosphorylation of RhoB by CK1 impedes actin stress fiber organization and epidermal growth factor receptor stabilization. *Exp. Cell Res.* **314**(15): 2811-2821.

Touchot N, Chardin P and Tavitian A (1987) Four additional members of the Ras gene superfamily isolated by an oligonucleotide strategy: molecular cloning of YPT-related cDNAs from a rat brain library. *Proc. Natl. Acad. Sci. U. S. A.* **84**(23): 8210-8214.

Toulmay A and Prinz WA (2013) Direct imaging reveals stable, micrometer-scale lipid domains that segregate proteins in live cells. *J. Cell Biol.* **202**(1): 35-44.

Trajkovic K, Hsu C, Chiantia S, Rajendran L, Wenzel D, Wieland F, Schwille P, Brugger B and Simons M (2008) Ceramide triggers budding of exosome vesicles into multivesicular endosomes. *Science* **319**(5867): 1244-1247.

Turner SJ, Zhuang S, Zhang T, Boss GR and Pilz RB (2008) Effects of lovastatin on Rho isoform expression, activity, and association with guanine nucleotide dissociation inhibitors. *Biochem. Pharmacol.* **75**(2): 405-413.

Uechi Y, Bayarjargal M, Umikawa M, Oshiro M, Takei K, Yamashiro Y, Asato T, Endo S, Misaki R, Taguchi T and Kariya K (2009) Rap2 function requires palmitoylation and recycling endosome localization. *Biochem. Biophys. Res. Commun.* **378**(4): 732-737.

Ullrich O, Horiuchi H, Bucci C and Zerial M (1994) Membrane association of Rab5 mediated by GDP-dissociation inhibitor and accompanied by GDP/GTP exchange. *Nature* **368**(6467): 157-160.

Ullrich O, Reinsch S, Urbe S, Zerial M and Parton RG (1996) Rab11 regulates recycling through the pericentriolar recycling endosome. *J. Cell Biol.* **135**(4): 913-924.

Ullrich O, Stenmark H, Alexandrov K, Huber LA, Kaibuchi K, Sasaki T, Takai Y and Zerial M (1993) Rab GDP dissociation inhibitor as a general regulator for the membrane association of rab proteins. *J. Biol. Chem.* **268**(24): 18143-18150.

Urade R, Hayashi Y and Kito M (1988) Endosomes differ from plasma membranes in the phospholipid molecular species composition. *Biochim. Biophys. Acta* **946**(1): 151-163.

Valero RA, Oeste CL, Stamatakis K, Ramos I, Herrera M, Boya P and Pérez-Sala D (2010) Structural determinants allowing endolysosomal sorting and degradation of endosomal GTPases. *Traffic* **11**(9): 1221-1233.

van Niel G, Charrin S, Simoes S, Romao M, Rochin L, Saftig P, Marks MS, Rubinstein E and Raposo G (2011) The tetraspanin CD63 regulates ESCRT-independent and -dependent endosomal sorting during melanogenesis. *Dev. Cell* **21**(4): 708-721.

Vega FM, Colomba A, Reymond N, Thomas M and Ridley AJ (2012) RhoB regulates cell migration through altered focal adhesion dynamics. *Open Biol* **2**(5): 120076.

Veit M, Sollner TH and Rothman JE (1996) Multiple palmitoylation of synaptotagmin and the t-SNARE SNAP-25. *FEBS Lett.* **385**(1-2): 119-123.

Verkruyse LA and Hofmann SL (1996) Lysosomal targeting of palmitoyl-protein thioesterase. *J. Biol. Chem.* **271**(26): 15831-15836.

Vlassov AV, Magdaleno S, Setterquist R and Conrad R (2012) Exosomes: current knowledge of their composition, biological functions, and diagnostic and therapeutic potentials. *Biochim. Biophys. Acta* **1820**(7): 940-948.

Vogt AB, Spindeldreher S and Kropshofer H (2002) Clustering of MHC-peptide complexes prior to their engagement in the immunological synapse: lipid raft and tetraspan microdomains. *Immunol. Rev.* **189**: 136-151.

Walsh CT, Garneau-Tsodikova S and Gatto GJ, Jr. (2005) Protein posttranslational modifications: the chemistry of proteome diversifications. *Angew. Chem. Int. Ed. Engl.* **44**(45): 7342-7372.

Wang DA and Sebti SM (2005) Palmitoylated cysteine 192 is required for RhoB tumor-suppressive and apoptotic activities. *J. Biol. Chem.* **280**(19): 19243-19249.

Wang M, Guo L, Wu Q, Zeng T, Lin Q, Qiao Y, Wang Q, Liu M, Zhang X, Ren L, Zhang S, Pei Y, Yin Z, Ding F and Wang HR (2014) ATR/Chk1/Smurf1 pathway determines cell fate after DNA damage by controlling RhoB abundance. *Nat Commun* **5**: 4901.

Wang Q, Pfeiffer GR, 2nd and Gaarde WA (2003) Activation of SRC tyrosine kinases in response to ICAM-1 ligation in pulmonary microvascular endothelial cells. *J. Biol. Chem.* **278**(48): 47731-47743.

Wang W, Yang L and Huang HW (2007) Evidence of cholesterol accumulated in high curvature regions: implication to the curvature elastic energy for lipid mixtures. *Biophys. J.* **92**(8): 2819-2830.

Ward DM, Griffiths GM, Stinchcombe JC and Kaplan J (2000) Analysis of the lysosomal storage disease Chediak-Higashi syndrome. *Traffic* **1**(11): 816-822.

Watson RT, Furukawa M, Chiang SH, Boeglin D, Kanzaki M, Saltiel AR and Pessin JE (2003) The exocytotic trafficking of TC10 occurs through both classical and nonclassical secretory transport pathways in 3T3L1 adipocytes. *Mol. Cell. Biol.* **23**(3): 961-974.

Wei ML (2006) Hermansky-Pudlak syndrome: a disease of protein trafficking and organelle function. *Pigment Cell Res.* **19**(1): 19-42.

Wennerberg K and Der CJ (2004) Rho-family GTPases: it's not only Rac and Rho (and I like it). *J. Cell Sci.* **117**(Pt 8): 1301-1312.

Wherlock M, Gampel A, Futter C and Mellor H (2004) Farnesyltransferase inhibitors disrupt EGF receptor traffic through modulation of the RhoB GTPase. *J. Cell Sci.* **117**(Pt 15): 3221-3231.

Whyte DB, Kirschmeier P, Hockenberry TN, Nunez-Oliva I, James L, Catino JJ, Bishop WR and Pai JK (1997) K- and N-Ras are geranylgeranylated in cells treated with farnesyl protein transferase inhibitors. *J. Biol. Chem.* **272**(22): 14459-14464.

Wideman JG, Leung KF, Field MC and Dacks JB (2014) The cell biology of the endocytic system from an evolutionary perspective. *Cold Spring Harb. Perspect. Biol.* **6**(4): a016998.

Williams RL and Urbe S (2007) The emerging shape of the ESCRT machinery. *Nat. Rev. Mol. Cell Biol.* **8**(5): 355-368.

Wubbolts R, Leckie RS, Veenhuizen PT, Schwarzmann G, Möbius W, Hoernschemeyer J, Slot JW, Geuze HJ and Stoorvogel W (2003) Proteomic and biochemical analyses of human B cell-derived exosomes. Potential implications for their function and multivesicular body formation. *J. Biol. Chem.* **278**(13): 10963-10972.

http://www.lipidlibrary.aocs.org

http://www.microvesicles.org

Yang X, Claas C, Kraeft SK, Chen LB, Wang Z, Kreidberg JA and Hemler ME (2002) Palmitoylation of tetraspanin proteins: modulation of CD151 lateral interactions, subcellular distribution, and integrin-dependent cell morphology. *Mol. Biol. Cell* **13**(3): 767-781.

Yang Z and Klionsky DJ (2010) Eaten alive: a history of macroautophagy. *Nat. Cell Biol.* **12**(9): 814-822.

Yeung T, Gilbert GE, Shi J, Silvius J, Kapus A and Grinstein S (2008) Membrane phosphatidylserine regulates surface charge and protein localization. *Science* **319**(5860): 210-213.

Yoshida T, Kawano Y, Sato K, Ando Y, Aoki J, Miura Y, Komano J, Tanaka Y and Koyanagi Y (2008) A CD63 mutant inhibits T-cell tropic human immunodeficiency virus type 1 entry by disrupting CXCR4 trafficking to the plasma membrane. *Traffic* **9**(4): 540-558.

Zhang H, Fan X, Bagshaw RD, Zhang L, Mahuran DJ and Callahan JW (2007) Lysosomal membranes from *beige* mice contain higher than normal levels of endoplasmic reticulum proteins. *J. Proteome Res.* **6**(1): 240-249.

Zheng H, Pearsall EA, Hurst DP, Zhang Y, Chu J, Zhou Y, Reggio PH, Loh HH and Law PY (2012) Palmitoylation and membrane cholesterol stabilize mu-opioid receptor homodimerization and G protein coupling. *BMC Cell Biol.* **13**: 6.

ADDENDUM

Traffic 2010; **11:** 1221–1233

doi:10.1111/j.1600-0854.2010.01091.x

Structural Determinants Allowing Endolysosomal Sorting and Degradation of Endosomal GTPases

Ruth A. Valero[1], Clara L. Oeste[1], Konstantinos Stamatakis[1,2], Irene Ramos[1], Mónica Herrera[1], Patricia Boya[3] and Dolores Pérez-Sala[1,*]

[1]Department of Chemical and Physical Biology, Centro de Investigaciones Biológicas, Consejo Superior de Investigaciones Científicas, 28040 Madrid, Spain
[2]Present address: Centro de Biología Molecular Severo Ochoa, CSIC, 28049 Madrid, Spain
[3]Department of Cellular and Molecular Medicine, Centro de Investigaciones Biológicas, Consejo Superior de Investigaciones Científicas, 28040 Madrid, Spain
**Corresponding author: Dolores Pérez-Sala, dperezsala@cib.csic.es*

Rapid control of protein degradation is usually achieved through the ubiquitin-proteasome pathway. We recently found that the short-lived GTPase RhoB is degraded in lysosomes. Moreover, the fusion of the RhoB C-terminal sequence CINCCKVL, containing the isoprenylation and palmitoylation sites, to other proteins directs their sorting into multivesicular bodies (MVBs) and rapid lysosomal degradation. Here, we show that this process is highly specific for RhoB. Alteration of late endosome lipid dynamics produced the accumulation of RhoB, but not of other endosomal GTPases, including Rab5, Rab7, Rab9 or Rab11, into enlarged MVB. Other isoprenylated and bipalmitoylated GTPases, such as H-Ras, Rap2A, Rap2B and TC10, were not accumulated into MVB and were stable. Remarkably, although TC10, which is highly homologous to RhoB, was stable, a sequence derived from its C-terminus (CINCCLIT) elicited MVB sorting and degradation of a green fluorescent protein (GFP)-chimeric protein. This led us to identify a cluster of basic amino acids (KKH) in the TC10 hypervariable region, constituting a secondary signal potentially involved in electrostatic interactions with membrane lipids. Mutation of this cluster allowed TC10 MVB sorting and degradation, whereas inserting it into RhoB hypervariable region rescued this protein from its lysosomal degradation pathway. These findings define a highly specific structural module for entering the MVB pathway and rapid lysosomal degradation.

Key words: hypervariable domain, isoprenylation, lysosomal degradation, palmitoylation, post-translational modification, protein sorting, RhoB, Rho proteins, TC10, U18666A

Received 21 February 2010, revised and accepted for publication 17 June 2010, uncorrected manuscript published online 21 June 2010, published online 13 July 2010

Lysosomal degradation of proteins plays a key role in cell homeostasis. It is generally believed that proteins degraded through the lysosomal pathway are mostly long-lived proteins, although various short-lived proteins can be degraded, at least in part, in lysosomes, including the ubiquitin E3 ligase MARCH1 (1), Jun, the component of adaptor protein 1 (AP1) transcription factor (2), and the signalling kinase Traf2 (3). Thus, lysosomal protein degradation may have important consequences for cell signalling.

The mechanisms through which proteins may reach lysosomes are multiple and in many cases only partially understood. Often, signals consisting in precise protein sequences or post-translational modifications, such as ubiquitination, trigger recognition of the protein by multiprotein complexes that constitute the endosomal sorting complexes required for transport (ESCRT) machinery inducing membrane invagination and multivesicular body (MVB) formation. For instance, monoubiquitination of cytosolic domains of membrane receptors leads to their sorting into MVB. Cellular components may also reach lysosomes through macroautophagy, where proteins and even organelles are engulfed in membranous structures called autophagosomes that finally will fuse with lysosomes to degrade their contents (4). In addition, some proteins reach the lysosomal lumen by specific interaction of the protein with the chaperone Hsc70 and the lysosomal receptor Lamp2a as in chaperone-mediated autophagy (5). Hypothetically, proteins associated with the cytosolic face of endosomes or MVB could also be delivered to their interior and reach lysosomes where they would be degraded (6,7).

The small GTPase RhoB is a short-lived protein located on the cytosolic side of late endosomes, which plays important roles in the traffic of signalling molecules and in tumour suppression (8,9). We have recently reported that RhoB can be sorted into MVB and be rapidly degraded by lysosomal proteases (7). Although the mechanisms governing this process are not fully understood, involvement of the ESCRT system is suggested by the observation that dominant-negative mutants of the ATPase VPS4 cause RhoB retention at the MVB-limiting membrane and stabilization of the protein. The lipid composition of late endosomes is also important for MVB biogenesis (10). The late endosome-specific lipid phospholipid bis(monoacylglycero)phosphate (BMP) (11), also called 2,2′-dioleoyl lysobisphosphatidic acid (LBPA), has been reported to play a key role in membrane invagination (12). The composition and dynamics of late endosome lipids are disrupted in the genetic disorder known as Niemann-Pick type C type 1 (NPC) disease (13). In this disease, mutations in the NPC1 protein, which regulates cholesterol transport, cause a massive accumulation of cholesterol in

late endosomal membranes with a concomitant increase in BMP (14,15). The hydrophobic amine U18666A mimics the NPC phenotype causing acute accumulation of cholesterol and BMP in late endosomes (15) and it is considered as an *in vitro* model for this disease (13,16). Interestingly, RhoB becomes trapped in dense endosomes when lipid dynamics are altered either pharmacologically, with U18666A, or by genetic disease, as in NPC cells (7).

Lipid modifications of small G-proteins play a key role in their subcellular localization (17). Several endosome-associated GTPases involved in the regulation of membrane traffic belong to the Rab family of small G-proteins and are mono- or bi-geranylgeranylated at their C-termini (18). RhoB is an isoprenylated and bipalmitoylated protein (19). RhoB modification by lipids is required for its association with MVB and its sorting into intraluminal vesicles (7). Importantly, this property is transferable to other proteins because a sequence containing the isoprenylation and palmitoylation sites of RhoB (CINCCKVL) elicits the lysosomal sorting and rapid degradation of stable proteins when fused to their C-terminal end (7). Several other small G-proteins, including H-Ras, TC10, Rap2A and Rap2B, possess bipalmitoylated and isoprenylated C-terminal sequences similar to that of RhoB (20,21). Of these proteins, H-Ras localizes mainly to the plasma membrane and various intracellular structures, including the endoplasmic reticulum, the Golgi complex, recycling endosomes (22,23), and to randomly moving nanoparticles known as rasosomes (24). TC10 has been detected at the plasma and perinuclear membranes, identified as components of the secretory or endosomal compartments (20,25), whereas Rap2 has been detected in secretory granules (26) and recycling endosomes (21). However, at present it is not known whether these proteins interact with or are degraded through the lysosomal pathway. To get insight into the specificity of the degradation pathway followed by RhoB, we have studied the subcellular distribution and stability of various endosome-associated small GTPases and the behaviour of several short chimeric proteins containing their C-terminal lipidation sequences.

Here, we describe that lysosomal targeting through isoprenylation and palmitoylation is highly specific for RhoB. Moreover, protein targeting and degradation mediated by this mechanism can be counteracted by the presence of basic residues close to the lipidation motif. These results provide novel insight into the structural determinants involved in endolysosomal targeting of small GTPases.

Results

RhoB accumulates into Lamp1-positive endosomes upon disruption of endosomal lipid dynamics

The compound U18666A provokes increased MVB membrane invagination and accumulation of cholesterol in BMP-rich MVB internal membranes that resemble the alterations observed in NPC disease (16). We have previously shown that treatment of cells with the compound U18666A induces a strong accumulation of RhoB inside dense compartments, which are stained with the probe for acidic compartments Lysotracker red (LTR) (7). To characterize U18666A-induced RhoB-positive structures in more detail, we monitored the distribution of the late endosome/lysosome integral membrane protein Lamp1 in RhoB-transfected cells. As it can be observed in Figure 1A, U18666A induced the accumulation of RhoB in structures that were delimited by Lamp1, indicating that they are formed from late endosomes/lysosomes, and that were clearly visible by differential interference contrast (DIC) as dense structures. Moreover, RhoB colocalized inside these Lamp1-delimited compartments with BMP and cholesterol, as revealed by immunofluorescence and filipin staining, respectively (Figure 1B). Finally, we confirmed that Lamp1-positive, U18666A-induced dense structures were acidic as evidenced by staining with LTR (Figure 1B). Taken together, these results indicate that dense compartments accumulating RhoB upon impairment of cholesterol traffic with U18666A correspond to altered MVB.

Selectivity of RhoB accumulation into MVB upon treatment with U18666A

Having observed a clear accumulation of RhoB inside MVB upon treatment with U18666A, we explored whether the distribution of other small GTPases, known to be associated with various endosomal compartments, suffered similar alterations. For this, we employed green fluorescent protein (GFP) constructs and LTR staining (Figure 2), as well as DIC (not shown) to monitor the dilated MVB induced by U18666A treatment in live cells. As expected from the results shown in Figure 1, GFP-RhoB strongly colocalized with LTR inside U18666A-induced dense endosomes (Figure 2). In contrast, Rab5, a GTPase associated with early endosomes (27), did not colocalize with LTR in control cells and did not accumulate in LTR-positive dilated structures in U18666A-treated cells. Interestingly, Rab7, known to associate with late endosomes and lysosomes (28), was clearly retained at the limiting membrane of dense MVB after U18666A treatment. Rab9, which has been reported to associate with late endosomes (29), partially colocalized with LTR in control cells, but remained at the periphery of the dilated LTR-positive compartments in U18666A-treated cells. Rab11, a GTPase described to be present in recycling endosomes (30), did not colocalize with LTR in control cells and did not accumulate in U18666A-induced LTR-positive compartments. Analysis of the fluorescence intensity profiles of the individual channels along the diameter of U18666A-induced MVB clearly shows the differential distribution of the various GTPases (Figure 2A, right panels). Therefore, whereas treatment of cells with U18666A produces the accumulation of RhoB inside dilated MVB colocalizing with LTR, a variety of endosome-associated GTPases, including Rab5, Rab7, Rab9 and Rab11, do not reach the interior of these structures in significant amounts. In particular, Rab7 and Rab9

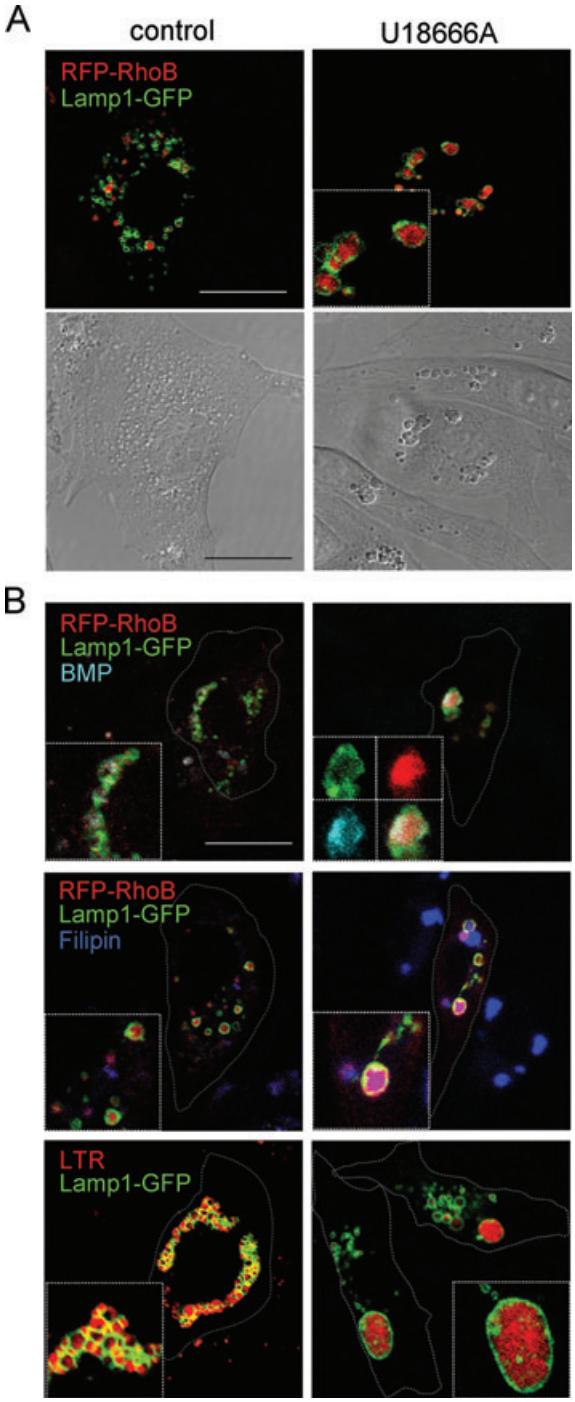

Figure 1: U18666A induces RhoB accumulation in enlarged MVB. A) BAECs transfected with tRFP-T-RhoB and Lamp1-GFP were treated with 10 M U18666A for 24 h, after which live cells were visualized by confocal microscopy. Single confocal sections (upper panels) and DIC images (lower panels) are shown. B) BAECs transfected as above were treated in the absence or presence of U18666A after which, BMP was detected by IF, cholesterol accumulation was evidenced by staining with filipin and acidic compartments were traced by LTR staining. Cell contours are indicated by dotted grey lines. Images shown are representative of four experiments. Bars, 20 m.

form a defined layer at the periphery of these organelles, whereas Rab5 is not associated with them. Because colocalization between the corresponding GFP constructs and LTR reflected the extent of accumulation of the respective proteins inside MVB, we quantified this parameter for the various GTPases used in this study. Figure 2B shows the increase in colocalization of the different GFP constructs with LTR induced by U18666A treatment with respect to untreated cells. These results clearly confirm the selective accumulation of RhoB in LTR-positive compartments in U18666A-treated cells.

Distribution of isoprenylated and bipalmitoylated GTPases in U18666A-treated cells

RhoB association with endosomal membranes is mediated by isoprenylation and bipalmitoylation (7,20). This triple-lipid anchor (Figure 3A), which is not present in Rab GTPases, could be involved in RhoB being trapped in invaginating vesicles of MVB. To assess whether other isoprenylated and bipalmitoylated GTPases follow the same pathway, we explored the subcellular localization of H-Ras, TC10, Rap2A and Rap2B in control and U18666A-treated cells. H-Ras appeared distributed at the cell membrane and intracellular vesicles that showed little or no colocalization with LTR, both in the absence and presence of U18666A (Figure 3B). The other isoprenylated and bipalmitoylated proteins appeared associated with the plasma membrane, but above all with intracellular vesicles, showing partial colocalization with LTR, indicative of their association with acidic compartments (Figure 3C). Upon treatment with U18666A, TC10, Rap2A and Rap2B showed a peripheral distribution with respect to the dilated MVB compartments, and remained mostly excluded from the intraluminal space. As shown in Figure 3D, the degree of colocalization of the various proteins with LTR did not increase in the presence of U18666A, thereby indicating the lack of internalization of the various constructs into LTR-positive compartments (Figure 3D). Therefore, possessing a sequence for isoprenylation and bipalmitoylation is not sufficient to confer susceptibility to U18666A-induced invagination into MVB.

Stability of several isoprenylated and bipalmitoylated small GTPases

Rapid degradation of RhoB requires both isoprenylation and palmitoylation (7,31). The possibility that other isoprenylated and palmitoylated proteins were subjected to rapid degradation was addressed by measuring the decay of the levels of GFP constructs of H-Ras, TC10, Rap2A and Rap2B, in comparison with GFP-RhoB, after blocking protein synthesis with cycloheximide (CHX) (Figure 4). Consistent with previous reports (32,33), GFP-H-Ras did not suffer rapid degradation. TC10, Rap2A and Rap2B constructs also showed higher stability than RhoB. Endogenous proteins followed the same pattern (results not shown). Taken together, these results indicate that bipalmitoylation and isoprenylation *per se* are not sufficient to direct MVB sorting and/or rapid protein

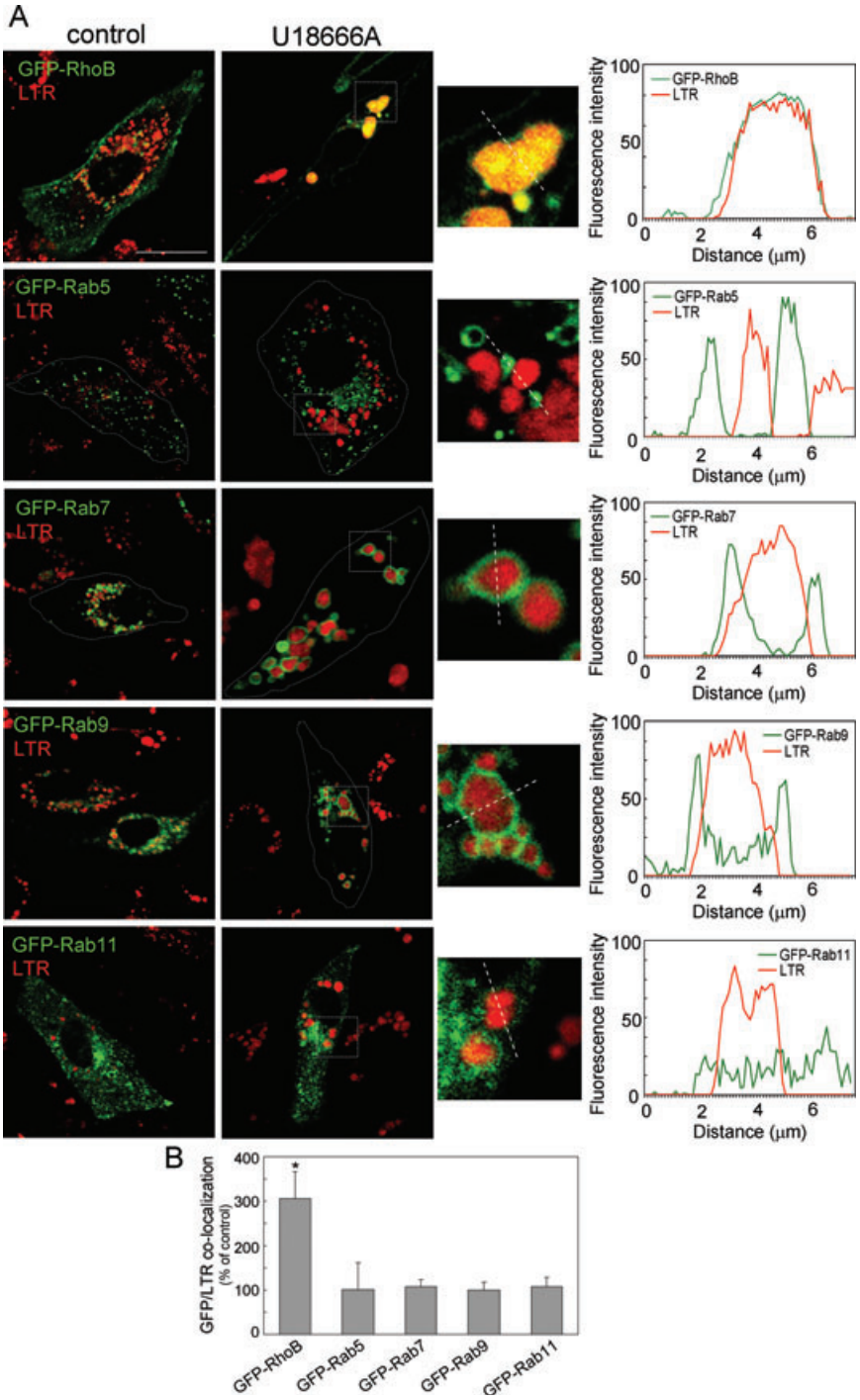

Figure 2: Effect of U18666A on the distribution of various endosomal GTPases. A) BAECs transfected with the indicated constructs were treated in the absence or presence of U18666A for 24 h and incubated with 25 nM LTR before visualization by confocal microscopy. Areas in insets are enlarged for better visualization of the lines along which fluorescence intensity profiles (left panels) have been obtained. Results are representative of four experiments with similar results. Bar, 20 m. B) The extent of colocalization of GFP and LTR signals in U18666A-treated cells was used as an index of the internalization of the corresponding GFP constructs into acidic compartments and is expressed as percentage of the values obtained in untreated cells for each construct. Results shown as average values of five determinations from three independent experiments ± SEM. *$p < 0.05$ versus the same condition in the absence of U18666A by Student's *t*-test.

degradation. Therefore, other structural determinants may contribute to allow MVB delivery and degradation. These structural determinants could be related to the different spacing of lipidic modifications or to differences inherent to the amino acid sequence, which are more substantial in the hypervariable domains of these proteins. To address these issues, we decided to explore the behaviour of short chimeras bearing the lipidation motifs from several GTPases.

Distribution and stability of chimeric proteins bearing the isoprenylation and palmitoylation sequences from small GTPases

We have previously shown that the chimeric protein GFP-CINCCKVL (GFP-8-RhoB), containing the RhoB C-terminal sequence, is sorted and degraded through a lysosomal pathway (7). Therefore, in the case of RhoB all necessary determinants for degradation are retained in this short sequence. To assess whether C-terminal sequences from

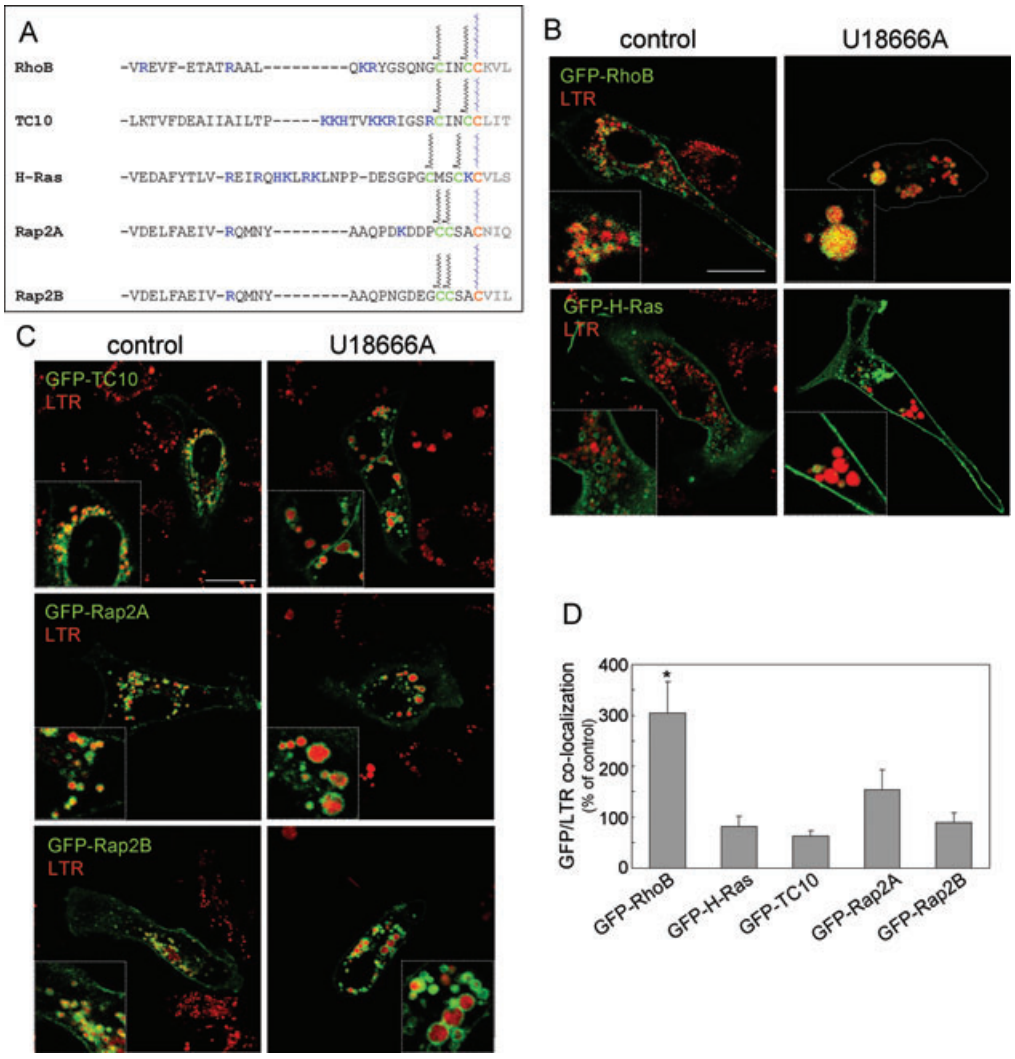

Figure 3: Localization of isoprenylated and bipalmitoylated GTPases in control and U18666A-treated cells. A) The C-terminal sequence of several isoprenylated and bipalmitoylated low-molecular weight GTPases is shown. Basic amino acids are depicted in blue, palmitoylation cysteines in green, isoprenylation cysteines in orange and amino acids removed by C-terminal proteolysis in grey. B and C) BAECs transfected with the indicated constructs were treated as above. Bars, 20 m. D) Colocalization of GFP and LTR signals was assessed as in Figure 2. *$p < 0.05$ versus the same condition in the absence of U18666A by Student's *t*-test.

other GTPases, isolated from the rest of the protein, could also follow this pathway, we generated chimeric proteins consisting of the isoprenylation and palmitoylation motifs from the various GTPases fused to the C-terminal end of GFP (Figure 5A). GFP alone showed a diffuse distribution throughout the cell and was completely excluded from the enlarged MVB in U18666A-treated cells (Figure 5B). Consistent with previous observations (7), GFP-8-RhoB, shown here as control, was clearly accumulated inside U18666A-induced MVB. The other chimeric proteins tested were partly associated with the plasma membrane and with intracellular vesicles, showing a variable degree of colocalization with LTR under control conditions. Interestingly, the construct bearing the C-terminal sequence from TC10 (GFP-8-TC10), which is highly similar to that of RhoB, clearly accumulated inside dense MVB in the presence of U18666A, showing intense colocalization with LTR (Figure 5C). In contrast, GFP-9-H-Ras and GFP-8-Rap2A, bearing the C-terminal sequences of H-Ras and Rap2A, respectively, did not substantially colocalize with LTR either in the absence or presence of U18666A, nor were they accumulated inside dense MVB to extents similar to GFP-8-RhoB or GFP-8-TC10. Therefore, sorting of isoprenylated and palmitoylated constructs into MVB appears to require specific sequences and/or spacing of lipidated residues. To assess this point, we have explored the localization of a construct bearing a sequence similar to that of GFP-8-TC10, in which the spacing between palmitoylation cysteines has been altered by substituting the CINCCLIT sequence for CCINCLIT (Figure S1). The resulting construct, GFP-8-TC10m, showed lesser association

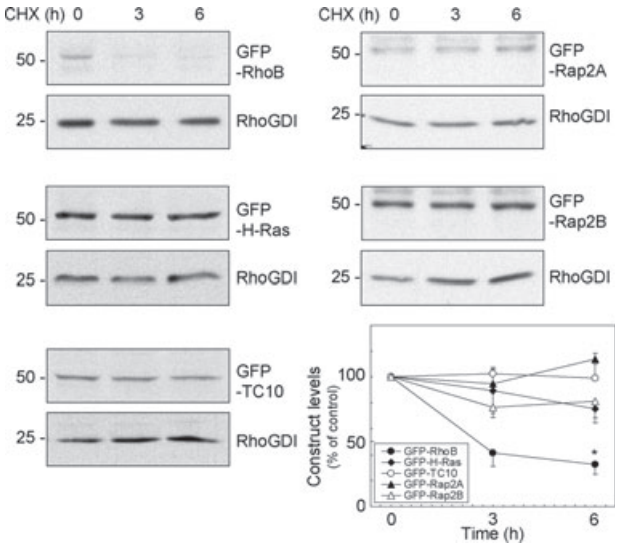

Figure 4: Stability of several fusion proteins of GFP with isoprenylated and bipalmitoylated proteins. BAECs were transiently transfected with the indicated constructs. Construct stability was assessed by blocking protein synthesis with 20 g/mL CHX and estimating the remaining levels by western blot with anti-GFP antibody. RhoGDI is used as a loading control. The graph shows the construct levels remaining after treatment with CHX for the indicated times. Results are shown as average values ± SEM of three different experiments. *$p < 0.05$ GFP-RhoB versus every other construct by Student's *t*-test.

with acidic compartments, it was not effectively accumulated into MVB upon U18666A treatment and displayed a more diffuse pattern, thus showing that the spacing of lipidatable residues may be critical for the function of the sorting signal. Nevertheless, the partition of GFP-8-TC10m into Triton-X-114 was indistinguishable from that of GFP-8-TC10, thus indicating that its lipidation was not impaired. We next explored the stability of the various chimeric proteins (Figure 6). Interestingly, both GFP-8-RhoB and GFP-8-TC10 showed reduced half-life with respect to unmodified GFP or to GFP fused to the C-terminal sequences of H-Ras or Rap2A. Thus, for the constructs herein studied, a correlation appears to exist between MVB sorting induced by treatment with U18666A and the susceptibility to undergo rapid lysosomal degradation. Therefore, the late endosome lipid environment appears to be critical for the function of the lysosomal-targeting signal. To confirm this point, we have used additional approaches. As we have previously mentioned, the lipid composition of late endosomes is profoundly altered in NPC disease (14,15). As it is shown in Figure S2A, the GFP-8-RhoB construct partially colocalized with acidic compartments in primary fibroblasts from control subjects. However, colocalization was greatly increased in fibroblasts from patients with NPC, thus showing that the distribution of the MVB-targeting construct reflects the lysosomal alterations occurring in this human genetic disease. In addition, we studied the effect of an anti-BMP antibody, which accumulates in late endosomes by endocytosis blocking BMP-dependent lipid dynamics (15). Anti-BMP induced a dilation of late endosomes, where GFP-8-RhoB could be detected both inside and at the periphery of these structures (Figure S2B). These observations confirm that the lipid environment of late endosomes is important for the function of the MVB sorting signal.

Role of basic residues in the hypervariable domains of GTPases in MVB sorting and rapid degradation

As shown above, a GFP construct bearing the last eight amino acids of TC10 (GFP-8-TC10) showed a pattern similar to that of GFP-8-RhoB, and was accumulated inside U18666A-induced compartments (Figure 5). This is in striking contrast with the fact that full-length GFP-TC10 was mainly localized at the limiting membrane of dense MVB in U18666A-treated cells (Figure 3C). This indicates that in the case of TC10, the C-terminal CINC-CLIT sequence may not be sufficient for accumulation of the protein in intraluminal vesicles of MVB. This could be because of the presence of other strong localization determinants in the TC10 molecule that prevented its intravesicular localization and degradation. Inspection of the RhoB and TC10 sequences reveals a high degree of homology (68%) with the main differences concentrating in the hypervariable domains (Figure 7A), where TC10 contains an additional cluster of basic residues 194KKH196. To probe the role of this region in TC10 localization and stability, we substituted these residues by non-charged residues. The resulting construct, GFP-TC10-NQN, clearly accumulated inside U18666A-induced structures (Figure 7B), as evidenced by a marked increase in the colocalization with LTR in U18666A-treated cells (Figure 7C), thus showing a sharp contrast with the behaviour of GFP-TC10 wt. As a proof of concept for the role of the basic residues in preventing MVB sorting, we designed the opposite experiment by introducing a cluster of basic amino acids in the equivalent position of the RhoB sequence (between aa 179 and 180). As it can be observed in Figure 7B,C, in clear contrast with GFP-RhoB wt, the mutant RhoB construct, termed GFP-RhoB-KKH, was clearly retained at the periphery of U18666A-induced MVB. Finally, we confirmed that the wild-type and chimeric proteins also showed a differential distribution in cells treated with other lysosomal inhibitors, such as chloroquine (Figure S3). Therefore, these findings suggest that the presence of basic residues in a position adjacent to the lipidation sequence trumps the activity of the isoprenylation/bipalmitoylation MVB-targeting signal.

We next assessed the stability of the wild-type and mutant RhoB and TC10 proteins. Remarkably, mutation of the polybasic cluster in TC10, as in GFP-TC10-NQN, clearly destabilized the protein (Figure 8). Conversely, the introduction of basic residues in the hypervariable region of RhoB clearly increased the stability of the resulting construct, GFP-RhoB-KKH, with respect to that of the wild-type construct. These results suggest that polybasic sequences upstream of the bipalmitoylated and isoprenylated motifs of certain GTPases, such as TC10, can

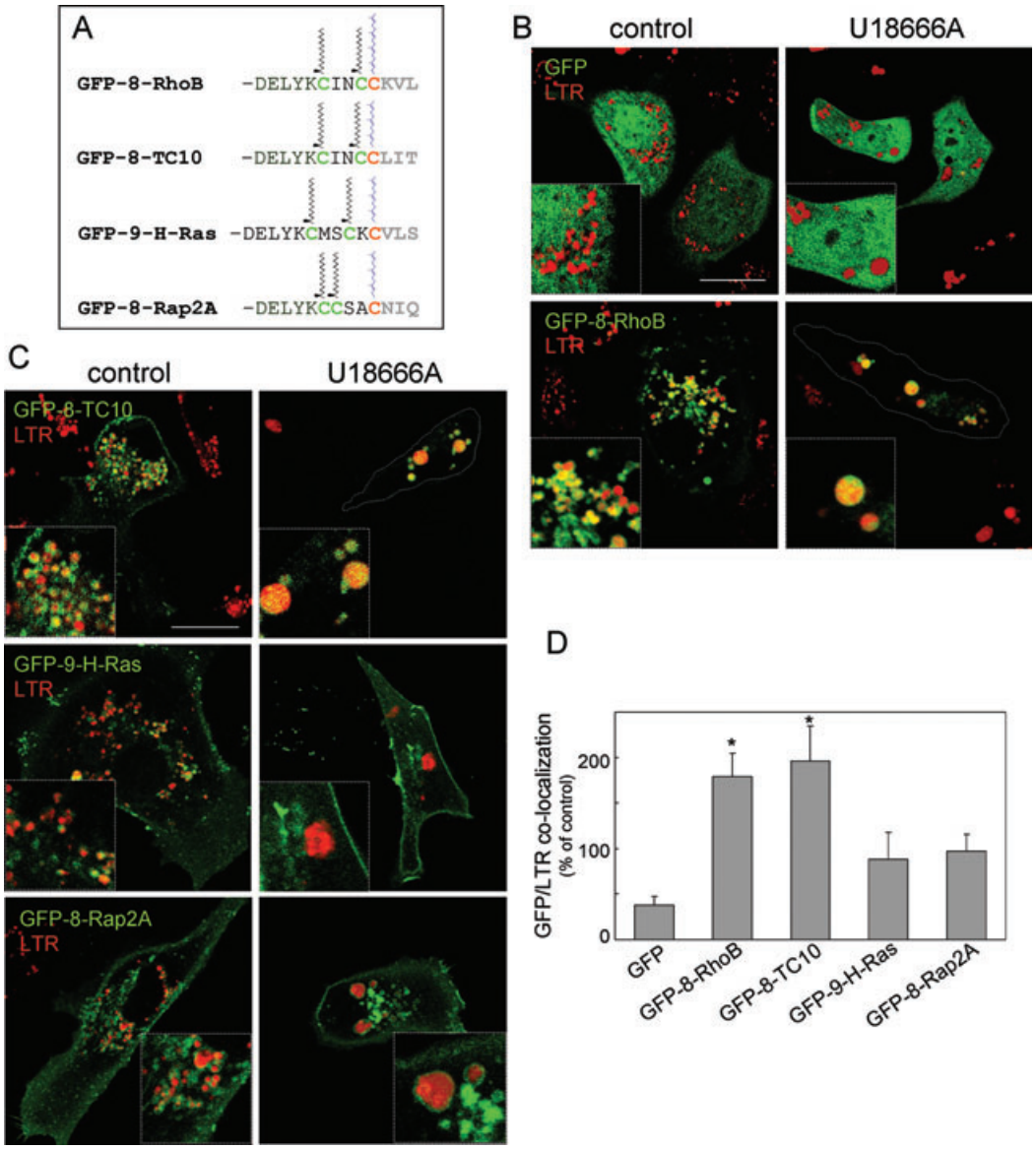

Figure 5: Effect of U18666A on the localization of chimeric proteins derived from the C-termini of isoprenylated and bipalmitoylated GTPases. A) The C-terminal sequence of the chimeric proteins constructed, consisting of GFP and the last eight amino acids of RhoB, TC10 or Rap2A or the last nine amino acids of H-Ras, is shown. Palmitoylation cysteines are shown in green, isoprenylation cysteines in orange and amino acids removed by C-terminal proteolysis in grey. B and C) BAECs transfected with the indicated constructs were treated as above. D) The extent of colocalization of GFP and LTR signals was used as an index of the internalization of the corresponding GFP constructs into acidic compartments and is shown as average values of five determinations from three independent experiments ± SEM. *$p < 0.05$ versus the same condition in the absence of U18666A by Student's *t*-test.

modulate their interaction with specific endosomal compartments, precluding their entry into the endolysosomal pathway and their targeting for degradation.

Role of basic residues in the hypervariable domains of RhoB or TC10 constructs in subcellular targeting

We next addressed the potential mechanisms by which the basic amino acid patch prevented the lysosomal-targeting signal from functioning. Stretches of basic amino acids at the hypervariable domains of other GTPases, such as K-Ras or Rac1, have been involved in their binding to negatively charged lipids at the plasma membrane (34). Therefore, we explored the presence of the various constructs at the plasma membrane. The results, shown in Figure 9A, indicate that the fraction of plasma membrane-associated protein was higher for GFP-RhoB than for GFP-TC10. The mutant constructs GFP-RhoB KKH and GFP-TC10 NQN showed an intermediate pattern with the latter showing more clear membrane association. Thus, in this case, basic residues appear not to

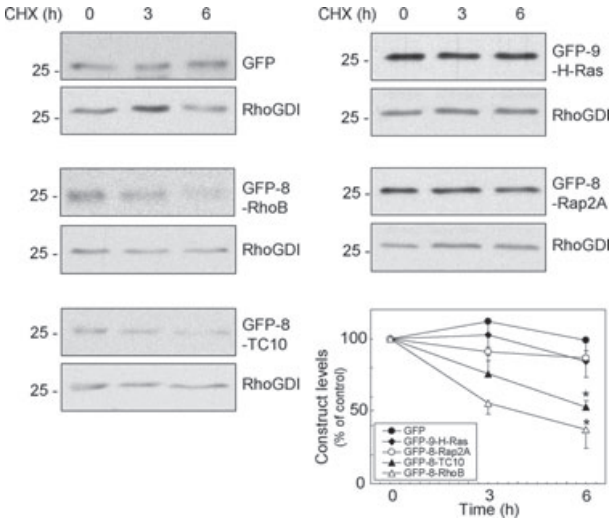

Figure 6: Stability of chimeric proteins consisting of GFP and the C-terminal sequences of isoprenylated and bipalmitoylated GTPases. BAECs were transiently transfected with the indicated constructs. Construct stability was assessed by blocking protein synthesis with CHX and estimating the remaining levels by western blot with anti-GFP antibody. Blots show the levels of the constructs of interest and of RhoGDI, as control. The graph shows the construct levels remaining after treatment with CHX for the indicated times. Results are shown as average values ± SEM of at least three different experiments. *$p < 0.05$ versus GFP by Student's *t*-test.

be sufficient to direct plasma membrane association. As TC10 is a bipalmitoylated protein, the presence of palmitate moieties could override and/or modulate the plasma membrane targeting role of basic residues.

To address this point, we explored the distribution of GFP-RhoB and GFP-TC10 in the presence of a palmitoylation inhibitor. Treatment with 2-bromopalmitate completely mislocalized RhoB leading to a diffuse cytosolic distribution, as we previously reported (7). Remarkably, inhibition of palmitoylation did not abolish plasma membrane or endomembrane association of GFP-TC10, suggesting a membrane targeting role of the basic residues present in this protein (Figure 9B). To confirm this, we studied the distribution of the GFP-RhoB-KKH and GFP-TC10-NQN mutants. Insertion of the KKH motif into GFP-RhoB resulted in endomembrane localization being more resistant to palmitoylation inhibition. Conversely, elimination of the KKH motif from GFP-TC10, as in the GFP-TC10-NQN construct, led to reduced plasma membrane binding with preserved endomembrane association upon 2-bromopalmitate treatment. Thus, these observations unveil a targeting role of basic residues: in the non-palmitoylated proteins the KKH motif may contribute to plasma membrane and/or endomembrane association, whereas in the palmitoylated proteins it may contribute to localization on specific endosomal membranes. A summary of these observations and the resulting hypothesis is depicted in Figure S4.

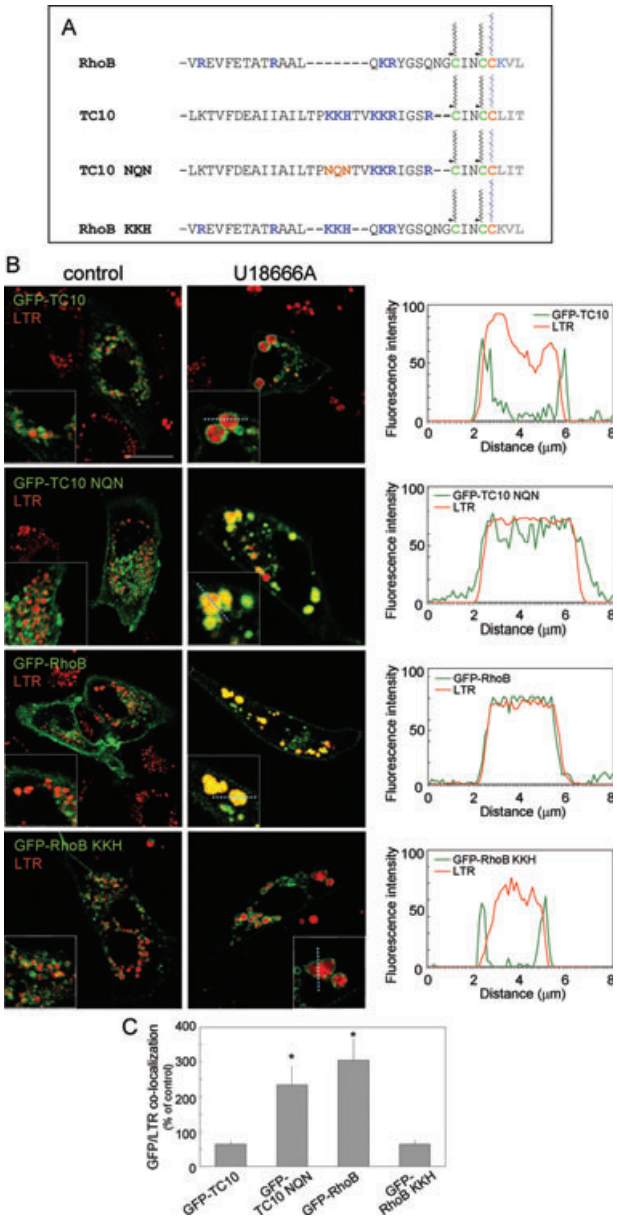

Figure 7: Role of basic residues in the hypervariable domains of TC10 and RhoB in U18666A-induced subcellular localization. A) The sequences of the hypervariable domains of RhoB, TC10 and the two constructs generated by mutating or inserting basic residues are shown. Basic amino acids are depicted in blue, palmitoylation cysteines in green and isoprenylation cysteines in orange. The non-polar residues introduced in TC10 in exchange for basic residues are shown in brown. B) BAECs transfected with the indicated constructs were treated in the absence or presence of U18666A for 24 h and incubated with 25 nM LTR before visualization by confocal microscopy. Bar, 20 m. Areas in insets are enlarged for better visualization of the lines along which fluorescence intensity profiles (left panels) have been obtained. Results are representative of four experiments with similar results. C) The extent of colocalization of GFP and LTR signals is shown. Results are average values of five determinations from three independent experiments ± SEM. *$p < 0.05$ versus the same condition in the absence of U18666A by Student's *t*-test.

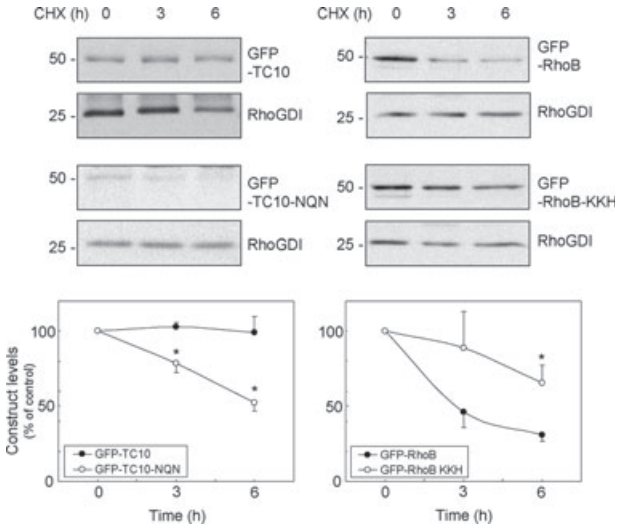

Figure 8: Role of basic residues in the hypervariable domain of GTPases in protein stability. BAECs were transfected with the indicated constructs and protein stability was assessed as described above. Graphs show the construct levels remaining after treatment with CHX for the indicated times. Results are shown as average values ± SEM of three different experiments. *$p < 0.05$ versus the same condition in the wild-type by Student's *t*-test.

Discussion

Lysosomal sorting and degradation of proteins plays an important role in cell homeostasis. The short-lived GTPase RhoB is targeted to a lysosomal pathway by its isoprenylated and bipalmitoylated C-terminal sequence. This property can be transferred to other proteins by fusion of this sequence (CINCCKVL). Small GTPases are post-translationally modified by one or two isoprenoid moieties and in some cases by palmitoylation. Here, we have studied whether other small GTPases follow a sorting and degradation pathway similar to that of RhoB. Our results show that lysosomal sorting is highly specific for RhoB. Of other sequences, only the closely related C-terminal sequence of TC10, CINCCLIT, displays a pattern similar to that of RhoB. Moreover, we have found that the presence of basic residues upstream of these lipidation sequences counteracts their effect on protein sorting and degradation.

In this work, we have used a compound blocking cholesterol dynamics, U18666A, as a tool to achieve increased membrane invagination of MVB (35). Using this compound, we have observed accumulation of RhoB inside organelles with the characteristics of dilated MVB, i.e. they are delimited by the late endosome/lysosome integral membrane protein Lamp1, are stained by the probe for acidic compartments LTR and accumulate cholesterol and the late endosome lipid BMP. The effect of U18666A appears to be highly specific of RhoB. First, none of the Rab endosomal GTPases studied, including Rab5, 7, 9 and 11, were accumulated in the intraluminal

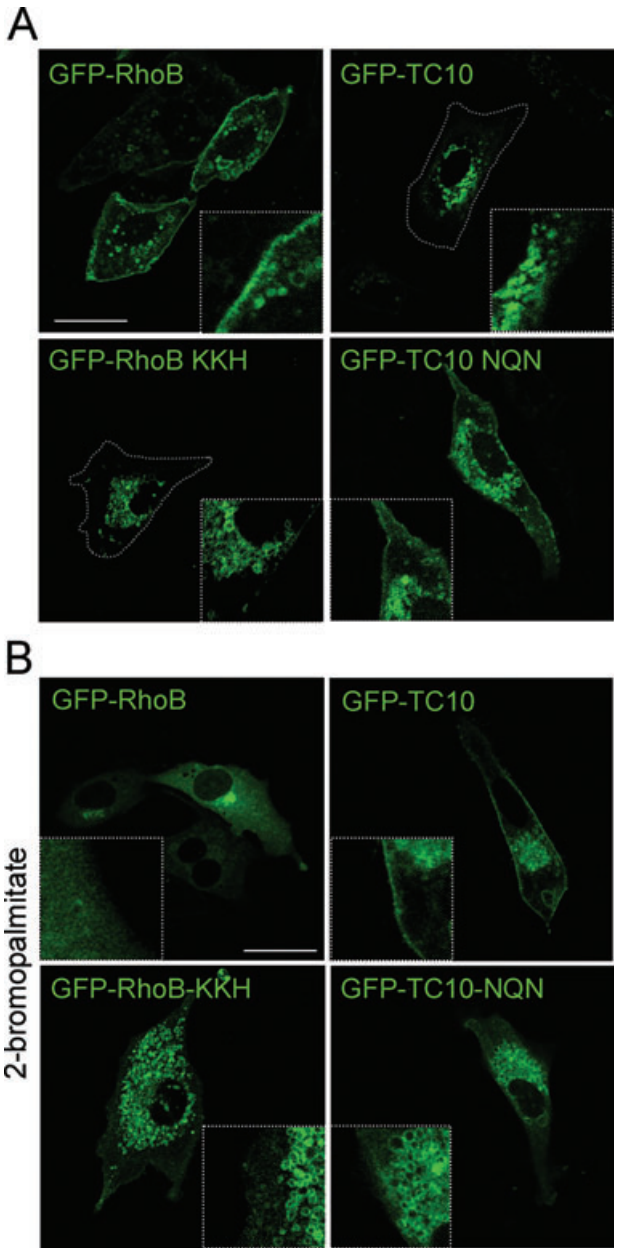

Figure 9: Role of basic residues in the hypervariable domain of endosomal GTPases in subcellular membrane targeting. A) BAECs were transfected with the indicated constructs and observed live by confocal microscopy. B) Cells were treated with 20 μM 2-bromopalmitate for 6 h before observation. Results shown are representative of at least four independent assays for every experimental condition.

space of U18666A-induced dilated MVB. Instead, Rab7 and 9 appear clearly associated at the periphery of these structures. It is interesting to note that, in NPC cells, Rab9 has been reported to be less susceptible to extraction from membranes by RhoGDI (36) and a reduced rate of dissociation of Rab7 from cholesterol-loaded endosomes has been evidenced (37). These effects could contribute to

the accumulation of Rab7 and Rab9 on U18666A-induced structures (36–38).

The specificity of RhoB internalization into MVB is also supported by the fact that other small GTPases bearing lipid moieties similar to those of RhoB, namely, one isoprenoid and two palmitate groups, including H-Ras, TC10, Rap2A and Rap2B, do not accumulate inside MVB upon U18666A treatment. Noteworthy, none of these proteins displayed the low stability typical of RhoB. These results were particularly striking in the case of TC10, because this protein is highly similar to RhoB. GFP-RhoB and GFP-TC10 showed differential endosomal localization patterns, both after U18666A and after chloroquine treatment, with the most obvious difference being the preferential presence of the construct at the limiting endosomal layer (GFP-TC10) or at the luminal space (GFP-RhoB). This suggests that in this experimental model, TC10 may occupy a more peripheral position in endosomes than RhoB.

It should be noted that although a correlation seems to exist between susceptibility to U18666A-induced accumulation into MVB of the various proteins and reduced stability, these two processes do not need to be causally related. Although access to the MVB compartment may be necessary for subsequent delivery to lysosomes, it may not be sufficient for rapid degradation. Certain MVB-sorted proteins can be recycled to the *trans* Golgi network or delivered to the plasma membrane, thus reflecting the existence of different types of luminal vesicles in MVB, of which, only a subset is targeted for lysosomal degradation (39,40). It should also be taken into account that we are employing resting cells throughout this work, thus we do not exclude the possibility that different localization and sorting patterns may arise upon cell stimulation.

The generation of short constructs containing only the isoprenylation and palmitoylation C-terminal sequences from these GTPases allowed us to confirm the contribution of these small structural motifs to protein sorting and degradation. In this case, both GFP-8-RhoB and GFP-8-TC10 displayed reduced stability, whereas the constructs bearing sequences from H-Ras and Rap2A (GFP-9-H-Ras and GFP-8-Rap2A, respectively) were more stable. The lipidation motifs from H-Ras and Rap2A differ from that of RhoB both in the spacing of the lipidated residues and in the nature of the remaining residues. Our results show that the spacing of lipidated residues is important for MVB sorting. This suggests that different positions of palmitoylatable residues within the sequence may probably result in a differential three-dimensional conformation of the lipidated C-terminus. This has been studied in detail in the case of H-Ras, for which it has been shown that residues within the lipidation motif establish specific contacts with the membrane (41). In turn, the lipidation motifs of RhoB and TC10 are highly similar. The spacing of the isoprenoid and palmitate moieties is the same. Moreover, after proteolytic removal of the three amino acids distal to the isoprenylated cysteine in the mature protein (17), the remaining sequences would be identical. Interestingly, with respect to the lipidic modifications, both RhoB and TC10 can be substrates for GGTase I and FTase *in vitro* (42), although RhoB has been shown to be preferentially geranylgeranylated in cells, whereas TC10 appears to be preferentially farnesylated (42). However, under our experimental conditions, the behaviour of GFP-8-RhoB and GFP-8-TC10 was highly similar with respect to the parameters assessed in this study, namely, susceptibility to U18666A-induced accumulation into MVB and protein stability. This may indicate that the nature of the isoprenoid lipid is not critical for lysosomal targeting and degradation. Future studies will address this issue in detail.

The fact that, whereas GFP-TC10 is stable in our assay, GFP-8-TC10 shows reduced stability highlights the importance of other regions of TC10 in avoiding lysosomal sorting and degradation. Given the high homology between RhoB and TC10, we delimited the regions bearing the most important differences to those comprised between amino acids 137 and 142 and between 192 and 198 of human TC10, the last one including several basic amino acids. Previous studies addressing the role of the stretches of basic amino acids located in the hypervariable domain of TC10 did not find a significant effect in TC10 localization and trafficking (25). However, a role for this region in protein stability had not been assessed previously. Our results show that these basic residues of TC10 play key roles in positioning the protein away from the intraluminal space of MVB and in protein stability. To assess the specific role of the basic residues, we have employed a palmitoylation inhibitor. Our results show that the fully processed TC10 protein preferentially binds to endomembranes. However, inhibition of palmitoylation unveils the capability of basic residues in TC10 hypervariable domain to preserve plasma membrane binding. The observation that plasma membrane association is clearly reduced in the GFP-TC10-NQN mutant indicates that basic residues in TC10 may be involved in electrostatic interactions with negatively charged lipids at the plasma membrane. Conversely, although introducing basic residues into RhoB does not appear to be sufficient to promote localization of the non-palmitoylated protein at the plasma membrane, it supports association with endomembranes, in clear contrast with RhoB wt, which is completely diffuse in 2-bromopalmitate-treated cells. The different extent of plasma membrane association of GFP-TC10 and GFP-RhoB-KKH upon inhibition of palmitoylation may be related to the different number and/or distribution of basic amino acids in the C-terminus of these proteins (Figures 7A and S4), as previously suggested (43). Ionomycin has been previously used to disrupt the electrostatic interaction of polybasic motif-bearing proteins with the plasma membrane by promoting Ca^{2+} entry, which masks negatively charged phospholipids in the inner leaflet of the plasma membrane (43). We have observed that ionomycin did not disrupt plasma membrane association of fully processed RhoB. Interestingly, ionomycin compromised the association of non-palmitoylated GFP-TC10 with the plasma

membrane (Valero et al., unpublished observations). This supports the involvement of the basic patch of TC10 in electrostatic interactions with negatively charged lipids, thus acting as a complementary targeting signal.

As palmitoylation is a reversible modification, taken together our results suggest that there may be an interplay between palmitoylation and electrostatic interactions in modulating protein localization. The presence of phosphatidylserine and other anionic lipids has been detected at the cytosolic side of both plasma membrane and endosomes (34,44,45). In the light of our findings, a hypothetical model could be proposed (Figure S4), by which basic amino acids in the hypervariable region of TC10 would enhance its interaction with the cytosolic side of endosomes, thereby preventing its sorting into MVB, directed otherwise, as in the case of RhoB, by a specific distribution of palmitoyl and isoprenoid moieties in resting cells.

Therefore, our observations contribute to the understanding of the role of hypervariable regions of small GTPases in specific subcellular localization. In the case of H-Ras, an isoprenylated and bipalmitoylated protein, basic residues in the hypervariable domain stabilize membrane binding and constitute a switch for the orientation of the protein and the interaction with effectors (46). In the case of RhoB, the hypervariable region has been involved in interactions with the microtubule-associated protein MAP1A, which are dependent on RhoB-GTP binding and affect EGF signalling (47). Residues in the hypervariable domain of other Rho proteins have been involved in modulation of protein degradation. In particular, phosphorylation of Ser188 in RhoA appears both to negatively regulate protein activity and protect it from proteasome-mediated degradation by enhancing its association with RhoGDI (48,49). A potential interaction with RhoGDI, in this case, secondary to RhoA silencing, has also been proposed as a mechanism for RhoB stabilization (50), although the physiological role of this effect remains to be elucidated.

Taken together, our results show that the absence of polybasic sequences in the hypervariable region of RhoB allows its delivery into the luminal space of MVB and its rapid lysosomal degradation. These results identify an important structural determinant influencing MVB sorting and degradation of endosome-associated GTPases. Moreover, they allow formulating the hypothesis that protein or lipid interactions involving the hypervariable domain of RhoB could influence its sorting and stability.

Materials and Methods

Reagents and antibodies

U18666A was from Merck4Biosciences (Spain). RPMI-1640 and bovine serum were from Invitrogen (GIBCO). Filipin, ionomycin and CHX were from Sigma. LTR was from Molecular Probes (Invitrogen). Anti-RhoB (sc-180) and anti-RhoGDI (sc-360) were from Santa Cruz Biotechnology. Anti-LBPA (BMP) was from Echelon Biosciences Inc. Anti-GFP was from Clontech.

Cell culture and treatments

Bovine aortic endothelial cells (BAECs) were obtained and cultured as previously described (7,31). Human primary fibroblasts from apparently healthy subjects and NPC disease patients were from Coriell Institute for Medical Research and were cultured according to their instructions. For treatments, cells were cultured in the absence of serum.

Plasmids and transfections

The tagRFP plasmid encoding a monomeric red fluorescent protein was from Evrogen. An S162T mutation was introduced in the tagRFP coding sequence using the Quickchange II kit and oligonucleotide 5′-GCCTGGAAGGCAGAACCGACATGGCCCTGAAG-3′ and its complementary oligonucleotide to generate tagRFP-T, which displays improved photostability (51). A plasmid for the expression of HA-RhoB was generously donated by Dr G. C. Prendergast. From this, a GFP-HA-RhoB plasmid was generated as previously described (31). tRFP-T-HA-RhoB was generated by cloning HA-RhoB into the *Bgl*II/*Eco*RI sites of tRFP-T. Lamp1-GFP was provided by Professor Jennifer Lippincott-Schwartz (NIH). GFP-Rab7 was kindly provided by Professor Cecilia Bucci (University of Copenhagen). GFP-Rab5 was generously provided by Professor Juan S. Bonifacino (NIH). GFP-Rab9A, GFP-Rap2A and GFP-Rap2B were from Genecopoeia. GFP-H-Ras was provided by Dr José María Rojas (ISCIII). A plasmid coding for human TC10 with an N-terminal haemagglutinin (HA) tag was used as template for amplification by polymerase chain reaction (PCR) with primers containing *Sac*I and *Eco*RI sites, respectively (sense: 5′-CCGAGCTCAAATGGGCTACCCCTATGATGTGCC-3′; antisense: 5′-CCGAATTCTCACGTAATTAAACAACAGTTTATAC-3′), for cloning of the PCR product into the same sites of pEGFP-C1 to generate GFP-HA-TC10. Constructs encoding chimeric proteins comprising GFP and the isoprenylation and palmitoylation sequences from the C-terminus of RhoB, TC10, H-Ras and Rap2A, were generated by PCR using pEGFP-C1 as a template. The forward primer was common for all constructs: 5′-GAGTAGAAGCTTATGGTGAGCAAGGGCGAGGAG-3′. Reverse primers were 5′-CCGAATTCTAGAGGACCTTGCAACAGTTGATACACTTGTACAGC TCGTCCATGC-3′ for generating GFP-CINCCKVL (GFP-8-RhoB); 5′-CC GAATTCTCACGTAATTAAACAACAGTTGATACACTTGTACAGCTCGTCCAT GC-3′ for GFP-CINCCLIT (GFP-8-TC10); 5′-CCGAATTCTCACGTAATTAA ACAGTTGATACAACACTTGTACAGCTCGTCCATGC-3′ for GFP-CCINCLIT (GFP-8-TC10m); 5′-CCGAATTCTACGACAACACGCATTTGCATGACATGCA CTTGTACAGCTCGTCCATGC-3′ for GFP-CMSCKCVLS (GFP-9-H-Ras) and 5′-CCGAATTCTACTGGATGTTGCAGGCGCTACAGCACTTGTACAGCTCGT CCATGC-3′ for GFP-CCSACNIQ (GFP-8-Rap2A). PCR products were digested with *Hind*III and *Eco*RI and cloned into pcDNA3.0. The triple mutant of GFP-HA-TC10 (K194N, K195Q, H196N; GFP-TC10-NQN) was prepared by using the Stratagene Quickchange kit with the oligonucleotide 5′-GGCTATCATAGCCATTTTAACTCCAAACCAAAACACTGTAAAAAAAAG AATAGG-3′ and its complementary reverse, following the instructions of the manufacturer. The triple mutant of GFP-HA-RhoB (insertion of KKH after L179, GFP-RhoB-KKH) was generated by annealing synthetic sense 5′-CAAGCGCGCCGCGCTGAAGAAACACCAGAAGCGCTACGGATCCCAG AATGGCTGCATCAACTGCTGCAAGGTGCTATGAGAATTCAAC-3′ and antisense oligonucleotides containing three inserted triplets, digesting with *Bss*HII and *Eco*RI and cloning the product into the same sites of the GFP-HA-RhoB plasmid. All constructs were confirmed by sequencing. For transfections, confluent cells in p35 plates were incubated with 1 g of DNA construct and 3 L of Lipofectamine 2000 (Invitrogen), according to the instructions of the manufacturer. Twenty-four hours after transfection, cells were treated with the various agents as indicated above.

Assessment of protein stability

Protein stability was estimated from the decay of the levels of the protein of interest in cells treated with a non-toxic concentration of CHX, as previously described (7,31). SDS–PAGE and western blot analysis were performed as described (7,31) using enhanced chemiluminiscence (ECL) detection (Amersham). Protein levels were estimated by image scanning of the ECL exposures and corrected by the signal given by an antibody

against RhoGDI, a protein the levels of which do not change under the experimental conditions used throughout the manuscript.

Confocal microscopy

For confocal microscopy of live cells, BAECs were cultured on glass bottom dishes (Mattek Corp.), transfected with fluorescent constructs, treated with the indicated agents and visualized directly on a confocal microscope (LEICA DMRE2). For immunofluorescence with anti-LBPA/BMP antibody, cells were fixed with 4% paraformaldehyde, incubated in the presence of 0.27% NH_4Cl, 0.38% glycine for 10 min and permeabilized with 0.05% saponin in PBS in the presence of anti-LBPA at 1:50 dilution. After washing with PBS, cells were incubated with anti-mouse Alexa 647 (Invitrogen) at 1:250 in 10% normal goat serum in PBS. For filipin staining, fixed cells were washed 3× with PBS, incubated with 1.5 mg/mL glycine in PBS for 10 min at room temperature and subsequently with 0.05 mg/mL filipin in 10% normal goat serum in PBS for 2 h. Unless otherwise stated, images shown are single Z-section images for colocalization assessment. All experiments were repeated at least 3× and representative results are shown.

Quantification and statistics

The degree of colocalization of the different constructs with LTR was analysed with software from Leica and Scion Corporation for image analysis. Results are presented as average values ± SD or SEM, as indicated. Average values were compared by Student's *t*-test for unpaired observations.

Acknowledgments

We are indebted to O. Hidalgo and M. T. Seisdedos (CIB, CSIC) for expert assistance with confocal microscopy. This work was supported by grants from MiCInn SAF2009-11642 and SAF2009-08086 and by RETICS RIRAAF from ISCIII, RD07/0064/0007 and PIE201020E031 from CSIC. C. L. O. has been supported by a JAE Intro fellowship from CSIC.

Supporting Information

Additional Supporting Information may be found in the online version of this article:

Figure S1: Effect of U18666A on the localization of a chimeric protein derived from the C-terminus of TC10 in which the spacing between palmitoylation cysteines has been altered. A) The C-terminal sequence of the chimeric protein GFP-8-TC10m is shown in comparison with that derived from wild-type TC10 (GFP-8-TC10). B) Cells transfected with the constructs indicated were treated in the absence or presence of U18666A for 24 h and incubated with 25 nM LTR before visualization by confocal microscopy. Bar, 20 m. C) BAECs were transfected with the indicated constructs and lysed in buffer containing 1% Triton-X-114. Partition of the constructs into the aqueous (a) and detergent (d) phases was performed as previously described (23) and their levels in each phase were assessed by western blot with anti-GFP antibody. Results are average values of two determinations and are presented as percentage of the total. The soluble protein RhoGDI is shown as a control. Blots shown are representative of two experiments performed in duplicate.

Figure S2: Effect of alteration of the lipid environment of late endosomes on the localization of the chimeric protein GFP-8-RhoB. A) Localization of GFP-8-RhoB in NPC disease cells. Human fibroblasts from healthy subjects (control) or NPC disease patients were transfected with GFP-8-RhoB. After 24 h in serum-free medium, the distribution of GFP-8 and LTR was visualized by confocal microscopy in live cells. The extent of colocalization of GFP and LTR signals in the two cell types is shown in the lower panel. Results are average values of five determinations from three independent experiments ± SEM, *$p < 0.05$ versus control cells by Student's *t*-test. B) Effect of anti-BMP antibodies on the localization of GFP-8-RhoB. BAECs were transfected with GFP-8-RhoB and incubated with anti-BMP or control antibody (hybridoma supernatant diluted 1:1 in culture medium) for 24 h before visualization by confocal microscopy. In the right panel, single fluorescence channels and overlay images of the inset are shown. Results are representative of three assays with similar results.

Figure S3: Role of basic residues in the hypervariable domains of TC10 and RhoB in subcellular localization in chloroquine-treated cells. BAECs transfected with the indicated constructs were treated in the absence or presence of 10 M chloroquine for 24 h and incubated with 25 nM LTR before visualization by confocal microscopy. Bar, 20 m. Shown are the single fluorescence channels and overlay sections. DIC images are shown in the right panels. Results are representative of four experiments with similar results.

Figure S4: Hypothetical model summarizing the subcellular localization, observed in this study, of the various GTPases and their mutants. In resting control cells, GFP-RhoB localizes to plasma membrane and endosomes whereas GFP-TC10 localizes mainly to endosomes. The GFP-RhoB KKH mutant shows a lower extent of plasma membrane binding than GFP-RhoB. The GFP-TC10 NQN mutant shows a higher extent of plasma membrane binding than TC10. GFP-RhoB and GFP-TC10 NQN are sorted into MVB, and accumulate in this compartment in U18666A-treated cells, whereas GFP-TC10 and GFP-RhoB KKH are retained at the limiting membrane of these structures. Upon inhibition of palmitoylation, GFP-RhoB becomes diffuse and cytosolic, whereas GFP-TC10 is clearly detected at the plasma membrane and on endosomes. The constructs GFP-RhoB KKH and GFP-TC10 NQN do not localize significantly to the plasma membrane in 2-bromopalmitate-treated cells, but retain their localization at endosomes. Therefore, mutation of the basic patch in TC10 reduces plasma membrane association in 2-bromopalmitate-treated cells. Plasma membrane association of non-palmitoylated GFP-TC10 but not of fully processed GFP-RhoB is sensitive to ionomycin treatment. Taken together, these observations suggest the existence of electrostatic interactions between the basic residues in the hypervariable domains of the various constructs (shown in blue) and the negatively charged lipids (represented by lipids with red 'heads') at the different membrane compartments. These interactions would favour the distribution of GTPases bearing basic hypervariable domains at the cytosolic side of late endosomes, whereas GTPases with less polar hypervariable domains would reach MVB intraluminal space in a higher proportion.

Please note: Wiley-Blackwell are not responsible for the content or functionality of any supporting materials supplied by the authors. Any queries (other than missing material) should be directed to the corresponding author for the article.

References

1. Jabbour M, Campbell EM, Fares H, Lybarger L. Discrete domains of MARCH1 mediate its localization, functional interactions, and post-transcriptional control of expression. J Immunol 2009;183:6500–6512.
2. Ikeda H, Kerppola TK. Lysosomal localization of ubiquitinated Jun requires multiple determinants in a lysine-27-linked polyubiquitin conjugate. Mol Biol Cell 2008;19:4588–4601.
3. Li L, Soetandyo N, Wang Q, Ye Y. The zinc finger protein A20 targets TRAF2 to the lysosomes for degradation. Biochim Biophys Acta 2009;1793:346–353.
4. Mizushima N, Levine B, Cuervo AM, Klionsky DJ. Autophagy fights disease through cellular self-digestion. Nature 2008;451:1069–1075.
5. Cuervo AM, Dice JF. A receptor for the selective uptake and degradation of proteins by lysosomes. Science 1996;273:501–503.
6. Lu A, Tebar F, Alvarez-Moya B, Lopez-Alcala C, Calvo M, Enrich C, Agell N, Nakamura T, Matsuda M, Bachs O. A clathrin-dependent pathway leads to KRas signaling on late endosomes en route to lysosomes. J Cell Biol 2009;184:863–879.
7. Pérez-Sala D, Boya P, Ramos I, Herrera M, Stamatakis K. The C-terminal sequence of RhoB directs protein degradation through an endo-lysosomal pathway. PLoS ONE 2009;4:e8117.
8. Sandilands E, Cans C, Fincham VJ, Brunton VG, Mellor H, Prendergast GC, Norman JC, Superti-Furga G, Frame MC. RhoB and actin polymerization coordinate Src activation with endosome-mediated delivery to the membrane. Dev Cell 2004;7:855–869.

9. Liu AX, Rane N, Liu JP, Prendergast GC. RhoB is dispensable for mouse development, but it modifies susceptibility to tumor formation as well as cell adhesion and growth factor signaling in transformed cells. Mol Cell Biol 2001;21:6906–6912.
10. Falguieres T, Luyet PP, Gruenberg J. Molecular assemblies and membrane domains in multivesicular endosome dynamics. Exp Cell Res 2009;315:1567–1573.
11. Kolter T, Sandhoff K. Principles of lysosomal membrane digestion: stimulation of sphingolipid degradation by sphingolipid activator proteins and anionic lysosomal lipids. Annu Rev Cell Dev Biol 2005; 21:81–103.
12. Matsuo H, Chevallier J, Mayran N, Le Blanc I, Ferguson C, Faure J, Blanc NS, Matile S, Dubochet J, Sadoul R, Parton RG, Vilbois F, Gruenberg J. Role of LBPA and Alix in multivesicular liposome formation and endosome organization. Science 2004;303:531–534.
13. Mukherjee S, Maxfield FR. Lipid and cholesterol trafficking in NPC. Biochim Biophys Acta 2004;1685:28–37.
14. Carstea ED, Morris JA, Coleman KG, Loftus SK, Zhang D, Cummings C, Gu J, Rosenfeld MA, Pavan WJ, Krizman DB, Nagle J, Polymeropoulos MH, Sturley SL, Ioannou YA, Higgins ME et al. Niemann-Pick C1 disease gene: homology to mediators of cholesterol homeostasis. Science 1997;277:228–231.
15. Kobayashi T, Beuchat MH, Lindsay M, Frias S, Palmiter RD, Sakuraba H, Parton RG, Gruenberg J. Late endosomal membranes rich in lysobisphosphatidic acid regulate cholesterol transport. Nat Cell Biol 1999;1:113–118.
16. Sobo K, Le Blanc I, Luyet PP, Fivaz M, Ferguson C, Parton RG, Gruenberg J, van der Goot FG. Late endosomal cholesterol accumulation leads to impaired intra-endosomal trafficking. PLoS ONE 2007;2: e851.
17. Pérez-Sala D. Protein isoprenylation in biology and disease: general overview and perspectives from studies with genetically engineered animals. Front Biosci 2007;12:4456–4472.
18. Leung KF, Baron R, Seabra MC. Thematic review series: lipid posttranslational modifications. Geranylgeranylation of Rab GTPases. J Lipid Res 2006;47:467–475.
19. Wang DA, Sebti SM. Palmitoylated cysteine 192 is required for RhoB tumor-suppressive and apoptotic activities. J Biol Chem 2005; 280:19243–19249.
20. Michaelson D, Silletti J, Murphy G, D'Eustachio P, Rush M, Philips MR. Differential localization of Rho GTPases in live cells: regulation by hypervariable regions and RhoGDI binding. J Cell Biol 2001; 152:111–126.
21. Uechi Y, Bayarjargal M, Umikawa M, Oshiro M, Takei K, Yamashiro Y, Asato T, Endo S, Misaki R, Taguchi T, Kariya K. Rap2 function requires palmitoylation and recycling endosome localization. Biochem Biophys Res Commun 2009;378:732–737.
22. Hancock JF, Parton RG. Ras plasma membrane signalling platforms. Biochem J 2005;389:1–11.
23. Gomez GA, Daniotti JL. H-Ras dynamically interacts with recycling endosomes in CHO-K1 cells: involvement of Rab5 and Rab11 in the trafficking of H-Ras to this pericentriolar endocytic compartment. J Biol Chem 2005;280:34997–35010.
24. Rotblat B, Yizhar O, Haklai R, Ashery U, Kloog Y. Ras and its signals diffuse through the cell on randomly moving nanoparticles. Cancer Res 2006;66:1974–1981.
25. Watson RT, Furukawa M, Chiang SH, Boeglin D, Kanzaki M, Saltiel AR, Pessin JE. The exocytotic trafficking of TC10 occurs through both classical and nonclassical secretory transport pathways in 3T3L1 adipocytes. Mol Cell Biol 2003;23:961–974.
26. Mollinedo F, Pérez-Sala D, Gajate C, Jiménez B, Rodríguez P, Lacal JC. Localization of rap1 and rap2 proteins in the gelatinase-containing granules of human neutrophils. FEBS Lett 1993;326:209–214.
27. Bucci C, Parton RG, Mather IH, Stunnenberg H, Simons K, Hoflack B, Zerial M. The small GTPase rab5 functions as a regulatory factor in the early endocytic pathway. Cell 1992;70:715–728.
28. Bucci C, Thomsen P, Nicoziani P, McCarthy J, van Deurs B. Rab7: a key to lysosome biogenesis. Mol Biol Cell 2000;11:467–480.
29. Ganley IG, Carroll K, Bittova L, Pfeffer S. Rab9 GTPase regulates late endosome size and requires effector interaction for its stability. Mol Biol Cell 2004;15:5420–5430.
30. Ullrich O, Reinsch S, Urbe S, Zerial M, Parton RG. Rab11 regulates recycling through the pericentriolar recycling endosome. J Cell Biol 1996;135:913–924.
31. Stamatakis K, Cernuda-Morollón E, Hernández-Perera O, Pérez-Sala D. Isoprenylation of RhoB is required for its degradation: a novel determinant in the complex regulation of RhoB expression by the mevalonate pathway. J Biol Chem 2002;277:49389–49396.
32. Haklai R, Weisz MG, Elad G, Paz A, Marciano D, Egozi Y, Ben-Baruch G, Kloog Y. Dislodgment and accelerated degradation of Ras. Biochemistry 1998;37:1306–1314.
33. Kim SE, Yoon JY, Jeong WJ, Jeon SH, Park Y, Yoon JB, Park YN, Kim H, Choi KY. H-Ras is degraded by Wnt/beta-catenin signaling via beta-TrCP-mediated polyubiquitylation. J Cell Sci 2009;122: 842–848.
34. Yeung T, Gilbert GE, Shi J, Silvius J, Kapus A, Grinstein S. Membrane phosphatidylserine regulates surface charge and protein localization. Science 2008;319:210–213.
35. Marchetti A, Mercanti V, Cornillon S, Alibaud L, Charette SJ, Cosson P. Formation of multivesicular endosomes in Dictyostelium. J Cell Sci 2004;117:6053–6059.
36. Ganley IG, Pfeffer SR. Cholesterol accumulation sequesters Rab9 and disrupts late endosome function in NPC1-deficient cells. J Biol Chem 2006;281:17890–17899.
37. Huynh KK, Gershenzon E, Grinstein S. Cholesterol accumulation by macrophages impairs phagosome maturation. J Biol Chem 2008;283:35745–35755.
38. Lebrand C, Corti M, Goodson H, Cosson P, Cavalli V, Mayran N, Faure J, Gruenberg J. Late endosome motility depends on lipids via the small GTPase Rab7. EMBO J 2002;21:1289–1300.
39. Bishop NE. Dynamics of endosomal sorting. Int Rev Cytol 2003; 232:1–57.
40. Piper RC, Katzmann DJ. Biogenesis and function of multivesicular bodies. Annu Rev Cell Dev Biol 2007;23:519–547.
41. Gorfe AA, Babakhani A, McCammon JA. H-ras protein in a bilayer: interaction and structure perturbation. J Am Chem Soc 2007; 129:12280–12286.
42. Roberts PJ, Mitin N, Keller PJ, Chenette EJ, Madigan JP, Currin RO, Cox AD, Wilson O, Kirschmeier P, Der CJ. Rho family GTPase modification and dependence on CAAX motif-signaled posttranslational modification. J Biol Chem 2008;283:25150–25163.
43. Yeung T, Terebiznik M, Yu L, Silvius J, Abidi WM, Philips M, Levine T, Kapus A, Grinstein S. Receptor activation alters inner surface potential during phagocytosis. Science 2006;313:347–351.
44. Urade R, Hayashi Y, Kito M. Endosomes differ from plasma membranes in the phospholipid molecular species composition. Biochim Biophys Acta 1988;946:151–163.
45. Leventis PA, Grinstein S. The distribution and function of phosphatidylserine in cellular membranes. Annu Rev Biophys 2010;39: 407–427.
46. Abankwa D, Hanzal-Bayer M, Ariotti N, Plowman SJ, Gorfe AA, Parton RG, McCammon JA, Hancock JF. A novel switch region regulates H-ras membrane orientation and signal output. EMBO J 2008;27:727–735.
47. Lajoie-Mazenc I, Tovar D, Penary M, Lortal B, Allart S, Favard C, Brihoum M, Pradines A, Favre G. MAP1A light chain-2 interacts with GTP-RhoB to control epidermal growth factor (EGF)-dependent EGF receptor signaling. J Biol Chem 2008;283:4155–4164.
48. Ellerbroek SM, Wennerberg K, Burridge K. Serine phosphorylation negatively regulates RhoA in vivo. J Biol Chem 2003;278: 19023–19031.
49. Rolli-Derkinderen M, Sauzeau V, Boyer L, Lemichez E, Baron C, Henrion D, Loirand G, Pacaud P. Phosphorylation of serine 188 protects RhoA from ubiquitin/proteasome-mediated degradation in vascular smooth muscle cells. Circ Res 2005;96:1152–1160.
50. Ho T, Merajver S, Lapière C, Nusgens B, Deroanne C. RhoA-GDP regulates RhoB protein stability. Potential involvement of RhoGDI alpha. J Biol Chem 2008;283:21588–21598.
51. Shaner NC, Lin MZ, McKeown MR, Steinbach PA, Hazelwood KL, Davidson MW, Tsien RY. Improving the photostability of bright monomeric orange and red fluorescent proteins. Nat Methods 2008;5:545–551.

OPEN ACCESS Freely available online

PLOS ONE

An Isoprenylation and Palmitoylation Motif Promotes Intraluminal Vesicle Delivery of Proteins in Cells from Distant Species

Clara L. Oeste[1], Mario Pinar[2], Kay O. Schink[3], Javier Martínez-Turrión[1], Harald Stenmark[3], Miguel A. Peñalva[2], Dolores Pérez-Sala[1]*

1 Department of Chemical and Physical Biology, Centro de Investigaciones Biológicas, Consejo Superior de Investigaciones Científicas, Madrid, Spain, **2** Department of Cellular and Molecular Biology, Centro de Investigaciones Biológicas, Consejo Superior de Investigaciones Científicas, Madrid, Spain, **3** Centre for Cancer Biomedicine, Faculty of Medicine, Oslo University Hospital, Oslo, Norway

Abstract

The C-terminal ends of small GTPases contain hypervariable sequences which may be posttranslationally modified by defined lipid moieties. The diverse structural motifs generated direct proteins towards specific cellular membranes or organelles. However, knowledge on the factors that determine these selective associations is limited. Here we show, using advanced microscopy, that the isoprenylation and palmitoylation motif of human RhoB (–CINCCKVL) targets chimeric proteins to intraluminal vesicles of endolysosomes in human cells, displaying preferential co-localization with components of the late endocytic pathway. Moreover, this distribution is conserved in distant species, including cells from amphibians, insects and fungi. Blocking lipidic modifications results in accumulation of CINCCKVL chimeras in the cytosol, from where they can reach endolysosomes upon release of this block. Remarkably, CINCCKVL constructs are sorted to intraluminal vesicles in a cholesterol-dependent process. In the lower species, neither the C-terminal sequence of RhoB, nor the endosomal distribution of its homologs are conserved; in spite of this, CINCCKVL constructs also reach endolysosomes in *Xenopus laevis* and insect cells. Strikingly, this behavior is prominent in the filamentous ascomycete fungus *Aspergillus nidulans*, in which GFP-CINCCKVL is sorted into endosomes and vacuoles in a lipidation-dependent manner and allows monitoring endosomal movement in live fungi. In summary, the isoprenylated and palmitoylated CINCCKVL sequence constitutes a specific structure which delineates an endolysosomal sorting strategy operative in phylogenetically diverse organisms.

Citation: Oeste CL, Pinar M, Schink KO, Martínez-Turrión J, Stenmark H, et al. (2014) An Isoprenylation and Palmitoylation Motif Promotes Intraluminal Vesicle Delivery of Proteins in Cells from Distant Species. PLoS ONE 9(9): e107190. doi:10.1371/journal.pone.0107190

Editor: Julie G. Donaldson, NHLBI, NIH, United States of America

Received May 20, 2014; **Accepted** August 7, 2014; **Published** September 10, 2014

Data Availability: The authors confirm that all data underlying the findings are fully available without restriction. All relevant data are within the paper and its Supporting Information files.

Funding: This work was supported by grants SAF2009-11642 and SAF2012-36519 from MINECO and RETIC RD12/0013/0008 to DPS, grants BIO2012-30695 from MINECO and S2010/BMD-2414 from Comunidad de Madrid to MAP, and grants from the Norwegian Cancer Society and the South-Eastern Norway Regional Health Authority to HS. CLO is supported by the FPI program from MINECO (BES-2010-033718). The stay of CLO at HS laboratory was supported by the short stay grant EEBB-I-12-04482 from MINECO. J. Martínez Turrión has been the recipient of a JAE Intro Fellowship from CSIC. The funders had no role in study design, data collection and analysis, decision to publish, or preparation of the manuscript.

Competing Interests: The authors have declared that no competing interests exist.

* Email: dperezsala@cib.csic.es

Introduction

Regulation of vesicular traffic is a key process for many cellular functions. Signal transduction by membrane receptors, protein delivery to specific compartments, membrane repair and exosome shedding or autophagy, among others, depend on compartmentalized traffic of molecules within the cell. Intracellular vesicles constitute a yet not fully characterized array of dynamic membranous compartments which are in continuous evolution and transformation, resulting in the acquisition of a specific protein and lipid composition [1,2]. These components can regulate the fate of proteins by sorting them through different types of intracellular vesicles that can come from or recycle back to the plasma membrane, send proteins along the secretory pathway from the Golgi or travel along trafficking routes through the late endosomal pathway to the lysosome to be degraded, among many other processes.

The endolysosomal pathway is subjected to a complex regulation by families of proteins or multiprotein structures which act in a concerted manner. Indeed, small GTPases of the Rab family play a fundamental role in endosome biogenesis and traffic, and undergo the so-called "Rab conversion", in which Rab5 from early endosomes is substituted by Rab7 at late endosomes, thus allowing progression of endosome maturation [3]. Incorporation of cytosolic proteins into this pathway is believed to occur through various mechanisms by recognizing target sequences or modifications that ultimately may trigger association with or internalization into endolysosomal vesicles. The endosomal sorting complexes required for transport (ESCRTs) constitute a well-established system of protein "machines" that work sequentially to induce the endosomal delivery of target proteins. Particular components of

ESCRTs recognize ubiquitinated proteins, induce membrane invagination and promote formation of multivesicular bodies (MVB), into which proteins are sorted [4]. Other means of lysosomal sorting include modification of e.g. soluble acid hydrolases with mannose 6-phosphate (M6P) and recognition by M6P receptors in the Golgi apparatus prior to endo-lysosomal trafficking, or M6P-independent sorting by association with proteins such as sortilin or LIMP-2 [5,6]. In the case of lysosomal transmembrane proteins, specific motifs such as dileucine or tyrosine-containing sequences can interact with clathrin-associated proteins and trigger lysosomal localization [7]. Furthermore, modifications such as phosphorylation and acylation of proteins at particular residues can also serve as vesicle-specific membrane anchors for peripheral membrane proteins [8].

One of several types of acylation, thioesterification of a palmitate molecule (C16:0) occurs at specific cysteine residues in a reversible manner and allows proteins to cycle between different subcellular localizations. In particular, palmitoylation is important for the sorting and localization of numerous integral membrane proteins such as the M6P receptor, tetraspanins (e.g. CD9, CD63 or CD81) or synaptotagmins [9–11]. Small GTPases of the Ras superfamily are isoprenylated at their C-termini. For several members of this family, including H-Ras, RhoB or TC10, isoprenylation is required for the subsequent palmitoylation of nearby cysteines, which allows their association with the plasma membrane or specific endolysosomal vesicles [12–15]. Thus, certain protein sequences, as well as specific types of protein posttranslational modifications play a key role in targeting proteins to membranes with subtle differences in protein and/or lipid composition.

The C-terminal sequence of RhoB (CINCCKVL) is palmitoylated and isoprenylated, and these modifications are required for its localization at the endolysosomal pathway [16]. Moreover, we have previously shown that this sequence directs the rapid lysosomal degradation of chimeric proteins in bovine aortic endothelial cells (BAEC) [16]. Here we have fused the CINCCKVL sequence (or "–8") to fluorescent proteins to explore its potential to promote endolysosomal localization in cells from different species. From our studies, CINCCKVL chimeras step forth as tunable targeting sequences which depend on posttranslational lipid modifications that can be regulated pharmacologically to finely modulate subcellular localization. Our results show that endolysosomal sorting of the chimeric proteins ending in the "–8" sequence operates in diverse cell types and is preserved in organisms as distant as fungi and humans.

Materials and Methods

Ethics statement

The study was conducted according to the Declaration of Helsinki principles and was approved by the Commission of Bioethics and Biosafety of Centro de Investigaciones Biológicas (Madrid, Spain) and by the Bioethics Committee of Consejo Superior de Investigaciones Científicas (Spain). All cell types used were from commercial sources (see below) or from established Cell Repositories (NIGMS Human Genetic Cell Repository at the Coriell Institute for Medical Research, Camden, NJ).

Materials

Cell culture media RPMI1640, DMEM, TC100 and supplements (Newborn calf serum, penicillin/streptomycin, glutamine, trypsin-EDTA) were from Gibco Life Technologies (Paisley, UK). NCTC 109 medium and chloroquine were from Sigma (Steinheim, Germany). Foetal bovine serum (FBS) was from Lonza Inc. (Walkersville, MD, USA). Lipofectamine 2000 and Lysotracker Red (LTR) were from Life Technologies (Carlsbad, CA, USA). U18666A was from Merck4Biosciences (Madrid, Spain). Anti-GFP was from Roche Diagnostics GmbH (Mannheim, Germany). Anti-Hsp90 (sc-7947), anti-RhoGDI (sc-360), and anti-vimentin (sc-6260) were from Santa Cruz Biotechnology (Santa Cruz, CA, USA). Anti-mouse Igs were from Dako (Copenhagen, Denmark). Anti-giantin was from Covance (Princeton, NJ, USA).

Plasmids

The following constructs were generous gifts: GFP-Rab7, from Prof. C. Bucci (University of Copenhagen); Lamp1-GFP, from Prof. J. Lippincott-Schwartz (NIH); GFP-Rab5, from Prof. J. Bonifacino (NIH). GFP-Rab11 was from Genecopoeia. The constructs GFP-8 (GFP-CINCCKVL), GFP-HA-RhoB and tRFP-T-HA-RhoB have been previously described [14]. The plasmid tRFP-T-8 containing a S162T mutation to improve photostability [17] was generated from tRFP-8 [16] by PCR, as previously described [14]. Dendra-8 (Dendra2-CINCCKVL) was generated from pDendra2-C (Clontech) by PCR, analogously to GFP-8, as described [16]. Briefly, the cDNA of Dendra-8 was generated by PCR using pDendra2-C as template and primers: forward, 5′-GCGCTAGCTCGAGGTACCGC-3′, and reverse, 5′-CCGAGCTCTAGAGGACCTTGCAACAGTTGATACAC-CACACCTGGCTGG-3′. The product was cloned in the NheI-SacI sites of pDendra2-C. The constructs GFP-CINCSKVL (GFP-8-C244S, isoprenylation defective GFP-8 mutant), GFP-SINSCKVL (GFP-8-C240, 243S, palmitoylation defective GFP-8 mutant) and the corresponding tRFP-T-8 mutants tRFP-T-CINCSKVL (tRFP-T-8-C242S) and tRFP-T-SINSCKVL (tRFP-T-8-C238, 241S), as well as the vector GFP-HA-RhoB X (expressing RhoB from *Xenopus laevis*, NCBI Acc. No.: NM_001096461.1), were generated by Genewiz Inc. (South Plainfield, NJ) by oligonucleotide synthesis and cloning into the parent vectors. The plasmid p1902 encoding Osmani GFP for fungi transformation has been previously described [18]. The vectors encoding GFP-8 and its C239, 242S (palmitoylation deficient) mutant for expression in fungi were constructed by gene synthesis and cloned into the HindIII-XmaI sites of p1902 (Genewiz).

Cell culture and transfections

The cell line [AG09309] (primary fibroblasts from control subjects) was obtained from the NIGMS Human Genetic Cell Repository (http://ccr.coriell.org/Sections/Collections/NIGMS/?SsId = 8) at the Coriell Institute for Medical Research (Camden, NJ) and was cultured according to the instructions provided. BAEC from Clonetics were cultured in RPMI1640 supplemented with 10% (vol/vol) newborn calf serum, and antibiotics (100 U/ml penicillin, 100 μg/ml streptomycin). HeLa adenocarcinoma cells from ATCC were cultured in DMEM supplemented with serum and antibiotics. *Xenopus laevis* A6 cells were obtained from Sigma and cultured at 28°C in NCTC 109 medium supplemented with 15% distilled H_2O, 2 mM glutamine, 10% FBS and antibiotics. High Five cells, derived from ovarian cells of the cabbage looper, *Trichoplusia ni*, were from Invitrogen. These cells were cultured at 28°C in TC100 medium supplemented with 10% FBS, penicillin-streptomycin as above and 10 μg/ml gentamycin. Transfection of cells at 80% confluence was performed with Lipofectamine2000 following the instructions of the manufacturer, using 1 μg of DNA and 3 μl (single transfections) or 4.5 μl (double transfections) of Lipofectamine per p35 dish. Unless otherwise indicated, after transfection, cells were allowed to recover for 24 h in complete medium before treatment with the indicated agents in the absence

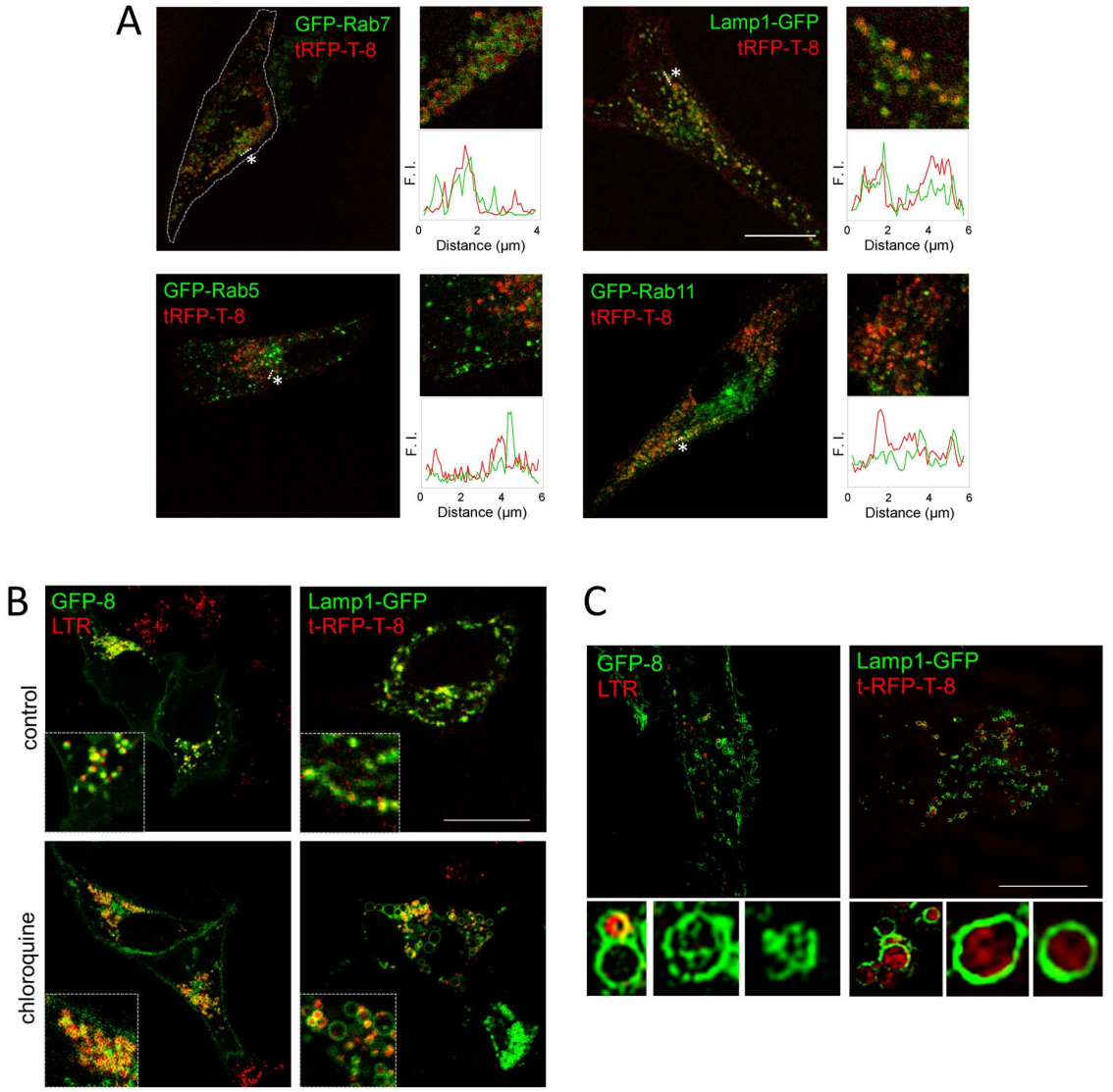

Figure 1. Localization of CINCCKVL chimeras in human cells. (A) Human fibroblasts were transfected with the indicated constructs and observed live by confocal microscopy after 16 h in serum-depleted medium. To the right of every condition, zoom-ins of original pictures and fluorescence intensity profiles along a section (see dotted lines marked by asterisks) are shown. The magnification used for zoom-ins is seven-fold with respect to the corresponding full-sized images. F.I., fluorescence intensity. (B) HeLa cells were transiently transfected with the indicated constructs and treated with 25 nM LTR for 15 min, where indicated, prior to live confocal microscopy observation. Bottom panels show cells that were treated with 10 μM chloroquine 24 h post-transfection for a further 24 h. Insets show details of the pictured cells. (C) Cells transfected as in (B) were visualized live by super-resolution microscopy (SIM). Insets show individual MVB and their ILV decorated with CINCCKVL fluorescent proteins. Scale bar, 20 μm.
doi:10.1371/journal.pone.0107190.g001

of serum. Imaging of live cells was performed 48 h after transfection to minimize its effects.

Aspergillus nidulans culture

Aspergillus nidulans was cultured on complete medium (MCA) or synthetic complete medium (SC) containing 1% glucose and 5 mM ammonium tartrate (i.e. 10 mM NH^{4+}) as carbon and nitrogen sources, respectively. GFP-8 and GFP-8-C239S, C242S were expressed under the control of the $gpdA^{mini}$ promoter, using a single-copy integration construct targeted to *pyroA*, as described previously [18]. Strains used in this work: MAD4688: wA2; pyroA4::[pyroA*-$gpdA^{mini}$::GFP-8-C239S, C242S]; pantoB100 and MAD4689: wA2; pyroA4::[pyroA*-$gpdA^{mini}$::GFP-8]; pantoB100.

Immunofluorescence

For immunofluorescence with anti-giantin antibody, cells were fixed in 4% paraformaldehyde for 20 min at r.t., washed twice in PBS and permeabilized with 0.05% saponin in PEM buffer (80 mM PIPES, 5 mM EGTA, 1 mM $MgCl_2$ pH 6.8) for 5 min. Incubation with anti-giantin at 1:500 dilution was carried out in PBS containing 0.05% saponin for 1 h. After PBS washes, cells

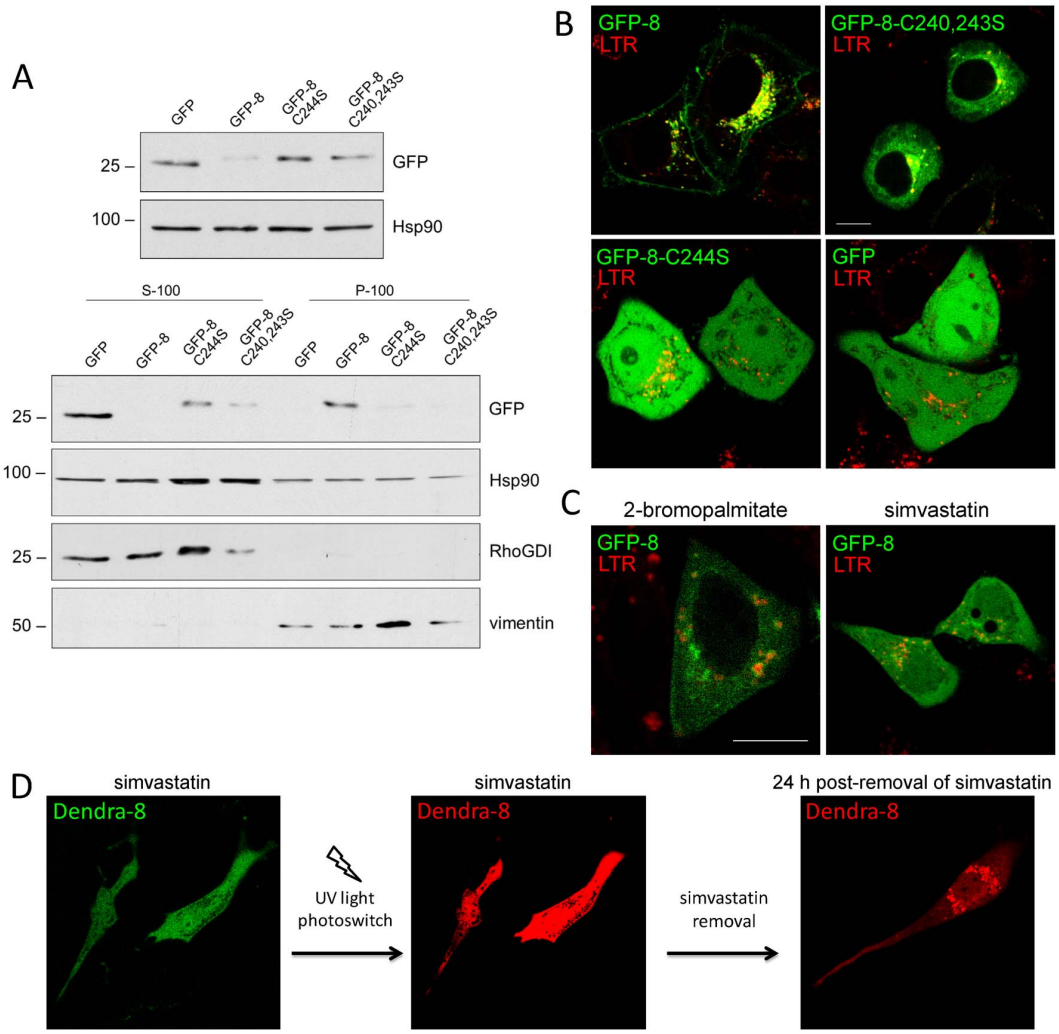

Figure 2. Endolysosomal localization of CINCCKVL-chimeric proteins depends on posttranslational processing. (A) HeLa cells were transiently transfected with the indicated constructs and 24 h later they were cultured in serum-free medium for another 24 h. Cell lysis and fractionation were achieved as described in the Experimental section. Upper panels show the amount of the constructs in total cell lysates and lower panels depict the levels of the constructs in S100 (soluble) and P100 (particulate) fractions, assessed by western blot with an anti-GFP antibody. Hsp90 was used as a loading control, RhoGDI as a marker of the soluble fraction and vimentin as a particulate fraction marker. Results are representative from three experiments with virtually identical results. The positions of the 25 and 100 kDa markers are shown for reference. (B) HeLa cells were transfected with GFP-8, its palmitoylation defective mutant (GFP-8-C240, 243S), its isoprenylation defective mutant (GFP-8-C244S) or GFP, as indicated, and stained with LTR prior to live confocal microscopy imaging. (C) GFP-8-transfected HeLa cells were treated with 20 μM 2-bromopalmitate for 6 h or 10 μM simvastatin for 24 h in serum-free medium and stained with LTR before live observation by confocal microscopy. (D) BAEC were transfected with Dendra-8 and treated with simvastatin for 24 h (left panel) prior to eliciting a green-to-red photoswitch using UV light (middle panel). Immediately after photoswitching simvastatin was removed and the localization of the red, photoconverted protein was assessed 24 h later (right panel). Scale bar, 10 μm.
doi:10.1371/journal.pone.0107190.g002

were incubated with anti-rabbit-Alexa 568 (Invitrogen) at 1:200 in 1% BSA in PBS for a further hour.

Microscopy

For live cell visualization, cells were cultured on glass-bottom dishes (Mattek Corp., Ashland, MA), transfected with fluorescent constructs, treated with the indicated agents and visualized directly on a confocal microscope (LEICA DMRE2 or LEICA SP5 Heidelberg, Germany). Unless otherwise stated, images shown are single channels or overlays of single Z-sections for co-localization visualization. All experiments were repeated at least three times and representative results are shown. Bars represent 20 μm unless otherwise indicated.

In vivo superresolution 3D structured illumination microscopy (SIM) imaging was performed on a Deltavision OMX V4 system (Applied Precision, a GE healthcare company, Issaqua, WA) equipped with an Olympus 60x NA 1.42 objective, cooled sCMOS cameras and 405, 488, 568 and 642 nm diode lasers. Z-stacks covering the whole cell were recorded with a Z-spacing of 125 nm. A total of 15 raw images (5 phases, 3 rotations) per plane were collected. Reconstruction and alignment of these raw images

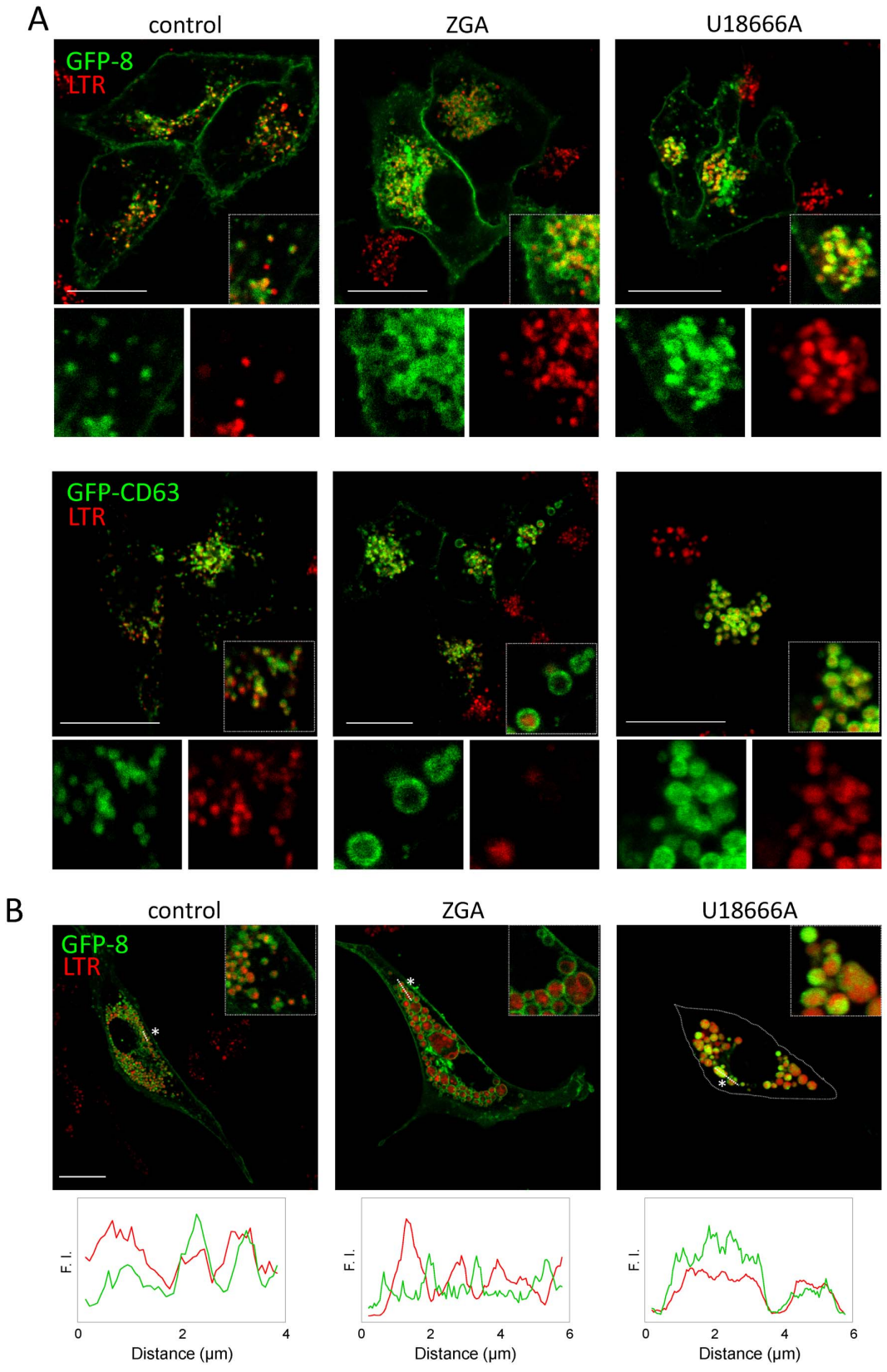
A
control
ZGA
U18666A
GFP-8
LTR
GFP-CD63
LTR
B
control
ZGA
U18666A
GFP-8
LTR
F. I.
Distance (μm)
0
2
4
6

Figure 3. Effects of agents modulating cholesterol synthesis and traffic on the distribution of CINCCKVL constructs. (A) HeLa cells were transfected with GFP-8 (upper panels) or GFP-CD63 (lower panels). 24 h later cells were treated with 100 μM ZGA or 10 μM U18666A for 24 h and stained with LTR as above. Insets show enlarged areas of interest. The single channels corresponding to the areas in insets are shown below each image. (B) BAEC were transfected with GFP-8 and treated with ZGA or U18666A as described in (A). Insets show enlarged areas of interest and lower panels depict fluorescence intensity profiles along a section (see dotted lines marked by asterisks).
doi:10.1371/journal.pone.0107190.g003

was performed using Softworx software. (Applied Precision, a GE healthcare company, Issaqua, WA).

Dendra-8 photoswitching and isoprenylation inhibition-and-release experiments were performed on transfected BAEC on glass-bottom dishes. The transfection medium was removed after 5 hours and replaced with serum-free medium with or without 10 μM simvastatin. Cells were observed 24 hours post-treatment on a confocal microscope (LEICA SP2) and photoswitching was performed by exposure to 405 nm UV light. The resulting green-to-red conversion was recorded in both channels. Simvastatin was either added or removed to the corresponding dishes in serum-free medium and photoconverted, red Dendra-8 was tracked 24 hours later by confocal microscopy.

For microscopy experiments in *Aspergillus*, hyphae were cultured in Lab-Tek chambers (Thermo Fischer Scientific, 115411; 0.3 ml of medium per well) at 25–28°C in pH 6.5 'watch minimal medium' (WMM) containing 100 mM sodium acetate and 5 mM ammonium tartrate as carbon and nitrogen sources, respectively. Hyphae were visualized on an inverted fluorescence microscope (Leica DMI6000B) equipped with an EL6000 external light source with metal halide lamp epifluorescence excitation, driven by Metamorph software (Molecular Dynamics) and coupled to a CCD camera (ORCA ER-II; Hamamatsu). Vacuoles were detected with CMAC (7-amino-4-chloromethylcoumarin, CellTracker Blue; Invitrogen C-2110).

Image analysis

Co-localization analysis was performed with LAS-AF software from Leica on single z-sections of images to obtain co-localization rates (expressed as percentages) and Pearson coefficients (coefficient $r \times 100$). At least 30 cells were analysed per experimental condition. Results are presented as average co-localization rates or Pearson coefficients ± standard error of mean (SEM) as indicated. Average values were compared by Student's t-test for unpaired observations.

Western blot

SDS-PAGE and Western blot analysis of HeLa cells were performed as described [16,19], using ECL detection (GE Healthcare, Buckinghamshire, UK). For analysis of cell fractions, S100 and P100 fractions were obtained by centrifugation of total cell lysates at 100,000×g for 1 h at 4°C, essentially as previously described [20].

Results

Fluorescent CINCCKVL constructs localize at endolysosomal compartments in human cells

To assess the ability of the CINCCKVL motif to induce endolysosomal localization in distant species, we first assessed the distribution of fluorescent CINCCKVL chimeric proteins in primary human fibroblasts, a species in which these constructs have not been characterized. Therefore, we co-transfected tRFP-T-CINCCKVL (tRFP-T-8) with fluorescent constructs of known components of various endosomal compartments. Fusion proteins of Rab family GTPases are commonly used as markers of particular endosomal vesicles, i.e. fluorescent constructs of Rab5 or Rab7 for early and late endosomes, respectively. As can be observed in Figure 1A, tRFP-T-8 localized inside vesicles delimited by GFP-Rab7 and the late endosome-lysosomal marker Lamp1-GFP. Under our conditions, tRFP-T-8 showed partial co-localization with GFP-Rab11, which typically localizes to recycling endosomes [21], and more limited co-localization with a fluorescent construct of Rab5 [22]. Thus, the tRFP-T-8 construct displays a selective localization at late endosomes-lysosomes in this cell type (Fig. 1A, see profiles).

In the widely used human cell line from cervical adenocarcinoma HeLa, CINCCKVL-chimeric proteins showed substantial co-localization with LTR (GFP-8/LTR co-localization rate: 62.6±2.5%) and tRFP-T-8 localized inside Lamp-1-GFP-positive vesicles which, as described above, became dilated when treated with cloroquine (Fig. 1B). GFP-8 also co-localized extensively with

Species	Protein	Accession no.	C-terminal sequence
Homo sapiens	RhoB	NM_004040	TRAALQKRYGSQNGCINCCKVL
Bos taurus	RhoB	NM_001077922	TRAALQKRYGSQNGCINCCKVL
Mus musculus	RhoB	AF481943	TRAALQKRYGSQNGCINCCKVL
Gallus gallus	RhoB	NM_204909.1	TRAALQKRYGTQNGCINCCKVL
Xenopus laevis	RhoB	NM_001096461.1	TRAALQKKHGRSGECMSCCKLL
Drosophila mojavensis	Rho-like	EDW09337	TRASLQVKKRKKRSGCWSLSCKLL
Schizosaccharomyces pombe	Rho2	NM_001019998.3	TRAALTVRDSENDKSSTKCCIIS
Aspergillus fumigatus	RasA	XM_748433	TRAPEGKMDVSEPGDNAGCCGKCVIM
Aspergillus nidulans	Rho2-like	AN4953	TRAALLTFDKRKSSCCIVL

Figure 4. C-terminal sequences of CINCCKVL-chimeric proteins, RhoB homologs and related proteins from diverse species. The C-terminal sequences of GFP-8 and tRFP-T-8 are shown on top, together with a schematic view of the lipidic modifications; palmitates are shown in black and the geranylgeranyl moiety in blue. The Pubmed accession numbers of genes coding for proteins bearing C-terminal sequences similar to that of RhoB are shown in the lower panel. Potential sites for palmitoylation are shown in red and the isoprenylation cysteine in green.
doi:10.1371/journal.pone.0107190.g004

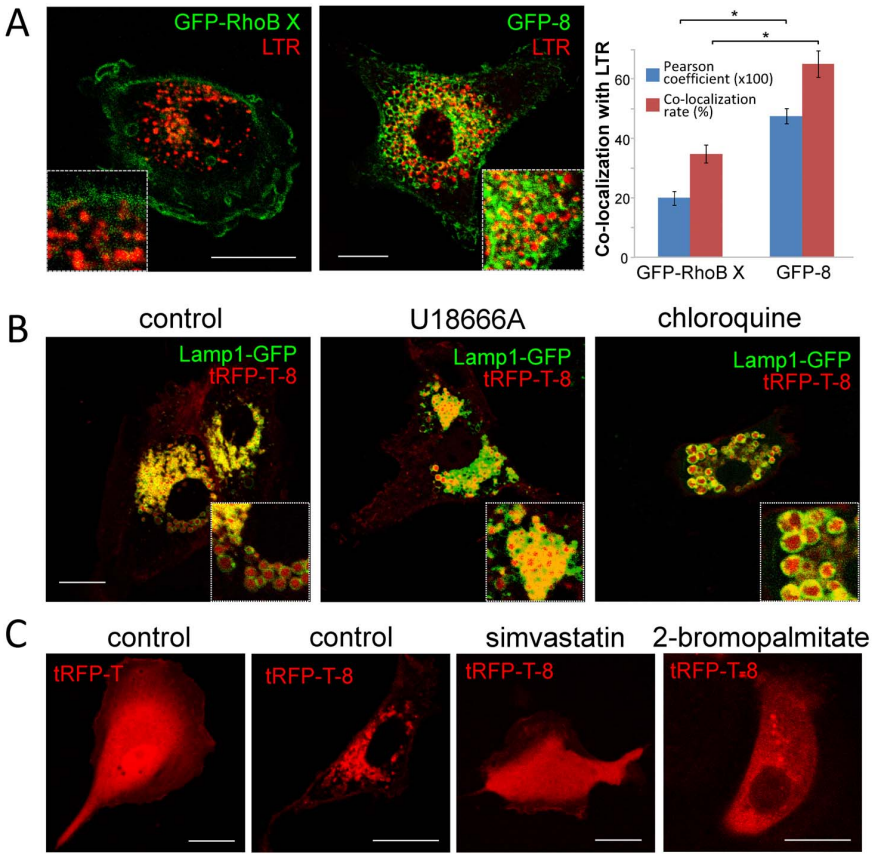

Figure 5. Localization of RhoB-related proteins in amphibian cells. (A) *Xenopus laevis* RhoB (GFP-RhoB X) or GFP-8 were expressed in *Xenopus laevis* A6 cells and acidic compartments were stained with LTR. The right panel depicts the extent of co-localization of GFP and LTR signals shown as Pearson coefficients (x100) or co-localization rates (in percentages). Results are average values of at least 30 cells per condition ± standard error of mean (SEM). *$p<1\times10^{-6}$ *vs* GFP-8 by Student's t-test. (B) Effect of agents altering lysosomal function on the distribution of tRFP-T-8. *Xenopus* A6 cells were co-transfected with Lamp1-GFP to mark lysosomes and tRFP-T-8, and treated with 10 μM U18666A or 10 μM chloroquine, as indicated. (C) Dependence of tRFP-T-8 localization on posttranslational modification in *Xenopus* cells. A6 cells were transfected with tRFP-T or tRFP-T-8 and treated with 10 μM simvastatin or 20 μM 2-bromopalmitate and imaged live by confocal microscopy.
doi:10.1371/journal.pone.0107190.g005

a fluorescent construct of CD63, a component of MVB that is used as a marker of intraluminal vesicles (ILV) (Fig. S1A). This prominent co-localization was confirmed in BAEC (Fig. S1B).

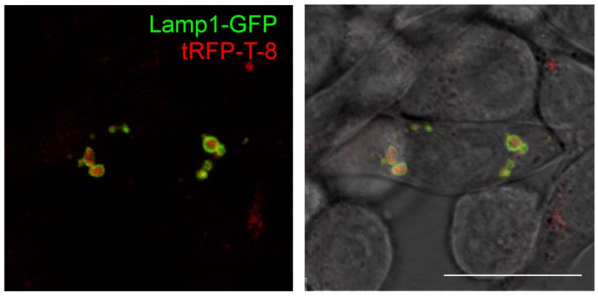

Figure 6. Localization of tRFP-T-8 in High Five insect cells. High Five cells were transfected with Lamp1-GFP and tRFP-T-8 and live cells were visualized by confocal microscopy. The overlays of single fluorescent z-sections alone and with the Differential Interference Contrast image are shown.
doi:10.1371/journal.pone.0107190.g006

Consistent with this and taking advantage of the higher localization precision obtained by *in vivo* super-resolution structural illumination microscopy (SIM), we further demonstrated the presence of both GFP-8 and tRFP-T-8 in the ILV of MVB (Fig. 1C). This suggests that this simple amino acid sequence can carry proteins to specific domains in endolysosomes, some of which are ultimately internalized to form vesicles inside MVBs. Inside these compartments, whereas tRFP-T-8 showed a more diffuse pattern, GFP-8 outlined the inner membranes, which could be attributed to the decrease in GFP fluorescence occurring in acidic pH environments [23].

Lipidation of CINCCKVL acts as an endolysosomal targeting switch

In RhoB, the CINCCKVL motif is subject to posttranslational processing at its cysteine residues by irreversible binding of an isoprenoid to its last cysteine and reversible palmitoylation of its two remaining cysteines. To explore the importance of these modifications in endolysosomal localization of CINCCKVL-chimeric proteins, we generated constructs in which the lipidation cysteines have been mutated. Total lysates from cells transfected with these constructs are shown in Figure 2A, upper panels. The

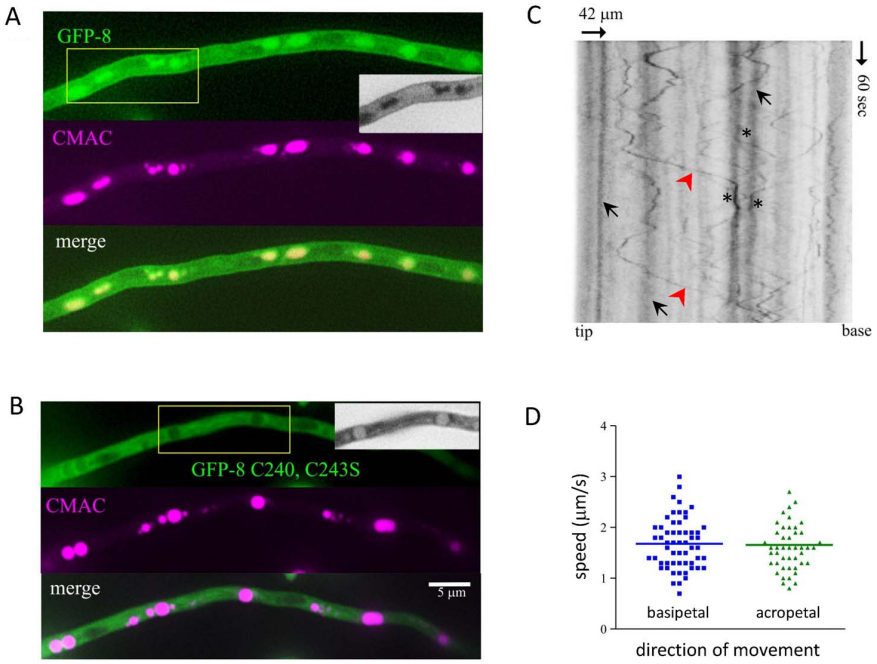

Figure 7. Localization of GFP-8 in *Aspergillus nidulans*. Strains of *Aspergillus nidulans* expressing GFP-8 or its palmitoylation deficient mutant (GFP-8-C240, 243S) were imaged as described in Methods. (A and B) show co-localization of the constructs with the vacuole marker, CMAC. Insets show grayscale images for better contrast. (C) Kymograph showing the movements of various GFP-8-positive compartments. Rapidly moving endosomes (likely corresponding to early endosomes) are marked by arrowheads (red), static vesicles (likely corresponding to vacuoles) are marked by arrows and potential points of contact between endosomes and vacuoles are depicted by asterisks. (D) Graph representing velocities of individual endosomes.
doi:10.1371/journal.pone.0107190.g007

degree of membrane association of the different constructs was assessed by subcellular fractionation into S100 (soluble) and P100 (membrane) fractions, followed by western blot (Fig. 2A, lower panels). Whereas GFP was fully soluble, GFP-8 was totally membrane bound. In turn, the isoprenylation and the palmitoylation defective mutants (GFP-8-C244S and GFP-8-C241, 243S, respectively) showed a predominant localization in the soluble fraction with a marginal amount appearing in P100 fractions.

Membrane localization of the different constructs was also assessed by confocal microscopy (Fig. 2B). Mutation of the palmitoylation cysteines in GFP-8 altered its typical localization, leading to the cytoplasmic distribution of the non-palmitoylatable construct (GFP-8-C241, 243S), which excluded the nucleus. This pattern has been observed for constructs that can be isoprenylated but not palmitoylated, such as GFP bearing only a CAAX motif [16]. In some cells, certain cytoplasmic accumulations of the GFP-8-C241, 243S construct were observed that corresponded to its presence at the Golgi, as indicated by their co-localization with the Golgi component giantin (Fig. S2). In contrast, mutation of the CAAX box cysteine (GFP-8-C244S) led to a diffuse distribution throughout the cytoplasm and nucleus, excluding some organelles (Fig. 2B). This pattern was indistinguishable from that of GFP and is typical of non-lipidated constructs, thus indicating that isoprenylation of GFP-8 is required for subsequent palmitoylation [24]. Similar results were obtained with tRFP-T-8 palmitoylation or isoprenylation-defective mutants (results not shown). Importantly, pharmacological inhibition of palmitoylation by means of treatment with 2-bromopalmitate or of isoprenylation (and subsequent palmitoylation) with simvastatin, resulted in a cellular distribution of GFP-8 analogous to that of the corresponding palmitoylation or isoprenylation-defective mutants (Fig. 2C). Therefore, association of CINCCKVL chimeras with membranes can be modulated pharmacologically by blocking lipidation of its cysteine residues. We took advantage of this feature to address the key issue of whether a non-lipidated, cytosolic pool of CINCCKVL protein can undergo lipidation to be sorted to the aforementioned membranes or whether sorting must occur on newly synthesized proteins. Using BAEC, which present low cytotoxicity upon treatment with simvastatin, and Dendra2, a protein capable of photoswitching from green to red fluorescence emission after UV light exposure, we set up a simvastatin-based approach to follow specific pools of a Dendra2-CINCCKVL fusion protein (Dendra-8, Fig. 2D). Treatment with simvastatin blocked processing of Dendra-8 rendering a pool of fully cytosolic green construct. This pool was photoswitched obtaining a soluble, non-isoprenylated red fluorescent CINCCKVL construct to follow. Releasing the isoprenylation inhibition by removal of simvastatin allowed endolysosomal targeting of the previously diffuse red construct, clearly demonstrating that preexisting CINCCKVL-chimeric proteins may undergo sorting from a cytosolic localization, depending on isoprenoid availability (Fig. 2D). The observed behavior establishes this sequence as a tunable targeting motif in live cells.

Impaired cholesterol dynamics alters sorting of CINCCKVL chimeras

Specific combinations of lipidic membrane anchors, such as that conferred by the CINCCKVL sequence, may promote protein association with membrane domains of a particular composition [15]. To address this issue, here we have tackled cholesterol

availability and traffic in the HeLa cell model (Fig. 3). Remarkably, inhibiting cholesterol biosynthesis with the squalene synthase inhibitor zaragozic acid (ZGA) induced the appearance of enlarged endolysosomes showing a diffuse localization of GFP-8, which in some of them appeared retained at the edge (Fig. 3A, upper panels). Some of these structures displayed a fainter or patchy LTR staining. In sharp contrast, U18666A, an agent that causes accumulation of cholesterol and of the endosomal lipid 2,2′-dioleoyl lysobisphosphatidic acid (LBPA), also known as bis(monoacylglycero)phosphate (BMP) in MVB [25], induced the formation of dense MVB containing GFP-8, as previously observed in BAEC [14]. Interestingly, GFP-CD63, a marker of MVB intraluminal structures, suffered alterations similar to those of GFP-8 in response to ZGA and U18666A (Fig. 3A, lower panels). Moreover, CD63 markedly co-localized with CINCCKVL constructs at the altered endolysosomes under all experimental conditions (Fig. S1C). In order to substantiate the importance of cholesterol availability for GFP-8 sorting, we treated BAEC with ZGA. Inhibition of cholesterol biosynthesis elicited the appearance of dilated MVB showing a peripheral distribution of GFP-8 (Fig. 3B) and CD63 (Fig. S1D). This cell type presents large endosomes, so that the differences between the alterations induced by ZGA and U18666A (shown here for reference) were more obvious, clearly showing the reduction of intraluminal content in ZGA-treated cells (Fig. 3B, see profiles). Taken together these results suggest that the specific modification of CINCCKVL chimeras induces their association with defined membrane domains, in a manner dependent on the presence or distribution of cholesterol, which appears to be required for their sorting.

Localization of CINCCKVL chimeric proteins in cells from non-mammalian species

The C-terminal sequence of RhoB is unique for this GTPase and it is conserved in mammalian species and in birds (Fig. 4). In lower species, the RhoB sequence displays a higher degree of variability, and in some cases a *bona fide* homolog of RhoB has not been identified (Fig. 4). Although several proteins can be found which possess CAAX boxes and potential sites for palmitoylation, the composition and/or spacing of these residues is not conserved with respect to the CINCCKVL sequence. Therefore, we wanted to assess whether CINCCKVL constructs would confer endolysosomal localization in more distant non-mammalian species.

The *Xenopus laevis* RhoB protein C-terminus contains one isoprenylation and two putative palmitoylation cysteine residues (Fig. 4). However, the composition of this sequence clearly differs from that of human RhoB in the presence of a basic amino acid cluster at position 181–183 (KKH), and in the amino acids located between the two palmitoylation cysteines (MS). These features are analogous to motifs present in the C-terminal segments of TC10 (KKH), an endosomal RhoB-related GTPase, and H-Ras (MS), which preferentially localize to recycling compartments and to the plasma membrane, respectively [12,14]. Consistent with this, we observed that GFP-tagged *Xenopus laevis* RhoB (GFP-RhoB X) was mainly localized at the plasma membrane in *Xenopus* A6 cells, and showed limited co-localization with LTR (Fig. 5A, left panel). In contrast, transfection of CINCCKVL chimeric proteins in *Xenopus* A6 cells resulted in a clear endolysosomal localization of the constructs, as revealed by the disposition of GFP-8 at LTR-positive compartments (Fig. 5A, middle panel), showing substantial co-localization with this lysosomal marker (Fig. 5A, right panel) and the presence of tRFP-T-8 inside vesicles delimited by Lamp1-GFP (Fig. 5B). Interestingly, human RhoB but not *Xenopus* RhoB fluorescent constructs extensively co-localized with CINCCKVL constructs in A6 cells (Fig. S3), thus stressing the importance of the differences in the sequence of RhoB from various species for targeting of the full-length protein. This also indicates that, although the RhoB C-terminal sequence is not fully conserved in *Xenopus laevis*, the mechanisms targeting CINCCKVL-chimeric proteins to endolysosomes are operative in this cell type.

We next assessed the distribution of these constructs in response to agents which disrupt endolysosomal dynamics and cholesterol traffic [16]. Treatment of A6 cells with U18666A led to a dramatic compaction of endolysomes, which accumulated tRFP-T-8 (Fig. 5B), and chloroquine caused accumulation of tRFP-T-8 inside enlarged endolysomes (Fig. 5B). Moreover, we confirmed that in these cells, targeting of CINCCKVL chimeric proteins was also dependent on their posttranslational processing by isoprenylation and palmitoylation. As shown in Fig. 5C, treatment with simvastatin abolished the distribution of tRFP-T-8 in endosomal vesicles and led to a diffuse distribution throughout the cytosol and the nucleus, indistinguishable from that of tRFP-T, thus confirming the importance of isoprenylation for tRFP-T-8 targeting in this cell type, as well. In contrast, inhibition of palmitoylation with 2-BP elicited the appearance of the protein in the cytosol, excluding the nucleus, as shown above for GFP-8 in Hela cells. Similar experiments were routinely carried out in other cell types used in this work and yielded analogous results (data not shown).

In order to ascertain the robustness of the CINCCKVL sequence as a determinant for endolysosomal localization, we went on to explore its localization in a cell line of an invertebrate. In High Five insect cells, tRFP-T-8 was fully localized inside vesicles delimited by Lamp1-GFP, thus suggesting its lysosomal targeting (Fig. 6). Interestingly, in insect cells the homology of Rho-related proteins with RhoB is more distant, both in terms of the number of cysteines located at the C-terminus and the nature of the surrounding amino acids (Fig. 4). Nevertheless, the sequence derived from the mammalian protein still promotes localization in lysosomal compartments.

Tracking endosomes with GFP-CINCCKVL in *Aspergillus nidulans*

Palmitoylation plays a key role in protein localization and sorting in lower eukaryotic organisms such as fungi [26]. Indeed, yeast have been seminal for the identification and characterization of the isoprenylation and palmitoylation machinery. The fungus *Aspergillus nidulans* expresses a potential Rho-related protein bearing one putative site for palmitoylation adjacent to the isoprenylation cysteine (Fig. 4). However, in this organism, the –CINCCKVL sequence is not conserved. In *Aspergillus nidulans* most GFP-8 fluorescence clearly localized in late endosomes and vacuoles, where it co-localized with 7-amino-4-chloromethylcoumarin (CMAC), a marker for hydrolase-containing acidic organelles (Fig. 7A) [27]. In addition, GFP-8 fluorescence was detected at endosomes showing bidirectional movement (see Video S1), which is dependent on microtubules [27]. In this model, GFP-8 also decorated the plasma membrane (Fig. 7A, inset) and septa (not shown). GFP-8 localization was dependent on its posttranslational modification since a palmitoylation-deficient mutant, GFP-8-C240, 243S, was fully cytosolic, excluding plasma membrane, septa, vacuoles and nuclei (Fig. 7B). Therefore, analogously to the observations in cells from higher organisms, the isoprenylation motif was not sufficient to promote the specific endolysosomal localization of this construct, although it led to nuclear exclusion. Nevertheless, the distribution of the GFP-8-C240, 243S construct was distinct from that of GFP, which, as observed in mammalian cells, showed a diffuse pattern throughout the nucleus and cytosol (not shown).

Aspergillus nidulans constitutes a well characterized model for monitorization of the endocytic process. Fluorescent constructs of endosomal proteins allow following the movement of these organelles by time-lapse microscopy and representation of their trajectories as kymographs to calculate endosomal speed [27]. Therefore, we took advantage of these possibilities to characterize the dynamics of GFP-8-positive compartments in more detail. Figure 7C shows a representative kymograph where nearly static traces correspond to vacuoles (arrows). In addition, the movement of various endosomes, both in basipetal and acropetal directions, can be monitored (arrowheads). Moreover, points of endosome-vacuole contact can be observed (asterisks). The velocities of the endosomes monitored are shown in Figure 7D. As can be observed, GFP-8-positive compartments show speeds ranging from less than 1 μm per second, to nearly 3 μm per second, the average velocities being practically the same for basipetal and acropetal movements. Therefore, GFP-8 marks the endolysosomal pathway in *Aspergillus nidulans*, suggesting that the targeting mechanisms for CINCCKVL constructs are also conserved in fungi.

Discussion

The combination of several lipidic modifications, like isoprenylation and palmitoylation constitute important determinants for protein localization in specific subcellular compartments. The spacing of the lipid moieties and the nature of the non-lipidated amino acids may contribute to the generation of unique structures with affinity for membrane domains or protein partners. Here we have shown that the isoprenylation and palmitoylation motif of the GTPase RhoB constitutes one such structure *per se* and is able to determine protein sorting to lysosomal compartments in cells from distant species, including fungi and humans.

Several mechanisms for sorting to MVBs have been reported. The classical mechanism implies ubiquitination of the cargo protein and association with components of the ESCRT machinery, which, according to some models may assemble sequentially to define invagination domains leading to the formation and ultimately the release of ILV [7,28,29]. Although under our conditions we have not detected ubiquitination of GFP-8 (unpublished observations), this mechanism cannot be excluded since ubiquitination-independent sorting of certain cargo by ESCRT-mediated processes has also been reported [30]. Recently, a late-endosome microautophagy-like process has been described, which depends on ESCRT I and III for vesicle formation and on Hsc70 for cargo selection, and may mediate the delivery into late endosomes of various cytosolic proteins [31]. Nevertheless, this process does not seem to be involved in sorting of CINCCKVL chimeric proteins since it is disrupted by U18666A, which as shown above, causes strong accumulation of GFP-8 in MVB. In turn, although the autophagic and endolysosomal pathways may converge at several levels, we have previously observed that GFP-8 and the autophagosomal marker RFP-LC3 show different distribution patterns [32], Moreover, endolysosomal targeting of CINCCKVL constructs occurs also in cells growing in complete medium, including human, *Xenopus* and insect cells (unpublished observations), thus indicating that induction of macroautophagy is not required for sorting. Lastly, in chaperone-mediated autophagy, unfolding of the protein occurs prior to entrance in the lysosome, leading to a loss of fluorescence [33]. Under our conditions, however, intra-lysosomal fluorescence of CINCCKVL-constructs is preserved, thus making this potential mechanism unlikely.

The fact that CINCCKVL proteins are targeted to human lysosomes and fungal vacuoles suggests the presence of conserved sorting mechanisms in these distant species. Indeed, extensive phylogenetic studies on Rab family proteins have unveiled the existence of more than 20 core Rab proteins in the latest eukaryotic common ancestor (LECA) which have suffered expansions *via* gene duplication or losses throughout eukaryotic evolution giving rise to modern Rabs [34,35]. Under our conditions, the Rab proteins that co-localize to a greater extent with CINCCKVL chimeras are encompassed in a proposed late endosomal LECA Rab family (group III), making it possible that particular Rabs of this conserved group could be involved in CINCCKVL sorting. Similarly, the ESCRT protein family is also conserved throughout eukaryotes, in particular ESCRT-I, -II, -III and -III-associated proteins, though ESCRT-0 proteins appear to be specific to Opisthokonta (fungi and animals/metazoans) [36]. Interestingly, although several tetraspanin homologs have been identified in fungi, including *Aspergillus* species [37], their location and/or role in vesicular traffic have not been studied. Therefore, the species studied here may share many of the MVB sorting machineries already present in the LECA, underscoring the conserved character of the fundamental trafficking proteins involved in later steps of the endolysosomal pathway.

In addition to the roles of proteins or protein complexes, lipids with a particular structure may contribute to the sorting process by forming targeting microdomains or through the induction of curvature which facilitates membrane invagination. This is the case of the late endosomal lipid LBPA/BMP [38]. Interestingly, we have observed that pharmacological disruption of MVB lipid dynamics with U18666A traps GFP-8 in this compartment in several species, including *Xenopus laevis*. Remarkably, inhibition of cholesterol biosynthesis with ZGA led to MVB alterations consisting in dilation and retention of ILV components, including CD63 and GFP-8, at the periphery of some of these dilated compartments. Results obtained recently in mice deficient in ^{24} sterol reductase, the last enzyme of the cholesterol biosynthetic pathway, in which a reduction in MVB intraluminal material has been reported, might serve as a clue to the behavior observed here in BAEC and HeLa cells [39]. It has been reported that most of the cholesterol present in endolysosomes is contained in ILV. Therefore, it is plausible that an overall metabolic cholesterol reduction would affect ILV more directly than other compartments [40]. Conversely, treatment of cells with methyl-β-cyclodextrin, widely used to deplete plasma membrane cholesterol, did not alter GFP-8 distribution, although a non-specific alteration of cell morphology, prior to cell rounding, was noticed (unpublished observations). Taken together, our results indicate that interaction with endosomal lipids is an important determinant in GFP-8 sorting.

In all species studied, palmitoylation appears as a key element for lysosomal localization of CINCCKVL chimeras. Protein palmitoylation has been involved in protein sorting, although its effects appear to be cell-type and protein-specific. The mannose receptor N-terminus is palmitoylated and blocking this modification induces lysosomal accumulation of this protein [9]. In the case of the protease-activated receptor 1, palmitoylation allows the correct utilization of tyrosine-based sorting signals, and a palmitoylation-deficient mutant, shows increased degradation in lysosomes [41]. In contrast, the Ca^{2+} sensor synaptotagmin 7 has been reported to be targeted to lysosomes by its palmitoylation-dependent association with the tetraspanin CD63 [42], although the examples of palmitoylation-driven endolysosomal association in mammalian cells are very scarce. In yeast, the palmitoylated protein Vac8 is targeted to the vacuolar membrane, although there is no evidence for vacuolar sorting [43]. Therefore, in most cases, palmitoylation directs proteins away from lysosomes (see

[44] and [16] and references therein), with only a few examples of palmitoylation-supported ILV sorting. Interestingly, as previously suggested [45], palmitoylation is also likely responsible for the lack of interaction of GFP-RhoB or GFP-8 with RhoGDI (Oeste et al., unpublished observations). Nevertheless, it would be interesting to assess whether non-palmitoylated constructs interact with RhoGDI in the cytosol.

The human RhoB sequence is not conserved in the lower species, in which its closest homologs are not endosomal proteins. Yet, CINCCKVL chimeric proteins show endolysosomal localization analogous to that found in mammalian cells. In insects, a clear homolog of RhoB has not been identified. However, several proteins exist that possess sequences for bipalmitoylation, although their potential lysosomal targeting has not been explored. In *Schizosaccharomyces pombe*, the RhoB homolog Rho2 has been reported to be mainly membrane bound and localize at the growing end(s) of the cell and the septation site [46]. Rho2 is isoprenylated and palmitoylated [26], although, as predicted from its CAAX box sequence, is farnesylated [47], whereas RhoB is mainly geranylgeranylated in cells [48]. However, when using constructs directing either farnesylation of geranylgeranylation of GFP-8, namely, GFP-CINCCKVL and GFP-CINCCLVM, we did not find significant differences in their lysosomal localization, thus indicating that the length of the isoprenoid moiety is not a critical factor (Oeste et al., unpublished observations). In addition, Rho2 only possesses one palmitoylation cysteine adjacent to the isoprenylation site. Also in yeast, there are examples of bipalmitoylated proteins, like RasA, which localizes at the plasma membrane, but appears in internal patches when palmitoylation is blocked [49]. However, in this case, the spacing of palmitates is different from that of CINCCKVL proteins (see Fig. 4). In this context, we have previously shown than the spacing of palmitates is key for fine-tuning protein localization. Moving the distal palmitoylation cysteine away from the isoprenylation site in a chimeric construct reduces its accummulation in MVB in response to alterations in lipid dynamics [14]. In *Aspergillus nidulans*, both the putative Rho2-like protein (Fig. 4) and GFP-8 would be expected to be geranylgeranylated and palmitoylated, although, to the best of our knowledge, a homolog for GGTase I has not been biochemically identified in this organism and the information available on potential geranylgeranyltransferases only stems from sequence homology analysis on database searches. It can be noted that CINCCKVL chimeras displayed some degree of plasma membrane localization, although it was dependent on the cell type under study and on the construct used, with GFP-8 decorating the plasma membrane to a higher extent than tRFP-T-8. Nevertheless, the most consistent localization of CINCCKVL chimeric proteins, when lipidated, is the endolysosomal compartment. It could be hypothesized that the specific structure formed upon CINCCKVL lipidation promotes the interaction with specific microdomains that require the presence of cholesterol. Indeed, domains rich in free cholesterol have been described in MVB of endothelial cells under particular cell culture conditions [50]. Moreover, the presence of lipid microdomains that segregate proteins in the yeast vacuole has been recently demonstrated in *Saccharomyces cerevisiae* [51].

One of the most striking conclusions of this work is that the CINCCKVL sequence takes a route to endolysosomes present in the lower species but not used, to the best of our knowledge, by their endogenous proteins. Our findings may motivate the search for proteins with analogous sequences that may be sorted through this pathway, as well as the use of cells from lower species to completely unveil the sorting mechanism. This information will allow elucidating whether this sequence has evolved in the higher species to ensure endolysosomal delivery of specific proteins. In summary, our observations support the interpretation that the structures generated by precise lipidation sequences, and in particular by the CINCCKVL motif, may specifically interact with defined membrane components for protein targeting and sorting. These findings may set the basis for exploring the sorting of lipidated sequences to specific microdomains involved in MVB biogenesis in diverse species.

Supporting Information

Figure S1 GFP-8 co-localization with the MVB/ILV marker, mCherry-CD63. (A) HeLa cells were co-transfected with GFP-8 and mCherry-CD63, serum-starved for 16 h and observed by live confocal fluorescence microscopy. (B) BAEC were treated as described for HeLa. Scale bar, 20 μm. (C) HeLa cells transfected as above were treated with ZGA or U18666A as in Figure 3. (D) BAEC transfected as in (A) were treated with ZGA as in Figure 3. Insets show enlarged areas of interest. The single channels corresponding to the areas in insets are shown below each image.
(TIF)

Figure S2 Golgi staining of cells transfected with GFP-8 and its mutants. HeLa cells transfected with GFP, GFP-8 or the mutants featured in Figure 2 were fixed after 16 h of serum deprivation and the Golgi compartment was stained by anti-giantin immunofluorescence, as described in Materials & Methods.
(TIF)

Figure S3 Localization of *Xenopus* or human RhoB chimeras in amphibian cells. *Xenopus laevis* A6 cells were co-transfected with the indicated constructs and observed live by confocal microscopy after 16 h in serum-depleted medium. Insets show enlarged areas of interest.
(TIFF)

Video S1 *Aspergillus nidulans* expressing GFP-8 and showing endosome movement.
(MOV)

Acknowledgments

We are grateful to R.A. Valero for performing preliminary experiments and to M.T. Seisdedos for expert assistance with confocal microscopy. The technical assistance of E. Reoyo and M.J. Carrasco is gratefully appreciated.

Author Contributions

Conceived and designed the experiments: DPS CLO MAP. Performed the experiments: CLO DPS JMT MP MAP. Analyzed the data: DPS CLO MP MAP. Contributed reagents/materials/analysis tools: MAP KOS HS. Contributed to the writing of the manuscript: DPS CLO MAP HS.

References

1. Platta HW, Stenmark H (2011) Endocytosis and signaling. Curr Opin Cell Biol 23: 393–403.
2. Huotari J, Helenius A (2011) Endosome maturation. EMBO J 30: 3481–3500.
3. Rink J, Ghigo E, Kalaidzidis Y, Zerial M (2005) Rab conversion as a mechanism of progression from early to late endosomes. Cell 122: 735–749.
4. Raiborg C, Stenmark H (2009) The ESCRT machinery in endosomal sorting of ubiquitylated membrane proteins. Nature 458: 445–452.

5. Ghosh P, Dahms NM, Kornfeld S (2003) Mannose 6-phosphate receptors: new twists in the tale. Nat Rev Mol Cell Biol 4: 202–212.
6. Coutinho MF, Prata MJ, Alves S (2012) A shortcut to the lysosome: the mannose-6-phosphate-independent pathway. Mol Genet Metab 107: 257–266.
7. Bonifacino JS, Traub LM (2003) Signals for sorting of transmembrane proteins to endosomes and lysosomes. Annu Rev Biochem 72: 395–447.
8. Braulke T, Bonifacino JS (2009) Sorting of lysosomal proteins. Biochim Biophys Acta 1793: 605–614.
9. Schweizer A, Kornfeld S, Rohrer J (1996) Cysteine34 of the cytoplasmic tail of the cation-dependent mannose 6-phosphate receptor is reversibly palmitoylated and required for normal trafficking and lysosomal enzyme sorting. J Cell Biol 132: 577–584.
10. Stipp CS, Kolesnikova TV, Hemler ME (2003) Functional domains in tetraspanin proteins. Trends Biochem Sci 28: 106–112.
11. Veit M, Sollner TH, Rothman JE (1996) Multiple palmitoylation of synaptotagmin and the t-SNARE SNAP-25. FEBS Lett 385: 119–123.
12. Adamson P, Paterson HF, Hall A (1992) Intracellular localization of the P21rho proteins. J Cell Biol 119: 617–627.
13. Pérez-Sala D (2007) Protein isoprenylation in biology and disease: general overview and perspectives from studies with genetically engineered animals. Front Biosci 12: 4456–4472.
14. Valero RA, Oeste CL, Stamatakis K, Ramos I, Herrera M, et al. (2010) Structural determinants allowing endo-lysosomal sorting and degradation of endosomal GTPases. Traffic 11: 1221–1233.
15. Aicart-Ramos C, Valero RA, Rodriguez-Crespo I (2011) Protein palmitoylation and subcellular trafficking. Biochim Biophys Acta 1808: 2981–2994.
16. Pérez-Sala D, Boya P, Ramos I, Herrera M, Stamatakis K (2009) The C-terminal sequence of RhoB directs protein degradation through an endo-lysosomal pathway. PLoS ONE 4(12): e8117.
17. Shaner NC, Lin MZ, McKeown MR, Steinbach PA, Hazelwood KL, et al. (2008) Improving the photostability of bright monomeric orange and red fluorescent proteins. Nat Methods 5: 545–551.
18. Pantazopoulou A, Penalva MA (2009) Organization and dynamics of the Aspergillus nidulans Golgi during apical extension and mitosis. Mol Biol Cell 20: 4335–4347.
19. Stamatakis K, Cernuda-Morollón E, Hernández-Perera O, Pérez-Sala D (2002) Isoprenylation of RhoB is required for its degradation: a novel determinant in the complex regulation of RhoB expression by the mevalonate pathway. J Biol Chem 277: 49389–49396.
20. Gharbi S, Garzón B, Gayarre J, Timms J, Pérez-Sala D (2007) Study of protein targets for covalent modification by the antitumoral and anti-inflammatory prostaglandin PGA_1: focus on vimentin. J Mass Spectrom 42: 1474–1484.
21. Ullrich O, Reinsch S, Urbe S, Zerial M, Parton RG (1996) Rab11 regulates recycling through the pericentriolar recycling endosome. J Cell Biol 135: 913–924.
22. Bucci C, Parton RG, Mather IH, Stunnenberg H, Simons K, et al. (1992) The small GTPase rab5 functions as a regulatory factor in the early endocytic pathway. Cell 70: 715–728.
23. Kneen M, Farinas J, Li Y, Verkman AS (1998) Green fluorescent protein as a noninvasive intracellular pH indicator. Biophys J 74: 1591–1599.
24. Wang DA, Sebti SM (2005) Palmitoylated cysteine 192 is required for RhoB tumor-suppressive and apoptotic activities. J Biol Chem 280: 19243–19249.
25. Sobo K, Le Blanc I, Luyet PP, Fivaz M, Ferguson C, et al. (2007) Late endosomal cholesterol accumulation leads to impaired intra-endosomal trafficking. PLoS ONE 2: e851.
26. Roth AF, Wan J, Bailey AO, Sun B, Kuchar JA, et al. (2006) Global analysis of protein palmitoylation in yeast. Cell 125: 1003–1013.
27. Abenza JF, Galindo A, Pinar M, Pantazopoulou A, de los Rios V, et al. (2012) Endosomal maturation by Rab conversion in Aspergillus nidulans is coupled to dynein-mediated basipetal movement. Mol Biol Cell 23: 1889–1901.
28. Williams RL, Urbe S (2007) The emerging shape of the ESCRT machinery. Nat Rev Mol Cell Biol 8: 355–368.
29. Nickerson DP, Russell MR, Odorizzi G (2007) A concentric circle model of multivesicular body cargo sorting. EMBO Rep 8: 644–650.
30. Dores MR, Chen B, Lin H, Soh UJ, Paing MM, et al. (2012) ALIX binds a YPX(3)L motif of the GPCR PAR1 and mediates ubiquitin-independent ESCRT-III/MVB sorting. J Cell Biol 197: 407–419.
31. Sahu R, Kaushik S, Clement CC, Cannizzo ES, Scharf B, et al. (2011) Microautophagy of cytosolic proteins by late endosomes. Dev Cell 20: 131–139.
32. Oeste CL, Seco E, Patton WF, Boya P, Pérez-Sala D (2013) Interactions between autophagic and endo-lysosomal markers in endothelial cells. Histochem Cell Biol 139: 159–170.
33. Koga H, Martinez-Vicente M, Macian F, Verkhusha VV, Cuervo AM (2011) A photoconvertible fluorescent reporter to track chaperone-mediated autophagy. Nat Commun 2: 386.
34. Klopper TH, Kienle N, Fasshauer D, Munro S (2012) Untangling the evolution of Rab G proteins: implications of a comprehensive genomic analysis. BMC Biol 10: 71.
35. Elias M, Brighouse A, Gabernet-Castello C, Field MC, Dacks JB (2012) Sculpting the endomembrane system in deep time: high resolution phylogenetics of Rab GTPases. J Cell Sci 125: 2500–2508.
36. Leung KF, Dacks JB, Field MC (2008) Evolution of the multivesicular body ESCRT machinery; retention across the eukaryotic lineage. Traffic 9: 1698–1716.
37. Lambou K, Tharreau D, Kohler A, Sirven C, Marguerettaz M, et al. (2008) Fungi have three tetraspanin families with distinct functions. BMC Genomics 9: 63.
38. Matsuo H, Chevallier J, Mayran N, Le Blanc I, Ferguson C, et al. (2004) Role of LBPA and Alix in multivesicular liposome formation and endosome organization. Science 303: 531–534.
39. Gilk SD, Cockrell DC, Luterbach C, Hansen B, Knodler LA, et al. (2013) Bacterial colonization of host cells in the absence of cholesterol. PLoS Pathog 9: e1003107.
40. Mobius W, van Donselaar E, Ohno-Iwashita Y, Shimada Y, Heijnen HF, et al. (2003) Recycling compartments and the internal vesicles of multivesicular bodies harbor most of the cholesterol found in the endocytic pathway. Traffic 4: 222–231.
41. Canto I, Trejo J (2013) Palmitoylation of protease-activated receptor-1 regulates adaptor protein complex-2 and -3 interaction with tyrosine-based motifs and endocytic sorting. J Biol Chem 288: 15900–15912.
42. Flannery AR, Czibener C, Andrews NW (2010) Palmitoylation-dependent association with CD63 targets the Ca2+ sensor synaptotagmin VII to lysosomes. J Cell Biol 191: 599–613.
43. Peng Y, Tang F, Weisman LS (2006) Palmitoylation plays a role in targeting Vac8p to specific membrane subdomains. Traffic 7: 1378–1387.
44. McCormick PJ, Dumaresq-Doiron K, Pluviose AS, Pichette V, Tosato G, et al. (2008) Palmitoylation controls recycling in lysosomal sorting and trafficking. Traffic 9: 1984–1997.
45. Michaelson D, Silletti J, Murphy G, D'Eustachio P, Rush M, et al. (2001) Differential localization of Rho GTPases in live cells: regulation by hypervariable regions and RhoGDI binding. J Cell Biol 152: 111–126.
46. Hirata D, Nakano K, Fukui M, Takenaka H, Miyakawa T, et al. (1998) Genes that cause aberrant cell morphology by overexpression in fission yeast: a role of a small GTP-binding protein Rho2 in cell morphogenesis. J Cell Sci 111 (Pt 2): 149–159.
47. Ma Y, Kuno T, Kita A, Asayama Y, Sugiura R (2006) Rho2 is a target of the farnesyltransferase Cpp1 and acts upstream of Pmk1 mitogen-activated protein kinase signaling in fission yeast. Mol Biol Cell 17: 5028–5037.
48. Roberts PJ, Mitin N, Keller PJ, Chenette EJ, Madigan JP, et al. (2008) Rho Family GTPase modification and dependence on CAAX motif-signaled posttranslational modification. J Biol Chem 283: 25150–25163.
49. Fortwendel JR, Juvvadi PR, Rogg LE, Asfaw YG, Burns KA, et al. (2012) Plasma membrane localization is required for RasA-mediated polarized morphogenesis and virulence of Aspergillus fumigatus. Eukaryot Cell 11: 966–977.
50. Amiya E, Watanabe M, Takeda N, Saito T, Shiga T, et al. (2013) Angiotensin II impairs endothelial nitric-oxide synthase bioavailability under free cholesterol-enriched conditions via intracellular free cholesterol-rich membrane microdomains. J Biol Chem 288: 14497–14509.
51. Toulmay A, Prinz WA (2013) Direct imaging reveals stable, micrometer-scale lipid domains that segregate proteins in live cells. J Cell Biol 202: 35–44.

Histochem Cell Biol
DOI 10.1007/s00418-012-1057-6

ORIGINAL PAPER

Interactions between autophagic and endo-lysosomal markers in endothelial cells

Clara L. Oeste · Esther Seco · Wayne F. Patton · Patricia Boya · Dolores Pérez-Sala

Accepted: 13 November 2012

Abstract Autophagic and endo-lysosomal degradative pathways are essential for cell homeostasis. Availability of reliable tools to interrogate these pathways is critical to unveil their involvement in physiology and pathophysiology. Although several probes have been recently developed to monitor autophagic or lysosomal compartments, their specificity has not been validated through co-localization studies with well-known markers. Here, we evaluate the selectivity and interactions between one lysosomal (Lyso-ID) and one autophagosomal (Cyto-ID) probe under conditions modulating autophagy and/or endo-lysosomal function in live cells. The probe for acidic compartments Lyso-ID was fully localized inside vesicles positive for markers of late endosome-lysosomes, including Lamp1-GFP and GFP-CINCCKVL. Induction of autophagy by amino acid deprivation in bovine aortic endothelial cells caused an early and potent increase in the fluorescence of the proposed autophagy dye Cyto-ID. Cyto-ID-positive compartments extensively co-localized with the autophagosomal fluorescent reporter RFP-LC3, although the time and/or threshold for organelle detection was different for each probe. Interestingly, use of Cyto-ID in combination with Lysotracker Red or Lyso-ID allowed the observation of structures labeled with either one or both probes, the extent of co-localization increasing upon treatment with protease inhibitors. Inhibition of the endo-lysosomal pathway with chloroquine or U18666A resulted in the formation of large Cyto-ID and Lyso-ID-positive compartments. These results constitute the first assessment of the selectivity of Cyto-ID and Lyso-ID as probes for the autophagic and lysosomal pathways, respectively. Our observations show that these probes can be used in combination with protein-based markers for monitoring the interactions of both pathways in live cells.

Keywords Endo-lysosomal pathway · Autophagy · Amino acid deprivation · Live cell fluorescence · Autophagosome marker · Endothelial cell

Introduction

The degradation of cell components is essential for homeostasis and it occurs through complex and highly regulated pathways. Both the endo-lysosomal and the autophagic pathways proceed through mechanisms linked to vesicular biogenesis and membrane trafficking.

The endo-lysosomal pathway begins at the plasma membrane and runs through several endosomal compartments leading to the lysosome, where membrane receptors and generally long-lived proteins are degraded. Early and late endosomes, multivesicular bodies and lysosomes bear distinct proteins such as Rab GTPases or integral membrane proteins (e.g. Lamp1) as well as a particular lipidic composition and increasingly acidic pH (Stenmark 2009). However, endo-lysosomal maturation involves molecular exchanges, fusion and budding events that blur the idea of distinct compartmentalization. Moreover, lysosomes

Electronic supplementary material The online version of this article (doi:10.1007/s00418-012-1057-6) contains supplementary material, which is available to authorized users.

C. L. Oeste · E. Seco · P. Boya · D. Pérez-Sala (✉)
Centro de Investigaciones Biológicas, Consejo Superior de Investigaciones Científicas, Ramiro de Maeztu, 9, 28040 Madrid, Spain
e-mail: dperezsala@cib.csic.es

W. F. Patton
Enzo Life Sciences, 10 Executive Blvd., Farmingdale, NY 11734, USA

Published online: 01 December 2012

degrade components of endocytic, autophagic or phagocytic origin, highlighting the convergence of these pathways (Saftig and Klumperman 2009). Given their pathophysiological importance, the search for selective markers of these pathways is an on-going task. Well-established markers of the endo-lysosomal pathway include fluorescent constructs of Rab5 and Rab7 for early and late endosomes, respectively (Bucci et al. 1992, 2000), and of Lamp1, for late endosomes and lysosomes (Patterson and Lippincott-Schwartz 2002). In addition, we recently described the localization of chimeric proteins bearing the C-terminal sequence of the endosomal GTPase RhoB (-CINCCKVL) in late endosomes and in the intraluminal vesicles of multivesicular bodies (Pérez-Sala et al. 2009). The dynamics of the endo-lysosomal pathway may be altered by lysosomotropic drugs. Many of these drugs, like chloroquine or chlorpromazine, will alter lysosomal flux, thus impairing also autophagic degradation and giving rise to enlarged lysosomes or lamellar bodies, which may represent the fusion of diverse organelles including late endosomes, lysosomes and autophagic vesicles, as suggested by the presence of markers of these various compartments (Pérez-Sala et al. 2009; Wang et al. 2011).

In a general sense, autophagy, or "self-eating" refers to a variety of complex and tightly regulated mechanisms by which cells sense nutrient levels and degrade cellular components to obtain molecules essential for cell homeostasis (please see Yang and Klionsky 2010 for review). In addition, autophagy is a general stress response that also degrades whole organelles, protein aggregates and intracellular pathogens. Initially considered a death mechanism it is clear now that autophagy plays critical roles in adaptation and survival. Three main types of autophagy have been defined, namely, *macroautophagy* (or autophagy), which involves the sequestration of cytosolic components into double-membrane vesicles which end up fusing with lysosomes, *microautophagy*, by which cytosolic constituents are directly sequestered into lysosomes, and *chaperone-mediated autophagy*, in which chaperones aid in transporting proteins bearing a specific sequence into lysosomes (Lee et al. 2012). The materials arising from degradation are delivered back to the cytosol for recycling or energy generation (reviewed in Chen and Klionsky 2011; Lee et al. 2012).

The autophagic and endo-lysosomal pathways may interact at several levels. Although it is generally accepted that autophagosomes fuse to lysosomes to deliver their contents for degradation, fusion at the level of early and late endosomes has also been reported (Dunn 1994; Liou et al. 1997; Berg et al. 1998). Given their multiple connections with other vesicular and degradative pathways, autophagy-specific processes are difficult to delineate. Therefore, the availability of well-characterized tools and assays is a critical issue (Klionsky et al. 2008, 2012; Mizushima et al. 2010).

The most widely used assay to monitor autophagy is the lipidation of the LC3 protein (microtubule-associated protein 1 light chain 3) that gives rise to LC3-II (Kabeya et al. 2000; Barth et al. 2010; Mizushima and Yoshimori 2007) and promotes its insertion into the membranes of autophagosomes (Barth et al. 2010; Mizushima et al. 2010). However, LC3 processing and dynamics in live cells are difficult to follow and their assessment requires transfection procedures, which are not exempt from artifacts (Klionsky et al. 2008). Therefore, there is an interest for the development of autophagy probes that can be used in live cells independently of transfection.

The recently developed Lyso-ID Red detection reagent (Lyso-ID) is an amphiphilic fluorescent probe that is actively sequestered in acidic compartments (Coleman et al. 2010) and is expected to stain lysosomes or lysosome-derived organelles arising upon block of lysosomal flux. However, it should not accumulate in early autophagosomes, which do not possess an acidic pH until the acquisition or activation of H^+-ATPase (Dunn 1994). Among the tools to monitor autophagy in live cells, the autofluorescent molecule monodansylcadaverine (MDC), has been reported to label autophagic vacuoles (Biederbick et al. 1995) and has been used as an autophagy probe (Munafo and Colombo 2001; Iwai-Kanai et al. 2008). MDC is a lysosomotropic agent reportedly showing increased fluorescence in hydrophobic environments (Niemann et al. 2000). Nevertheless, MDC specificity is controversial since in some works MDC staining was indistinguishable from that of lysosomal probes (Bampton et al. 2005). The Cyto-ID green reagent (Cyto-ID) is a cationic amphiphilic dye the fluorescence of which has been reported to increase upon autophagy induction (Warenius et al. 2011), hypothetically due to compartmentalization in the hydrophobic environment of autophagic vesicles. However, this probe has not been validated through co-localization studies with probes for autophagosomes. Moreover, its selectivity in combination with markers of other degradative compartments has not been assessed.

In this work, we have carried out a detailed study of the co-localization of Lyso-ID and Cyto-ID with well-known markers of autophagic and endo-lysosomal pathways in live cells. Our results show that Lyso-ID specifically stains acidic compartments bearing late-endosome/lysosome markers, whereas Cyto-ID fluorescence is highly sensitive to amino acid deprivation displaying extensive co-localization with RFP-LC3 and partial co-localization with lysosomal probes. These observations highlight the potential of these probes for monitoring both pathways in live cells.

Materials and methods

U18666A was from Merck4Biosciences (Spain). Chloroquine, 3-methyladenine (3-MA), rapamycin, leupeptin and E-64d were from Sigma. Culture media and supplements, Lipofectamine 2000 and Lysotracker Red (LTR) were from Life Technologies (Carlsbad, CA). Cyto-ID Green Detection Reagent for autophagy monitoring (Cyto-ID) and Lyso-ID Red Detection Reagent (Lyso-ID) were from Enzo Life Sciences.

Cell culture

Bovine aortic endothelial cells (BAEC) were obtained from Lonza, Inc., (Walkersville, MD) and cultured in RPMI1640 medium supplemented with penicillin/streptomycin and 10 % calf serum from Gibco (Life Technologies). BAEC were used between passages 5 and 12 and were grown to near confluence for experiments. HeLa cells were cultured in high glucose DMEM with 10 % FBS and penicillin/streptomycin. HeLa cells stably transfected with GFP-LC3 were kindly provided by Dr. Aviva Tolkovsky (Bampton et al. 2005).

Modulation of autophagy and the lysosomal pathway

Treatment of BAEC with the various agents used was carried out in serum-free medium. This situation induces a near-quiescent state and does not reduce cell viability (Hernández-Perera et al. 1998). Control cells received an equivalent amount of vehicle as required. For induction of autophagy, cells were incubated in amino acid-free medium (EBSS) for the times indicated. All further treatments and staining procedures were performed also in this medium to avoid autophagy reversion. The autophagy inducer rapamycin was used at 200 nM overnight, whereas the autophagy inhibitor 3-MA was added at 1.5 mg/ml for 6 h in medium containing or devoid of amino acids, as indicated. In order to disrupt the endo-lysosomal pathway, cells were treated with 10 μM U18666A or chloroquine for 20 h. U18666A causes an entrapment of cholesterol and bis(monoacylglycero)phosphate (BMP)-rich membranes into late endosomes and an inhibition of the dynamics of internal vesicles (Kobayashi et al. 1999; Sobo et al. 2007). At the concentrations used in this study, chloroquine inhibits lysosomal protein degradation and induces lysosome enlargement but does not impair the accumulation of probes for acidic compartments (Pérez-Sala et al. 2009), nor induces significant changes in lysosomal pH as estimated with Lysosensor DND-160 (Invitrogen) following the instructions of the manufacturer: control 4.4 ± 0.03, chloroquine 4.5 ± 0.09, average ± SD of three determinations.

Plasmids and transfections

Lamp1-GFP was a gift from Prof. Jennifer Lippincott-Schwartz (NIH, Bethesda, MD). RFP-LC3 was from Prof. Tamotsu Yoshimori (Research Institute for Microbial Diseases, Osaka, Japan). The construct GFP-CINCCKVL (GFP-8) containing the last eight amino acids from the GTPase RhoB has been previously described (Pérez-Sala et al. 2009; Valero et al. 2010). Cells at 80 % confluence were transfected with Lipofectamine 2000 (Life Technologies) following the manufacturer's instructions. For transfection of single constructs, 1 μg of plasmid plus 3 μl of Lipofectamine were used per 35 mm dish, whereas for co-transfections, DNA/Lipofectamine mixtures were prepared with 1 μg of each construct plus 4.5 μl of the transfection reagent. After transfection, cells were allowed to recover for 24 h in complete medium before treatments. Unless otherwise stated, imaging of live cells was performed 48 h after transfection to minimize its effects.

Staining with lysosomal or autophagosomal small molecule probes

Several variations to the manufacturer's recommended staining procedures were introduced in order to enhance probe performance. Lyso-ID and Cyto-ID were diluted in the total volume of serum-free culture medium to be used for staining at 37 °C for 30 min. This was found to improve the maintenance of endothelial cell morphology and viability during cell imaging. Incubation in the presence of serum reduced the intensity of the staining in BAEC. In experiments in which autophagy was induced by incubation of cells with EBSS, staining and washing (for autophagy reversion experiments) was also performed in this medium. LTR staining was performed by incubation of cells with 25 nM LTR for 15 min at 37 °C. In the case of Cyto-ID/LTR co-staining, LTR was added to the medium of cells that had been incubated with Cyto-ID for 15 min, left for an additional 15 min to co-stain and visualized immediately afterwards. For MDC staining, cells were incubated with 50 μM MDC (Sigma) for 10 min at 37 °C, and washed three times with the medium used for treatment before visualization.

Confocal microscopy

For live cell confocal microscopy, cells were cultured on glass bottom dishes (Mattek Corp., Ashland, MA, USA), transfected with fluorescent constructs, treated with the indicated agents and visualized directly on a confocal microscope (LEICA DMRE2, Heidelberg, Germany). Unless otherwise stated, images shown are single Z-section images for co-localization assessment and scale bars represent 20 μm. Images were obtained shortly after staining

to minimize loss of fluorescence. Care was taken to briefly observe cells under the UV lamp before imaging to minimize fading of the probes. In the case of Lyso-ID, this was also important to avoid organelle damage, as it has been described for other lysosomal dyes (Jaiswal et al. 2007; Alvarez et al. 2011). For MDC visualization, the excitation and emission wavelengths were set at 351 and 500 nm, respectively.

Image analysis

Co-localization analysis was performed with LAS-AF software from Leica as follows. Single Z-sections of images with multiple cells were analyzed to obtain co-localization rates and Pearson coefficients. For stained cells, whole-field images were analyzed, whereas in the case of transfected cells, ROIs including transfected cells and excluding non-transfected cells were delimited prior to image analysis. At least 30 cells, for co-localization studies or 100 cells, for RFP-LC3 distribution were analysed per experimental condition. Results are presented as mean co-localization rates expressed as percentages, which were comparable to the corresponding mean Pearson coefficients (not shown).

Western blot

In preparation for SDS-PAGE, cells were homogenized by forced passes through a $26^{1/2}$-gauge needle in 50 mM Tris, pH 6.8, 10 % glycerol, 2 % SDS, 0.1 mM β-mercaptoethanol, 50 mM sodium fluoride and 0.1 mM sodium orthovanadate containing 2 μg/ml of the protease inhibitors leupeptin and aprotinin as well as 1.3 mM Pefablock. Protein concentration was estimated by the BCA method (Pierce Chemical, Rockford, IL, USA). Volumes equivalent to 30 μg of protein were run on 15 % SDS-polyacrylamide gels and transferred to Immobilon-P membranes (Millipore, Bedford, MA, USA) using a semi-dry transfer method. Blots were incubated with monoclonal anti-LC3B (Cell Signaling Technologies, Beverly, MA, USA) or anti-actin (Sigma-Aldrich Chemicals, St Louis, MO, USA) antibodies at 1:1,000 dilution and proteins of interest were detected by ECL (GE Healthcare, Buckinghamshire, UK). Blots were quantified using ImageJ software (US National Institutes of Health, Bethesda, MD, USA).

Results

Lyso-ID is localized in late-endosomes/lysosomes

In order to assess the performance of Lyso-ID, we used it in combination with Lamp1-GFP, a fluorescent construct of the well-known protein constituent of late endosomes and lysosomes and with GFP-CINCCKVL (GFP-8), a protein-based probe that localizes to the endosomal pathway in endothelial cells (Pérez-Sala et al. 2009; Valero et al. 2010). We observed that Lyso-ID was accumulated inside vesicles that were delimited by Lamp1-GFP (Fig. 1a) and by GFP-8 (Fig. 1b) thus indicating their endo-lysosomal nature. Incubation of BAEC with chloroquine led to the formation of giant vesicular bodies, as we previously reported (Pérez-Sala et al. 2009), in which Lyso-ID was accumulated. In addition, this probe accumulated in the dense bodies induced by U18666A, an agent which disrupts late endosome dynamics (Valero et al. 2010). The patterns obtained with Lyso-ID were similar to those observed with the widely used lysosomal probe LTR (Fig. S1). Therefore, these observations indicate that in living cells Lyso-ID is confined to a late-endosomal/lysosomal compartment.

Characterization of Cyto-ID distribution upon autophagy induction by amino acid deprivation in BAEC

Bovine aortic endothelial cells have been reported to undergo autophagy in response to nutrient deprivation induced by incubation in the presence of 2-deoxy-glucose or by incubation in glucose-deficient medium (Wang et al. 2011; Du et al. 2012). However, autophagy induction by a classical stimulus such as amino acid deprivation, to the best of our knowledge, has not been reported. Interestingly, in this model, amino acid deprivation by incubation in EBSS medium resulted in a time-dependent decrease of endogenous LC3-I and II levels (Fig. 2a). This was likely due to consumption caused by degradation, as previously reported in other models (Sato et al. 2007; Mizushima and Yoshimori 2007). Consistent with this, inhibition of lysosomal degradation with protease inhibitors (leupeptin plus E-64d, Fig. 2a, right panels) or with chloroquine (not shown) attenuated the disappearance of LC3-I/II and increased the proportion of LC3-II. Control cells for these assays were serum starved. Serum deprivation per se induced only minor changes in LC3 levels (Fig. 2a). A detailed assessment of the kinetics and distribution of the autophagosomal fluorescent reporter RFP-LC3 and the fluorescent probe Cyto-ID upon autophagy induction in live cells is shown in Fig. S2. In control cells, transfected RFP-LC3 (Fig. S2a) showed a predominantly diffuse distribution, although cells with some localized accumulations of RFP-LC3 could also be observed (21 ± 2 % of cells, average ± SEM of a least four experiments). Amino acid deprivation induced an increase in the proportion of cells showing bright RFP-LC3 aggregates (49 ± 5 % of cells after 6 h, $p < 0.01$ by Student's t test vs. control, and

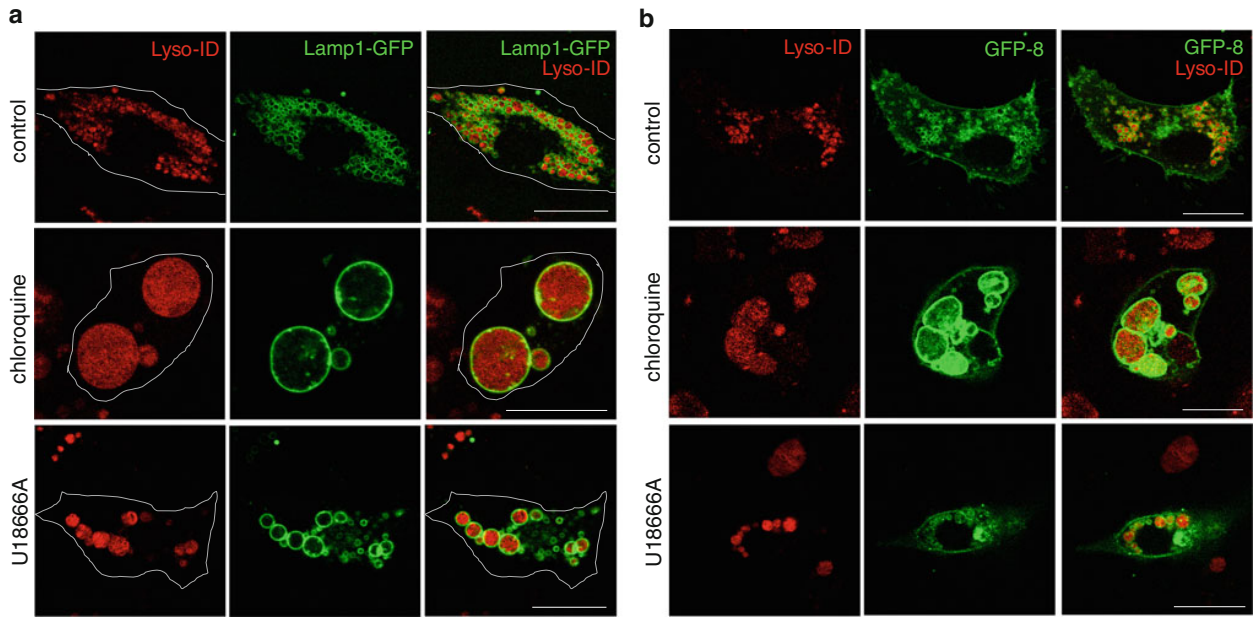

Fig. 1 Distribution of Lyso-ID dye, Lamp1-GFP and GFP-8. BAEC transiently transfected with Lamp1-GFP (**a**) or GFP-8 (**b**) were treated with the indicated agents in the absence of serum for 20 h. After treatment, cells were stained with Lyso-ID. *Scale bar* 20 μm

79 ± 1 % of cells after 24 h, $p < 0.01$ by Student's t test vs. control and 3 h EBSS). Interestingly, Cyto-ID staining was negligible in control cells and increased rapidly upon amino acid deprivation (Fig. S2b), in such a way that virtually all cells showed a bright particulate fluorescent pattern as early as 30 min after amino acid withdrawal. This pattern was consistent up to 24 h incubation in EBSS. Quantitation of Cyto-ID fluorescence by flow cytometry showed a maximal increase 3 h after amino acid withdrawal followed by a slow decline, with intensity remaining 2.7-fold higher than that of control cells after 24 h (not shown). Taken together, these observations show that both transfected RFP-LC3 and Cyto-ID reflect autophagy induction but with different kinetics, with the pattern obtained with Cyto-ID being more homogeneous in the cell population and with a more rapid induction reflecting alterations induced by amino acid deprivation under our experimental conditions.

To assess the nature of Cyto-ID-labeled structures, we next performed Cyto-ID-RFP-LC3 co-localization studies (Fig. 2b). Co-localization of Cyto-ID with RFP-LC3-positive accumulations was obvious from 3 h (38 ± 9.5 % co-localization, average ± SEM of at least six determinations, $p < 0.01$ by Student's t test vs. control), and was substantial after 20 h (80 ± 3.7 % co-localization, $p < 0.01$ by Student's t test vs. control and 3 h EBSS). Treatment in the presence of protease inhibitors, leupeptin plus E-64d, increased the size of vesicles positive for both probes, indicative of RFP-LC3/autophagosomal material accumulation after blocking lysosomal degradation (Fig. 2c).

In order to substantiate the correlation between autophagy and Cyto-ID staining, we assessed this parameter after modulation of autophagy induction by well-known agents (Fig. 3). Reversion of autophagy by incubation with amino acid-containing medium for 30 min was sufficient to lose most of the Cyto-ID signal. On the other hand, treatment of BAEC in the presence of the autophagy inhibitor 3-MA during amino acid deprivation clearly reduced Cyto-ID fluorescence. Finally, the autophagy inducer rapamycin elicited a detectable increase in the Cyto-ID signal, which could be evidenced also by flow cytometry (not shown). In contrast, staining with MDC was undistinguishable in control and amino acid-deprived cells (Fig. S3), and overlap with the Cyto-ID signal was absent in control cells, which were not stained with Cyto-ID, and partial in amino acid-deprived cells. Taken together, these observations indicate the existence of a good correlation between autophagy induction and Cyto-ID staining.

Localization of Cyto-ID in combination with lysosomal probes

Next, we assessed whether Cyto-ID and Lyso-ID or LTR could be used in combination, and if so, if these probes retained selectivity for autophagosomal or lysosomal pathways (Fig. 4). Upon autophagy induction by incubation in EBSS, co-localization between Cyto-ID and either

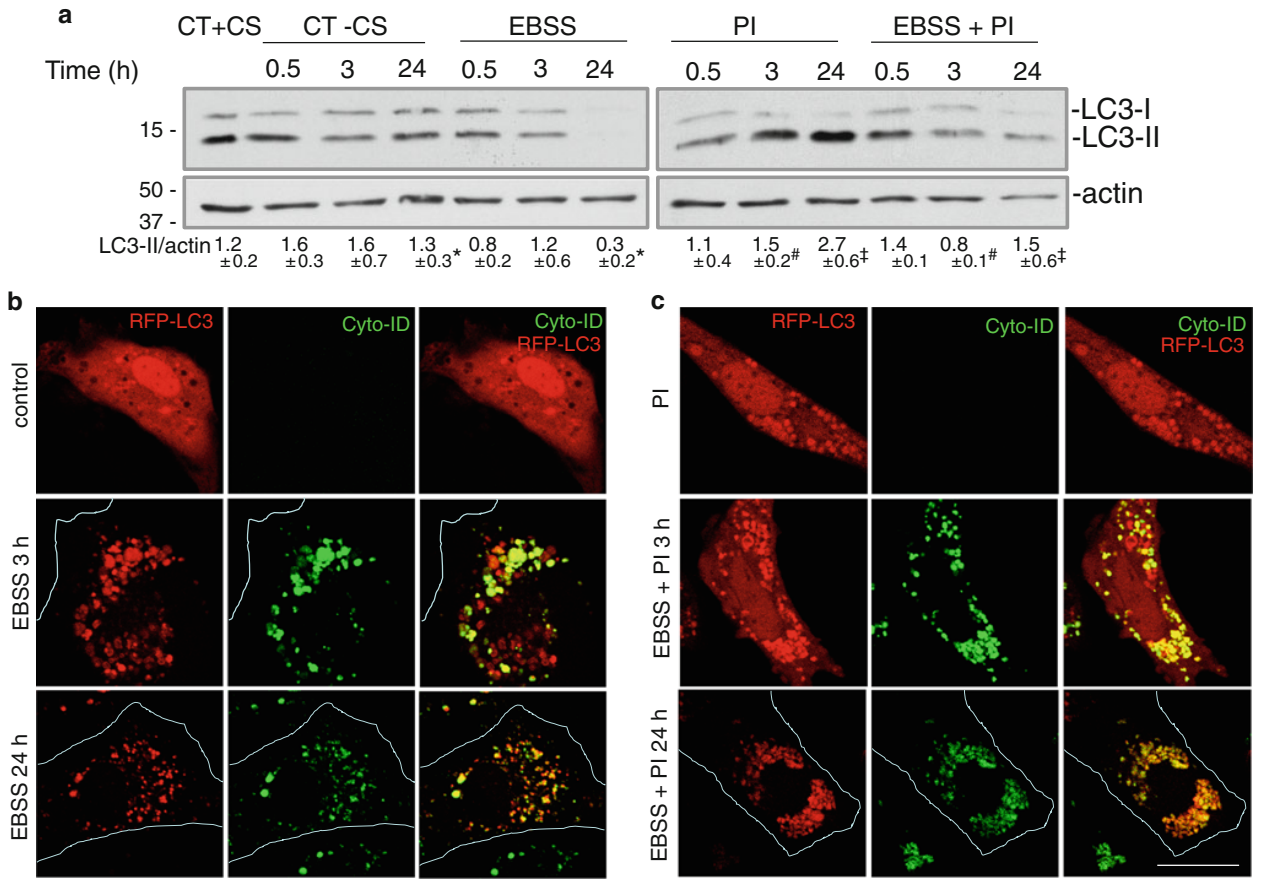

Fig. 2 Induction of autophagy by amino acid deprivation in BAEC and characterization of Cyto-ID distribution. **a** Western blotting was performed as described in "Materials and methods" to detect endogenous LC3B levels upon amino acid starvation (EBSS) and/or treatment with 10 μg/ml of the protease inhibitors leupeptin and E-64d (PI) for the times indicated. Results are representative of three experiments. The ratio of LC3 II/actin (average values ± standard error of mean) is shown below (*pairs of symbols* indicate conditions between which statistically significant differences were found, $p < 0.05$ by Student's t test). *CT + CS* control medium plus calf serum, *CT − CS* control medium minus calf serum. **b**, **c** Co-localization of Cyto-ID and RFP-LC3 was assessed in BAEC transfected with RFP-LC3 and incubated in serum-free medium or EBSS in the absence (**b**) or presence (**c**) of protease inhibitors. Cyto-ID staining was performed as indicated in "Materials and methods" and cells were immediately imaged by confocal microscopy. Individual sections are shown

lysosomal probe was partial (60 ± 4.1 % with LTR and 30 ± 4.8 % with Lyso-ID) and compartments positive only for Cyto-ID or for LTR or Lyso-ID could be detected, as well as compartments with mixed staining suggestive of fusion events (Fig. 4a, b, see detail). To obtain additional evidence of the existence of independent autophagosomal and endo-lysosomal structures under these experimental conditions we co-transfected cells with RFP-LC3 and GFP-8 (Fig. 4c). These constructs showed different distribution patterns, both under control conditions and after autophagy induction (see co-localization profiles). Taken together, these results indicate that Cyto-ID stains defined compartments, some of which are non-acidic. Whether these compartments represent early autophagosomes not yet fused with lysosomes warrants further investigation.

Finally, we explored the distribution of these probes in cells treated with agents known to disrupt the lysosomal pathway. The giant acidic vesicles induced by chloroquine showed a weak diffuse Cyto-ID signal (Fig. 5a, b), which increased after autophagy induction with EBSS. Interestingly, RFP-LC3 also gave a faint signal in chloroquine-induced vesicles, which increased in EBSS-cultured cells (Fig. 5c). However, although co-localization of Cyto-ID and lysosomal probes was extensive in these compartments, individual lysosomes (stained with lysosomal probes only) could still be detected. A stronger Cyto-ID signal was also observed in most, but not all, of the compartments induced by treatment with U18666A (Fig. S4a, b). Thus, disruption of the lysosomal pathway affects Cyto-ID and Lyso-ID staining differently.

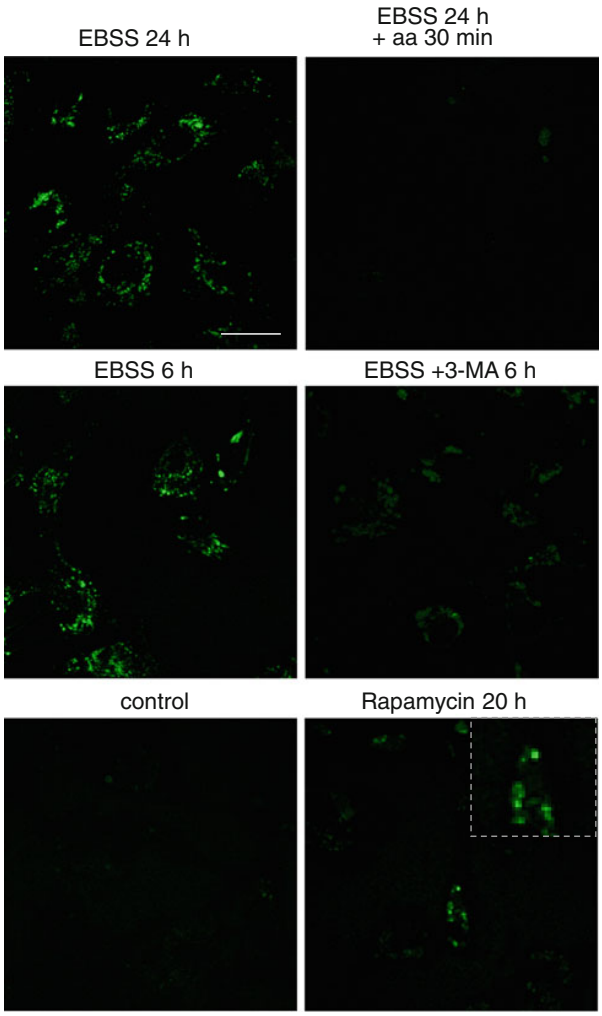

Fig. 3 Effect of modulators of autophagy on Cyto-ID staining in BAEC. *Top panels* BAEC treated with EBSS for 24 h and stained with Cyto-ID were incubated with amino acid-containing medium (aa) for 30 min, as indicated, and immediately imaged by confocal microscopy. *Middle panels* BAEC were incubated in EBSS with or without 1.5 mg/ml of 3-methyladenine (3-MA) for 6 h and stained with Cyto-ID as previously described. *Bottom panels* BAEC were incubated in serum-free medium with vehicle or 200 nM rapamycin overnight and stained with Cyto-ID immediately before confocal imaging

Remarkably, we observed that staining with Cyto-ID in the presence of Lyso-ID resulted in a weaker Cyto-ID staining than with Cyto-ID alone or Cyto-ID plus LTR (Fig. S4c). This could account for the lower values obtained for Cyto-ID/Lyso-ID co-localization compared to the Cyto-ID/LTR combination. Although this observation does not preclude the use of both probes in combination since the quenching effect can be overcome by adjusting the settings for data acquisition, the detection conditions are not optimal, and in this case combination of Cyto-ID with other lysosomal probes may offer better performance.

Localization of Lyso-ID and Cyto-ID in HeLa cells

In order to assess the behaviour of Cyto-ID and Lyso-ID in a different cell type, we used HeLa cells. As it is shown in Fig. 6a, Lyso-ID showed little overlap with GFP-LC3 under control conditions or upon amino acid deprivation, the co-localization increasing, as expected, in the presence of chloroquine. In turn, Cyto-ID staining was negligible under control conditions and increased upon amino acid deprivation showing a clear overlap with RFP-LC3 (Fig. 6b).

Discussion

Autophagy is a key process in cell homeostasis which involves de novo generation of organelles in a short time frame along with traffic and fusion processes with other vesicular compartments, i.e., endo-lysosomes. Therefore, there is great interest in the development of tools that allow monitoring autophagy in live cells in real time. In this work, we have assessed the distribution of various probes intended to monitor lysosomal and autophagic pathways. Our results show that in live BAEC, endo-lysosomes and autophagosomes can be distinguished using various probes, including LTR, Lyso-ID and GFP-8 for endo-lysosomes and RFP-LC3 for autophagosomes. Moreover, the Cyto-ID probe labels structures distinct from acidic vesicles and responds to various stimuli which modulate autophagy, displaying a substantial co-localization with RFP-LC3 in this experimental model. Therefore, more detailed identification of the precise target(s) of Cyto-ID may provide key information for the study of autophagy.

Under our experimental conditions, Lyso-ID showed high selectivity for acidic compartments as demonstrated by its localization inside vesicles delimited by Lamp1-GFP and GFP-8. Moreover, it reflected the alterations induced by disrupting lysosomal function with chloroquine or inhibiting late endosome dynamics with U18666A. Mechanistically, the recently developed probe Cyto-ID is based upon similar principles as MDC. Analogously to MDC, selective labelling of autophagic vesicles by Cyto-ID is thought to arise from its interaction with the hydrophobic lamellar structures associated with autophagic vesicles (Niemann et al. 2000). However, MDC may accumulate into acidic compartments due to an ion trapping-mediated mechanism and yield substantial basal labelling overlapping with acidic vesicles (Munafo and Colombo 2001, Bampton et al. 2005). Indeed, we observed that MDC gave intense vesicle staining which was undistinguishable under control conditions and upon autophagy induction. In contrast, staining with Cyto-ID under control conditions was negligible. This may be due to the titratable functional

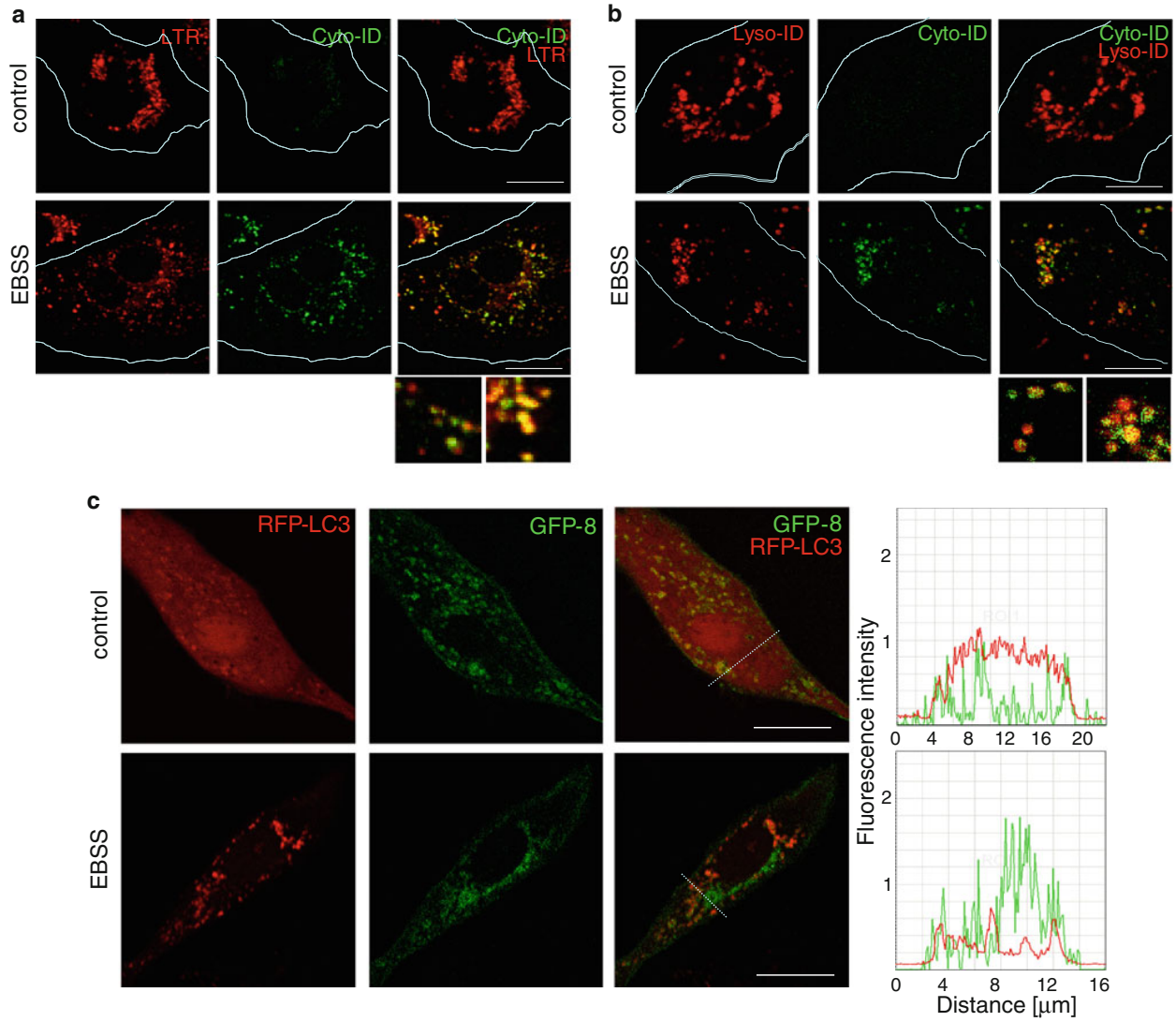

Fig. 4 Co-localization of autophagic and endo-lysosomal probes in BAEC. **a**, **b** BAEC were incubated in serum-free medium (control) or EBSS for 20 h prior to staining with Cyto-ID and LTR (**a**) or Lyso-ID (**b**) as described in "Materials and methods". **c** BAEC were co-transfected with RFP-LC3 and GFP-CINCCKVL (GFP-8). *Right panels* show the fluorescence intensity of the single channels along the lines depicted in the images

groups introduced in this dye to prevent its accumulation within lysosomes. After autophagy induction, the overlap between Cyto-ID and MDC labelling was only partial. Moreover, upon amino acid deprivation, it was possible to detect bright Cyto-ID compartments, which were not stained by lysosomal probes, thus indicating that Cyto-ID stains more than just acidic vesicles. Conversely, under all experimental conditions, acidic (LTR- or Lyso-ID-positive) vesicles were observed that were not stained by Cyto-ID, probably reflecting a different lipidic composition. Nevertheless, care should be exercised when using these probes and ideally they should be used in combination with compartment-specific markers. However, it should be taken into account that protein-based fluorescent probes for autophagy are not free of potential artifacts since both RFP and GFP tend to oligomerize when overexpressed in cells, and the use of constitutive expression plasmids may not reflect effects related to transcriptional or post-transcriptional regulation.

In contrast to glucose deprivation-induced autophagy in BAEC (Wang et al. 2011; Du et al. 2012), we found that the most obvious effect of amino acid deprivation in this cell type is a decrease in the levels of both endogenous proteins LC3-I and II, probably due to an increase in degradation dynamics, since it was attenuated by treatment with protease inhibitors. Noteworthy, serum starvation in

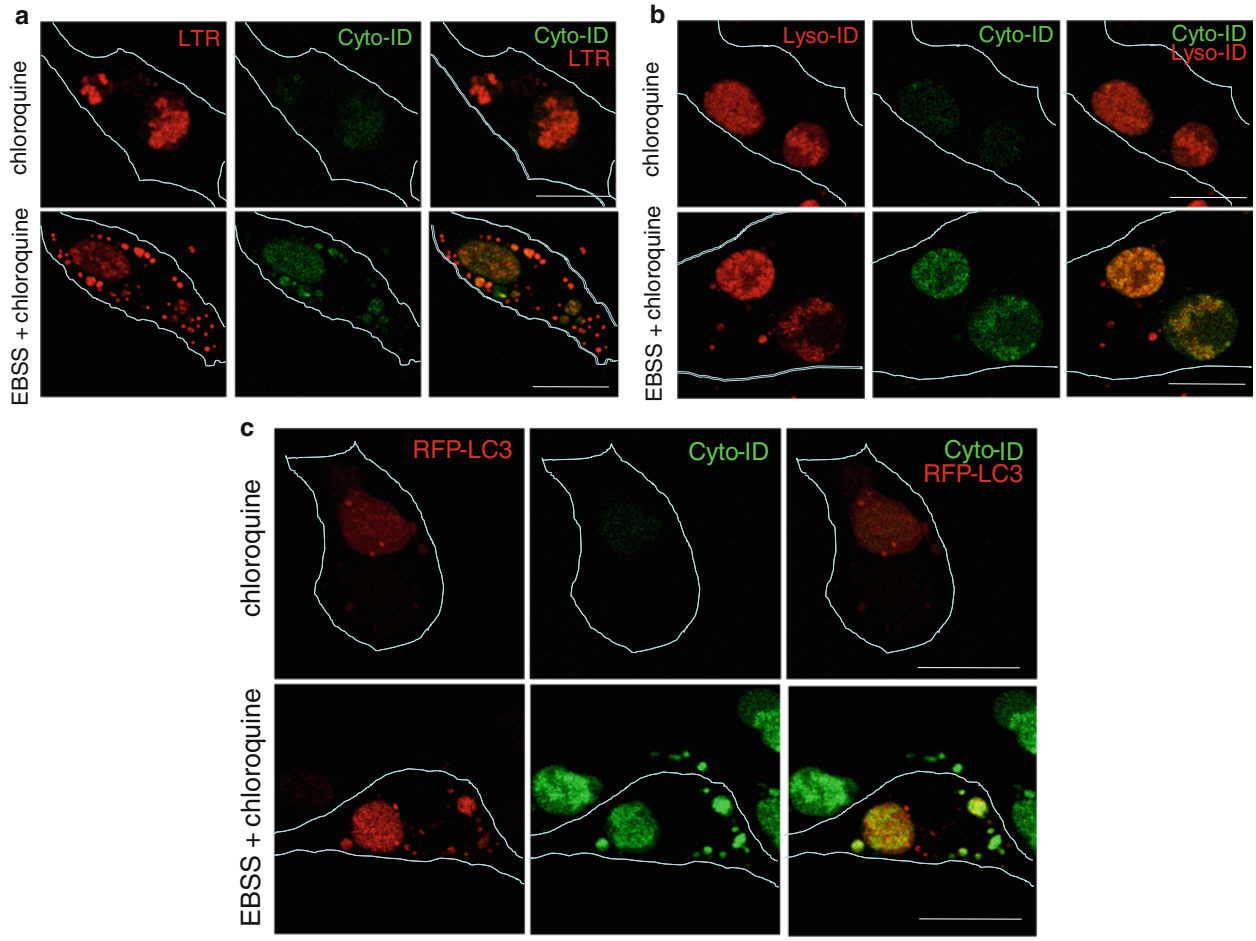

Fig. 5 Effect of chloroquine on the distribution of endo-lysosomal and autophagy probes in BAEC. **a**, **b** Cells were treated with chloroquine in serum-free medium or EBSS, as indicated. Chloroquine was used at 10 μM. **c** BAEC transfected with RFP-LC3 were treated with chloroquine as in (**a**, **b**). Staining with Cyto-ID and LTR or Lyso-ID was performed as detailed in "Materials and methods"

BAEC did not result in increased autophagy, as revealed by the LC3 blot and by the absence of RFP-LC3 accumulations, nor altered Cyto-ID staining. Interestingly, the three different assays shown in Figs. 2a and S2 revealed different features of amino acid deprivation-induced BAEC autophagy: endogenous LC3 decreased from 3 h, exogenous RFP-LC3 illustrated the punctate distribution typical of association with autophagosomes, which increased clearly after 3–6 h and the putative small molecule probe for autophagic vesicles Cyto-ID readily formed bright dots upon amino acid starvation. This may indicate that Cyto-ID partitions more rapidly and homogeneously than exogenous RFP-LC3 into membranous structures upon autophagy induction. This could also account for the differences in fluorescence intensity of the RFP-LC3 and Cyto-ID signals in compartments positive for both probes. The pattern obtained with Cyto-ID did not vary in transfected and non-transfected cells, thus ruling out the possibility that it could be influenced by transfection-related membrane perturbations. It should be noted that transient transfection was performed here due to the impossibility of establishing stably transfected cell lines from primary culture BAEC. Nevertheless, being a putative lipid-binding probe, labelling with Cyto-ID could be affected by agents altering vesicle membrane composition. In this vein, impairment of cholesterol traffic by treatment with U18666A, a pharmacological model of Niemann–Pick Type C disease, induced the appearance of dense acidic bodies. Nevertheless, not all of these dense structures were labelled by Cyto-ID. Interestingly, similarly to our observations, previous studies showed that only some of the dense compartments induced by U18666A treatment were positive for LC3 (Ishibashi et al. 2009), although at present there is no agreement as to whether U18666A induced-alterations reflect increased autophagy (Ishibashi et al. 2009; Pacheco et al. 2007). Treatment of cells with chloroquine may also pose some questions. The observation that the Cyto-ID signal inside chloroquine-induced compartments appears to

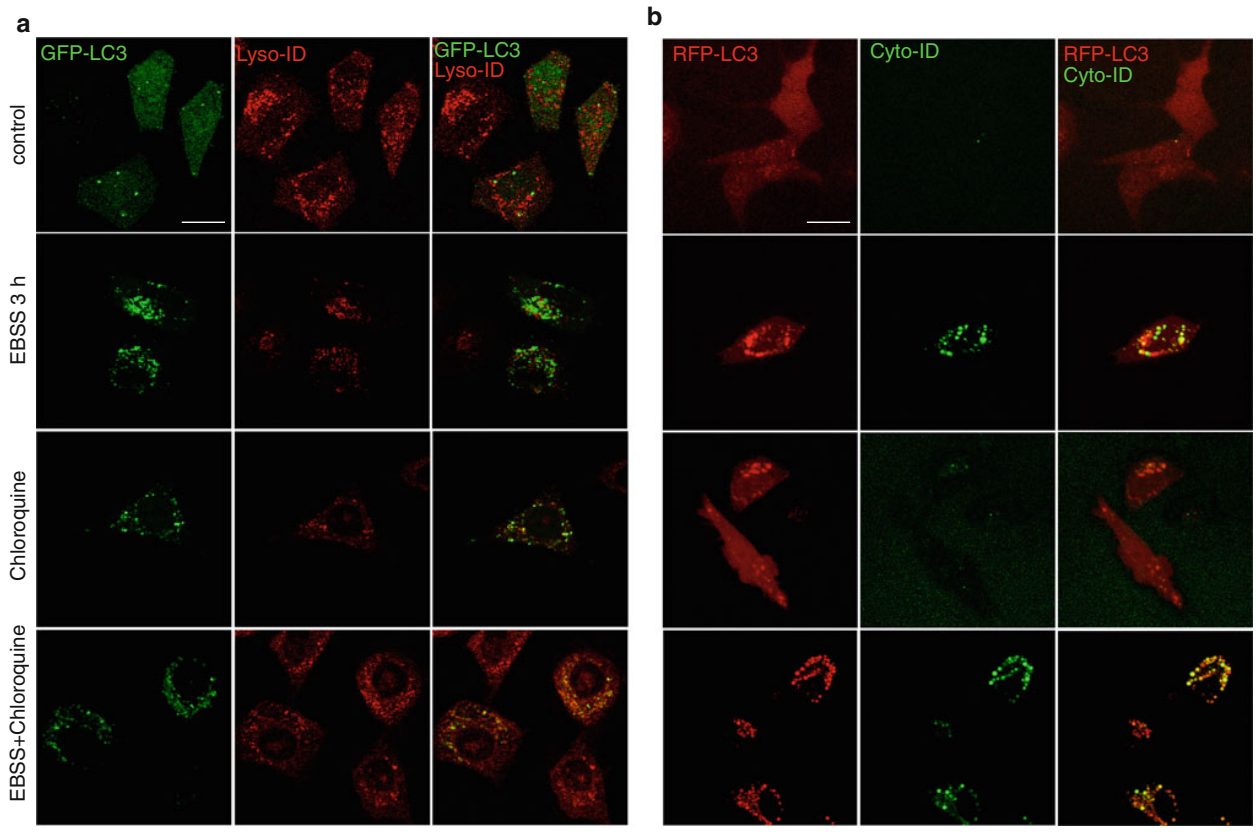

Fig. 6 Localization of Lyso-ID and Cyto-ID probes with fluorescent constructs of the autophagosomal reporter LC3 in HeLa. HeLa cells were stably (**a**) or transiently (**b**) transfected with the indicated LC3 constructs. Cell treatments and labelling with the probes were as indicated in "Materials and methods". Images shown are representative from two experiments and correspond to individual sections

be lower than that of EBSS-induced vesicles could be due to a lesser accumulation of the probe, this in turn being related to chloroquine-induced minor pH changes and/or to the heterogeneous nature of membranes accumulated in these structures.

One important observation of this work is that independent structures labeled selectively with autophagy probes or with endo-lysosomal probes can be observed under our experimental conditions. Moreover, merging structures were observed, which could be indicative of fusion events between autophagosomes and endo-lysosomes.

In view of the numerous assays for monitoring the autophagic pathway being developed, the results herein presented provide novel information on the usefulness and limitations of several widely accepted as well as recently developed autophagy probes and stress the importance of using various approaches in combination in order to minimize misinterpretations in the analysis of this complex process.

Acknowledgments This work was supported by grants SAF2009-11642 (financed in part by Plan E), and SAF2012-36519 (MINECO), RETIC RD07/0007/64 and PIE201020E031 to DPS, and by SAF2009-08086 to PB. CLO is the recipient of a fellowship from the FPI Program (MINECO).

References

Alvarez M, Villanueva A, Acedo P, Canete M, Stockert JC (2011) Cell death causes relocalization of photosensitizing fluorescent probes. Acta Histochem 113:363–368. doi:10.1016/j.acthis.2010.01.008

Bampton ET, Goemans CG, Niranjan D, Mizushima N, Tolkovsky AM (2005) The dynamics of autophagy visualized in live cells: from autophagosome formation to fusion with endo/lysosomes. Autophagy 1:23–36

Barth S, Glick D, Macleod KF (2010) Autophagy: assays and artifacts. J Pathol 221:117–124. doi:10.1002/path.2694

Berg TO, Fengsrud M, Stromhaug PE, Berg T, Seglen PO (1998) Isolation and characterization of rat liver amphisomes. Evidence for fusion of autophagosomes with both early and late endosomes. J Biol Chem 273:21883–21892

Biederbick A, Kern HF, Elsasser HP (1995) Monodansylcadaverine (MDC) is a specific in vivo marker for autophagic vacuoles. Eur J Cell Biol 66:3–14

Bucci C, Parton RG, Mather IH, Stunnenberg H, Simons K, Hoflack B, Zerial M (1992) The small GTPase rab5 functions as a regulatory factor in the early endocytic pathway. Cell 70:715–728

Bucci C, Thomsen P, Nicoziani P, McCarthy J, van Deurs B (2000) Rab7: a key to lysosome biogenesis. Mol Biol Cell 11:467–480

Chen Y, Klionsky DJ (2011) The regulation of autophagy—unanswered questions. J Cell Sci 124:161–170. doi:10.1242/jcs.064576

Coleman J, Xiang Y, Pande P, Shen D, Gatica D, Patton WF (2010) A live-cell fluorescence microplate assay suitable for monitoring vacuolation arising from drug or toxic agent treatment. J Biomol Screen 15:398–405

Du J, Teng RJ, Guan T, Eis A, Kaul S, Konduri GG, Shi Y (2012) Role of autophagy in angiogenesis in aortic endothelial cells. Am J Physiol Cell Physiol 302:C383–C391. doi:10.1152/ajpcell.00164.2011

Dunn WA Jr (1994) Autophagy and related mechanisms of lysosome-mediated protein degradation. Trends Cell Biol 4:139–143

Hernández-Perera O, Pérez-Sala D, Navarro-Antolín J, Sánchez-Pascuala R, Hernández G, Díaz C, Lamas S (1998) Effects of the 3-hydroxy-3-methylglutaryl-CoA reductase inhibitors, atorvastatin and simvastatin, on the expression of endothelin-1 and endothelial nitric oxide synthase in vascular endothelial cells. J Clin Invest 101:2711–2719

Ishibashi S, Yamazaki T, Okamoto K (2009) Association of autophagy with cholesterol-accumulated compartments in Niemann–Pick disease type C cells. J Clin Neurosci 16:954–959

Iwai-Kanai E, Yuan H, Huang C, Sayen MR, Perry-Garza CN, Kim L, Gottlieb RA (2008) A method to measure cardiac autophagic flux in vivo. Autophagy 4:322–329

Jaiswal JK, Fix M, Takano T, Nedergaard M, Simon SM (2007) Resolving vesicle fusion from lysis to monitor calcium-triggered lysosomal exocytosis in astrocytes. Proc Natl Acad Sci USA 104:14151–14156. doi:10.1073/pnas.0704935104

Kabeya Y, Mizushima N, Ueno T, Yamamoto A, Kirisako T, Noda T, Kominami E, Ohsumi Y, Yoshimori T (2000) LC3, a mammalian homologue of yeast Apg8p, is localized in autophagosome membranes after processing. EMBO J 19:5720–5728. doi:10.1093/emboj/19.21.5720

Klionsky DJ, Abeliovich H, Agostinis P, Agrawal DK, Aliev G, Askew DS, Baba M, Baehrecke EH, Bahr BA, Ballabio A, Bamber BA, Bassham DC, Bergamini E, Bi X, Biard-Piechaczyk M, Blum JS, Bredesen DE, Brodsky JL, Brumell JH, Brunk UT, Bursch W, Camougrand N, Cebollero E, Cecconi F, Chen Y, Chin LS, Choi A, Chu CT, Chung J, Clarke PG, Clark RS, Clarke SG, Clave C, Cleveland JL, Codogno P, Colombo MI, Coto-Montes A, Cregg JM, Cuervo AM, Debnath J, Demarchi F, Dennis PB, Dennis PA, Deretic V, Devenish RJ, Di Sano F, Dice JF, Difiglia M, Dinesh-Kumar S, Distelhorst CW, Djavaheri-Mergny M, Dorsey FC, Droge W, Dron M, Dunn WA, Jr., Duszenko M, Eissa NT, Elazar Z, Esclatine A, Eskelinen EL, Fesus L, Finley KD, Fuentes JM, Fueyo J, Fujisaki K, Galliot B, Gao FB, Gewirtz DA, Gibson SB, Gohla A, Goldberg AL, Gonzalez R, Gonzalez-Estevez C, Gorski S, Gottlieb RA, Haussinger D, He YW, Heidenreich K, Hill JA, Hoyer-Hansen M, Hu X, Huang WP, Iwasaki A, Jaattela M, Jackson WT, Jiang X, Jin S, Johansen T, Jung JU, Kadowaki M, Kang C, Kelekar A, Kessel DH, Kiel JA, Kim HP, Kimchi A, Kinsella TJ, Kiselyov K, Kitamoto K, Knecht E, Komatsu M, Kominami E, Kondo S, Kovacs AL, Kroemer G, Kuan CY, Kumar R, Kundu M, Landry J, Laporte M, Le W, Lei HY, Lenardo MJ, Levine B, Lieberman A, Lim KL, Lin FC, Liou W, Liu LF, Lopez-Berestein G, Lopez-Otin C, Lu B, Macleod KF, Malorni W, Martinet W, Matsuoka K, Mautner J, Meijer AJ, Melendez A, Michels P, Miotto G, Mistiaen WP, Mizushima N, Mograbi B, Monastyrska I, Moore MN, Moreira PI, Moriyasu Y, Motyl T, Munz C, Murphy LO, Naqvi NI, Neufeld TP, Nishino I, Nixon RA, Noda T, Nurnberg B, Ogawa M, Oleinick NL, Olsen LJ, Ozpolat B, Paglin S, Palmer GE, Papassideri I, Parkes M, Perlmutter DH, Perry G, Piacentini M, Pinkas-Kramarski R, Prescott M, Proikas-Cezanne T, Raben N, Rami A, Reggiori F, Rohrer B, Rubinsztein DC, Ryan KM, Sadoshima J, Sakagami H, Sakai Y, Sandri M, Sasakawa C, Sass M, Schneider C, Seglen PO, Seleverstov O, Settleman J, Shacka JJ, Shapiro IM, Sibirny A, Silva-Zacarin EC, Simon HU, Simone C, Simonsen A, Smith MA, Spanel-Borowski K, Srinivas V, Steeves M, Stenmark H, Stromhaug PE, Subauste CS, Sugimoto S, Sulzer D, Suzuki T, Swanson MS, Tabas I, Takeshita F, Talbot NJ, Talloczy Z, Tanaka K, Tanida I, Taylor GS, Taylor JP, Terman A, Tettamanti G, Thompson CB, Thumm M, Tolkovsky AM, Tooze SA, Truant R, Tumanovska LV, Uchiyama Y, Ueno T, Uzcategui NL, van der Klei I, Vaquero EC, Vellai T, Vogel MW, Wang HG, Webster P, Wiley JW, Xi Z, Xiao G, Yahalom J, Yang JM, Yap G, Yin XM, Yoshimori T, Yu L, Yue Z, Yuzaki M, Zabirnyk O, Zheng X, Zhu X, Deter RL (2008) Guidelines for the use and interpretation of assays for monitoring autophagy in higher eukaryotes. Autophagy 4:151–175

Klionsky DJ et al (2012) Guidelines for the use and interpretation of assays for monitoring autophagy. Autophagy 8:445–454

Kobayashi T, Beuchat MH, Lindsay M, Frias S, Palmiter RD, Sakuraba H, Parton RG, Gruenberg J (1999) Late endosomal membranes rich in lysobisphosphatidic acid regulate cholesterol transport. Nat Cell Biol 1:113–118

Lee J, Giordano S, Zhang J (2012) Autophagy, mitochondria and oxidative stress: cross-talk and redox signalling. Biochem J 441:523–540. doi:10.1042/BJ20111451

Liou W, Geuze HJ, Geelen MJ, Slot JW (1997) The autophagic and endocytic pathways converge at the nascent autophagic vacuoles. J Cell Biol 136:61–70

Mizushima N, Yoshimori T (2007) How to interpret LC3 immunoblotting. Autophagy 3:542–545

Mizushima N, Yoshimori T, Levine B (2010) Methods in mammalian autophagy research. Cell 140:313–326. doi:10.1016/j.cell.2010.01.028

Munafo DB, Colombo MI (2001) A novel assay to study autophagy: regulation of autophagosome vacuole size by amino acid deprivation. J Cell Sci 114:3619–3629

Niemann A, Takatsuki A, Elsasser HP (2000) The lysosomotropic agent monodansylcadaverine also acts as a solvent polarity probe. J Histochem Cytochem 48:251–258

Pacheco CD, Kunkel R, Lieberman AP (2007) Autophagy in Niemann–Pick C disease is dependent upon Beclin-1 and responsive to lipid trafficking defects. Hum Mol Genet 16:1495–1503

Patterson GH, Lippincott-Schwartz J (2002) A photoactivatable GFP for selective photolabeling of proteins and cells. Science 297:1873–1877

Pérez-Sala D, Boya P, Ramos I, Herrera M, Stamatakis K (2009) The C-terminal sequence of RhoB directs protein degradation through an endo-lysosomal pathway. PLoS ONE 4(12):e8117

Saftig P, Klumperman J (2009) Lysosome biogenesis and lysosomal membrane proteins: trafficking meets function. Nat Rev Mol Cell Biol 10:623–635. doi:10.1038/nrm2745

Sato K, Tsuchihara K, Fujii S, Sugiyama M, Goya T, Atomi Y, Ueno T, Ochiai A, Esumi H (2007) Autophagy is activated in colorectal cancer cells and contributes to the tolerance to nutrient deprivation. Cancer Res 67:9677–9684. doi:10.1158/0008-5472.CAN-07-1462

Sobo K, Le Blanc I, Luyet PP, Fivaz M, Ferguson C, Parton RG, Gruenberg J, van der Goot FG (2007) Late endosomal cholesterol accumulation leads to impaired intra-endosomal trafficking. PLoS One 2(9):e851

Stenmark H (2009) Rab GTPases as coordinators of vesicle traffic. Nat Rev Mol Cell Biol 10:513–525. doi:10.1038/nrm2728

Valero RA, Oeste CL, Stamatakis K, Ramos I, Herrera M, Boya P, Pérez-Sala D (2010) Structural determinants allowing

endo-lysosomal sorting and degradation of endosomal GTPases. Traffic 11:1221–1233

Wang Q, Liang B, Shirwany NA, Zou MH (2011) 2-Deoxy-D-glucose treatment of endothelial cells induces autophagy by reactive oxygen species-mediated activation of the AMP-activated protein kinase. PLoS One 6(2):e17234

Warenius HM, Kilburn JD, Essex JW, Maurer RI, Blaydes JP, Agarwala U, Seabra LA (2011) Selective anticancer activity of a hexapeptide with sequence homology to a non-kinase domain of cyclin dependent kinase 4. Mol Cancer 10:72. doi:10.1186/1476-4598-10-72

Yang Z, Klionsky DJ (2010) Mammalian autophagy: core molecular machinery and signaling regulation. Curr Opin Cell Biol 22:124–131

OPEN ACCESS Freely available online

PLoS one

The C-Terminus of H-Ras as a Target for the Covalent Binding of Reactive Compounds Modulating Ras-Dependent Pathways

Clara L. Oeste[1☯], Beatriz Díez-Dacal[1☯], Francesca Bray[1], Mario García de Lacoba[1], Beatriz G. de la Torre[2], David Andreu[2], Antonio J. Ruiz-Sánchez[3], Ezequiel Pérez-Inestrosa[3], Carlota A. García-Domínguez[4], José M. Rojas[4], Dolores Pérez-Sala[1]*

1 Department of Chemical and Physical Biology, Centro de Investigaciones Biológicas, Consejo Superior de Investigaciones Científicas, Madrid, Spain, **2** Department of Experimental and Health Sciences, Universitat Pompeu Fabra, Barcelona, Spain, **3** Department of Organic Chemistry, Faculty of Sciences, University of Málaga, Málaga, Spain, **4** Unidad de Biología Celular, Área de Biología Celular y del Desarrollo, Centro Nacional de Microbiología, Instituto de Salud Carlos III, Madrid, Spain

Abstract

Ras proteins are crucial players in differentiation and oncogenesis and constitute important drug targets. The localization and activity of Ras proteins are highly dependent on posttranslational modifications at their C-termini. In addition to an isoprenylated cysteine, H-Ras, but not other Ras proteins, possesses two cysteine residues (C181 and C184) in the C-terminal hypervariable domain that act as palmitoylation sites in cells. Cyclopentenone prostaglandins (cyPG) are reactive lipidic mediators that covalently bind to H-Ras and activate H-Ras dependent pathways. Dienone cyPG, such as 15-deoxy-$\Delta^{12,14}$-PGJ_2 (15d-PGJ_2) and Δ^{12}-PGJ_2 selectively bind to the H-Ras hypervariable domain. Here we show that these cyPG bind simultaneously C181 and C184 of H-Ras, thus potentially altering the conformational tendencies of the hypervariable domain. Based on these results, we have explored the capacity of several bifunctional cysteine reactive small molecules to bind to the hypervariable domain of H-Ras proteins. Interestingly, phenylarsine oxide (PAO), a widely used tyrosine phosphatase inhibitor, and dibromobimane, a cross-linking agent used for cysteine mapping, effectively bind H-Ras hypervariable domain. The interaction of PAO with H-Ras takes place in vitro and in cells and blocks modification of H-Ras by 15d-PGJ_2. Moreover, PAO treatment selectively alters H-Ras membrane partition and the pattern of H-Ras activation in cells, from the plasma membrane to endomembranes. These results identify H-Ras as a novel target for PAO. More importantly, these observations reveal that small molecules or reactive intermediates interacting with spatially vicinal cysteines induce intramolecular cross-linking of H-Ras C-terminus potentially contributing to the modulation of Ras-dependent pathways.

Citation: Oeste CL, Díez-Dacal B, Bray F, García de Lacoba M, de la Torre BG, et al. (2011) The C-Terminus of H-Ras as a Target for the Covalent Binding of Reactive Compounds Modulating Ras-Dependent Pathways. PLoS ONE 6(1): e15866. doi:10.1371/journal.pone.0015866

Editor: Ben C. B. Ko, Chinese University of Hong Kong, Hong Kong, Special Administrative Region, People's Republic of China

Received August 26, 2010; **Accepted** November 25, 2010; **Published** January 6, 2011

Funding: This work was supported by European Union Cooperation in the field of Scientific and Technical research (COST) Action CM1001, grant SAF2009-11642 from Ministerio de Ciencia e Innovación and Red Temática de Investigación Cooperativa from Instituto de Salud Carlos III (Spain) RD07/0064/0007 to DP-S and RD07/0064/0000 to EP-I. Work at Universitat Pompeu Fabra was supported by grants BIO2005-07592-CO2-02 and BIO2008-04487-CO3-02 from Ministerio de Ciencia e Innovación (Spain) to DA, and by the regional government of Catalunya (SGR2005-00494). JMR's work is supported by Fondo de Investigaciones Sanitarias-Intrasalud (PS09/00562) and Red Temática de Investigación Cooperativa RD06/0020/0003 from Instituto de Salud Carlos III, and the Spanish Association Against Cancer (AECC). CLO is the recipient of a predoctoral fellowship from the Formación de Personal Investigador (FPI) program (Ministerio de Ciencia e Innovación, Spain, BES-2010-033718). CAG-D is the recipient of a fellowship from Fondo de Investigaciones Sanitarias-Beca de Formación en Investigación. The funders had no role in study design, data collection and analysis, decision to publish, or preparation of the manuscript.

Competing Interests: The authors have declared that no competing interests exist.

* E-mail: dperezsala@cib.csic.es

☯ These authors contributed equally to this work.

Introduction

Ras proteins are key regulators of cellular proliferation, survival or senescence. In addition to their role in cellular physiology, Ras proteins are involved in many pathophysiological processes. In fact, mutations in the Ras genes are found in 30% of human cancers [1]. Therefore, since their discovery, Ras oncogenes have been the subject of intense research. The three Ras genes, H-, N-, and K-Ras display extensive homology but also important distinctive features (reviewed in [2,3]).

Ras proteins are GTP-binding proteins which hydrolyze GTP with the concourse of GTPase activating proteins. Ras activity is controlled by a cycle between the GTP-bound active state and the GDP-bound inactive state. In the GTP-bound state, Ras proteins may interact with effectors including Raf, PI3K and RalGDS, among others [3,4], to activate various signaling pathways with impact on cell cycle regulation, cytoskeleton organization, transcriptional regulation or membrane trafficking. Ras activity is subjected to a complex modulation at many different levels. Ras activation, requiring the exchange of bound GDP for GTP, can occur by interaction with GTP exchange factors (GEFs), which in turn may transduce signals from growth factor receptors or sense levels of intracellular mediators, including calcium and diacylglycerol. In addition, GDP-GTP exchange can be favoured by the

direct action of reactive oxygen or nitrogen species, such as nitric oxide, on Ras proteins [5].

Posttranslational modifications of Ras proteins play a key role in their localization and activity. All Ras proteins are isoprenylated at a cysteine residue present in the CAAX box located at the C-termini [6]. In addition, whereas H-Ras is palmitoylated at two cysteine residues present in the hypervariable domain (C181 and C184), N-Ras contains a single palmitoylation site (C181) and K-Ras4B possesses no cysteine residues but its interaction with cellular membranes is favoured by the presence of a polybasic domain. These differences are critical to determine the traffic and site of action of Ras proteins (reviewed in [4,7]). Thus, H-Ras is located mainly at the plasma membrane and in endosomes and traffics to the plasma membrane through the conventional secretory pathway. In contrast, K-Ras4B has been reported to interact with microtubules, although the pathway by which it reaches the plasma membrane is not well characterized. In the case of H-Ras, a palmitoylation-depalmitoylation cycle regulates recycling of the protein between the plasma membrane and the Golgi. Moreover, palmitate groups are important for determining the interaction of H-Ras with specific membrane microdomains, its membrane insertion and orientation and its presence in internal membranes, which in turn may influence the engagement of various signaling pathways [8,9].

Cyclopentenone prostaglandins (cyPG) are reactive lipidic mediators that are generated by dehydration of their parent PG. PGE-type PG give rise to cyPG of the A-series. The J series of cyPG arise from dehydration of PGD_2 by a sequence of well characterized steps giving rise to the single enone PGJ_2 and to the dienone PG 15d-PGJ_2 and Δ^{12}-PGJ_2 [10,11]. These prostanoids are produced in increased amounts in situations associated with inflammation or oxidative stress and they have been shown to influence cell proliferation and contribute to the resolution of inflammation [12]. cyPG contain an α,β-unsaturated carbonyl group in the cyclopentenone ring. Electrophilic carbons conjugated with this group can suffer the attack of nucleophiles, such as sulphur atoms, and form Michael adducts. Through this mechanism, cyPG may covalently modify proteins, leading to alteration of protein structure and function [13]. We have previously shown that several cyPG may bind to Ras proteins, and that this correlates with Ras activation, as evidenced by an increase in the levels of Ras in its active conformation, and an activation of Ras dependent pathways [14]. Interestingly, we observed that modification and activation of Ras proteins by cyPG with different structure are site-selective. Single enone PG, like PGA_1 or PGJ_2 preferentially bound to C118 in H-Ras, which is located in the GTP binding site, whereas cyPG with dienone structure preferentially bound to the C-terminal segment containing C181 and C184 [15]. Interestingly, this preferential binding resulted in the selective modification of the different Ras proteins: while dienone cyPG selectively bound to H-Ras, single enone cyPG could bind to the three Ras proteins, H-, N- and K-Ras4B, because all three possess the C118 residue. In light of these data, we formulated the hypothesis that, dienone cyPG, possessing two electrophilic carbons, could react simultaneously with two different cysteine residues. The fact that H-Ras is the only Ras protein possessing two nearby cysteine residues could constitute the structural basis for its selective modification by cyPG with dienone structure. Moreover, this observation raised the possibility that the C-terminus of H-Ras could be the target for other bifunctional cysteine reagents. Here we have characterized the modification of the C-terminal region of H-Ras by cyPG dienones as well as by other bifunctional cysteine reagents and explored the functional consequences of this modification. Since palmitoylation is a reversible modification, our results suggest that the reactive cysteines present in the H-Ras C-terminus may also be targeted by various small molecules or biological intermediates with reactivity towards vicinal thiols, with diverse consequences on H-Ras localization and function.

Results

cyPG with dienone structure bind simultaneously to C181 and C184 of H-Ras C-terminus

cyPG dienones, such as 15d-PGJ_2 and Δ^{12}-PGJ_2, can covalently modify H-Ras by preferentially binding the C-terminal peptide containing C181 and C184 [15]. Given the bifunctional nature of these dienones, the possibility exists that they simultaneously bind to both cysteine residues. To investigate this point we have used a synthetic peptide corresponding to the tryptic fragment K170-K185 (m/z 1662.7) from H-Ras C-terminus.

Incubation of K170-K185 with 15d-PGJ_2 gave rise to the appearance of a peak of m/z 1979.80 corresponding to the addition of one PG molecule (Fig. 1A). Moreover, as previously noted [14,15], several peaks compatible with the oxidation of the modified peptide (m/z 1994.9 and 2010.7) were observed. Reduction and alkylation of the control peptide by subsequent treatment with DTT and iodoacetamide gave the expected peaks (m/z 1719.6 and 1776.6) corresponding to the carbamidomethylation of one and two cysteines, respectively. Addition of 15d-PGJ_2 to the K170-K185 peptide was not reversed by DTT. Interestingly, carbamidomethylation of the 15d-PGJ_2-modified peptide upon treatment with iodoacetamide was nearly undetectable, suggesting that the 15d-PGJ_2-modified peptide was basically devoid of free cysteines. Similar results were obtained when the H-Ras C-terminal peptide was modified by Δ^{12}-PGJ_2, another cyPG with dienone structure giving rise to a modified peptide with m/z 1997.5. These results, summarized in Fig. 1B, contrast with the behavior of PGJ_2, a single enone cyPG, which we have previously shown to form one- or two-cyPG adducts (m/z 1997.4 and 2331.7, respectively) with the H-Ras C-terminal peptide, thus showing binding to single cysteine residues [15]. Taken together these results indicate that modification of K170-K185 by cyPG dienones may involve intramolecular cross-linking of both C181 and C184. The C-terminal peptide of H-Ras does not show a defined structure in solution [16], but it adopts a precise conformation upon interaction with membranes [17]. Cross-linking between C181 and 184 could impose a more rigid conformation and potentially alter H-Ras membrane interactions. A theoretical molecular model illustrating the feasibility of 15d-PGJ_2-induced intramolecular cross-linking of the K170-K185 peptide is shown in Fig. 1C.

The small molecule bifunctional reagent phenylarsine oxide cross-links C181 and C184 of the H-Ras C-terminal peptide

In view of the ability of cyPG with dienone structure to simultaneously bind the cysteine residues of the H-Ras hypervariable domain, we tested other small bifunctional molecules for cross-linking of these two cysteines. The tyrosine phosphatase inhibitor phenylarsine oxide (PAO, mass 168.02), widely used in signal transduction studies and as an endocytosis inhibitor [18,19], is also known to form adducts with proteins by reacting with vicinal sulfhydryl groups of proteins forming thioarsine rings [20,21,22]. Incubation of K170-K185 with PAO resulted in the formation of an adduct of m/z 1812.7 (Fig. 2A), with a mass increment of 150, compatible with the formation of a cross-link between C181 and C184 and one PAO molecule, which implies

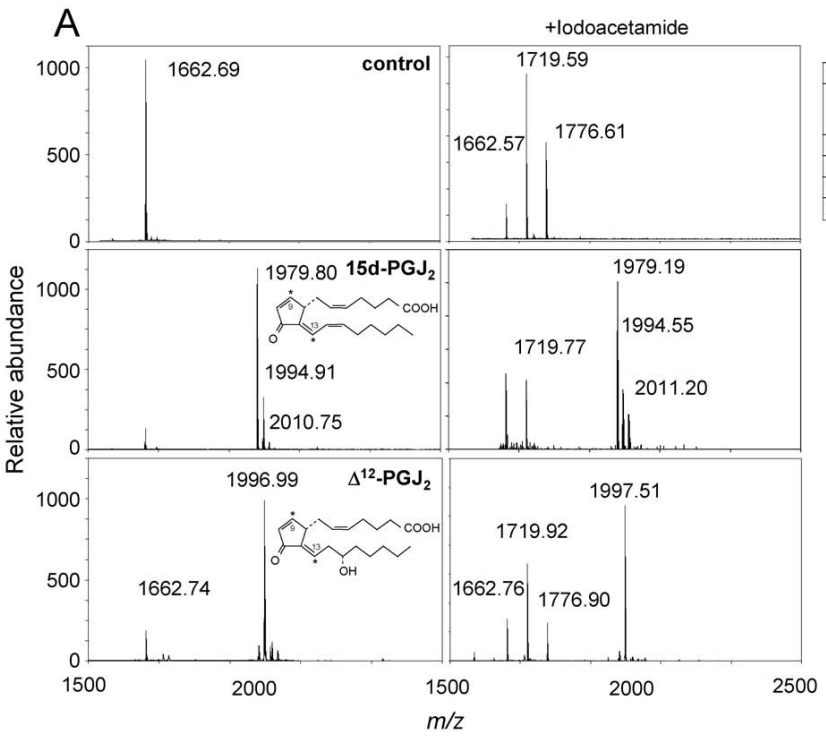

K170-K185	KLNPPDESGPGCMSCK		
	Theoretical m/z of the peptides for which compatible peaks were observed experimentally		
		+ CAM	+2 CAM
Unmodified peptide	1662.73	1719.73	1776.73
15d-PGJ_2 adduct (+316.5)	1979.23	-	-
Δ^{12}-PGJ_2 adduct (+334.5)	1997.23	-	-

Figure 1. Modification of the K170-K185 peptide from the C-terminal region of H-Ras by cyPG. (A) The synthetic K170-K185 peptide was incubated with the indicated cyPG and the resulting adducts analyzed by MALDI-TOF MS. When indicated, incubation mixtures were treated with 50 mM iodoacetamide after addition of 10 mM DTT. Spectra presented are representative from at least three independent assays per experimental condition. Structures of the cyPG used are shown in insets. Electrophilic carbons are marked by asterisks. (B) Summary of the theoretical peptide adducts for which compatible peaks were observed experimentally. +CAM indicates that the peak is compatible with the formation of carbamidomethyl cysteine subsequent to iodoacetamide treatment. (C) Ribbon diagram for the theoretical backbone structure of the H-Ras K170-K185 peptide (in green) modified by addition of 15d-PGJ_2 to cysteines 181 and 184. The side-chains of the cysteine residues and the 15d-PGJ_2 ligand are displayed in yellow and a default atom-type color scheme, respectively.
doi:10.1371/journal.pone.0015866.g001

the loss of the oxygen atom of the PAO molecule plus two hydrogen atoms (Fig. 2B). Analysis of this 1812.7 peak by MALDI-TOF-TOF MS/MS gave fragments compatible with the incorporation of PAO at the proposed sites (Fig. 2C). The smallest fragment detected containing the mass increment compatible with PAO addition corresponded to ion y5 of sequence CMSCK, confirming the site of modification. Figure 2D depicts a homology molecular model of the H-Ras C-terminal peptide after cross-linking elicited by PAO binding.

In contrast with the cross-linking by cyPG with dienone structure, PAO addition was fully reversible upon treatment with excess DTT. Thus, PAO-modified K170-K185 underwent carbamidomethylation at one or two cysteines after incubation with DTT and iodoacetamide (Fig. 3A, upper panels). Given the reversibility of PAO addition by competing agents like DTT, we were interested in exploring whether PAO-induced modification of the K170-K185 H-Ras peptide would occur in the presence of a biologically relevant thiol compound at concentrations close to those encountered in vivo. Interestingly, the presence of glutathione (GSH) in the incubation mixture reduced the proportion of PAO-peptide adduct formed in a concentration-dependent manner, as it can be deduced from the abundance of modified (m/z 1812.7) vs parent (m/z 1662.7) peptide (Fig. 3A, lower panels). However, a substantial proportion of PAO-peptide adduct could still be detected at GSH concentrations of up to 10 mM, thus suggesting that H-Ras modification by PAO could occur in cells. Remarkably, at 10 mM GSH, peaks of m/z 1967. 7 and 2272.8, compatible with the mono and di-glutathiolation of K170-K185 were also observed. A summary of the species encountered in the MS analysis of the K170-K185 peptide adducts after treatment with the various agents used is shown in Fig. 3B.

PAO binds to H-Ras C-terminus in vitro and in intact cells

In view of the above results we explored whether PAO could bind to the full length H-Ras protein in vitro, and if so, whether the peptide containing C181 and C184 was the preferred site for interaction. As it can be observed in Fig. 4A incubation of full-length H-Ras with PAO resulted in the formation of an adduct containing one PAO molecule bound to H-Ras, as clearly detected by MALDI-TOF MS analysis. Moreover, tryptic digestion of the modified protein revealed the appearance of a peak with m/z 1812.7 as the main modified peptide, which corresponded to the addition of one PAO molecule to the K170-K185 tryptic peptide (Fig. 4B). We have previously reported that biotinylated 15d-PGJ_2 (15d-PGJ_2-B) binds to H-Ras in vitro and in intact cells at the same peptide [14,15]. Therefore, we explored the capacity of PAO to block the binding of 15d-PGJ_2-B to H-Ras, by using a gel-based assay. Pre-incubation with PAO clearly reduced the incorporation of 15d-PGJ_2-B into H-Ras in vitro (Fig. 4C). This could be evidenced both by the reduction of the H-Ras-associated biotin signal (28%±7 reduction with respect to vehicle-treated Ras, mean ± standard deviation of three assays), and by the reduction

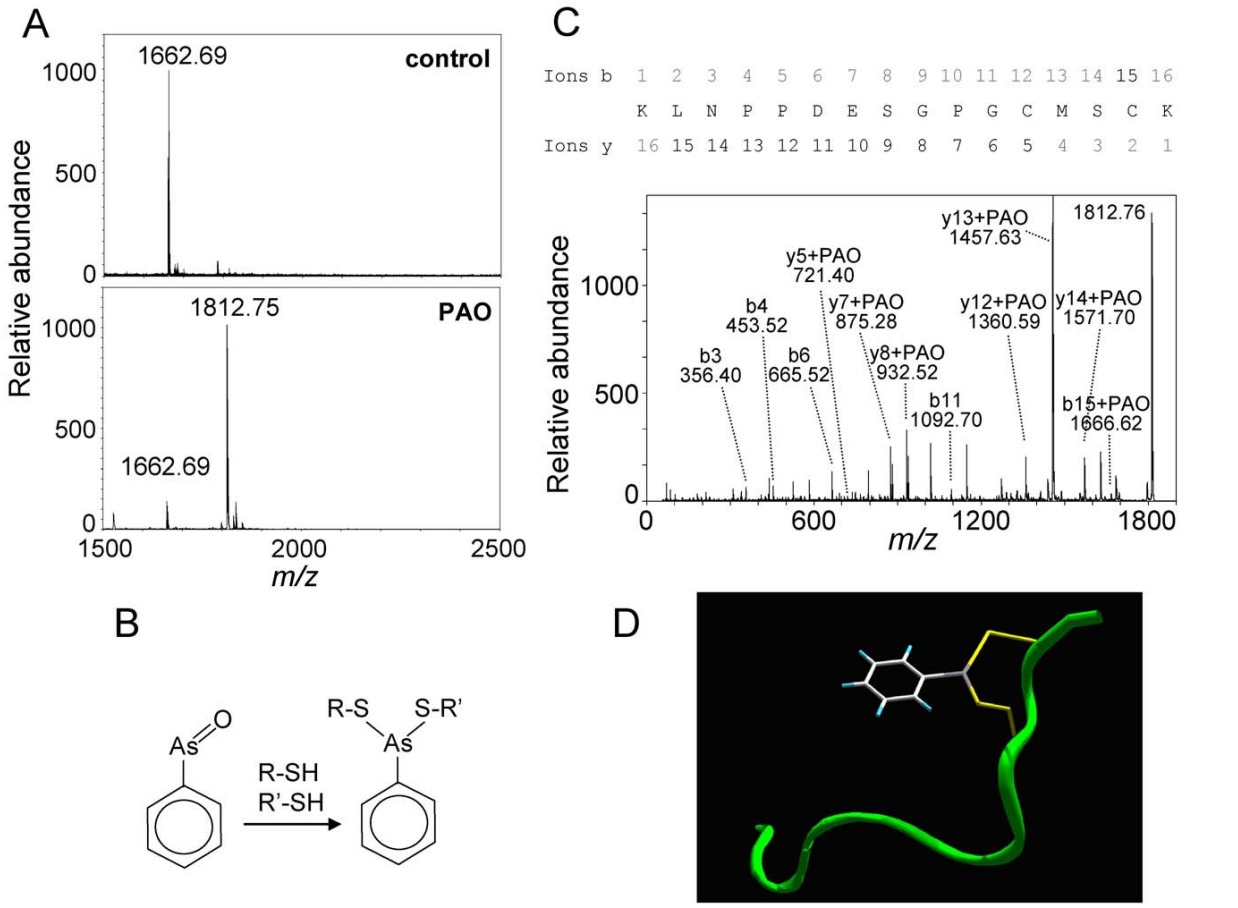

Figure 2. Modification of the K170-K185 peptide by PAO. (A) The K170-K185 peptide was incubated with PAO and analyzed by MALDI-TOF MS. Results are representative from at least four assays. (B) Scheme of the formation of a PAO adduct with two thiol groups. (C) Analysis of the PAO-peptide adduct by MALDI-TOF-TOF MS/MS analysis. The sequence of the peptide with the fragments generated is shown for reference. (D) Ribbon diagram for the theoretical backbone structure of H-Ras K170-K185 peptide model (in green) modified by PAO addition. The side-chains of the cysteine residues and PAO are displayed in yellow and a default atom-type color scheme, respectively.
doi:10.1371/journal.pone.0015866.g002

of the amount of 15d-PGJ_2-B modified protein, which appears as a higher molecular weight band (marked by an asterisk), as we have previously described [15]. We next explored the effect of PAO on 15d-PGJ_2-B binding to H-Ras in intact cells by using COS-7 cells transiently transfected with an expression vector for AU5-tagged H-Ras. Consistent with previous reports, AU5-H-Ras appeared in cell lysates as a doublet, reflecting different degrees of post-translational processing, with the lower band corresponding to the fully processed H-Ras protein [6]. Incubation with PAO markedly reduced the extent of modification of H-Ras by 15d-PGJ_2-B in COS-7 cells (Fig. 4D). Quantification of the biotin signal corrected by AU5-H-Ras protein levels yielded a 55% ±6 reduction (mean ± standard deviation of three experiments) in 15d-PGJ_2-B incorporation into H-Ras in PAO pre-treated cells. These results indicate that PAO binds to the C-terminus of H-Ras in intact cells.

Functional consequences of H-Ras modification by PAO

Binding of dienone cyPG or of PAO, as displayed in the theoretical models, would likely alter the conformational tendencies, and, more importantly, the chemical nature of H-Ras C-terminus. In addition, since the hypervariable domain cysteine residues are sites of palmitoylation, incorporation of PAO could have consequences for the membrane binding or the hydrophobicity of the modified protein. Therefore, we explored whether treatment of cells with PAO led to alterations in H-Ras subcellular distribution. Treatment of AU5-H-Ras transfected COS-7 cells with PAO led to a decrease in the amount of membrane associated H-Ras, as evidenced by cell fractionation into P100 and S100 fractions (Fig. 5A). Partition into the detergent Triton-X114 has been shown to constitute an assay for protein hydrophobicity [23] and it has been used as an index of H-Ras lipidation [24]. Indeed, isoprenylation has been shown to increase the proportion of H-Ras partitioning into the Triton-X114 phase, this being further increased by palmitoylation [6]. A Triton X-114 partition assay showed that treatment of AU5-H-Ras transfected cells with PAO reduced the amount of H-Ras protein in the detergent phase in a concentration-dependent manner, mostly at the expense of the upper component of the AU5-H-Ras doublet, with a concomitant increase in the protein recovered in the aqueous fraction (Fig. 5B). Therefore, these results suggest that PAO impairs lipidation of H-Ras in cells. We were then interested in assessing the effect of PAO on H-Ras function. Given the reversible nature of PAO binding we employed a Raf Ras binding domain (Raf-RBD) redistribution assay, which allows exploring Ras activation in intact cells. The

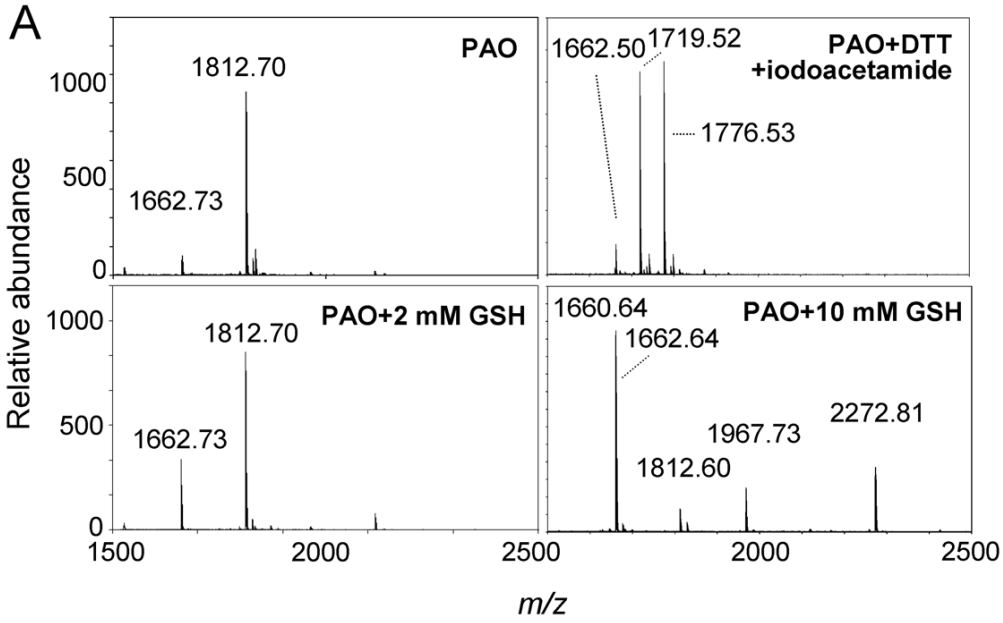

B

K170-K185	KLNPPDESGPGCMSCK		
	Theoretical m/z of the peptides for which compatible peaks were observed experimentally		
		+ CAM	+2 CAM
Unmodified peptide	1662.73	1719.73	1776.73
PAO adduct (+150.0)	1812.73	-	-
Mono GSH adduct (+305.0)	1967.73	-	-
Bis-GSH adduct (+610.0)	2272.73	-	-

Figure 3. Effect of reducing agents on PAO modification of the K170-K185 peptide. (A) In the upper panels, the K170-K185 peptide was incubated with PAO and analyzed by MALDI-TOF MS. In the right panel, the incubation mixture was treated with 10 mM DTT and subsequently with 50 mM iodoacetamide. In the lower panels, the K170-K185 peptide was incubated with PAO in the presence of the indicated concentrations of GSH before analysis by MALDI-TOF MS. (B) Summary of the theoretical *m/z* of peptides for which compatible peaks were observed experimentally in the assays shown in (A).
doi:10.1371/journal.pone.0015866.g003

YFP-RBD construct showed a diffuse distribution in transiently transfected COS-7 cells. Treatment with EGF led to a more irregular intracellular YFP-RBD pattern and, above all, to the appearance of defined accumulations of the fluorescent construct at the cell periphery, in some cases at the edge of membrane ruffle-like structures, thus indicating the recruitment of YFP-RBD by activated Ras at the plasma membrane (Fig. 6A). Incubation with PAO caused intracellular redistribution of YFP-RBD, resulting in a more particulate pattern. Interestingly, pre-treatment with PAO completely blocked EGF-induced recruitment of YFP-RBD to the plasma membrane. This indicates that Ras activation at the plasma membrane is blocked by PAO. Quantitation of these results is shown in Fig. 6B.

We next explored Ras activation by means of a RBD pull-down assay (Fig. 6C). EGF clearly activated H-Ras in this assay, as deduced from the increase in the retention of AU5-H-Ras on RBD beads. No AU5 signal was detected in the pull-down from cells transfected with empty vector (results not shown). Notably, treatment with PAO alone induced the retention on RBD beads of the slower migrating AU5-H-Ras band and did not reduce EGF-induced Ras activation in this assay. Taken together these results suggest that PAO treatment targets H-Ras in intact cells and alters H-Ras-mediated signaling by selectively blocking EGF-mediated Ras activation at the cell membrane and potentially inducing Ras-Raf interaction at other locations.

The cysteine cross-linking agent dibromobimane targets H-Ras hypervariable domain

The results shown above suggest that small molecules interacting with spatially vicinal cysteines may induce an intramolecular cross-linking of H-Ras hypervariable domain and alter Ras distribution and signaling. To further substantiate this point, we studied the effect of dibromobimane (DBB, mass 350.01), a reagent known to cross-link cysteine residues within 3–6 Å distance [25]. DBB was shown to bind K170-K185 by MS analysis (Fig. 7A). The *m/z* of the modified peptide (1850.81) was compatible with addition of one DBB molecule to C181 and C184, according to the reaction depicted in Fig. 7B (expected mass increment 188.0). Formation of peptide dimers was not detected, again suggesting the occurrence of intramolecular cysteine cross-linking by DBB. Moreover, reduction and alkylation with iodoacetamide did not result in carbamidomethylation of the DBB-modified peptide, thus ruling out the presence of free cysteines. As observed for PAO, treatment of full length H-Ras with DBB reduced the modification of the protein by 15d-PGJ_2-B, suggesting that DBB binds to H-Ras at the C-terminal peptide

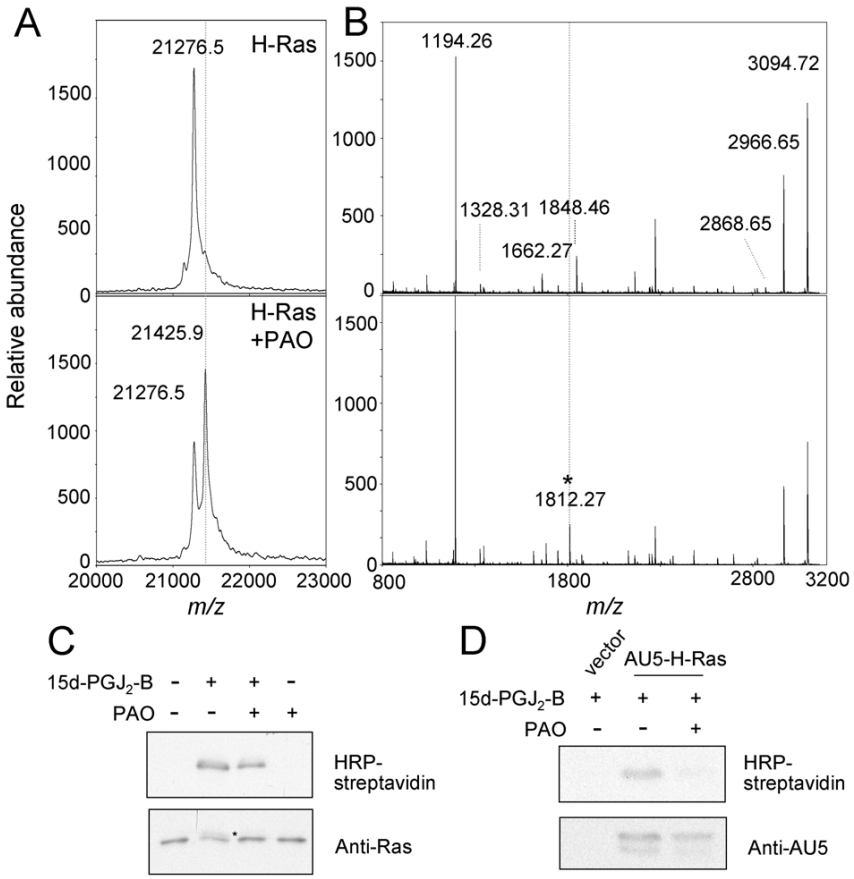

Figure 4. PAO binds to the C-terminal peptide of H-Ras in vitro and in cells. (A) Full length H-Ras was incubated with PAO and analyzed by MALDI-TOF MS. (B) Control or PAO-treated H-Ras was subjected to tryptic digestion and the resulting peptides analyzed by MALDI-TOF MS. The peak of *m/z* 1812.27, corresponding to the formation of an adduct between PAO and the K170-K185 peptide, is marked by an asterisk. Dotted lines mark the positions equivalent to those of the modified species in the untreated samples. (C) H-Ras at 5 μM was incubated with 50 μM PAO for 30 min before addition of 1 μM biotinylated 15d-PGJ_2 (15d-PGJ_2-B) for 1 h. (D) COS-7 cells were transiently transfected with empty vector or a plasmid coding for AU5-H-Ras. 24 h after transfection cells were pre-treated with vehicle or 1 μM PAO for 90 min before incubation with 5 μM 15d-PGJ_2-B for 90 min. Incubation mixtures from (C) and cell lysates from (D) were analysed by SDS-PAGE followed by transfer to membrane and detection of incorporated biotin with horseradish peroxidase (HRP)-streptavidin and of the Ras protein by immunoblot with anti-pan Ras or anti-AU5 antibody and enhanced chemiluminescence (ECL). Results shown are representative of at least three assays.
doi:10.1371/journal.pone.0015866.g004

(Fig. 7C). Indeed, direct binding of DBB to H-Ras could be evidenced by fluorescence detection of the gels, taking advantage of the fluorogenic properties of this compound upon replacement of both bromines [25] (Fig. 7C). Although DBB has been widely used in cysteine mapping studies in vitro, its effects in cultured cells have not been explored. Therefore, at this point we went on to assess whether DBB recapitulated some of the effects of PAO in intact cells. A concentration of 50 μM DBB was required to detect binding of this compound to intracellular components, as observed by confocal fluorescence microscopy (results not shown). This concentration did not affect cell viability nor elicited morphological changes. Under these conditions, treatment of AU5-H-Ras-transfected cells with DBB reduced the levels of the upper component of AU5-H-Ras doublet (Fig. 7D) and led to the virtual disappearance of this band from the detergent phase in the Triton X-114 partition assay (Fig. 7E). Finally, using the Raf-RBD redistribution assay, we observed that in the presence of DBB, YFP-RBD adopted a particulate intracellular pattern and EGF failed to induce the translocation the YFP-RBD construct to the cell periphery or to membrane ruffle-like structures (Fig. 7F). Therefore, DBB markedly alters H-Ras homeostasis and function.

Discussion

Ras proteins are critical signaling molecules that integrate information from growth factor receptors and intracellular mediators. Ras proteins may sense changes in calcium concentration or redox state and engage various signaling pathways leading to the regulation of basic cellular functions. The ability of Ras proteins to act as sensors of various stimuli in different cell compartments relies in part in the complex array of posttranslational modifications they can undergo. Ras proteins may be subjected to isoprenylation and accompanying modifications, proteolysis and carboxyl methylation, phosphorylation, palmitoylation, ubiquitination and various non-enzymatic modifications including nitrosylation, thiolation or addition of lipid electrophiles [14,26,27,28]. Here we show that the C-terminal end of H-Ras proteins may be the target for both endogenous reactive molecules

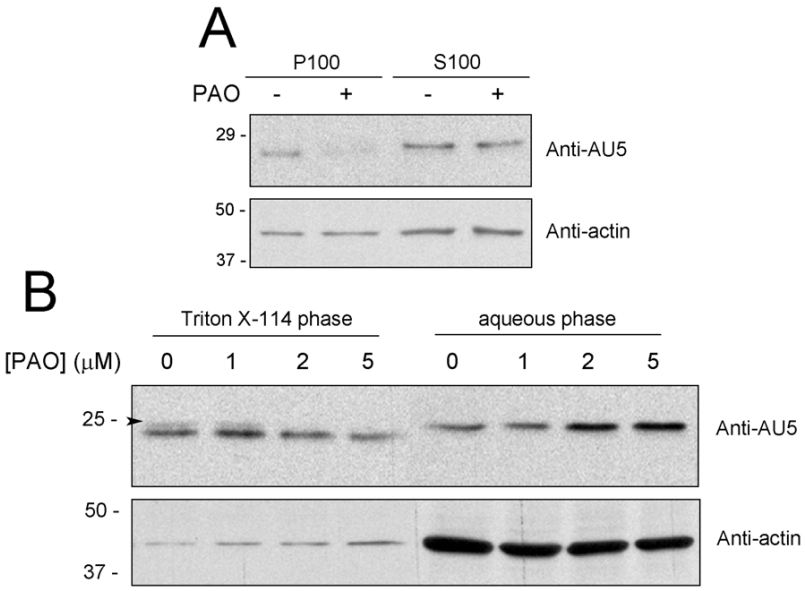

Figure 5. Effect of PAO on H-Ras subcellular localization. (A) COS-7 cells were transiently transfected with expression vectors coding for AU5-H-Ras wt. After serum starvation for 16 h, cells were treated with vehicle or 1 μM PAO for 1 h. Cells were lysed and postnuclear supernatants were separated into S100 and P100 fractions by ultracentrifugation at 200,000× g for 30 min. (B) AU5-H-Ras transfected cells were treated with the indicated concentrations of PAO for 90 min and cell lysates were subjected to fractionation in Triton-X114. The amount of AU5-H-Ras present in the various fractions was estimated by western blot with anti-AU5 antibody (upper panels). The upper component of the H-Ras doublet is indicated by an arrowhead. Levels of actin were assessed as control (lower panels). Blots shown are representative of three assays.
doi:10.1371/journal.pone.0015866.g005

and exogenous chemicals that cross-link nearby cysteines, thus opening new possibilities for the regulation of Ras proteins and potentially for H-Ras-selective signaling.

In this and previous works we have reported that Ras proteins are targets for modification by endogenous electrophilic eicosanoids, like cyPG and isoprostanes [14,15]. From a structural point of view, different patterns of modification by eicosanoids with different structure were encountered, with single enone compounds preferentially modifying C118, which is present in all three Ras proteins, and dienone compounds, like 15d-PGJ_2, binding preferentially to the C-terminal peptide containing C181 and 184, present only in H-Ras. Analogously to the selective modification and activation of H-Ras, but not N-Ras or K-Ras4B, by 15d-PGJ_2 [15], we have observed that PAO, shown here to modify H-Ras, did not affect the electrophoretical mobility or activation of AU5-K-Ras4B (results not shown). This suggests that the presence of two close cysteine residues in the hypervariable domain of H-Ras may be the main determinant for its selective modification by cyPG dienones, and possibly by other bifunctional cysteine reagents.

In this context, various recent evidences suggest that cyPG dienones could preferentially modify proteins containing cysteines in close proximity. Given the stability of this modification, this could result in intra- or inter-molecular cross-linking. Indeed, we have recently reported that dienone cyPG, like 15d-PGJ_2 and Δ^{12}-PGJ_2 induce cross-linking of the P1-1 isoform of glutathione S-transferase (GST), which is involved in cancer chemoresistance, through a mechanism likely involving cysteine residues present in different GSTP1-1 monomers [29]. Moreover, 15d-PGJ_2 has also been shown to directly cross-link c-Jun monomers in vitro [30]. In view of these findings it would be interesting to explore whether proteins with neighboring cysteines important for function, such as thioredoxins, tyrosine phosphatases, Rho proteins or Hsp90 constitute preferential targets for cyPG with dienone structure [20,31,32].

It should be taken into account that the cysteine residues of H-Ras targeted by the agents used in this study are the palmitoylation cysteines located in the hypervariable domain. Since H-Ras palmitoylation plays a key role in subcellular localization [8], modification of these cysteine residues could be expected to alter H-Ras distribution. We previously observed that treatment of cells with 15d-PGJ_2 did not disrupt membrane association of H-Ras, although an increased extractability in detergent was noted, indicative of potential changes in H-Ras membrane microdomain distribution [15]. The results presented here indicate that C181 and C184 of H-Ras can be targeted by several bifunctional molecules of diverse structure, such as PAO and DBB. Our results indicate that H-Ras modification by these agents takes place in vitro and in cells. Moreover, treatment with PAO decreases H-Ras hydrophobicity and membrane binding. In turn, the most obvious effect of DBB under the conditions studied is a reduction in the levels of the upper component of the H-Ras doublet, putatively the non-palmitoylated form, causing its disappearance from the detergent fraction. A reduction in the levels of the slower migrating form of H-Ras was also observed with high (10 μM) PAO concentrations (results not shown). Whether the decrease in the detection of the upper H-Ras band is due to protein aggregation, degradation or other mechanisms, it will be the subject of further studies.

Palmitoylation is a reversible modification, with a half-life that has been measured as approximately 20 min compared to the 20 h half-life of the protein [33]. In addition, Ras depalmitoylation can be stimulated by Ras activation [4], whereas S-nitrosocysteine treatment has been reported to modulate palmitate turnover by stimulating H-Ras deacylation and allowing subsequent reacylation [34]. It is possible therefore, that during the palmitoylation-depalmitoylation cycle of H-Ras, C181 and C184 may become

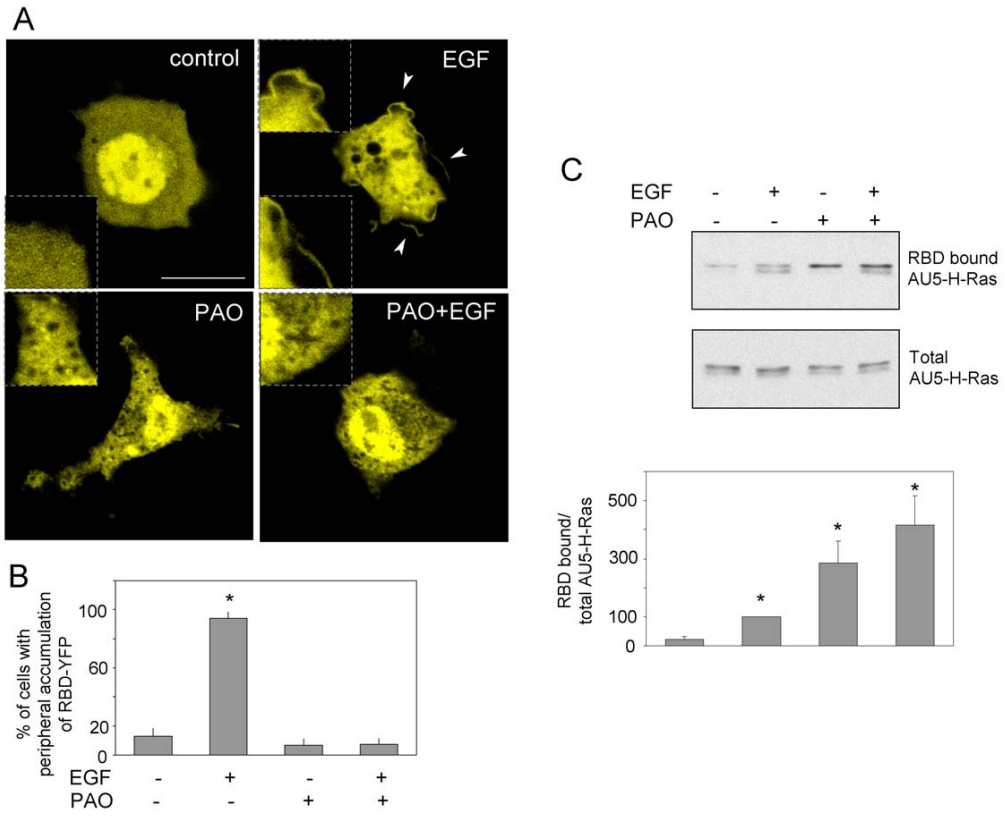

Figure 6. Effect of PAO on Ras activation. (A) COS-7 cells were transfected with YFP-RBD, serum starved for 16 h and pre-incubated with vehicle or 1 μM PAO for 1 h before stimulation with 100 nM EGF. Cells were visualized live by confocal fluorescence microscopy. Shown are representative images from at least five experiments with similar results. Dotted inserts show enlarged areas from the same cells for better visualization. Arrowheads mark the accumulation of YFP-RBD at defined locations of the cell periphery. Bar, 20 μm. At least 40 cells were monitored per experimental condition and the percentage of cells showing accumulations of YFP-RBD at the cell periphery is shown in (B) as average values ± standard error of mean (SEM) of five independent experiments. (C) Cells were treated as above and cell lysates were subjected to pull-down on GST-RBD beads for collection of Ras in its active conformation. Levels of RBD-bound and total AU5-H-Ras were assessed by western blot. Results shown are representative of three assays. The lower panel presents the quantitation of RBD-bound AU5-H-Ras/total AU5-H-Ras ratios from three independent experiments as average values ± SEM. *$p<0.05$ vs vehicle.
doi:10.1371/journal.pone.0015866.g006

available for chemical modification by various agents or by oxidation. Depending on its stability, this modification could interfere with subsequent palmitoylation and palmitoylation-dependent subcellular localization or microdomain partitioning of H-Ras. According to the current knowledge, depalmitoylation of H-Ras would occur subsequently to activation and allow recycling of the protein towards the Golgi complex, where it would be re-palmitoylated. Indeed, non-palmitoylatable versions of H-Ras have been found to localize primarily on the Golgi and signal mainly from this platform in response to growth factor stimulation [8]. In addition, active H-Ras has been detected at the endoplasmic reticulum and on recycling endosomes in route towards the plasma membrane [35]. Interestingly, mutation of C184 for a more hydrophobic leucine residue has been proposed to be able to substitute for the presence of palmitate at this position and support binding of H-Ras to plasma membrane and recycling endosomes [35]. In light of our data, it would be tempting to hypothesize that the modification of C181 and C184 of H-Ras through the addition of electrophilic endogenous mediators or chemical agents could differentially affect the site of action of this GTPase depending on the structure and/or hydrophobicity of the bound molecule.

We have previously shown that modification of Ras proteins by various eicosanoids, including 15d-PGJ_2, PGA_1 [15], Δ^{12}-PGJ_2 or 8-iso-PGA_1 (Oeste et al., unpublished results), correlates with activation of Ras-dependent pathways, although the precise site of H-Ras activation by these various eicosanoids needs to be studied in detail. Here we have observed that PAO induces an increase in H-Ras binding to RBD. Moreover, the observations that both PAO and DBB induce a cytosolic particulate pattern of YFP-RBD in cells could be indicative of the activation of Ras proteins in endomembranes. Although further work is needed to establish this point, our results with PAO selectively blocking redistribution of YFP-RBD towards the plasma membrane (live cell assay), but not the total RBD binding capacity of H-Ras after EGF stimulation (pull-down assay) would support this hypothesis. Moreover, we observed retention of the slower migrating form of H-Ras on RBD beads upon treatment with PAO. Whether this band represents PAO-modified protein and its precise subcellular localization will be the subject of future studies.

In this work we have used various electrophilic agents as tools to target the palmitoylation cysteines of H-Ras. However, it should be kept in mind that the compounds used may bind to multiple cellular targets. Moreover, thiol-reactive compounds may alter the

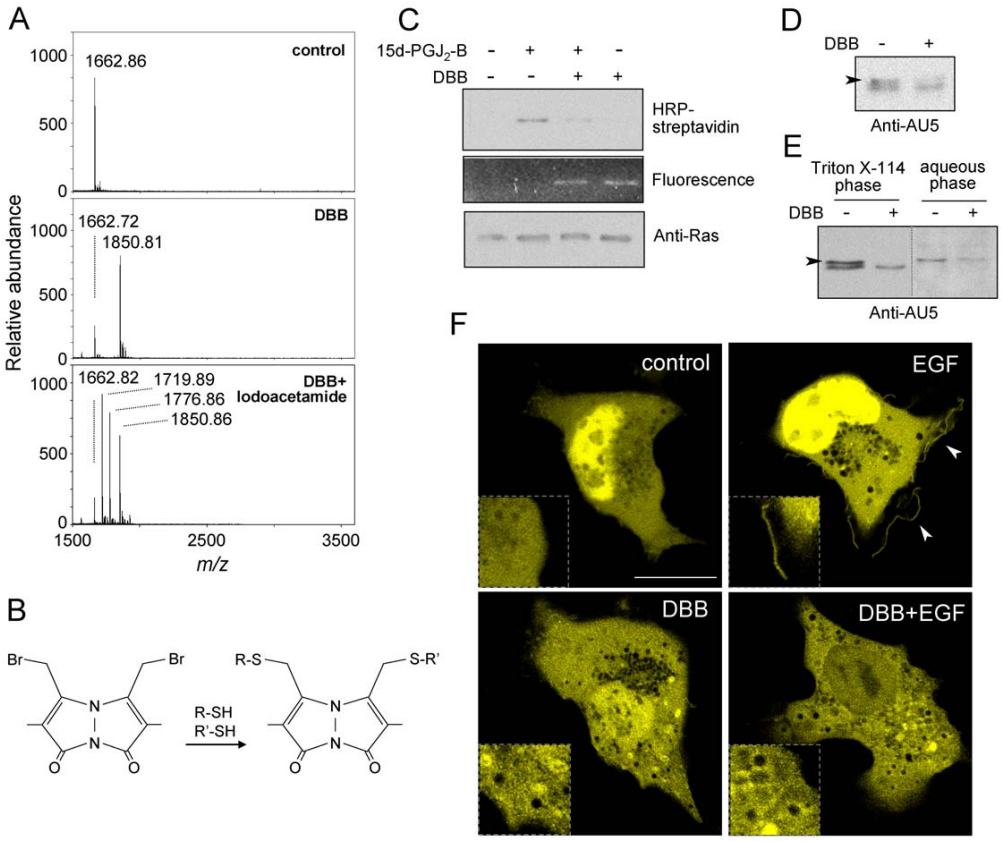

Figure 7. Interaction of the bifunctional reagent DBB with H-Ras. (A) Modification of the K170-K185 peptide by DBB. The K170-K185 peptide was incubated with DBB, as described in the Methods section. When indicated the incubation mixture was subjected to reduction and alkylation with iodoacetamide to modify free cysteines. Results are representative of three independent assays. (B) Scheme of the cross-linking of two thiol groups by DBB. (C) Competition of 15d-PGJ_2-B binding to H-Ras by DBB. H-Ras at 5 μM was incubated with 50 μM DBB for 30 min before addition of 1 μM 15d-PGJ_2-B for 1 h. Incorporation of the biotinylated PG was assessed by SDS-PAGE, protein blot and detection with horseradish peroxidase (HRP)-streptavidin (upper panel). Incorporation of DBB (middle panel) and total H-Ras levels (lower panel) were assessed by fluorescence detection and western blot with anti-pan Ras antibody, respectively. (D) COS-7 cells transfected with the AU5-H-Ras vector were treated in the absence or presence of 50 μM DBB for 1 h. Aliquots from total cell lysates (10 μg of protein) were analyzed by SDS-PAGE. The upper component of the AU5-H-Ras doublet is indicated by an arrowhead. (E) COS-7 cells transfected with the AU5-H-Ras vector were treated with DBB and subjected to fractionation in Triton-X114 as above. In (D) and (E) levels of AU5-H-Ras were assessed by western blot with anti-AU5 antibody. The dotted line marks where lanes from the same gel have been cropped. (F) COS-7 cells transfected with YFP-RBD as above were treated with 50 μM DBB for 1 h before stimulation with 100 nM EGF, as indicated, and visualized live by confocal fluorescence microscopy. Dotted inserts show enlarged areas from the same cells for better visualization. Arrowheads mark the accumulation of YFP-RBD at defined locations of the cell periphery. Bar, 20 μm. Shown are representative images from three experiments with similar results.
doi:10.1371/journal.pone.0015866.g007

cellular redox state and have an impact on the oxidative modifications of proteins [21,36]. In particular, PAO, widely used as a tyrosine phosphatase inhibitor in cells, may interfere with numerous signaling pathways [20,21]. Indeed, interaction of PAO with Ras signaling pathways has been reported to lead to diverse effects, in some cases of complex interpretation. PAO has been reported to block Ras activation by insulin in murine fibroblasts [37], but not to reduce EGF-induced Ras activation in HEK-293 cells [38]. Our results showing that H-Ras proteins can be direct targets for modification by this compound add further complexity to this picture and call attention to the need of interpreting these results cautiously.

In summary, our results show that bifunctional cysteine reagents can target the hypervariable region of H-Ras and that this interaction may have multifaceted consequences for Ras distribution and signaling.

Materials and Methods

Materials

The prostanoids used throughout this study were from Cayman Chemical (Ann Arbor, MI). Human recombinant H-Ras was from Calbiochem-Novabiochem (San Diego, CA). Anti-AU5 monoclonal antibody was from Berkeley Antibody Company (Berkeley, CA), anti-pan Ras (Ab-3) was from Merck. Phenylarsine oxide (PAO), dibromobimane (DBB) and epidermal growth factor (EGF) were purchased from Sigma-Aldrich (St. Louis, MO). Raf-Ras binding domain (Raf-RBD) protein agarose beads were from Cytoskeleton, Inc.

Synthesis of H-Ras C-terminal peptide

Peptide KLNPPDESGPGCMSCK, corresponding to amino acids K170 to K185 of human H-Ras, henceforth referred to as

K170-K185, was chosen as a model because it is the major modified peptide detected after tryptic digestion of 15d-PGJ_2- and Δ^{12}-PGJ_2-treated H-Ras [15]. The peptide was produced by solid phase methods [39] in an ABI 433A synthesizer (Applied Biosystems, Foster City, CA), using Fmoc (9-fluorenylmethoxy carbonyl) chemistry and 0.1-mmol-scale FastMoc protocols. After chain assembly, it was cleaved from the resin by acidolysis with trifluoroacetic acid/water/ethanedithiol/triisopropylsilane (94:2.5:2.5:1 v/v, 90 min, 25°C), precipitated with chilled methyl tert-butyl ether, redissolved in 10% (v/v) acetic acid and lyophilized. Purification by preparative HPLC (Phenomenex C_{18} column, 21.2×250 mm, 10 μm particle size, linear gradient of solvent B into A –solvent A, 0.045% TFA in H_2O; solvent B, 0.036% in acetonitrile– over 35 min, 25 ml/min flow rate) yielded fractions containing the target dithiol peptide in highly pure form, with a mass of 1662.73 by MALDI-TOF mass spectrometry.

Plasmids and transfections

The plasmids pCEFL-KZ-AU5 and pCEFL-KZ-AU5-H-Ras wt have been previously described [14]. An expression plasmid containing the Ras-binding domain of cRaf (RBD) fused to the Yellow Fluorescent Protein (pEYFP-RBD) was prepared from a RBD-pECFP plasmid generously donated by Dr. MR Philips. COS-7 cells were grown in DMEM supplemented with 10% fetal bovine serum, 2 mM glutamine, 100 U/ml penicillin and 100 μg/ml streptomycin. Transient transfections were performed using Lipofectamine 2000 (Invitrogen), according to the instructions of the manufacturer. Treatments with the various agents used were performed in the absence of serum. Prostanoids and PAO were added in DMSO (vehicle) and control cells received an equivalent amount of vehicle.

Analysis of the interaction between H-Ras and small molecules in vitro

H-Ras or K170-K185 Ras peptide were incubated at 5 μM in the presence of prostanoids, DBB or PAO at 50 μM or vehicle (DMSO), as previously described [15]. For some experiments, H-Ras incubation mixtures were then subjected to digestion with trypsin for 4 h at 37°C. When indicated, aliquots of H-Ras, tryptic digests or K170-K185 peptide were subsequently incubated with 10 mM DTT for 30 min followed by 50 mM iodoacetamide for 30 min at r.t. before purification on ZipTip C18 (Millipore) and MALDI-TOF MS analysis on an AUTOFLEX III MALDI-TOF-TOF instrument (Bruker-Franzen Analytik, Bremen, FRG) operated in the positive mode, as reported in detail [15]. Selected peptides were further analyzed by MALDI-TOF-TOF MS/MS.

Interaction of 15d-PGJ_2-B and recombinant H-Ras was also explored by SDS-PAGE, protein transfer to Immobilon-P membranes and detection of incorporated biotin with horseradish peroxidase (HRP)-Streptavidin and enhanced chemiluminescence (ECL), as previously described [14]. Direct binding of DBB to H-Ras was assessed by visualization of the gel under UV light on a Gel-Doc XR Imaging System (Bio-Rad), as described [25]. Unreacted DBB, which is essentially non-fluorescent, becomes fluorescent upon cross-linking (excitation maximum 385 nm, emission, 477 nm).

Molecular-building procedure

Structural studies on H-Ras indicate that the C-terminal segment lacks a defined structure in solution [16]. Therefore, we used a molecular-building approach for modelling this peptide. The recognition of an overall fold for the H-Ras K170-K185 peptide was based on the threading prediction from the THREADER program [40]. A three-dimensional model for the sequence of the K170-K185 peptide was built using a knowledge-based protein modelling method based on the given pair-wise target-template sequence alignment to the 156-171 spanning region of the 2.4 Å resolution X-ray structure of a CRISP family Ca^{2+}-blocker (PDB code 1wvr) as template. This particular template was chosen on the basis of its high sequence identity with the Ras C-terminal peptide (sequence alignment shows a 44% sequence identity with a ratio of aligned/gap positions of 16/0 as yielded by a global alignment algorithm), its low-density map of inter-residues interactions and a relatively high relation of surface/buried residues. Nevertheless, it should be taken into account that the structure obtained is a theoretical homology model, which serves the purpose, not of defining a structure for the K170-K185 H-Ras peptide, but of illustrating the feasibility of the modifications described. The 3D-configurations of 15d-PGJ_2 and PAO ligands were obtained from the PubChem database (http://pubchem.ncbi.nlm.nih.gov, CID codes 5280885 and 4778, respectively). Computational resources from the SWISS-MODEL homology modeling server [41] were used to achieve the final structural model for the K170-K185 peptide. The structure alignment of the 156–171 spanning region of 1wvr with the K170-K185 peptide model shows a likely identical fold, with a backbone-atoms root-mean-square deviation of 0.12 Å. The stereochemical quality of that model and its structural self-consistency were assessed with PROCHECK [42] and Verify-3D [43] programs, respectively. The initial molecular conformations for the adducts were subjected to a constrained energy minimization step in order to remove steric clashes. Computations were performed with the MacroModel 9.5 software (Schrödinger Suite 2007 Update 2, 2007). Final figures were carried out with the Swiss-Pdb Viewer v4.0 program (http://www.expasy.org/spdbv/).

Binding of 15d-PGJ_2-B to Ras proteins in intact cells

COS-7 cells transiently transfected with Ras plasmids were incubated with 15d-PGJ_2-B for 2 h. Cells were lysed in 50 mM Tris-HCl, pH 7.5, 0.1 mM EDTA, 0.1 mM EGTA, 0.1 mM 2-mercaptoethanol, 0.5% SDS containing protease inhibitors (2 μg/ml each of leupeptin, aprotinin and pepstatin, and 1.3 mM ABMSF), and incorporation of 15d-PGJ_2-B into Ras proteins was assessed by western blot with HRP-streptavidin, essentially as described [14].

Analysis of H-Ras localization and activation

The effect of PAO on H-Ras subcellular localization was assessed by obtaining S100 and P100 fractions, as described [44]. H-Ras hydrophobicity was assessed by partition in Triton X-114, as previously described [45]. Briefly, COS-7 cells transfected with AU5-H-Ras and treated with the indicated agents were lysed in 20 mM Tris HCl, pH 7.5, 150 mM MaCl, 1% Triton X-114, containing protease inhibitors as above, for 1 h at 4°C with occasional shaking. After 3 min incubation at 37°C lysates were centrifuged at 12000 rpm for 3 min for phase separation. Aqueous phase was collected and the detergent phase was re-extracted with lysis buffer without Triton X-114. The second aqueous phase was discarded and the detergent phase was resuspended in a volume of buffer, without detergent, equal to the starting volume of lysate used for fractionation. Equal volumes of aqueous and detergent phases were analyzed by SDS-PAGE and western blot.

H-Ras activation in intact cells was monitored by two complementary assays. For a Ras activation-redistribution assay, COS-7 cells cultured on glass bottom dishes from Mattek Corp. (Ashland, MA) were transiently transfected with YFP-RBD and serum starved for 16 h, after which they were stimulated with the

indicated compounds. The distribution of YFP-RBD was observed by confocal fluorescence microscopy in live cells using a Leica DMRE2 microscope (LEICA, Heidelberg, Germany). In this assay, YFP-RBD shows a diffuse distribution in non-stimulated cells, whereas Ras activation recruits YFP-RBD causing its accumulation in defined areas [8]. For quantitation, the proportion of cells showing plasma membrane-associated YFP-RBD was assessed. All experiments were repeated at least three times and representative results are shown. For a Raf RBD pull-down assay, cells were lysed in 25 mM Hepes, pH 7.5, 150 mM NaCl, 10% glycerol, 10 mM $MgCl_2$, 1% NP-40, 1 mM EDTA, 0.25% deoxycholic acid containing 25 mM FNa, 1 mM sodium orthovanadate, 10 μg/ml leupeptin and aprotinin and 1.3 mM ABMSF. Cell lysates were incubated with Raf-RBD agarose beads with rotary shaking for 1 h at 4°C. After extensive washing, bound proteins were eluted by incubation for 5 min at 95°C in Laemmli sample buffer. The amount of AU5-H-Ras retained on Raf-RBD beads and that present in total cell lysates used for pull-down was assessed by western blot.

Statistical analysis

The data shown are the mean ± SE of at least three experiments. Statistical significance was estimated with the Student's t test for unpaired observations. A p value of less than 0.05 was considered significant.

Acknowledgments

We thank Dr. V. de los Ríos for help with mass spectrometry, MT Seisdedos for expert assistance with fluorescent microscopy, MJ Carrasco for technical help and Prof. F.J. Cañada for helpful comments and discussion.

Author Contributions

Conceived and designed the experiments: DP-S. Performed the experiments: CLO BD-D FB MGdL. Analyzed the data: DP-S CLO BD-D DA JMR EPI. Contributed reagents/materials/analysis tools: MGL DA BGdlT JMR CAG-D AJR-S EPI. Wrote the paper: DP-S DA MGdL.

References

1. Barbacid M (1987) ras genes. Ann Rev Biochem 56: 779–827.
2. Pérez-Sala D, Martínez-A C, Rebollo A (1999) Novel aspects of Ras proteins biology: regulation and implications. Cell Death Differ 6: 722–728.
3. Malumbres M, Barbacid M (2003) RAS oncogenes: the first 30 years. Nat Rev Cancer 3: 459–465.
4. Omerovic J, Laude AJ, Prior IA (2007) Ras proteins: paradigms for compartmentalised and isoform-specific signalling. Cell Mol Life Sci 64: 2575–2589.
5. Heo J, Prutzman KC, Mocanu V, Campbell SL (2005) Mechanism of free radical nitric oxide-mediated Ras guanine nucleotide dissociation. J Mol Biol 346: 1423–1440.
6. Hancock JF, Magee AI, Childs JE, Marshall CJ (1989) All ras proteins are polyisoprenylated but only some are palmitoylated. Cell 57: 1167–1177.
7. Pérez-Sala D (2007) Protein isoprenylation in biology and disease: general overview and perspectives from studies with genetically engineered animals. Front Biosci 12: 4456–4472.
8. Chiu VK, Bivona T, Hach A, Sajous JB, Silletti J, et al. (2002) Ras signalling on the endoplasmic reticulum and the Golgi. Nat Cell Biol 4: 343–350.
9. Plowman SJ, Hancock JF (2005) Ras signaling from plasma membrane and endomembrane microdomains. Biochim Biophys Acta 1746: 274–283.
10. Uchida K, Shibata T (2008) 15-Deoxy- $\Delta^{12,14}$-prostaglandin J_2: an electrophilic trigger of cellular responses. Chem Res Toxicol 21: 138–144.
11. Díez-Dacal B, Pérez-Sala D (2010) Anti-inflammatory prostanoids: focus on the interactions between electrophile signalling and resolution of inflammation. TheScientificWorldJOURNAL 10: 655–675.
12. Rajakariar R, Hilliard M, Lawrence T, Trivedi S, Colville-Nash P, et al. (2007) Hematopoietic prostaglandin D_2 synthase controls the onset and resolution of acute inflammation through PGD_2 and 15-deoxy-$\Delta^{12,14}$ -PGJ_2. Proc Natl Acad Sci U S A 104: 20979–20984.
13. Cernuda-Morollón E, Pineda-Molina E, Cañada FJ, Pérez-Sala D (2001) 15-Deoxy-$\Delta^{12,14}$-prostaglandin J_2 inhibition of NF-κB DNA binding through covalent modification of the p50 subunit. J Biol Chem 276: 35530–35536.
14. Oliva JL, Pérez-Sala D, Castrillo A, Martínez N, Cañada FJ, et al. (2003) The cyclopentenone 15-deoxy- $\Delta^{12,14}$-prostaglandin J_2 binds to and activates H-Ras. Proc Natl Acad Sci U S A 100: 4772–4777.
15. Renedo M, Gayarre J, García-Domínguez CA, Pérez-Rodríguez A, Prieto A, et al. (2007) Modification and activation of Ras proteins by electrophilic prostanoids with different structure are site-selective. Biochemistry 46: 6607–6616.
16. Thapar R, Williams JG, Campbell SL (2004) NMR characterization of full-length farnesylated and non-farnesylated H-Ras and its implications for Raf activation. J Mol Biol 343: 1391–1408.
17. Gorfe AA, Babakhani A, McCammon JA (2007) H-ras protein in a bilayer: interaction and structure perturbation. J Am Chem Soc 129: 12280–12286.
18. Wang Q, Pfeiffer GR, 2nd, Gaarde WA (2003) Activation of SRC tyrosine kinases in response to ICAM-1 ligation in pulmonary microvascular endothelial cells. J Biol Chem 278: 47731–47743.
19. Covian-Nares JF, Smith RM, Vogel SS (2008) Two independent forms of endocytosis maintain embryonic cell surface homeostasis during early development. Dev Biol 316: 135–148.
20. Gerhard R, John H, Aktories K, Just I (2003) Thiol-modifying phenylarsine oxide inhibits guanine nucleotide binding of Rho but not of Rac GTPases. Mol Pharmacol 63: 1349–1355.
21. Gilge JL, Fisher M, Chai YC (2008) The effect of oxidant and the non-oxidant alteration of cellular thiol concentration on the formation of protein mixed-disulfides in HEK 293 cells. PLoS One 3: e4015.
22. He X, Ma Q (2009) Induction of metallothionein I by arsenic via metal-activated transcription factor 1: critical role of C-terminal cysteine residues in arsenic sensing. J Biol Chem 284: 12609–12621.
23. Bordier C (1981) Phase separation of integral membrane proteins in Triton X-114 solution. J Biol Chem 256: 1604–1607.
24. Gomez GA, Daniotti JL (2005) H-Ras dynamically interacts with recycling endosomes in CHO-K1 cells: involvement of Rab5 and Rab11 in the trafficking of H-Ras to this pericentriolar endocytic compartment. J Biol Chem 280: 34997–35010.
25. Sinz A, Wang K (2001) Mapping protein interfaces with a fluorogenic cross-linker and mass spectrometry: application to nebulin-calmodulin complexes. Biochemistry 40: 7903–7913.
26. Lander HM, Hajjar DP, Hempstead BL, Mirza UA, Chait BT, et al. (1997) A molecular redox switch on p21ras. Structural basis for the nitric oxide-p21ras interaction. J Biol Chem 272: 4323–4326.
27. Mallis RJ, Buss JE, Thomas JA (2001) Oxidative modification of H-ras: S-thiolation and S-nitrosylation of reactive cysteines. Biochem J 355: 145–153.
28. Kim SE, Yoon JY, Jeong WJ, Jeon SH, Park Y, et al. (2009) H-Ras is degraded by Wnt/beta-catenin signaling via beta-TrCP-mediated polyubiquitylation. J Cell Sci 122: 842–848.
29. Sánchez-Gómez FJ, Díez-Dacal B, Pajares MA, Llorca O, Pérez-Sala D (2010) Cyclopentenone prostaglandins with dienone structure promote cross-linking of the chemoresistance-inducing enzyme Glutathione Transferase P1-1. Mol Pharmacol 78: 723–733.
30. Pérez-Sala D, Cernuda-Morollón E, Cañada FJ (2003) Molecular basis for the inhibition of AP-1 DNA binding by 15-deoxy-$\Delta^{12,14}$-prostaglandin J_2. J Biol Chem 278: 51251–51260.
31. Shibata T, Yamada T, Ishii T, Kumazawa S, Nakamura H, et al. (2003) Thioredoxin as a molecular target of cyclopentenone prostaglandins. J Biol Chem 278: 26046–26054.
32. Pérez-Sala D, Boya P, Ramos I, Herrera M, Stamatakis K (2009) The C-terminal sequence of RhoB directs protein degradation through an endo-lysosomal pathway. PLoS ONE 4(12): e8117.
33. Rocks O, Peyker A, Kahms M, Verveer PJ, Koerner C, et al. (2005) An acylation cycle regulates localization and activity of palmitoylated Ras isoforms. Science 307: 1746–1752.
34. Baker TL, Booden MA, Buss JE (2000) S-Nitrosocysteine increases palmitate turnover on Ha-Ras in NIH 3T3 cells. J Biol Chem 275: 22037–22047.
35. Misaki R, Morimatsu M, Uemura T, Waguri S, Miyoshi E, et al. (2010) Palmitoylated Ras proteins traffic through recycling endosomes to the plasma membrane during exocytosis. J Cell Biol 191: 23–29.
36. Ishii T, Uchida K (2004) Induction of reversible cysteine-targeted protein oxidation by an endogenous electrophile 15-deoxy-$\Delta^{12,14}$-prostaglandin J_2. Chem Res Toxicol 17: 1313–1322.
37. Medema RH, Burgering BM, Bos JL (1991) Insulin-induced p21ras activation does not require protein kinase C, but a protein sensitive to phenylarsine oxide. J Biol Chem 266: 21186–21189.
38. Tong XK, Hussain NK, Adams AG, O'Bryan JP, McPherson PS (2000) Intersectin can regulate the Ras/MAP kinase pathway independent of its role in endocytosis. J Biol Chem 275: 29894–29899.
39. Fields GB, Noble RL (1990) Solid phase peptide synthesis utilizing 9-fluorenylmethoxycarbonyl amino acids. Int J Pept Protein Res 35: 161–214.
40. McGuffin LJ, Jones DT (2003) Improvement of the GenTHREADER method for genomic fold recognition. Bioinformatics 19: 874–881.

41. Arnold K, Bordoli L, Kopp J, Schwede T (2006) The SWISS-MODEL workspace: a web-based environment for protein structure homology modelling. Bioinformatics 22: 195–201.
42. Laskowski RA, MacArthur MW, Moss DS, Thornton JM (1993) PROCHECK: a program to check the stereochemical quality of protein structures. J Appl Cryst 26: 283–291.
43. Eisenberg D, Luthy R, Bowie JU (1997) VERIFY3D: assessment of protein models with three-dimensional profiles. Methods Enzymol 277: 396–404.
44. Gharbi S, Garzón B, Gayarre J, Timms J, Pérez-Sala D (2007) Study of protein targets for covalent modification by the antitumoral and anti-inflammatory prostaglandin PGA_1: focus on vimentin. J Mass Spectrom 42: 1474–1484.
45. Valero RA, Oeste CL, Stamatakis K, Ramos I, Herrera M, et al. (2010) Structural determinants allowing endo-lysosomal sorting and degradation of endosomal GTPases. Traffic 11: 1221–1233.

OTHER RELATED PUBLICATIONS

Oeste CL and Pérez-Sala D (2014) Modification of cysteine residues by cyclopentenone prostaglandins: interplay with redox regulation of protein function. *Mass Spectrom. Rev.* **33**(2): 110-125.

Garzón B, Oeste CL, Díez-Dacal B and Pérez-Sala D (2011) Proteomic studies on protein modification by cyclopentenone prostaglandins: expanding our view on electrophile actions. *J. Proteomics* **74**(11): 2243-2263.

Martínez AE, Sánchez-Gómez FJ, Díez-Dacal B, Oeste CL and Pérez-Sala D (2012) 15-Deoxy-Delta(12,14)-prostaglandin J2 exerts pro- and anti-inflammatory effects in mesangial cells in a concentration-dependent manner. *Inflamm Allergy Drug Targets* **11**(1): 58-65.